Case No. 84739

IN THE SUPREME COURT OF THE STATE OF NEVADA

Electronically Filed
Nov 08 2022 04:38 p.m.
Elizabeth A. Brown
Clerk of Supreme Court

ADAM SULLIVAN, P.E., NEVADA STATE ENGINEER, et al.

Appellants,

vs.

LINCOLN COUNTY WATER DISTRICT, et al.

JOINT APPENDIX

VOLUME 37 OF 49

Conceptual Model of Groundwater Flow for the Central Carbonate-Rock Province: Clark, Lincoln, and White Pine Counties Groundwater Development Project

November 2009

PREPARED IN COOPERATION WITH
THE BUREAU OF LAND MANAGEMENT

Suggested citation:
Southern Nevada Water Authority, 2009, Conceptual model of groundwater flow for the Central Carbonate-Rock Province—Clark, Lincoln, and White Pine Counties Groundwater Development Project: Southern Nevada Water Authority, Las Vegas, Nevada, 416 p.

SE ROA 50335

PREFACE

This report was prepared by the Southern Nevada Water Authority in cooperation with the U.S. Department of Interior's Bureau of Land Management. The U.S. Geological Survey served as technical advisor to the Bureau of Land Management in the preparation of this report.

This Page Intentionally Left Blank

CONTENTS

SE ROA 50339

JA_15740

CONTENTS (CONTINUED)

SE ROA 50340

JA_15741

SE ROA 50341

JA_15742

CONTENTS (CONTINUED)

CONTENTS (CONTINUED)

FIGURES

FIGURES (CONTINUED)

FIGURES (CONTINUED)

Figures (Continued)

PLATES

NUMBER **TITLE**

This Page Intentionally Left Blank

TABLES

TABLES (CONTINUED)

TABLES (CONTINUED)

TABLES (CONTINUED)

SE ROA 50355

JA_15756

ACRONYMS

3D	three-dimensional
AGU	agricultural unit
ANCOVA	analysis of covariance
BARCASS	Basin and Range Carbonate Aquifer System Study
Barker GRFM	Barker generalized radial flow model
BCM	Basin Characterization Model
BLM	Bureau of Land Management
CCRP	Central Carbonate-Rock Province
CDF	cumulative density function
CI	confidence interval
COV	coefficient of variation
CRFS	Colorado Regional Ground-Water Flow System
CWP	Cooperative Water Project
DEM	digital elevation model
DMV	dense meadowland vegetation
DOE	U.S. Department of Energy
DRI	Desert Research Institute
DST	drill-stem test
DSV	dense shrubland vegetation
DVFS	Death Valley Flow System
DVRFS	Death Valley Regional Flow System
DWV	dense woodland vegetation
EIS	environmental impact statement
ET	evapotranspiration
GIS	geographic information system
GSLDFS	Great Salt Lake Desert Flow System
GVFS	Goshute Valley Flow System
HA	hydrographic area
HGU	hydrogeologic unit
K	hydraulic conductivity
LVVSZ	Las Vegas Valley Shear Zone
LVVWD	Las Vegas Valley Water District
MSAVI	Modified Soil Adjusted Vegetation Index
MSV	moderate shrubland vegetation
MVFS	Meadow Valley Flow System

SE ROA 50356

JA_15757

MWV	moderate woodland vegetation
NA	not applicable
NAD83	North American Datum of 1983
NCDC	National Climatic Data Center
NDVI	Normalized Difference Vegetation Index
NDWR	Nevada Division of Water Resources
NE	not estimated
NED	National Elevation Dataset
NPU	non-phreatophytic unit
NRCS	Natural Resources Conservation Service
NTS	Nevada Test Site
NWIS	National Water Information System
NWR	National Wildlife Refuge
OWU	open water unit
PET	potential evapotranspiration
PRISM	Parameter-elevation Regressions on Independent Slopes Model
RASA	Regional Aquifer-System Analysis
RMU	regional modeling unit
SEBAL	Surface Energy Balance Algorithm for Land
SNJV	Stoller-Navarro Joint Venture
SNOTEL	SNOwpack TELemetry
SNWA	Southern Nevada Water Authority
SWReGAP	Southwest Regional Gap Analysis Project
UGS	Utah Geological Survey
UNLV	University of Nevada, Las Vegas
UNR	University of Nevada, Reno
USAF	U.S. Air Force
USGS	U.S. Geological Survey
UTM	Universal Transverse Mercator
WRCC	Western Regional Climate Center
WRFS	White River Flow System
WY	Water Year

ABBREVIATIONS

°C	degrees Celsius
°F	degrees Fahrenheit
ac	acre
afy	acre-feet per year
amsl	above mean sea level
bgs	below ground surface
cfs	cubic feet per second
cm	centimeter
ft	foot
ft^2	square feet
ft^3	cubic feet
gpm	gallons per minute
hr	hour
in.	inch
km	kilometer
km^2	square kilometer
m	meter
m^2	square meter
mi	mi
mi^2	square mile
yr	year

This Page Intentionally Left Blank

1.0 INTRODUCTION

The purpose of this report is to describe the development of a conceptual model of groundwater flow within the Central Carbonate-Rock Province (CCRP) of Nevada and Utah. The extent of the Project study area (i.e., the regional model area) is shown in Figure 1-1. The groundwater flow model supports the Southern Nevada Water Authority's (SNWA) Clark, Lincoln, and White Pine Counties Groundwater Development Project (hereinafter referred to as the Project), including the acquisition of water rights from the Nevada State Engineer and rights-of-way from the Bureau of Land Management (BLM). This conceptual model was developed and used to construct and calibrate a regional numerical groundwater flow model. The numerical model was used as part of the environmental analysis for the Project. Specifically, the numerical model was used to simulate groundwater development scenarios to evaluate the range of potential water-related effects of the Project's groundwater production at the regional scale. All work relating to BLM issuance of rights-of-way was subjected to review by a panel assembled by BLM. Summary descriptions of the Project background, relevant previous and on-going investigations, purpose and scope, and the BLM review process are presented in this section, followed by a description of the contents of this report.

1.1 Project Background

To reduce reliance on Colorado River water resources and buffer the impacts of long-term droughts on the Colorado River system, SNWA has identified plans to develop in-state non-Colorado River water resources (SNWA, 2004). These additional resources will augment the current water resource portfolio identified in the SNWA Water Resource Plan (SNWA, 2008b). The Project will develop and convey groundwater rights and applications held by SNWA in five basins in eastern Nevada. Figure 1-2 shows the project basins and proposed points of diversion.

The Project consists of groundwater production, conveyance and treatment facilities, and power conveyance facilities, most of which will be located on federal lands managed by BLM. Consequently, in 2004, SNWA applied to BLM for rights-of-way to construct, operate, and maintain the Project facilities. BLM issuance of these rights-of-way is a federal action, which must comply with the National Environmental Policy Act of 1969, the Endangered Species Act of 1973, and other federal regulations. BLM has determined that preparation of an Environmental Impact Statement (EIS) is required to assess the potential effects that may result from permitting the rights-of-way, including the potential indirect effects of the proposed groundwater development. This conceptual model of groundwater flow was prepared in support of the development of the numerical groundwater flow model, which was used in the EIS process for the analysis of the potential indirect effects of the Project.

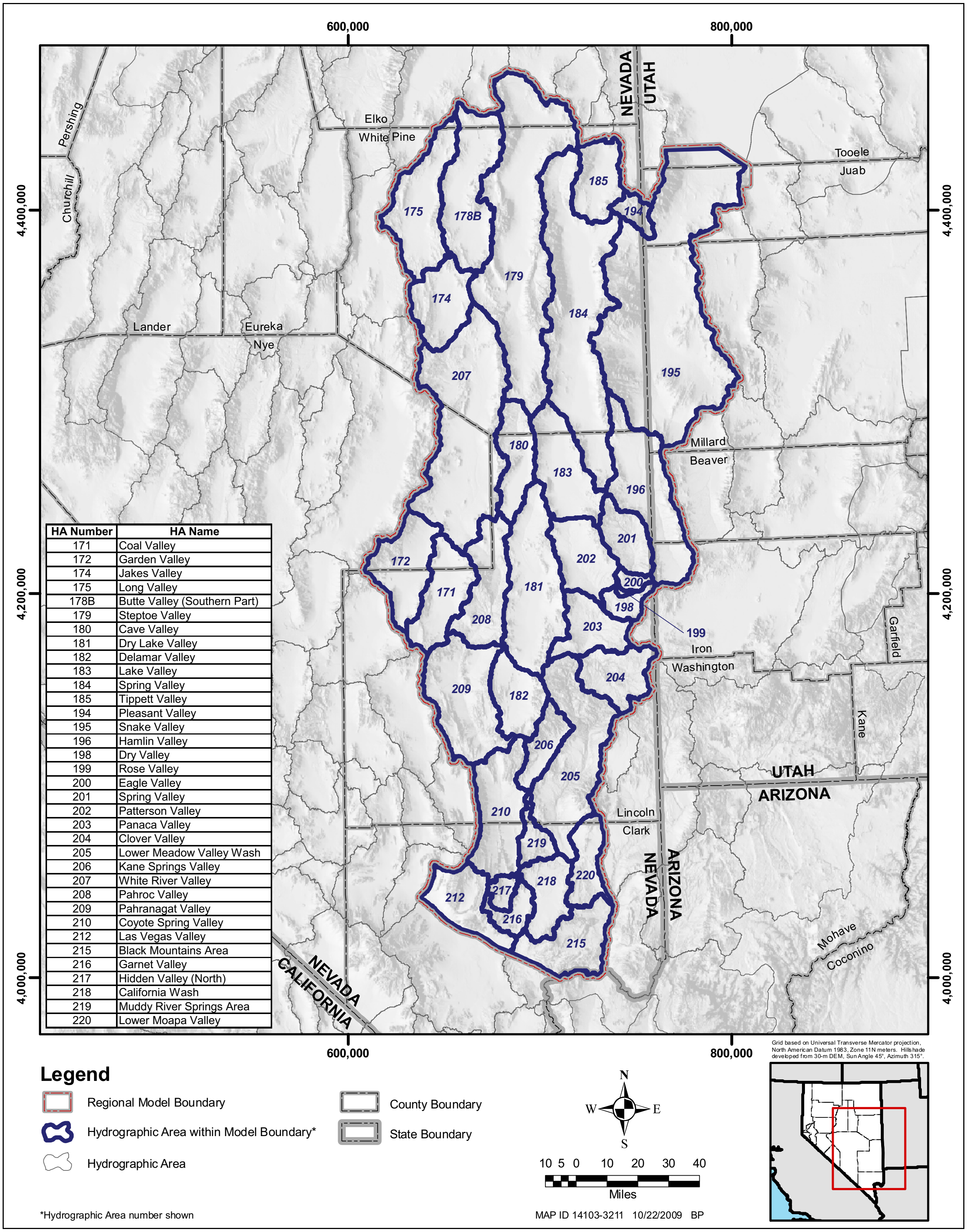

HA Number	HA Name
171	Coal Valley
172	Garden Valley
174	Jakes Valley
175	Long Valley
178B	Butte Valley (Southern Part)
179	Steptoe Valley
180	Cave Valley
181	Dry Lake Valley
182	Delamar Valley
183	Lake Valley
184	Spring Valley
185	Tippett Valley
194	Pleasant Valley
195	Snake Valley
196	Hamlin Valley
198	Dry Valley
199	Rose Valley
200	Eagle Valley
201	Spring Valley
202	Patterson Valley
203	Panaca Valley
204	Clover Valley
205	Lower Meadow Valley Wash
206	Kane Springs Valley
207	White River Valley
208	Pahroc Valley
209	Pahranagat Valley
210	Coyote Spring Valley
212	Las Vegas Valley
215	Black Mountains Area
216	Garnet Valley
217	Hidden Valley (North)
218	California Wash
219	Muddy River Springs Area
220	Lower Moapa Valley

Figure 1-1
Location of Study Area

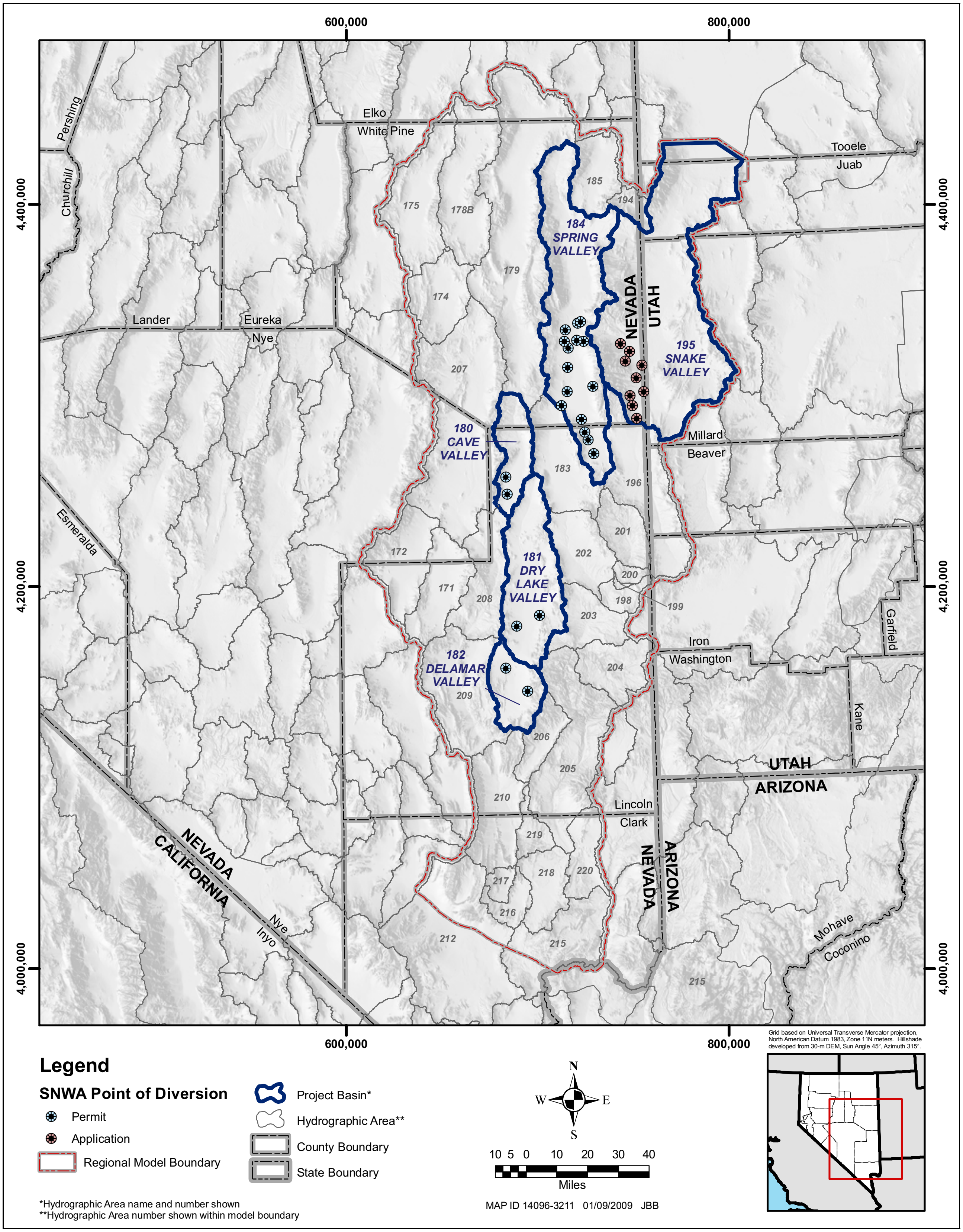

Figure 1-2
Location of Project Basins and Points of Diversion

1.2 Relevant Investigations

Many documents reporting the findings of various studies were reviewed to support development of the numerical model. A large number of them contain information that is relevant to the conceptual model described in this report. Of particular interest are major studies that provide information on the geology and/or hydrology of the study area or portions of it. Such studies are briefly described in this section. Others are called out as appropriate in this report. Major investigations of interest include the following:

- Nevada Division of Water Resources (NDWR)/U.S. Geological Survey (USGS) Reconnaissance Investigations
- U.S. Air Force (USAF) MX Missile-Siting Investigation–Water Resources Program Study
- Great Basin Regional Aquifer-System Analysis (RASA) Study conducted by the USGS
- Studies conducted by the Las Vegas Valley Water District (LVVWD)/SNWA, including those in cooperation with other agencies
- Basin and Range Carbonate Aquifer System Study (BARCASS) conducted by the USGS in cooperation with other agencies
- Groundwater and surface-water evapotranspiration study in hydrographic areas of the Southern Colorado Regional Ground-Water Flow System (CRFS) (DeMeo et al., 2008)

Information derived from recent or on-going studies, such as BARCASS or work conducted by SNWA and cooperating agencies, was given the highest consideration, as these studies incorporate more recent data and analysis methods.

1.2.1 NDWR/USGS Reconnaissance Investigations

During the late 1940s to the early 1980s, the USGS, in cooperation with the NDWR, completed reconnaissance-level hydrologic evaluations or reevaluations of nearly every valley in Nevada. The purpose of the studies was to provide a general appraisal of the groundwater resources as quickly as possible (Eakin, 1963a). The results of these studies are presented in two report series, the USGS Water Resources Bulletin Series and the NDWR/USGS Ground-Water Resources—Reconnaissance Series. The Reconnaissance Series describes estimates of groundwater recharge, groundwater discharge, and perennial yields for each valley or area in Nevada. The recharge estimates presented in these reports were based on a method developed by Maxey and Eakin (1949), using the groundwater-balance method and an empirical relationship between precipitation and groundwater recharge. A more detailed description of the Maxey and Eakin (1949) method is provided in Section 9.1.1.1. An index of the hydrographic areas (HA) of Nevada and the associated publications is presented in Rush (1968a).

Using the Bulletin and Reconnaissance Series, Scott et al. (1971) provided a hydrologic summary for the 232 hydrographic areas in Nevada in a report titled *Nevada's Water Resources—Nevada Water*

Resources Report No. 3. The report was one in a series of reports prepared for the development of a Nevada State Water Plan and included precipitation, surface-water runoff, and groundwater recharge data in addition to perennial and system yield data for each hydrographic area.

1.2.2 U.S. Air Force MX Missile-Siting Investigation–Water Resources Program Study

In the late 1970s and early 1980s, hydrogeologic evaluations were conducted in support of the USAF MX Missile-Siting Investigation–Water Resources Program Study. The purpose of these evaluations was to assess the potential for water-supply development in 36 hydrographic areas in the Great Basin region that were proposed for the deployment of the MX missile system. This program involved literature reviews, exploratory drilling, aquifer testing, groundwater sampling for water-quality analysis, and the development of groundwater flow models to assist in predicting potential impacts of pumping in some valleys. Development of groundwater from the basin-fill aquifers was the preferred water-supply source; most of the valleys had adequate unappropriated groundwater supplies in the basin fill to meet estimated water requirements (Ertec Western, Inc., 1981b). These studies are documented in several reports by Ertec Western, Inc., (1981a through e) and summarized by Bunch and Harrill (1984).

1.2.3 Great Basin Regional Aquifer-System Analysis Study

The Great Basin RASA study took place in the 1980s and was undertaken as part of the USGS national RASA program. The main purpose of this program was to develop a geologic, hydrologic, and geochemical framework for regional aquifer systems nationwide (Harrill et al., 1988) to support effective future groundwater management (Harrill and Prudic, 1998). The results of the RASA study are described in nearly 60 reports, including the USGS Professional Paper 1409 series (1409A through H). The first report of this series, Harrill and Prudic (1998), provides a summary of the RASA study.

Previous RASA reports for the Great Basin region include the USGS Hydrologic Atlas HA-694 series, which consists of the following documents:

- USGS Hydrologic Atlas HA-694-A (Plume and Carlton, 1988) describes the hydrogeology of the Great Basin region.
- USGS Hydrologic Atlas HA-694-B (Thomas et al., 1986) describes water levels in the basin-fill deposits and the potentiometric surface in consolidated rocks of the carbonate-rock province of the Great Basin region.
- USGS Hydrologic Atlas HA-694-C (Harrill et al., 1988) describes interpretations of groundwater-budget components including interbasin flow locations and magnitudes.

Another RASA report for the Great Basin region is that of Prudic et al. (1995). Prudic et al. (1995) present a conceptual evaluation of regional groundwater flow based on a numerical groundwater flow model. The two-layer model was used to simulate the concept of numerous shallow-flow regions superimposed upon fewer deep-flow regions. The Reconnaissance Series provides the basic estimates of recharge and discharge for this regional flow model.

1.2.4 LVVWD/SNWA/Co-operator Studies

Work conducted by LVVWD, SNWA, and co-operators in the study area includes past studies and on-going data collection efforts. Selected studies of interest have been documented in the following reports:

- Desert Research Institute (DRI) Publication No. 41054 (Hess and Mifflin, 1978) produced by the DRI under contract with LVVWD describes a feasibility study about groundwater development from the carbonate aquifers of Nevada. The report includes a compilation of information on the carbonate rocks in eastern and southern Nevada and a plan for further studies.

- The Cooperative Water Project (CWP) Report Series consists of a series of 19 reports published by LVVWD in support of groundwater applications filed with the Nevada State Engineer's Office in 1989 as part of its CWP.

- Reports prepared to support the water-rights hearings and EIS activities include (1) a USGS report containing estimates of groundwater budgets for selected basins of the study area (Nichols, 2000); (2) a LVVWD report on water resources and groundwater modeling of the White River and Meadow Valley flow systems (LVVWD, 2001); (3) an SNWA report on water resources evaluation for Spring Valley (SNWA, 2006); and (4) an SNWA report on water resources evaluation for Cave, Dry Lake, and Delamar valleys (SNWA, 2007).

- A multiple-volume report, *Baseline Characterization Report for Clark, Lincoln, and White Pine Counties Groundwater Development Project* (SNWA, 2008a), prepared by SNWA for BLM describes the baseline conditions for the Project study area in support of the EIS.

Currently, SNWA continues data collection and analysis activities in support of water-right acquisition and development in the area. These activities are part of several studies within the study area. Some are being conducted in cooperation with other agencies, such as USGS, DRI, and NDWR among others. These studies include geophysical surveys, surface-water and groundwater monitoring, well installation and testing, and evapotranspiration (ET) and weather-station data collection. The current status of the well installation and testing activities and the ET studies is provided in Appendix A.

1.2.5 BARCASS

BARCASS was a study created as a result of federal legislation enacted in December 2004 (Section 131 of the Lincoln County Conservation, Recreation, and Development Act of 2004 [U.S. Congress, 2004]). The purpose of BARCASS was to investigate the groundwater flow system underlying parts of White Pine and Lincoln counties, Nevada, and adjacent areas in Utah. Participating agencies included USGS, DRI, and a designee from the State of Utah. The BARCASS area coincides with the northern portion of the study area described in this report (Figure 1-3). Twelve hydrographic areas in the Great Basin were included in BARCASS. Of those twelve, Long, Butte, Steptoe, Spring, Tippett, Snake (including Pleasant and Hamlin), Lake, White River, and Jakes valleys are included within the scope of this study. BARCASS includes the most recent evaluation of ET within the northern part of the study area (Moreo et al., 2007; Smith et al., 2007; Welch et al., 2008).

The BARCASS findings have been documented in a series of reports as follows:

- Summary report (Welch et al., 2008)
- Geophysical framework investigations (Watt and Ponce, 2007)
- Recharge distribution (Flint and Flint, 2007)
- Mapping of ET units (Smith et al., 2007)
- ET rate measurements (Moreo et al., 2007)
- Water-level surface maps (Wilson, 2007)
- Delineated irrigated acreage (Welborn and Moreo, 2007)
- Methodology for mapping vegetation using satellite imagery (Cablk and Kratt, 2007)
- Steady-state water budget accounting model (Lundmark, 2007; Lundmark et al., 2007)
- Groundwater-chemistry interpretations (Hershey et al., 2007)
- Recharge estimates using the chloride mass-balance method (Mizell et al., 2007)
- Uncertainty analysis of groundwater ET estimates (Zhu et al., 2007)

1.2.6 Southern Colorado Regional Groundwater Flow System ET Study

USGS, in cooperation with the National Park Service, BLM, and the U.S. Fish and Wildlife Service, recently conducted a study to quantify the amount of groundwater and surface-water ET in the southern part of the Colorado Regional Groundwater Flow System, Nevada, Utah, and Arizona (DeMeo et al., 2008). Their study area includes 12 hydrographic areas and a portion of two others (Figure 1-3): Clover Valley (HA 204), Kane Springs Valley (HA 206), Lower Meadow Valley Wash (HA 205), Tule Desert (HA 221), Coyote Spring Valley (HA 210), Virgin River Valley (HA 222), Muddy River Springs Area (HA 219), Hidden Valley (North) (HA 217), Garnet Valley (HA 216), California Wash (HA 218), Lower Moapa Valley (HA 220), and the part of the Black Mountains Area (HA 215) north of Las Vegas Valley and the Lake Mead shear zones. All of these basins, except Tule Desert and Virgin River Valley, are located in the CCRP model area (Figure 1-3). The methodology followed by DeMeo et al. (2008) to delineate the ET areas is similar to that of BARCASS (Welch et al., 2008). Their ET rates are based on a combination of newly collected and reported data. The newly collected data consist of micrometeorological measurements at four sites. The four sites were located on the Virgin River floodplain (dense woodland), along the Muddy River (moderate woodland), in Rainbow Canyon (moderate shrubland), and in Lower Meadow Valley Wash (dense shrubland).

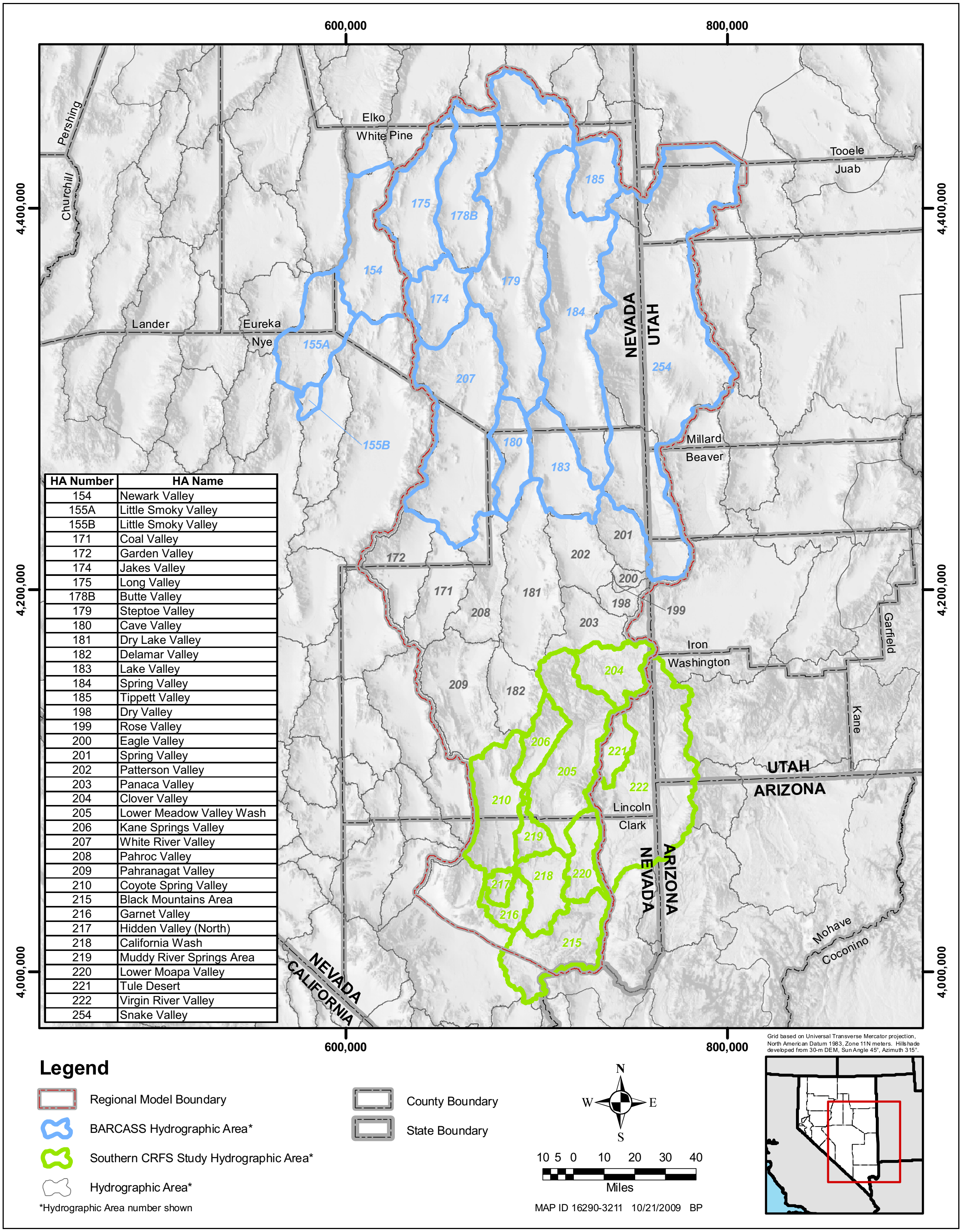

HA Number	HA Name
154	Newark Valley
155A	Little Smoky Valley
155B	Little Smoky Valley
171	Coal Valley
172	Garden Valley
174	Jakes Valley
175	Long Valley
178B	Butte Valley
179	Steptoe Valley
180	Cave Valley
181	Dry Lake Valley
182	Delamar Valley
183	Lake Valley
184	Spring Valley
185	Tippett Valley
198	Dry Valley
199	Rose Valley
200	Eagle Valley
201	Spring Valley
202	Patterson Valley
203	Panaca Valley
204	Clover Valley
205	Lower Meadow Valley Wash
206	Kane Springs Valley
207	White River Valley
208	Pahroc Valley
209	Pahranagat Valley
210	Coyote Spring Valley
215	Black Mountains Area
216	Garnet Valley
217	Hidden Valley (North)
218	California Wash
219	Muddy River Springs Area
220	Lower Moapa Valley
221	Tule Desert
222	Virgin River Valley
254	Snake Valley

Figure 1-3
Location of BARCASS and Southern CRFS ET Study Areas

1.3 Purpose and Scope

This section describes the overall purpose and scope of the hydrologic evaluation conducted in support of the EIS process and explains the purpose and scope of the conceptual model presented in this report.

1.3.1 Overall Purpose and Scope

The purpose of the hydrologic evaluation was to compile and analyze the available hydrogeologic information to support the EIS process and to develop the analytical tools to assist in the analysis of the indirect effects associated with the proposed groundwater withdrawal.

The hydrologic evaluation included the development of a regional three-dimensional (3D) numerical model of the flow systems underlying the study area. Each of the flow systems underlying the study area consists of three subsystems identified by their depth and the lengths of their flow paths: regional, intermediate, and local as described by Tóth (1963) and Freeze and Cherry (1979). See Section 5.2.1 for a description of these subsystems. The numerical model included the regional and intermediate portions of the flow system and served as a tool for performing preliminary regional-scale simulations of the effects of groundwater withdrawal. The simulation results, in turn, were used to preliminarily evaluate the potential water-related effects on the environment. As monitoring and testing data become available in the future, the model will be improved and used as a water-resource management tool.

The overall scope of work of the hydrologic evaluation included four major steps:

1. The preparation of a report documenting the baseline conditions within the study area titled *Baseline Characterization Report for Clark, Lincoln, and White Pine Counties Groundwater Development Project* (SNWA, 2008a).

2. The development of a conceptual model of groundwater flow in the flow systems underlying the study area. All components of this conceptual model, except for historical groundwater use and its effects on the flow system, are documented in this report.

3. The development of a numerical model calibrated to available observations. This step included the analysis of historical groundwater use and its effects on the flow systems and is documented in a report titled *Transient Numerical Model of Groundwater Flow for the Central Carbonate-Rock Province Clark, Lincoln, and White Pine Counties Groundwater Development Project* (SNWA, 2009b).

4. The use of the resulting transient model to evaluate future water-use scenarios, including groundwater withdrawals from the proposed SNWA wells, which are documented in a report titled *Simulation of Groundwater Development Scenarios Using the Transient Numerical Model of Groundwater Flow for the Central Carbonate-Rock Province: Clark, Lincoln, and White Pine Counties Groundwater Development Project* (SNWA, 2009a).

The study area extends over parts of Lincoln, White Pine, and Clark counties in Nevada and over Tooele, Juab, Millard, Beaver, and Iron counties in Utah encompassing the five project basins: Cave Valley (HA 180), Dry Lake Valley (HA 181), Delamar Valley (HA 182), Spring Valley (HA 184), and Snake Valley (HA 195) (Figure 1-1). The study area also includes basins where the water conveyance pipelines will be constructed to move the water from the project basins to the intended place of use in Las Vegas Valley. Originally, the eastern boundary of the model area coincided with the boundary of Snake Valley. During the course of this work, the model boundary was extended to include the portion of Fish Springs Flat that comprises Fish Springs.

1.3.2 Purpose and Scope of the Conceptual Model

The purpose of the conceptual model was to assemble the available hydrogeologic information into simplified components that provide a complete description of the flow system. The main components of the conceptual model are as follows:

- Hydrogeologic framework and hydraulic properties
- Groundwater occurrence and movement
- Predevelopment water budget
    - Groundwater discharge to the surface
    - Subsurface interbasin flow
    - Precipitation recharge
- Historical water use

All components of the conceptual model listed above, except historical water use, are described in this document. The historical water use and its effects are described in the numerical model report (SNWA, 2009b). In this hydrologic evaluation, the conceptual model served as an intermediate step in the development of the numerical model. Its components form the basis of the numerical model.

The conceptual model was developed for the flow systems underlying the Project study area (Figure 1-1). The scope of work included the evaluation, analysis, and simplification of the information contained in the baseline report (SNWA, 2008a) and additional information from various sources described in the document.

1.4 BLM Review Process

A Hydrology Technical Group was assembled by BLM in the early stages of the technical work conducted in support of the EIS. The primary objective of this group was to provide technical advice and recommendations to BLM, so they could ensure that the hydrologic data analysis and numerical model development satisfy the analysis requirements of the EIS.

The BLM Hydrology Technical Group members are as follows:

- BLM (Nevada, Utah, and Denver regional offices)
- USGS
- ENSR/AECOM (EIS consultant)

- Nevada State Engineer's Office (Observing)

The Hydrology Technical Group review process included meetings and conference calls to discuss and resolve technical issues. It also included formal reviews of preliminary reports and work products, including data compilation and analysis, and modeling files or results. This group conducted the report reviews and provided review comments to SNWA and Earth Knowledge, Inc., a consultant to SNWA. ENSR/AECOM was selected by BLM as a third-party contractor to assist in the preparation of the EIS. The Nevada State Engineer's Office participated in the technical meetings but in an observation capacity only.

1.5 Document Contents

This report consists of 12 sections and 9 appendixes. A brief description of the contents of each is provided.

Section 1.0 is this introduction.

Section 2.0 is a general description of the study area, including physiography, climate, soil and vegetation, and land and water uses.

Section 3.0 provides a description of the general approach to modeling groundwater flow in the study area and the specific approach used to conduct the hydrologic evaluation and develop the conceptual model. The description includes the method used to derive estimates of the water budgets for the flow systems and their basins.

Section 4.0 provides a description of the hydrogeologic framework model.

Section 5.0 describes the occurrence and movement of groundwater within the study area.

Section 6.0 describes available methods of deriving spatial distributions for precipitation and presents previously reported precipitation volumes.

Section 7.0 describes groundwater discharge, including groundwater ET and the springs that are relevant to the groundwater flow system at the regional scale.

Section 8.0 presents the directions and relative volumes of interbasin groundwater flow.

Section 9.0 presents methods used to estimate potential recharge and discusses the estimates of recharge and predevelopment groundwater budgets.

Section 10.0 presents the derived predevelopment groundwater budget.

Section 11.0 provides a summary of the contents of this report.

Section 12.0 provides a list of references cited in this report.

Appendix A provides the status of selected ongoing SNWA field data collection activities.

Appendix B presents maps of the extent and topography of all regional modeling units (RMUs).

Appendix C describes the hydraulic property data analysis.

Appendix D contains precipitation station data.

Appendix E contains literature ET data, including a compilation of phreatophyte rooting depths, ET station data, and the data analysis conducted to derive potential evapotranspiration (PET) rates.

Appendix F contains the details of the groundwater ET and interbasin flow volume calculations, including the ET and precipitation rates used in the analysis, the groundwater ET volume calculations, and the details of the Monte Carlo simulations conducted to estimate the uncertainty of groundwater ET and interbasin flow estimates.

Appendix G presents the relevant spring discharge data and an analysis of the geothermal gradient for the study area, which was used to derive initial estimates of the springs' source depths.

Appendix H provides additional information in support of interbasin flow estimates.

Appendix I describes the recharge and groundwater budget calculations using the Excel® Solver.

2.0 Study Area Description

The study area for the conceptual model was selected to encompass the five project basins and other neighboring basins (Figure 2-1). Each project basin is described in SNWA (2008a). This section provides a general overview of the physiographic setting, climate, soil and vegetation, geologic setting, groundwater flow systems, and land and water-use status of the study area.

2.1 Physiography

The study area is located within the Basin and Range Province described by Fenneman (1931) (Figure 2-1) and consists of a series of parallel to subparallel, north-trending mountain ranges separated by elongated alluvial valleys. According to Rowley and Dixon (2000), this region has undergone the most severe structural extension of the continental crust of any location in the world. The alluvial valleys are further classified by Heath (1984) as being in the Alluvial Basins Groundwater Region of the western United States. The study area is also part of the Carbonate-Rock Province of eastern Nevada and western Utah described by Plume and Carlton (1988) (Figure 2-1).

2.2 Climate

The climate within the study area is variable and influenced by the large range in latitude, variations in elevation, and the barrier provided by the Pacific mountain systems to the west, which prevents winds off the Pacific Ocean from reaching Nevada (Houghton et al., 1975). Temperatures within the study area have large daily and annual variations because the clear skies of Nevada allow for heating of the ground in the day and radiant cooling at night. Mean daily temperatures across the area (from Las Vegas to Ely) vary by approximately 20°F. Temperatures greater than 90°F are common in the summer at lower elevations, while cooler temperatures of about 30°F are experienced at higher elevations.

Precipitation in the study area varies by season and is the result of frontal systems originating in the Pacific Ocean, low pressure systems in the Great Basin, and summer thundershowers (Houghton et al., 1975). The amount of precipitation varies across the area with Ely, Nevada, receiving an annual average of 9.7 in., while Las Vegas receives an annual average of 4.4 in. (WRCC, 2008). The study area lies within the northeast, south-central, and extreme south climatic divisions defined by Houghton et al. (1975). Precipitation within each of the basins is generally least on the valley floor and greatest in the mountains. For much of the study area, annual precipitation ranges from 8 to 12 in. with the precipitation increasing with increasing elevation. Large precipitation events, mainly in the form of snowfall, are more common in the winter months in the high-elevation areas but are of short duration, and high-intensity rainfall events associated with isolated thunderstorms are common in the summer, causing flash floods in the lower elevations. These conditions have prevailed in

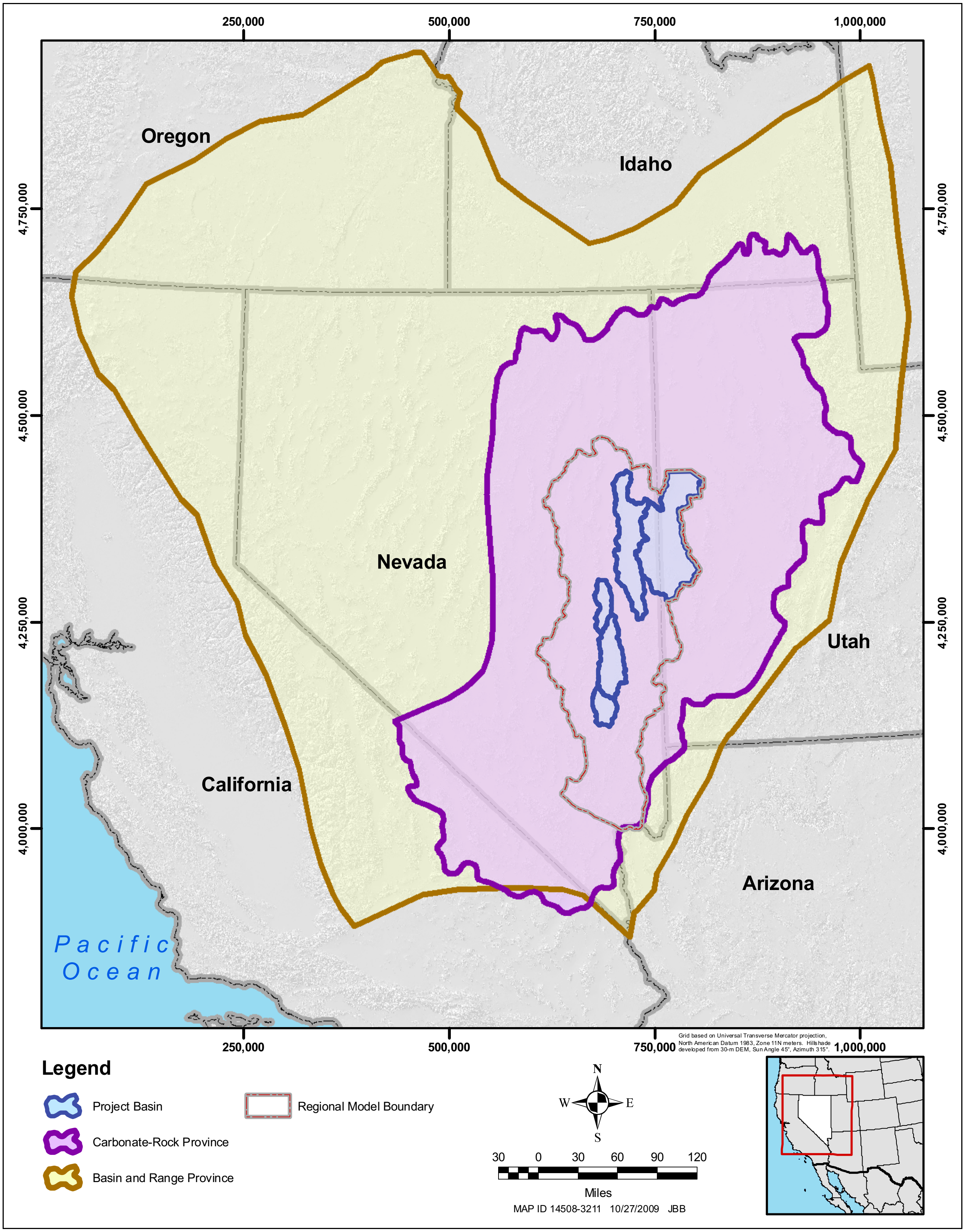

Figure 2-1
Location of Study Area within the Basin and Range Province

historic time, but during the pluvial episodes of the Pleistocene Epoch, the climate was much wetter and temperatures were 48°F to 55°F cooler (Tuttle, 1990).

Wind speed and direction are controlled by prevailing storm tracks and orographic effects induced by the basin and range topography. Evaporation rates within the study area are controlled by low humidity, abundant sunshine, and dry winds. The Las Vegas area is the warmest and driest part of the study area and has the lowest relative humidity. The annual evaporation rates range from approximately 45 to 72 in./yr (Houghton et al., 1975). Available records (Eakin, 1963a and b; Rush, 1964; Hood and Rush, 1965; Rush and Kazmi, 1965) suggest that evaporation from May through September accounts for most of the annual total evaporation in each of the valleys in the study area.

2.3 Soil and Vegetation

Generally, the basins of the study area (in the Great Basin) have thick sequences of fill material resulting from thousands of years of erosion from the surrounding mountains and volcanic activity in the area. Some of these valleys are occupied by playas (temporary lakes), which normally have a very high salt concentration as a result of evaporation.

The study area encompasses parts of the Mojave Desert and the Great Basin ecological systems. The exact boundary between the Mojave Desert and the Great Basin is vague, but the two systems can be distinguished by the occurrence of different vegetation communities and plant species.

The Mojave Desert scrub, or creosote bush scrub, is the dominant vegetation community within the Mojave Desert. The occurrence of this vegetation community is one of the main characteristics distinguishing the Mojave Desert from the Great Basin. Although, creosote bush (*Larrea tridentata*) and white bursage (*Ambrosia dumosa*) dominate this community, the Mojave Desert is a diverse landscape with a variety of other shrubs, yuccas (*Yucca spp.*), cholla (*Opuntia spp.*), and cacti.

The valley floors of the Great Basin are typical of a xeric sagebrush-shrubland community with big sagebrush (*Artemisia tridentata*) as the dominant species, which also distinguishes the Great Basin from the Mojave Desert. Big sagebrush is not typically found in the Mojave Desert. Common companions include greasewood (*Sarcobatus vermiculatus*), green and rubber rabbitbrush (*Chrysothamnus viscidiflorus* and *Chrysothamnus nauseosus*), snakeweed (*Gutierrezia sarothrae*), spiny hopsage (*Grayia spinosa*), and littleleaf and gray horsebrush (*Tetradymia glabrata* and *Tetradymia canescens*). More saline-tolerant species include shadscale (*Atriplex confertifolia*), saltgrass (*Distichlis spicata*), and winterfat (*Ceratoides lanata*). Greasewood also occurs on and around playas or in salt-encrusted soils. Riparian species, such as cottonwood (*Populus fremontii*), willow (*Chilopsis linearis*), tules (*Scirpus spp.*), and cattails (*Typha spp.*), occur within the spring complexes. The pinyon-juniper community dominates the higher elevations of the Great Basin, and the dominant trees are pinyon pine (*Pinus monophylla*) and Utah juniper (*Juniperus osteosperma*). Shrubs in this community can include snakeweed, green and rubber rabbitbrush, western serviceberry (*Amelanchier alnifolia*), various currants, and gooseberries and snowberry (*Symphoricarpos spp.*) (Mozingo, 1987).

Most of the plant groups that occupy the valley floor are referred to as phreatophytes. Phreatophytes were first defined by Meinzer (1927) as plants that are able to obtain a perennial and secure supply of water by sending their roots down to the groundwater table. This plant assemblage is composed primarily of greasewood, saltgrass, and rabbitbrush. Spiny hopsage, shadscale, and big sagebrush, although not generally considered phreatophytic, can occur within this assemblage. Phreatophytes have the ability to use both soil moisture and shallow groundwater to survive in desert environments via transpiration. ET, a combination of evaporation and transpiration of water, is a key component when estimating groundwater discharge in a basin; therefore, identifying the location of phreatophytes within a basin and quantifying their groundwater use are important when evaluating basin-water budgets.

The phreatophytic areas for each valley, including their distribution and volumes of water use, within the study area will be described in further detail in Section 7.0 of this report.

2.4 Geologic Setting

A brief description of the geology of the area, including the units present and the main structural events, is included in this section. The detailed descriptions, including maps and cross sections, may be found in Volume 1 of SNWA (2008a).

The geology of the study area is dominated by a thick sequence of Paleozoic carbonates overlying Proterozoic to early Cambrian quartzites and shales above a Precambrian metamorphic core complex. The total thickness of the Paleozoic carbonates is between 30,000 and 33,000 ft in parts of the study area (Tschanz, 1960; Tschanz and Pampeyan, 1961). Occasional shale and quartzite units are interbedded with the carbonates. Tertiary volcanic rocks are commonly found above the pre-Cenozoic sediments. These volcanic rocks erupted from several caldera complexes and are locally intruded by cogenetic plutons. Preceding, intermixed with, and postdating the volcanic rocks are volcaniclastic sedimentary units, which generally thicken toward the southern part of the model area. These Cenozoic sediments include Oligocene to Miocene limestone and Oligocene to Holocene sands and gravels. The latest depositional episode was the creation of the valley fill within the basins of the region, as those basins were formed. This valley fill is dominated by clay, silt, sands, and gravels, is of Quaternary age, and is largely in stream channels and playa areas. Three most recent episodes produced present-day topography and geologic features controlling groundwater flow. The three events are as follows:

1. The Late Devonian to Late Mississippian Antler compressive deformation resulted in a number of thrust faults and created a highland to the northwest of the study area. Erosion of the highland resulted in Mississippian shales, sands, and gravels deposited within the study area.

2. The Late Jurassic to early Tertiary Sevier compressive deformation thrust western facies Paleozoic carbonates and related sediments over eastern facies continental and near-shore sediments, most of which are Permian to Jurassic in age.

3. The Cenozoic basin-range extensional deformation began with the formation of detachment faults over uplifted areas, commonly areas of Jurassic and Tertiary plutons. These detachments continued during the volcanic episode of extension, where gaps created by extension allowed the intrusion of Tertiary magma that created the caldera complexes and

Tertiary volcanics. Following the volcanic episode, the existing basin-range topography formed because of motion along steeply dipping normal faults as the crust cooled and continued to stretch.

The Paleozoic carbonate rocks have little primary porosity and permeability but have developed secondary permeability through fractures and faults resulting from repeated folding and faulting events. Groundwater is transmitted through these openings. Some of the fractures have been enlarged by dissolution as water moves through them. The high spring discharges in parts of Pahranagat Valley, White River Valley, and the Muddy River Springs Area, as well as the cave system in Snake Valley, demonstrate groundwater movement in solution openings and fracture systems, at least locally in parts of the study area.

The primary permeability of the Paleozoic clastic and Tertiary volcanic rocks exposed in some of the surrounding mountains in the area is also very low. The rocks' transmissive properties are enhanced through secondary fracturing, which in some cases provide a network of openings through which water moves (Eakin, 1963c).

The unconsolidated sand and gravel of the valley fill in some of the valleys are capable of transmitting large amounts of groundwater. In some of the valleys where silty clay and clay dominate, however, water may be transmitted very slowly.

2.5 Groundwater Flow Systems

The basis of a flow system is interbasin flow. The first recognition of interbasin flow in the study area was documented by Mendenhall (1909) who suggested that the source of many of the desert springs in southern Nevada is from distant mountains, rather than from rainfall in the area immediately surrounding the springs. Later, Meinzer (1917) noted that, although bedrock separating the basin blocks was considered impermeable for the most part, water from a valley near Tonopah, Nevada, leaks through a mountain range into an adjacent valley. The dry playas are found in some valleys of the northern study area. The groundwater table of these dry playas is well below the playa surface. Carpenter (1915) recognized that, if a basin receives recharge but has no surface discharge of groundwater, the groundwater must flow to adjacent lower basins where discharge takes place. However, many valleys receiving heavy recharge in the northern study area discharge groundwater internally through phreatophytic ET. In addition, it is also recognized that, at depth, some amount of water following a groundwater gradient and permeable section flows from this basin to the lower basins.

Five groundwater flow systems are entirely or partially within the study-area domain (Figure 2-2 and Plate 1). These flow systems are finite three-dimensional bodies, bounded by the top of the saturated zone at the top, low hydraulic-conductivity geologic units at the bottom, and variable hydrogeologic features, corresponding to the hydrographic-area boundaries of the peripheral basins, on the sides. Flow into or out of the flow systems may occur through any of the boundaries. As will be discussed in Section 5.0, the boundaries of the flow systems in the study area are subject to interpretation. The five flow systems, as depicted in Plate 1, have been interpreted for this study to support the simplified version of the conceptual model. Most of the flow system boundaries, but not all, correspond to the

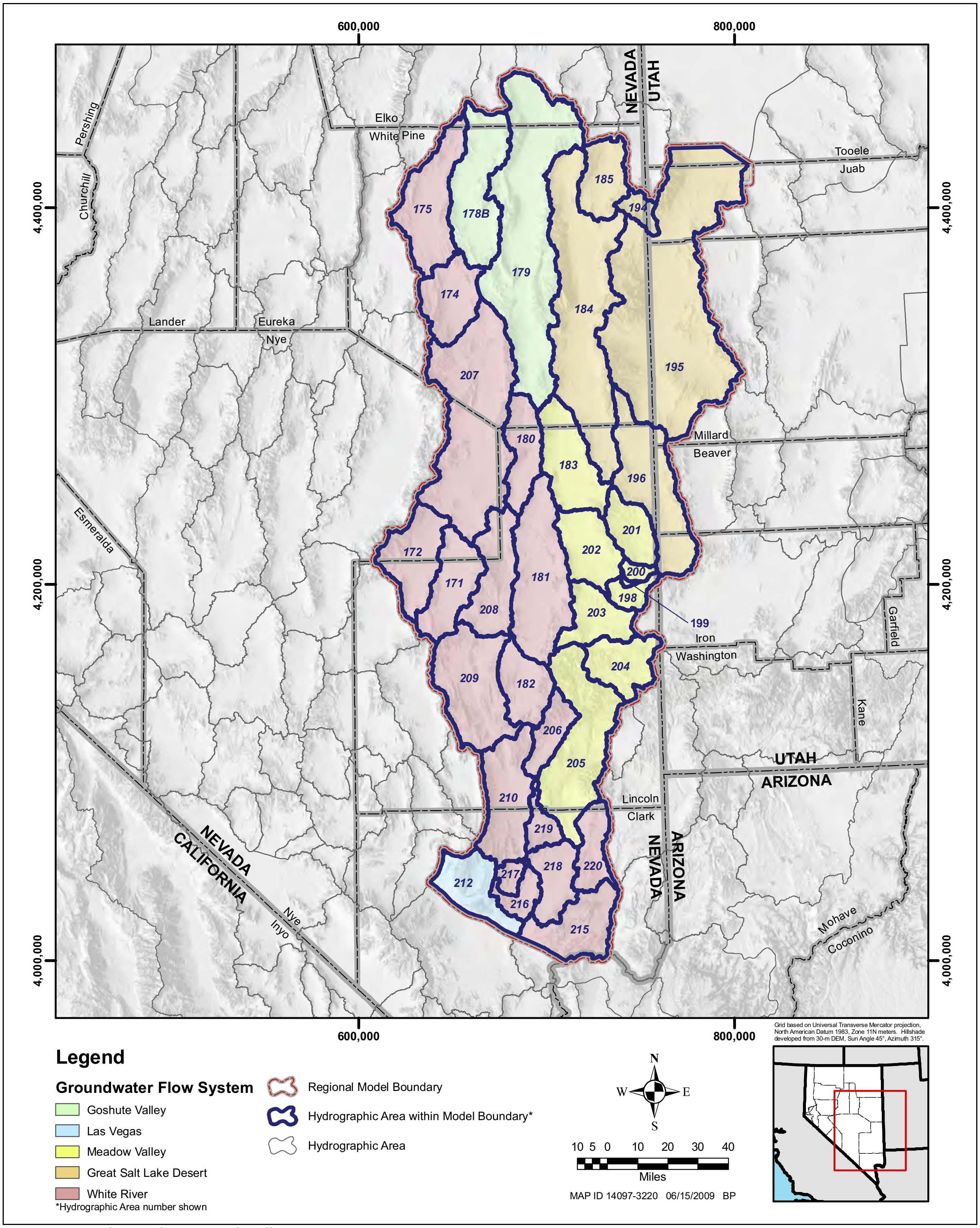

Note: See Plate 1 for more details.

Figure 2-2
Regional Flow Systems within Study Area

interpretation of Harrill et al. (1988) in U.S. Geological Survey Hydrologic Investigations Atlas HA-694-C. These flow systems are as follows:

- Goshute Valley Flow System (GVFS)
- Great Salt Lake Desert Flow System (GSLDFS)
- Las Vegas Flow System
- Meadow Valley Flow System (MVFS)
- White River Flow System (WRFS)

The top boundary of the flow systems of interest is assumed to correspond to the top of the saturated zone, not including perched groundwater. In general, recharge occurs at the higher-altitude areas of the top boundary (mountains), and discharge occurs at lower-altitude areas of the top boundary (the valley bottoms). Water from precipitation recharges the system through the top surface as direct infiltration of precipitation on the mountain block or as infiltration of mountain-front runoff on the alluvial aprons and valley bottoms. Groundwater discharges from the flow systems through the top boundary via evaporation from open water bodies fed by groundwater and/or by groundwater ET.

The bottom boundary of the flow systems is assumed to correspond to that part of the flow systems where groundwater flow is either unlikely or negligible. For this study, a depth of -10,000 ft amsl was selected as a cutoff for the bottom of the flow systems. The resulting flow domain includes most of the aquifers occurring within the study area. Some deep portions of the carbonate aquifer were cut off in some areas. This simplification should not affect the model of regional flow because this depth most probably represents the maximum depth of groundwater circulation; at depths greater than 10,000 ft amsl, groundwater circulation is unlikely. Others have used similar cutoff depths to represent the bottom of groundwater flow models in this region. For example, Faunt et al. (2004) used a cutoff depth of -4,000 m amsl (-13,000 ft amsl) in the model of the Death Valley Regional Flow System (DVRFS) (in Faunt et al., 2004). DOE (1997) used the same cutoff value of -4,000 m amsl in its regional model of the Nevada Test Site (NTS), an earlier version of the DVRFS model. This cutoff depth was supported by low estimates of horizontal hydraulic conductivities extrapolated from relationships of hydraulic conductivity versus depth (IT, 1996). IT (1996, n.p.) states "for depths of 3,000 m and more, the extrapolated hydraulic conductivity (K) values are less than 10^{-7} m/day, which are representative of virtually impermeable media."

Under ideal conditions, the lateral boundaries of the flow systems should correspond to natural hydrologic boundaries. This may be feasible for small local flow systems where the boundaries may be identified by aquifer testing, but it is not feasible for large flow systems such as those underlying the study area. In this case, the lateral boundaries of the groundwater flow systems of the study area (Figure 2-2) were generally selected to correspond to hydrographic-area boundaries. An exception is the southern end of the western boundary where the flow system was extended to the Las Vegas Valley Shear Zone (LVVSZ), including a portion of Las Vegas Valley. The LVVSZ is considered to be impermeable to transverse groundwater flow. A preliminary identification of permeable boundary segments was reported in SNWA (2008a). The locations of the permeable boundary segments were revised and finalized during the estimation of annual lateral boundary flow volumes, which are described in Section 8.0.

2.6 Land and Water-Use Status

Current land-status patterns in the study area are shown on Figure 2-3. Population density of the area is very low, so urban and commercial land uses are very limited. Over 90 percent of the land in the study area is owned by the Federal government through the Department of Interior bureaus; private ownership accounts for less than 4 percent. Irrigation cropland and rangeland are the two largest land-use activities in the area and occur predominantly in the valley bottoms. Cropland irrigation is mostly undertaken around the communities while rangeland activities are spread throughout the valleys on both government-owned and private lands.

According to the Nevada State Engineer (Smales and Harrill, 1971), the first major water use in Nevada coincides with the mining boom starting in 1849. Most of the water was diverted from streams to nearby mills to process the mining ores. Some water was used for irrigation purposes to support the mining community. From 1849 to 1860, the mining community was the main water user in Nevada. The livestock industry began in Nevada around 1870. Irrigation by surface water to produce forage crops began to increase starting then. Water use continued to expand in Nevada with the building of dams and reservoirs starting in 1903. Major water needs continued to be satisfied by surface water up to the early 1940s when the state began experiencing notable growth. At that time, groundwater use became more significant. However, prior to that time, by 1937, Boulder Dam (now Hoover Dam) had been completed, and Lake Mead had been filled. Spring flow records at the Muddy, Rogers, and Blue Point springs indicate that filling the lake has not significantly affected the majority of the flow system of the study area. Thus, although Lake Mead is man-made, approximate predevelopment conditions are assumed to prevail up to 1945 and include Lake Mead.

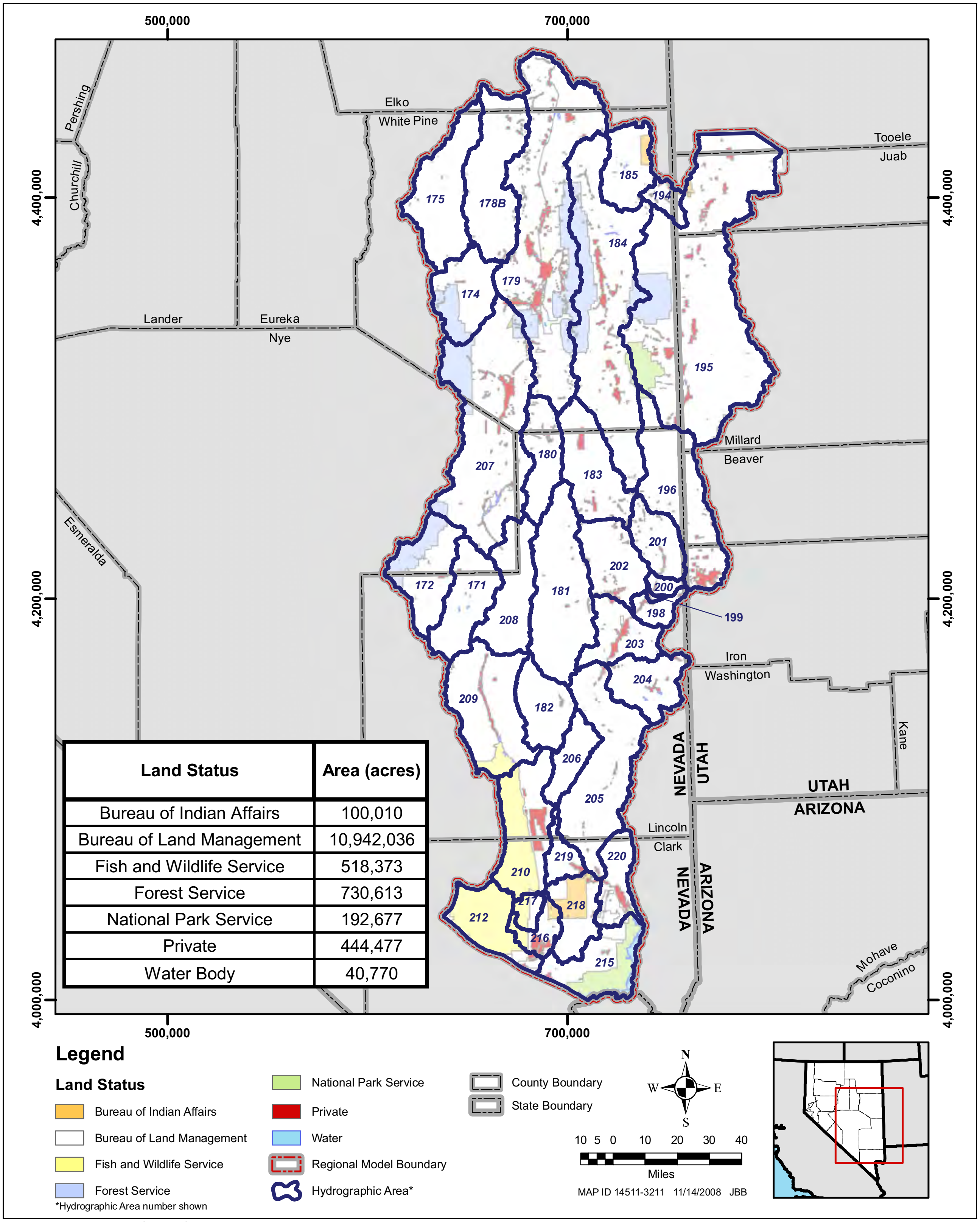

Land Status	Area (acres)
Bureau of Indian Affairs	100,010
Bureau of Land Management	10,942,036
Fish and Wildlife Service	518,373
Forest Service	730,613
National Park Service	192,677
Private	444,477
Water Body	40,770

Source: NDWR (2007)

Figure 2-3
Land-Status Patterns within Study Area

SE ROA 50380

JA_15781

This Page Intentionally Left Blank

3.0 Technical Approach

A description of the technical approach used to develop the groundwater flow model is presented in this section. The general approach is described first, followed by the approach used for developing the conceptual model.

3.1 General Approach

The general approach for the model development consisted of the following steps:

1. Development of a three-dimensional conceptual model for the flow systems of the study area, including estimates of groundwater-budget components (e.g., precipitation, recharge, groundwater discharge by ET, and interbasin inflow and outflow).

2. Development of a numerical model for the flow systems of the study area, including:

   - Construction of the numerical model based on the conceptual model.

   - Calibration of the numerical model to predevelopment steady-state conditions and transient conditions that span from 1945 to 2004.

3. Simulation of alternate groundwater development scenarios using the transient numerical model to evaluate:

   - Effects of proposed pumping.
   - Cumulative effects of historical groundwater use and proposed pumping.

The approach followed to develop the conceptual model (Step 1) is described in the remainder of this section. The specific approaches followed to complete Steps 2 and 3 are described in the corresponding reports (SNWA, 2009a and b) that document the CCRP model development and use (see Section 1.3.1).

3.2 Conceptual Model Development

The CCRP conceptual model was developed following the standards designed for groundwater flow modeling by the American Society for Testing and Materials (ASTM, 1996). The conceptual model consists of several conceptual submodels, each of which describes a set of abstractions of the physical components and processes of the flow system. The conceptual submodels are based on extensive reviews of previous scientific investigations and the available geologic and hydrologic data compiled and evaluated. The conceptual submodels work together as one conceptual model to provide a simplified interpretation of the flow systems that are the basis of the numerical groundwater flow model. These submodels consist of the following:

- Simplified hydrogeologic framework
- Groundwater occurrence and movement
- Predevelopment groundwater budget
- Historical groundwater use and effects

During development of the conceptual model, an extensive effort was spent on compiling available data and collecting additional data to support the conceptualization process. These efforts, along with a summary of the conceptualization process, are described within this section. Historical groundwater use and effects are described in the numerical model report (SNWA, 2009b).

3.2.1 Data Compilation, Collection, and Evaluation

The conceptual model described in this report was based on extensive reviews of previous scientific investigations and the available geologic and hydrologic data. These investigations include detailed and reconnaissance-level geologic, hydrologic, and geochemical investigations of the project basins and adjacent basins (Figure 1-2). A summary of studies that are relevant to this study is presented in Section 1.2 and throughout this report.

Substantial data collection efforts were also completed. Data collection activities during the 2003 to 2008 field seasons included drilling and testing SNWA monitor and test wells, geologic mapping, vegetation mapping, water-chemistry sampling, depth-to-groundwater measurements, and stream flow measurements. These data augmented existing hydrologic, geologic, and chemistry databases compiled by SNWA. Additionally, data compilation and collection efforts have been enhanced through cooperative agreements between SNWA and the University of Nevada, Reno (UNR), DRI, and USGS. These agreements involve long-term monitoring of hydrologic conditions, geophysical studies, and other selected studies to evaluate groundwater discharge, water chemistry, and groundwater flow routing. These efforts are documented in various technical reports, including SNWA (2008a), and this report.

These data were evaluated to determine their quality and limitations. Data were filtered to remove poor quality and erroneous records. The final data sets were applied in data analyses completed in support of a series of geologic, hydrologic, and geochemical investigations to assess the water resources of the project basins and adjacent basins. Recent data and interpretations developed as part of BARCASS were given priority and were incorporated in the conceptual model as appropriate. The results of the data evaluation and analyses are documented in SNWA (2008a) and are summarized in this report.

3.2.2 Simplified Hydrogeologic Framework

The hydrogeologic framework was developed through simplification of the geologic framework described in Volume 1 of SNWA (2008a). The development process consisted of four steps: (1) development of a geologic framework, (2) simplification into a hydrogeologic framework,

(3) simplification into an RMU model, and (4) assignment of hydraulic properties to the RMUs and significant structures. Steps 1 and 2 are described in SNWA (2008a). The final simplification process (Step 3) consisted of grouping units based on their hydraulic properties and structural positions. The development of the simplified hydrogeologic framework is described in more detail in Section 4.0 of this report.

3.2.3 Groundwater Occurrence and Movement

Groundwater occurrence and movement were deduced from the available data, particularly the following data types:

- Simplified hydrologic framework (discussed in previous subsection)
- Potentiometric head and water-level data under natural conditions
- Locations of major surface-water features (springs and streams)
- Distributions and rates of groundwater recharge from precipitation
- Locations of groundwater ET areas under natural conditions
- Locations of interbasin inflow and outflow under natural conditions

The interpretation of groundwater occurrence and movement within the flow system of the study area is described in Section 5.0. The information used to derive this interpretation originates from many sources. Detailed information on potentiometric levels and surface water, including streams and springs, is described in SNWA (2008a). Relevant information is summarized in this report as appropriate.

3.2.4 Predevelopment Groundwater Budget

A quantitative estimate of the predevelopment water budget is very important to the development of a groundwater flow model. The estimated budget represents predevelopment, long-term, mean annual conditions and includes precipitation recharge, groundwater discharge by ET and/or springs, and interbasin inflow and outflow. Given that precipitation recharge cannot be measured directly, it must be estimated in some manner. The three principal methods to estimate recharge include groundwater-balance methods, soil-water-balance methods, and chloride mass-balance methods.

Groundwater-balance methods yield estimates of recharge by balancing the total discharge against recharge and subsurface inflows for a system. Examples of such methods include Maxey and Eakin (1949) and variations on that method, such as those converting the traditional step function to a power function. Power functions have also been developed to describe the relationship between precipitation and recharge in Idaho, India, and Arizona. Soil-water-balance methods focus on the processes that control net infiltration through the uppermost layers of surficial materials in a given area and have been used in Nevada through the development of the INFIL and Basin Characterization Model (BCM) models. The chloride mass-balance method yields estimates of groundwater recharge in arid and semiarid environments, based on annual precipitation and known chloride concentrations of precipitation and groundwater in targeted aquifers. Each of these three principal methods will be described in greater detail in Section 9.0.

For the purpose of this study, the groundwater-balance method was selected. In this method, the total recharge to the system (precipitation recharge plus inflow) is equated to the total discharge from the system (groundwater ET plus outflow), and unknown components of the budget are estimated using trial-and-error or optimization methods. The optimization method as implemented in the Excel® Solver was used in this study (Section 3.2.4.4). Groundwater ET is estimated independently and is treated as a known quantity in the groundwater-balance method. Recharge is expressed as the sum of the product recharge efficiencies and precipitation volumes over a series of discrete zones. Assuming that precipitation is known, the recharge efficiencies are the primary unknown variables in the groundwater-balance method. However, other budget components that cannot be measured or estimated with sufficient confidence (interbasin flow rates in this case) may also be treated as unknown variables in the groundwater-balance method. However, constraints derived from the information available on the unknown variables (recharge efficiencies and interbasin flow volumes) are essential to finding a reasonable solution. The process used for development of the groundwater budgets is presented in Figure 3-1.

Groundwater budgets were derived for four flow systems of the study area (GVFS, MVFS, GSLDFS, and WRFS). No separate solution was sought for the small portion of Las Vegas Valley located within the model area. Recharge for this area was calculated using the solution derived for the nearest flow system, namely the WRFS.

3.2.4.1 Spatial Distribution of Precipitation

An estimate of the spatial distribution of precipitation is needed to estimate groundwater ET and the spatial distribution of recharge. The precipitation distribution for this study was derived using the Parameter-elevation Regressions on Independent Slopes Model (PRISM) method (Daly et al., 1994, 1997, 1998, 2008). The PRISM method incorporates important physical processes and uses state-of-the-art spatial methods for determining the precipitation distributions. The precipitation distribution over the study area was extracted from the 800-m PRISM grid, and the quality of this distribution was evaluated. The distribution was integrated by hydrographic area to obtain yearly precipitation volumes for all basins in the study area, and the resulting volumes were compared to previous estimates. One-inch precipitation bands within predefined potential recharge areas were extracted from the PRISM grid for use in the Excel® Solver. Details describing the PRISM precipitation distribution are presented in Section 6.0.

3.2.4.2 Groundwater Discharge to the Surface

Groundwater discharges to the surface primarily through the process of ET and spring flow. Groundwater may also discharge to the surface directly into streams through the process of upward leakage. Estimates of groundwater ET were made using the simplifying assumption that the volume of groundwater ET discharging from a given ET area is equal to the volume of total ET reduced by the volume of precipitation on that area. Groundwater ET was estimated using two methods. Method 1 was developed as part of this study and was applied to most of the southern basins of the study area. Method 2 was used and described by Welch et al. (2008) and DeMeo et al. (2008) and was applied to all northern basins and two southern basins of the study area. These methods are presented in Section 7.0.

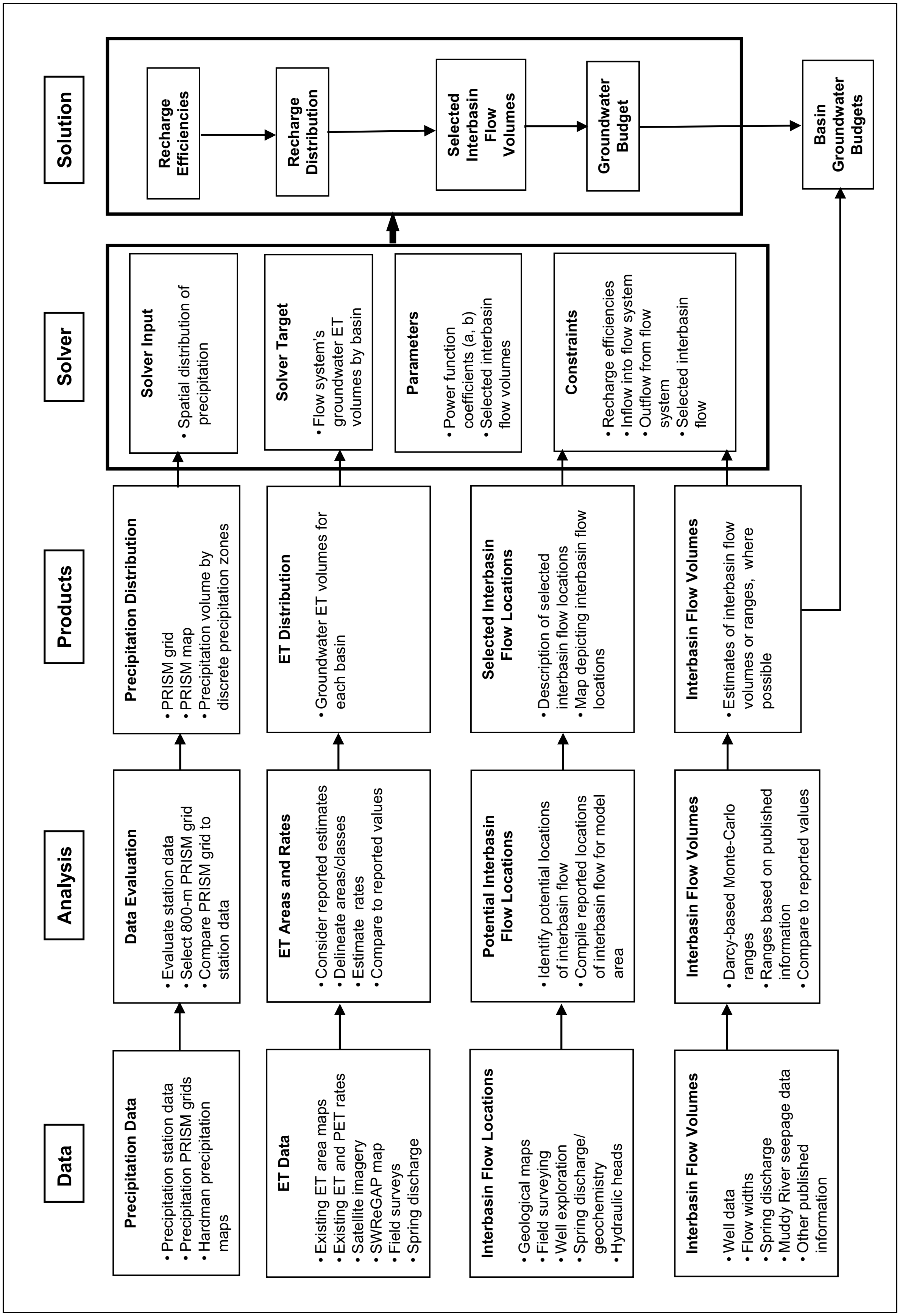

Figure 3-1
Process Used to Derive Groundwater Budgets for the Flow Systems of the Study Area

For Method 1, potential areas of groundwater ET were delineated and classified, and published ET rates were compiled and evaluated. Appropriate rates were selected, adjusted to local PET conditions, and applied to the delineated potential groundwater ET areas in each basin. The PRISM precipitation grid was then used to remove the ET associated with precipitation as the source.

For Method 2, potential areas of groundwater ET were delineated and classified similarly to Method 1 but with more detail. Groundwater ET rates were derived from the literature and/or field measurements and were multiplied by the corresponding potential groundwater ET areas to obtain estimates of annual volumes of groundwater ET.

3.2.4.3 Interbasin Groundwater Flow

Locations and volumes of interbasin flow are needed to constrain the groundwater-budget solutions. The selected flow-routing configuration, presented in Section 8.0, matches the interpretation of Harrill et al. (1988) for the most part. Flow ranges for each permeable boundary segment were estimated for each flow system. Constraints on interbasin flow volumes were developed using spring and stream flow gage records and groundwater elevations. Interbasin flow volumes across the external lateral boundaries of the model domain were estimated using Darcy's equation and Monte Carlo simulations. This method consisted of conducting multiple calculations of flux across a given flow-boundary segment to derive stochastic estimates of the flux. Interbasin flow for selected basin boundaries was also estimated by the Excel® Solver along with available information from the literature. The interbasin flow estimates are described in Section 8.0.

3.2.4.4 Recharge Estimation

The groundwater-balance method was used to estimate recharge for each flow system, using estimates of other budget components that can be measured within the bounds of reasonable uncertainty (e.g., precipitation, groundwater discharge to the surface). A relationship between recharge efficiencies and precipitation was derived that yielded a balanced groundwater budget for the flow system. This was completed using the spatial distribution of precipitation and estimates of groundwater ET and outflow previously discussed.

The groundwater-balance method was implemented using the Excel® Solver (Appendix I). The Excel® Solver is designed to find optimal solutions to numerical problems in which the main variables requiring a solution are the recharge efficiencies for a given flow system. The resultant recharge efficiencies were applied to the precipitation distribution to derive a recharge distribution. Using the recharge distribution, recharge estimates for each basin were calculated and used to develop the groundwater budget for the entire flow system and each of its basins. A different set of efficiencies was derived for each of the four flow systems in the study area.

For this analysis, it was assumed that only precipitation rates at or above 8 in./yr contribute to groundwater recharge (effective precipitation). The volume of precipitation below 8 in./yr is assumed to account for losses to soil-moisture deficits and ET (Anderson et al., 1992). The method described above was applied to each of the flow systems within the study area, except Las Vegas, and is described in detail in Section 9.0 and Appendix I.

4.0 HYDROGEOLOGIC FRAMEWORK

The Central Carbonate-Rock Province encompasses the entire study area and provides a degree of hydraulic connectivity between the many hydrographic areas composing the flow systems of the study area. A simplified hydrogeologic framework model of the flow systems underlying the study area was constructed to support the conceptualization of groundwater flow within these flow systems. The corresponding hydrogeologic surficial map and cross sections are presented in Plates 2 and 3. The area of the hydrogeologic framework model is slightly larger than the area of the conceptual model of groundwater flow (Plate 1). This section is organized as follows:

1. Construction of hydrogeologic framework model (SNWA, 2008a)
2. Improvements made after SNWA (2008a) was published
3. Construction of simplified hydrogeologic framework model (i.e., an RMU model)
4. Description of simplified hydrogeologic units (RMUs)
5. Identification of significant structural features
6. Description of hydraulic properties

4.1 Construction of Hydrogeologic Framework Model

The construction of the hydrogeologic framework model is described in detail in SNWA (2008a). The approach consisted of developing a detailed geologic framework and then simplifying it into a hydrogeologic framework. These two major steps are summarized in the following text.

4.1.1 Geologic Framework

The available published and unpublished geologic information was collected, compiled, and reviewed by geologists with extensive mapping experience within the study area. Relevant information included geologic maps, cross sections, and reports. In addition, information derived from boreholes, geophysical studies, and geologic field work was also considered. From this information and expert interpretations, a detailed geologic framework model was developed that consists of (1) surficial geologic maps in digital form (north and south) and descriptions of the geologic units; (2) a map of the major faults in digital form and a detailed description of the history of the area; and (3) several geologic cross sections in digital form (north and south) tied into the geologic maps. Detailed descriptions of this step may be found in Volume 1 of SNWA (2008a).

4.1.2 Hydrogeologic Framework

The geologic framework was simplified into a hydrogeologic framework by combining geologic units of similar hydraulic properties and spatial extent into hydrogeologic units (HGUs), which may be classified as aquifers, aquitards, or intermediate units. The geologic cross sections were also simplified to represent hydrogeologic cross sections. The areal extent of each HGU was then defined based on the hydrogeologic maps and cross sections. The hydrogeologic maps and cross sections were also used to identify major structural features that may control groundwater flow. Detailed descriptions of the hydrogeologic framework, including a surficial map and cross sections, may be found in Volume 1 of SNWA (2008a).

4.2 Improvements Made after SNWA (2008a) Was Published

Improvements made to the hydrogeologic framework after completion of SNWA (2008a) included (1) a more detailed evaluation of the geology of the Fish Springs Range to better understand the relationship between Fish Springs and Snake Valley, (2) the addition of new gravity data for Snake Valley, and (3) the reinterpretation of major structural features in the southern basins. These improvements were incorporated into the simplified hydrogeologic model described later in this section.

4.2.1 Detailed Hydrogeology of Fish Springs Range

During the CCRP model development, the eastern boundary of the flow domain was extended to include the portion of Fish Springs Flat that comprises Fish Springs. As a result, a more detailed evaluation of the hydrogeology of the Fish Springs Range, which separates Fish Springs from Snake Valley, was conducted.

The Fish Springs Range in Utah (Plate 4) is a 5-mi-wide, 20-mi-long, north-trending, jagged horst that rises abruptly from its base at less than 4,900 ft elevation to a height of 8,500 ft. It is bounded on the west by the northern extension of Tule Valley (Stephens, 1977), which is separated by scattered, mostly unnamed low hills from north-draining Snake Valley farther west. The two valleys join each other west of the northern Fish Springs Range as they enter the southwestern end of the broad Great Salt Lake Desert (Gates and Kruer, 1981), the ultimate sink of the Great Salt Lake Desert groundwater flow system (Harrill et al., 1988).

The Fish Springs Range is bounded on the east by Fish Springs Flat (Bolke and Sumsion, 1978), which separates Fish Springs range from the Dugway Range, Thomas Range, and Drum Mountains to the east. Fish Springs Flat drains north into the Great Salt Lake Desert. Both Tule Valley and Fish Springs Flat are dominated by deposits of pluvial Pleistocene Lake Bonneville (Plate 4) (Sack, 1990; Oviatt, 1991). An east-west county line, between Juab County to the south and Tooele County to the north, passes a half mile north of the Fish Springs Range; this line is the southern end of the Dugway Proving Ground (Clark et al., 2007), a large military base. The northern end of Fish Springs Flat, largely south of the county line and the Dugway Proving Ground, contains a large (26,000 afy) (Bolke and Sumsion, 1978) spring complex consisting of Fish Springs and other springs of slightly saline water. This spring complex and discharge area, about 4.5 mi east-west by 6 mi north-south, has been set aside as the Fish Springs National Wildlife Refuge (NWR) managed by the U.S. Fish and Wildlife Service.

The Fish Springs Range is made up largely of moderately west-dipping Middle Cambrian to Middle Devonian carbonate rocks (Kepper, 1960; Hintze, 1980a and b; Morris, 1987). These rocks of the

SE ROA 50389

JA_15790

lower carbonate aquifer rest on Lower Cambrian siliciclastic (basement confining zone) rocks that are exposed only in a few places on the eastern side of the range and underlie the range. All rocks in the range are intensely faulted by north-striking basin-range faults, with the range-front faults on both sides of the range being the largest. The range-front fault zone on the eastern side is of especially large displacement, and the basin beneath Fish Springs Flat is probably at least 3,000 ft thick (Plate 4), although the exact thickness is unknown. This main north-south fault zone, which uplifted the range, is still active and has a component of Holocene and late Pleistocene movement (Black et al., 2003). This zone not only formed many youthful fault scarps but also localized the springs of the Fish Springs complex. Many of these springs are warm, indicating deep circulation of groundwater in the fractures of the fault zone. Just north of the NWR, one northeast-trending string of springs is termed Wilson Health Springs (Hintze, 1980a) because it was the site of a former commercial spa. These springs, now on the Dugway Proving Ground, include several fumaroles, whose constructional edifice of spring deposits is evident. These hot springs further document the deep circulation of groundwater, here along a northeast-striking fault zone.

North-striking attenuation faults and thrust faults are mapped in the Fish Springs Range (Hintze, 1978, 1980a and b). More importantly, east-striking, oblique-slip faults also have been mapped throughout the range (Hintze, 1980a and b). Some large displacements appear to control the small Fish Springs lead-silver mining district, formerly mined on the western side of the northern part of the range (Olivera, 1975; Christiansen, 1977). A concentrated series of such east-striking faults occurs at Sand Pass, which separates the southern end of the Fish Springs Range from the northern end of the somewhat higher and larger House Range. This east-striking fault zone makes up the Sand Pass transverse zone, first noticed by Stoeser (1993) and later recognized by Rowley (1998) and Rowley and Dixon (2001) to extend as far east as the Wasatch front and to continue west to define the northern side of the east-trending Kern Mountains of Nevada. Stoeser (1993) noted that the zone is the southern boundary for the major east-west Tintic-Deep Creek volcanic belt in Utah, which is of Tertiary age. At Sand Pass, the southern end of the Fish Springs Range is about 2 mi west of the northern end of the House Range, suggesting left-lateral offset of the ranges along the transverse zone. In addition, small intrusions are present at the pass (Chidsey, 1978). Furthermore, in contrast to the Fish Springs Range, the main bounding fault zone of the House Range is on the western side, and the rocks in the range dip east. Like the main bounding fault zone of the Fish Springs Range, the main fault zone of the House Range is a fault zone of large displacement that includes Holocene and late Pleistocene movement (Black et al., 2003); the scarp on the western side of the House Range is as imposing as that on the eastern side of the Fish Springs Range.

4.2.2 Gravity Data for Snake Valley

This subsection presents the interpretation of gravity data, not available when the Baseline Report (SNWA, 2008a) was published, collected from new stations in Snake Valley in east-central Nevada and west-central Utah (Mankinen and McKee, 2009). Analyzing gravity data helps delineate anomalies that can then be used to identify the overall shape of the basins, to provide estimates of the depth to pre-Cenozoic basement rocks, and to locate buried structures beneath the sedimentary cover.

Gravity data from the new stations were combined with previously available data and were reduced using standard gravity corrections (Blakely, 1995). The derived Bouguer gravity anomaly was adjusted by subtracting the regional isostatic field. This adjustment removed long-wavelength variations in the gravity field that are inversely related to topography. Therefore, the resulting isostatic residual gravity anomaly (Figure 4-1) is a reflection of local density distributions within middle to upper crustal levels.

The isostatic gravity field (Figure 4-1) indicates several gravity anomalies, two of which are located along the eastern boundary of Snake Valley. The largest of these two gravity anomalies occurs along most of the Confusion Range. The second one occurs along the Fish Springs Range to the north. Mankinen and McKee (2009) used the gravity inversion method derived by Jachens and Moring (1990) to estimate the thickness of Cenozoic volcanic rock and sedimentary basin fill.

Among other findings, Mankinen and McKee's (2009) analysis reflected that the maximum basin depth in Snake Valley is about 3,000 m and occurs at Snake Valley's northern end. Also, the maximum basin-fill thicknesses in Pine and Wah Wah valleys and in the Sevier Lake area are about 3,000, 2,000, and 1,000 to 1,500 m, respectively. In contrast, the Tule Valley basin is shallow with a maximum depth of about 1,000 m.

4.2.3 Reinterpretation of Structural Features in Southern Basins

Recent photogeologic interpretations and limited field work (Page et al., 2005; Scheirer et al., 2006; Scheirer and Andreasen, 2008) have provided insight into the hydrogeology of the southern part of the area. Based on this work, selected structural features were reinterpreted as significant to groundwater flow in the southern part of the study area. These features consist of middle Miocene to Holocene basin-range faults of north, east, and northwest trends. These faults are interpreted to be connected and to form a path for groundwater flow from southern Coyote Spring Valley to the Muddy River Springs Area and eventually to Lake Mead. These faults are also interpreted to have hydraulic conductivities large enough to move groundwater through this area as evidenced by the spring and stream flow in the Muddy River Springs Area. These faults constitute a structural zone from Coyote Spring Valley to Lake Mead (Scheirer and Andreasen, 2008). These faults were directly added to the simplified hydrogeologic model that is discussed in Sections 4.3 and 4.4.

4.3 Construction of Simplified Hydrogeologic Framework Model

The simplified hydrogeologic framework consists of simplified hydrogeologic units, also called RMUs, and a set of major structural features that are interpreted to directly affect groundwater flow. The simplification process consisted of grouping HGUs into RMUs based on their hydraulic properties and structural positions. The unit grouping was then applied to the surficial maps, the unit extent maps, and the cross sections. A closer evaluation and simplification of the structural features that may play a role in groundwater flow were also made.

The construction of the simplified RMU framework consisted of the following steps:

1. Simplification of HGUs into RMUs. The RMUs are the Upper Valley Fill (UVF), Lower Valley Fill (LVF), Cretaceous Plateau Sediments (Kps), Upper Aquitard (UA), Upper Carbonate (UC) and Lower Carbonate (LC), Basement Rocks (BASE), and Intrusive Rocks (PLUT). RMUs and HGUs, and their relationships to each other, are described in Table 4-1.

SE ROA 50391

JA_15792

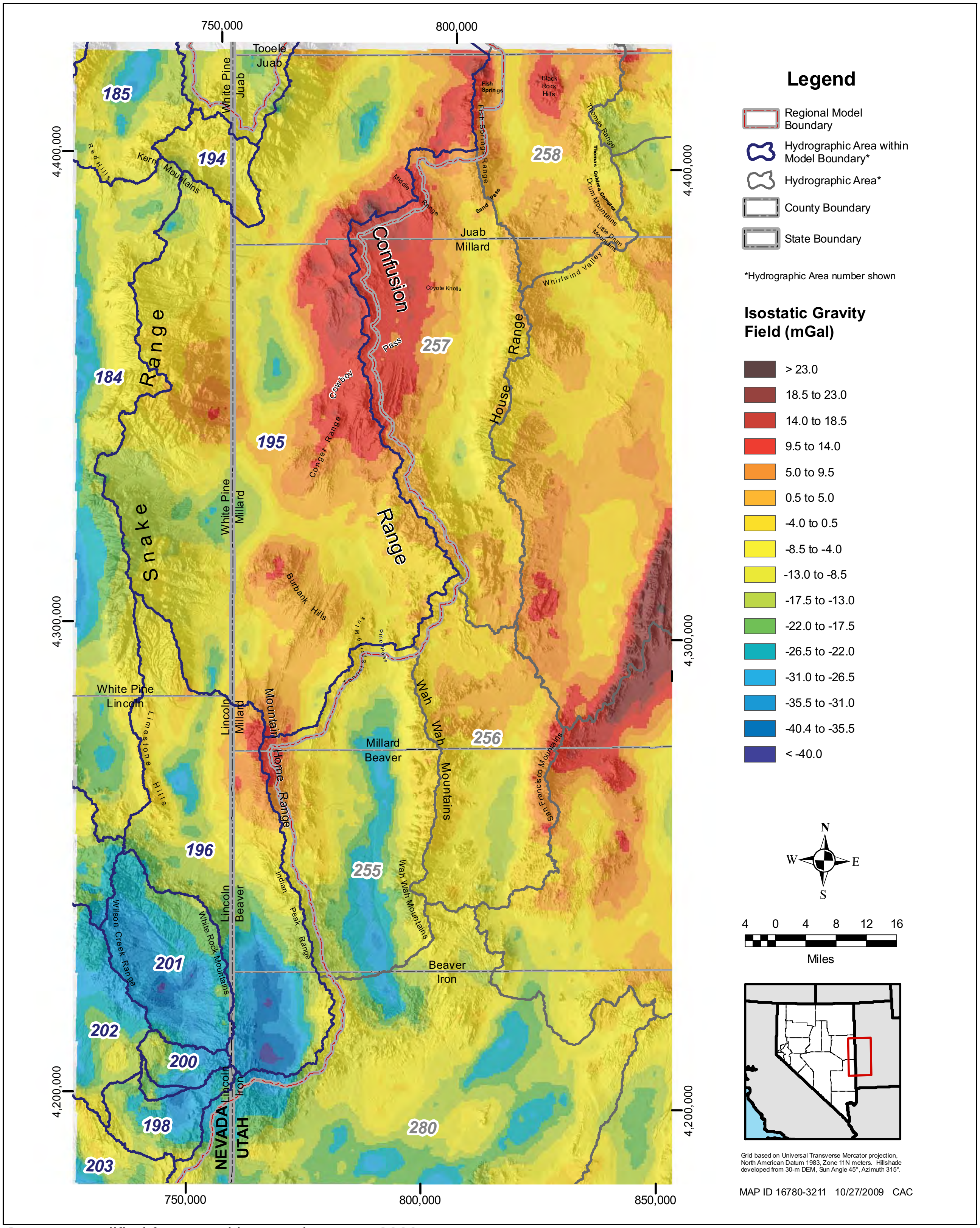

Source: Modified from Mankinen and McKee, 2009

Figure 4-1
Isostatic Gravity Field in Snake Valley and Vicinity

Table 4-1
Description of Hydrogeologic Units and Regional Modeling Units

RMU	RMU Description	HGU	HGU Description
UVF	Upper Valley Fill	QTb	Quaternary and Tertiary basalt - Quaternary and late Tertiary mafic volcanic rocks. Generally permeable but not hydrologically significant regionally because typically thin.
		QTs	Quaternary and Tertiary sediments - Includes sediments younger than the volcanic section but may include older sediments where volcanic rocks are minor or nonexistent. Also includes playa deposits. Generally moderate permeability but may be high where fractured, commonly a significant aquifer.
LVF	Lower Valley Fill	Tv	Tertiary volcanic rocks - Miocene to Eocene volcanic rocks. Good to moderate permeability, commonly a significant aquifer.
		Tos	Older Tertiary sediments - Primarily created for the cross sections; includes the older Tertiary alluvial and lacustrine section below the volcanic section. Of moderate permeability where fractured.
Kps	Cretaceous Plateau Sediments	KTRs	Cretaceous to Triassic siliciclastic rocks - Thicker where near the Colorado Plateau and generally of low permeability. More abundant in the southern part of the geologic study area. A confining unit of limited extent.
UC	Upper Carbonate Rocks	PIPc	Permian and Pennsylvanian carbonate rocks - Includes Ely Limestone, Bird Spring Formation, Park City Group, and other units. May include thin Triassic carbonate rocks in the Butte Mountains. Also includes Permian red beds, undifferentiated. A highly permeable aquifer.
UA	Upper Aquitard	Ms	Mississippian siliciclastic rocks - Includes Chainman Shale, Scotty Wash Quartzite, Diamond Peak Formation, and Eleana Formation. The Chainman Shale and Scotty Wash Quartzite are not differentiated in Lincoln County, except in the Egan and Schell Creek ranges. Where mapped, is considered a confining unit of low permeability.
LC	Lower Carbonate Rocks	MOc	Mississippian to Ordovician carbonate rocks - Joana Limestone (Monte Cristo Formation) to Pogonip Group, also includes thin Chainman Shale in most of Lincoln and Clark counties. The Pilot Shale, Eureka Quartzite, Guilmette Formation, Simonson Dolomite, Sevy Dolomite, and Laketown Dolomite are also included. A highly permeable aquifer.
		Ꞓc	Cambrian carbonate rocks - Includes the Bonanza King, Highland Peak, Lincoln Peak, and Pole Canyon formations. A highly permeable aquifer.
BASE	Basement	ꞒpꞒs	Cambrian and Precambrian siliciclastic rocks - Includes the Wood Canyon Formation, Prospect Mountain and Stirling quartzites, Chisholm Shale, Lyndon Limestone, and Pioche Shale. Generally impermeable except where fractured.
		pꞒm	Precambrian metamorphic rocks - Precambrian X, Y, and Z high-grade metamorphic rocks, generally Early Proterozoic. Also includes the Johnnie Formation in the south and the McCoy Creek and Trout Creek groups in the Schell Creek, Deep Creek, and Snake ranges. Impermeable except where fractured.
PLUT	Plutons	TJi	Tertiary to Jurassic intrusive rocks - Includes all plutons. Generally impermeable except where fractured.

Source: SNWA (2008a, Vol. 1)

The LC was further subdivided into three RMUs based on location and structural positioning within the framework. Those resulting RMUs are the LC1, LC2, and LC3. To account for the overthrown Kps unit bounding the LC at the Summit/Willow Tank Thrust fault, the Kps was subdivided into two RMUs, Kps1 and Kps2.

2. Simplification of a surficial hydrogeologic map into an RMU map (Plate 2).

3. Simplification of hydrogeologic cross sections into RMU cross sections (Plate 3).

4. Preparation of digital unit extent maps for each RMU using the surficial RMU map and the RMU cross sections. The interpretation of the unit extents were limited to a minimum thickness of 500 ft. The RMU extents were then digitized as polygons and inspected for errors. Corrections were made as necessary.

5. Development of structural contour maps for each RMU in which the contours represent the elevation of the top of the RMU. The contours were digitized as polylines and inspected for errors. With two exceptions, the structure contour maps for all RMUs were derived directly from the HGU framework. The two exceptions were the interpretations of the UVF and the surface elevations for the Kps1 (i.e., the upper unit of the Kps). The entire extent of the UVF and Kps1 units are exposed at the land surface. To ensure consistency with the land surface, the 30-m digital elevation model (DEM) was used in place of an interpretation of the land-surface elevations.

Major structural features included in the RMU model are those described in detail in the HGU model (SNWA, 2008b). They were not subjected to further simplification as were the HGUs. The only change is the addition of the structural features reinterpreted to form a conduit for groundwater flow from southern Coyote Spring Valley to the Muddy River Springs Area to Lake Mead (Section 4.2.3). A summary description is provided later in this section.

4.4 Description of Simplified Hydrogeologic Units (RMUs)

The resulting simplified hydrogeologic units, or RMUs, are described in this section. The descriptions are supported by a series of maps and cross sections. A surficial map of the RMUs showing the locations of the RMU cross sections is presented on Figure 4-2 and Plate 2. The RMU cross sections are presented in Plate 3. Maps of the extent and topography of all RMUs are presented on Figures B-1 through B-12 (Appendix B).

4.4.1 Upper Valley Fill (UVF)

The UVF RMU (Figure B-1) consists of basin-fill sediments and volcanic rocks of Miocene to Holocene age. The basin-fill sediments accumulated in down-faulted basins through erosion of the surrounding mountain ranges. Some of the minor sections of volcanic rocks deposited at the same time as the basin-fill sediments were combined with thick, interbedded, basin-fill sediments. Local thicknesses of the UVF can be more than 10,000 ft (SNWA, 2008a). The basin fill consists of boulders, gravels, cobbles, sands, silts, and clays. The UVF is considered a significant aquifer where

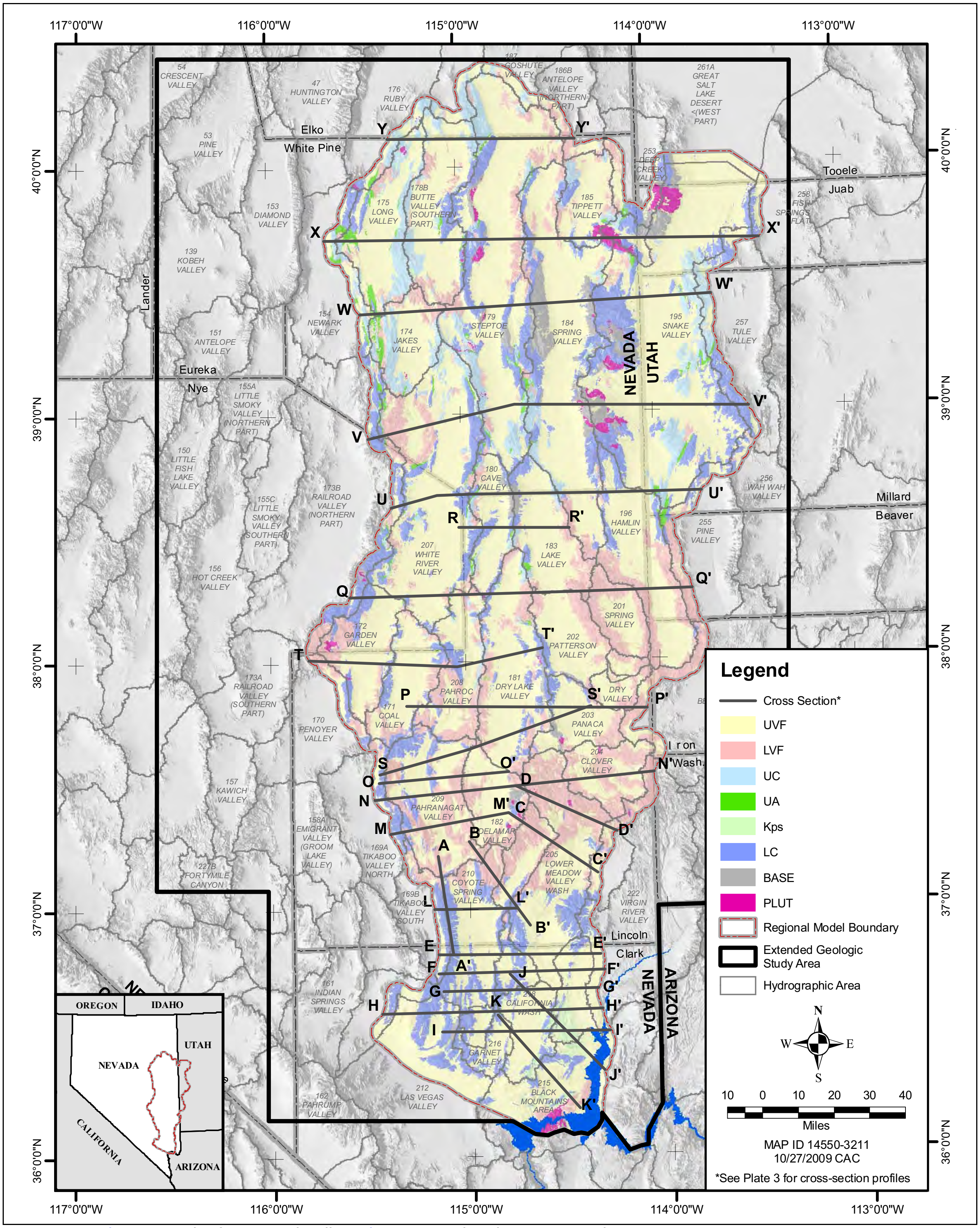

Note: See Plates 2 and 4 for more details. Plate 3 contains the cross sections.

Figure 4-2
Surficial RMU Map and Locations of Cross Sections

SE ROA 50395

JA_15796

present in the region. Generally, the sediments forming this unit are unconsolidated near the surface but become both increasingly compressed at depth as the overburden pressure increases and semi-consolidated (partially indurated). The compression of the basin-fill sediments causes their horizontal hydraulic conductivity to decrease with depth (see Section 4.6). In addition, finer-grained sediments where present within this RMU may act as confining units or aquitards (SNWA, 2008a).

4.4.2 Lower Valley Fill (LVF)

The LVF RMU (Figure B-2) consists of discontinuous Tertiary and Cretaceous sediments as well as middle Tertiary volcanic rocks. These rocks are composed of conglomerates, sandstones, siltstones, nonwelded to densely welded ash-flow tuffs, ash-fall tuffs, and lava flows. The LVF RMU occurs throughout the study area in a discontinuous manner (Figure B-2) and may behave as an aquifer or an aquitard depending on the specific types of rocks present at that location.

4.4.3 Intrusive Rocks (PLUT)

The PLUT RMU consists entirely of intrusive rocks, including granodiorites, quartz monzonites, and granites. Throughout the study area, the PLUT RMU is found sporadically, with several large irregularly shaped bodies along the eastern edge of the area. The PLUT RMU is considered an aquitard where present, although water may be transmitted through fractures (Figure B-12).

4.4.4 Cretaceous Plateau Sediments (Kps)

The Kps RMU consists of Cretaceous to Triassic siliciclastic rocks, including sandstones, siltstones, shales, and limestones of the Aztec, Chinle, Moenkopi, and Kaibab Formations, and is primarily located on the Colorado Plateau. The Kps is present in the southern portion of the study area (Figures B-3 and B-4).

The Summit/Willow Tank thrust fault causes the Kps to be split by carbonate rocks along the trace of the fault (Figures B-3 and B-4). To accommodate this geometry in the numerical groundwater flow model, the Kps was divided into an upper unit—Kps1—and a lower unit—Kps2. The Kps1 is a small-unit extent that represents the hanging wall of the Summit/Willow Tank thrust. The extent was derived by outlining where the Kps was present at the surface of the North Muddy Mountains. In addition to the Kps2's representing the footwall of the Summit/Willow Tank thrust, it also depicts the remaining regional representation of the Kps outside of the Kps1 extent. The southern portion of the Kps1 extent is bounded by the Glendale thrust fault to the west and a concealed lateral fault at the west end of the Black Mountains to the east. The remaining edges of the extent were truncated by the margins of the study-area boundary. The northern portion of the Kps2 extent is a long narrow band stretching from the southeast end of the Meadow Valley Mountains to the south edge of the Caliente Caldera Complex. A considerably smaller third piece of the Kps2 extent covers the minor Kps south of the Mormon Mountains.

4.4.5 Upper Aquitard (UA)

The UA RMU (Figure B-5) consists of Mississippian siliciclastic rocks, including quartzites and shales of the Chainman Shale, Scotty Wash Quartzite, Diamond Peak Formation, Eleana Formation, and others. The UA is predominantly found in the northern portion of the study area (Figure B-5) and is considered an aquitard where present, as indicated by its name.

4.4.6 Upper Carbonate (UC) and Lower Carbonate (LC)

The LC and UC RMUs (Figures B-6 through B-9) consist of Cambrian to Pennsylvanian carbonate rocks, including limestones and dolomites with lesser amounts of shale, siltstone, sandstone, and quartzites. The LC is present throughout the study area, while the UC is predominantly present in the northern areas.

Overthrown blocks caused by major thrust faults disrupt the LC's regional continuity. Therefore, the LC was divided into three layers: LC1, LC2, and LC3. The LC1 primarily depicts the LC affected by thrust faulting bounded by the Kps1 and Kps2 RMUs. Two components make up the LC1: a southern portion, generally affected by the Glendale Thrust fault, and a northern portion, mostly affected by the Tule Springs thrust fault that eases the LC transition between the Delamar Mountain calderas and the Caliente Caldera Complex (Plate 3). The LC2 represents the LC present at the hanging wall of the Gass Peak thrust fault. For simplicity, the entire area west of the Gass Peak thrust fault was included as LC2. Moving north along the Gass Peak thrust fault, the LC discontinuity was reduced. This allowed for the northern margin of the LC2 extent to be stopped at the Pahranagat Shear Zone (Plate 3). The LC3 is the largest piece of LC that represents the footwalls of both the LC1 and the LC2 RMUs as well as the remaining lower carbonate not affected by thrust faults.

4.4.7 Basement Rocks (BASE)

The BASE RMU consists of Precambrian metamorphic and Precambrian and early Cambrian clastic rocks. This unit is considered a major aquitard throughout the study area. It is buried deeply in most areas and constitutes the basement of the flow system in those areas (Figures B-10 and B-11).

Much like the LC, overthrown blocks of basement rock are present at the Gass Peak thrust fault. The BASE unit was separated into a Base1 unit and a Base2 unit to account for the repeating units caused by the thrusting fault (Plate 2). Base1 represents the basement rock present at the hanging wall of the Gass Peak thrust fault. The extent of Base1 is very similar to the LC1 extent with the exception of an outcrop band of basement rock in the Las Vegas Range (Plate 2). Base2 predominantly represents the regional extent of the basement rock. However, it also represents the basement rock of the footwall at the Gass Peak thrust fault. The Base2 extent covers the entire model area with the exception of areas where intrusive rocks (PLUT) exist.

SE ROA 50397

JA_15798

4.5 Identification of Significant Structural Features

Major structural features that play a significant role in groundwater flow are summarized here essentially as described for the HGU model in SNWA (2008a). The only exception is the reinterpretation of the faults in the southern part of the study area.

Major structural features in the study area were defined by identifying the fault structures and classifying them as “structurally significant” or “less structurally significant.” Structurally significant faults include faults that are clearly basin-bounding faults, faults that cause large juxtaposition of geologic units (range-front faults), faults that exhibit a large disturbance due to HGUs, and structures that have large cross-fault impedance. Less structurally-significant faults include normal faults with only minor displacements, low-angle detachment faults, and faults not necessarily defined as basin-bounding faults. Major structural features of interest are shown in Plate 2.

Among the structurally-significant features in the study area are those faults that act as conduits or barriers and control movement of groundwater flow. Examples of major structurally-significant faults in the study area are normal basin and range faults bounding or defining range fronts; strike-slip lateral faults, such as the Pahranagat Shear Zone and the Kane Springs fault zone; caldera-bounding structures, such as the Caliente caldera complex, Indian Peak caldera, and the Fortification Range caldera; and thrust faults such as the Gass Peak and Glendale/Muddy Mountains thrust faults.

Strike-slip faults are defined as faults on which the movement is parallel to fault strike. These faults can act as either conduits or barriers to flow depending on the orientation of the fault with respect to hydraulic gradients. The Pahranagat Shear Zone (Plate 2) is an example of a left-lateral strike-slip fault zone. This fault defines the southern extent of Pahranagat Valley and probably serves as a transverse barrier to southward-moving groundwater flow through the valley. This fault zone, in part, may impede southward flow (barrier) but may also divert flow laterally (conduit) to the west-southwest along the northern side of the fault zone (Rowley and Dixon, 2004).

Calderas are the result of volcanic activity throughout much of the Tertiary period. Calderas are the source of thick sequences of ash-flow tuffs and lavas with variable permeabilities. The volcanic rocks, when densely welded, are moderately to highly permeable; bedded and nonwelded tuffs display low permeabilities. These low-permeability volcanic rocks act like dams to groundwater flow. Groundwater moves through the calderas by faults that post-date the calderas’ conception. Six calderas are present in the study area: the White River Caldera; the Indian Peak Caldera Complex; the Caliente Caldera; the Narrow Canyon Caldera; the Boulder Canyon Caldera; and the Kane Springs Wash Caldera (Plate 2). The Indian Peak Caldera Complex is the largest caldera of the group and has at least four structurally-significant faults that run entirely through or just short of the caldera margin. These normal faults could provide conduits for north-south groundwater flow through the caldera (Dixon et al., 2007).

Compressive deformation events, primarily in the southern part of the study area, were a result of major thrust faulting. Blocks of older units faulted over younger units created large zones of disruption (gouge zones), and other fracture fillings formed along the thrust faults. These gouge zones may act as barriers to groundwater flow. However, with the inception of basin and range extensional faulting overprinting the thrust faults, many of the thrust faults’ influences on groundwater flow are diminished (Dixon et al., 2007). Structural stacking of part of the stratigraphic sequence by motion along the Gass Peak and Glendale/Muddy Mountains thrust faults required designation of separate hydrostratigraphic units for the formations present above and below these thrust faults as described by SNWA (2008a).

4.6 Description of Hydraulic Properties

Information on the hydraulic properties of the components of the framework model was used to support the development of the numerical groundwater flow model. Relevant information included delineation of natural zones with similar hydraulic properties, hydraulic property estimates, and hydraulic properties of major structures.

4.6.1 Natural Zonation Features

As described in SNWA (2008a, Volume 1), the hydrogeology of the study area and surrounding region is the result of three tectonic episodes and an intervening episode of extensive volcanism. Major aspects of the hydrogeology of the study area were incorporated into the hydrogeologic framework model. These included the spatial configuration of the hydrogeologic units and major structures as described in SNWA (2008a, Volume 1) and earlier in this section as part of the RMU model. However, other more detailed aspects of the hydrogeology of the study area were used to delineate natural zones of similar hydraulic properties in the numerical model, if needed during model calibration. These aspects consisted of alluvial deposition patterns in the UVF RMU and distinctive features created by the Basin-and-Range extensional-deformation episode and the volcanism episode, not accounted for in the RMU framework model.

4.6.1.1 Alluvial Deposition Patterns

The valley-fill sediments were mostly deposited by streams in closed basins with coarse-grained materials generally accumulating on the alluvial aprons and the finer materials accumulating near the center of the basins (SNWA, 2008a). Although the stratigraphy of the basin-fill sediments consists of intertonguing beds of all lithologies, the sediment deposition process created four areas of similar lithologies: playas, stream channels, alluvial fans, and valley bottoms. The boundaries of these natural zones were delineated using the following information:

- County geologic maps (Longwell et al., 1965; Tschanz and Pampeyan, 1970; Hose and Blake, 1976; Ekren et al., 1977; Kleinhampl and Ziony, 1985; Coats, 1987; Hintze and Davis, 2002a and b)
- A map of pluvial lakes (Mifflin and Wheat, 1979)
- Topography represented in the USGS DEM
- Landsat imagery

Playa deposits were identified primarily using the county geologic maps (Longwell et al., 1965; Tschanz and Pampeyan, 1970; Hose and Blake, 1976; Ekren et al., 1977; Kleinhampl and Ziony, 1985; Coats, 1987; Hintze and Davis, 2002a and b). Some of the county geologic maps, however, did not delineate playa deposits (e.g., White Pine County). As a result, a map of pluvial lakes (Mifflin and Wheat, 1979) and satellite imagery were used to supplement the county geologic maps to identify the playa deposits. The satellite maps were also used to delineate stream channel zones within the valley-fill sediments.

The boundaries of major stream channel deposits within the UVF were delineated using a combination of the groundwater ET extent map (based on satellite imagery) and the county geologic maps (Longwell et al., 1965; Tschanz and Pampeyan, 1970; Hose and Blake, 1976; Ekren et al., 1977; Kleinhampl and Ziony, 1985; Coats, 1987; Hintze and Davis, 2002a and b). A map of the National Hydrography Dataset was used to verify the locations of the identified stream channels (Simley and Carswell, 2009).

The lower boundaries of the alluvial fans were delineated from an analysis of the slope of the topography from the USGS DEM. The valley bottoms were defined as the UVF extent less the extents of the other three zones.

The delineated UVF zones are shown in Figure 4-3. The alluvial fans and stream deposits constitute the most permeable zones, and the playa deposits are the least permeable zones. The permeability of the valley bottoms is in between these two extremes. The delineated zones support the zonation of the UVF into more refined parameter zones used in the numerical model. The refined parameter zones can be used as necessary.

4.6.1.2 Basin-and-Range Extensional Deformation

The aspects of the Basin-and-Range extensional-deformation episode that can be used to delineate natural zones of hydraulic properties include the extension of the terrains that existed prior to this episode and the deep basins and mountain ranges produced during the episode.

Extensional Terrains

SNWA (2008a) described the Basin-and-Range extensional-deformation episode and explicitly incorporated the major hydrogeologic features it generated in the RMU model. These features consist of the RMU spatial distribution (extent and thickness) and major structural features, including significant faults. Other effects of this extensional episode, including smaller faults and numerous fractures, particularly in the carbonate aquifer, could not be explicitly incorporated in the framework model. However, these effects could be incorporated in the numerical model through the creation of zones of different hydraulic conductivities.

Dettinger and Schaefer (1996) have suggested that various areas of the carbonate-rock province have gone through lesser or greater degrees of extension. They describe these areas as follows:

> Regionally, in areas of extreme extension, carbonate rocks that elsewhere serve to connect and integrate flow in basin-fill and volcanic-rock aquifers have been

SE ROA 50400

JA_15801

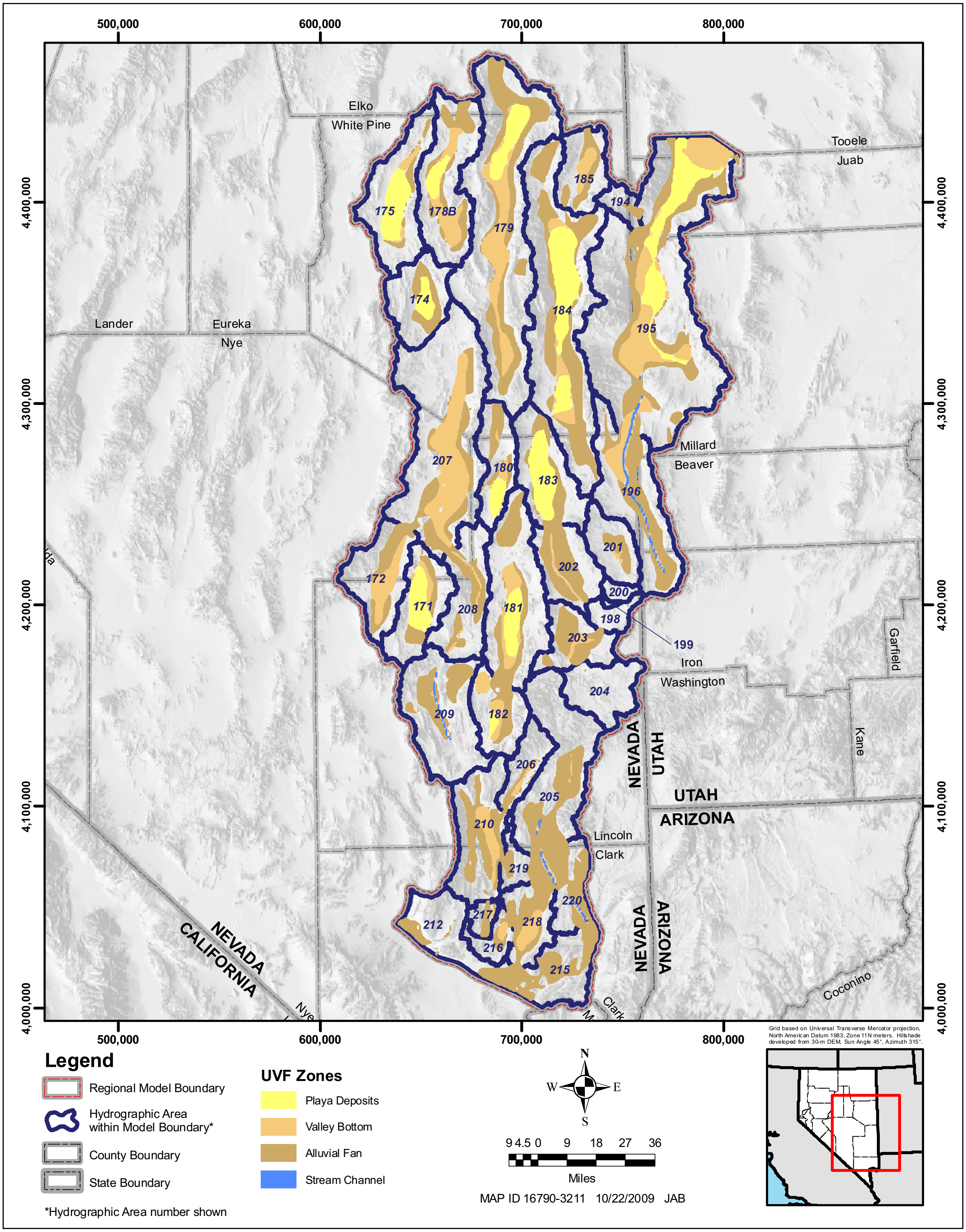

Figure 4-3
Main Alluvial Deposition in UVF Zones in Model Area

themselves extended and removed. In areas of slight extension, carbonate rocks are thick, continuous aquifers that allow for broadly integrated flow.

Figure 4-4 shows areas of slight extension and extreme extension as interpreted by Dettinger and Schaefer (1996) within the study area. These authors further described the extended areas as follows:

> Geologic descriptions of extensional remnants in the eastern Great Basin show numerous geographic parallels between structurally extended terrain and regional ground-water flow systems. In particular, some large areas of slight extension underlie major ground-water flow systems and may connect the upgradient, recharge-rich parts of the systems with their distal, discharge areas. Other areas of slight extension are not connected to recharge areas and contain only minor or local ground-water flow systems. Areas of extreme extension generally underlie single-basin flow systems that discharge from broad areas of basin fill.

Terrain extension stretches geologic units, thereby reducing their thicknesses and causing faults and fractures to form (hammer on glass effect [SNWA, 2008a]). Brittle geologic units, particularly carbonate rocks, are more susceptible to the effects of extension. Slight extension does not significantly reduce the thickness of the geologic units but enhances hydraulic conductivities by creating faults and fractures. This means that slightly extended carbonate rocks mostly retain their original thickness but have enhanced permeability. In areas of extreme extension, the carbonate aquifer is thin and perhaps absent. Volcanics rocks and valley fill may also be thin or absent in these areas, exposing the basement rocks. It is in these areas of extreme extension that detachment faulting occurs. Thus, areas of slight and extreme extension may be translated into corresponding zones of hydraulic conductivities as follows:

- Areas of slight extension correspond to sections of thick carbonate units with generally moderate large-scale hydraulic conductivities but large transmissivities due to the relatively unaltered original thicknesses of the carbonate aquifer. Note that hydraulic conductivities may still be very large along the strike of major faults.

- Areas of extreme extension correspond to sections of thin or absent carbonates units. Where carbonate units may still be present despite the stretching, they would be thin and highly fractured and therefore have large hydraulic conductivities but low transmissivities. In areas where they are absent, the basement rocks (BASE RMU) would have been exposed by the extreme extension of the carbonate aquifer.

The extended terrains delineated by Dettinger and Schaefer (1996) for the study area are shown in Figure 4-4. The available hydraulic-conductivity values derived from aquifer tests conducted in the carbonate aquifer are posted on this map in an attempt to support the zonation of the carbonate aquifer. Unfortunately, the available data are insufficient to draw a definite conclusion. Nonetheless, it was decided to incorporate these zones into the numerical model and use them during model calibration only if necessary. Incorporating these zones into the numerical model also allowed testing of the underlying assumption that hydraulic conductivities may be different depending on the degree of terrain extension.

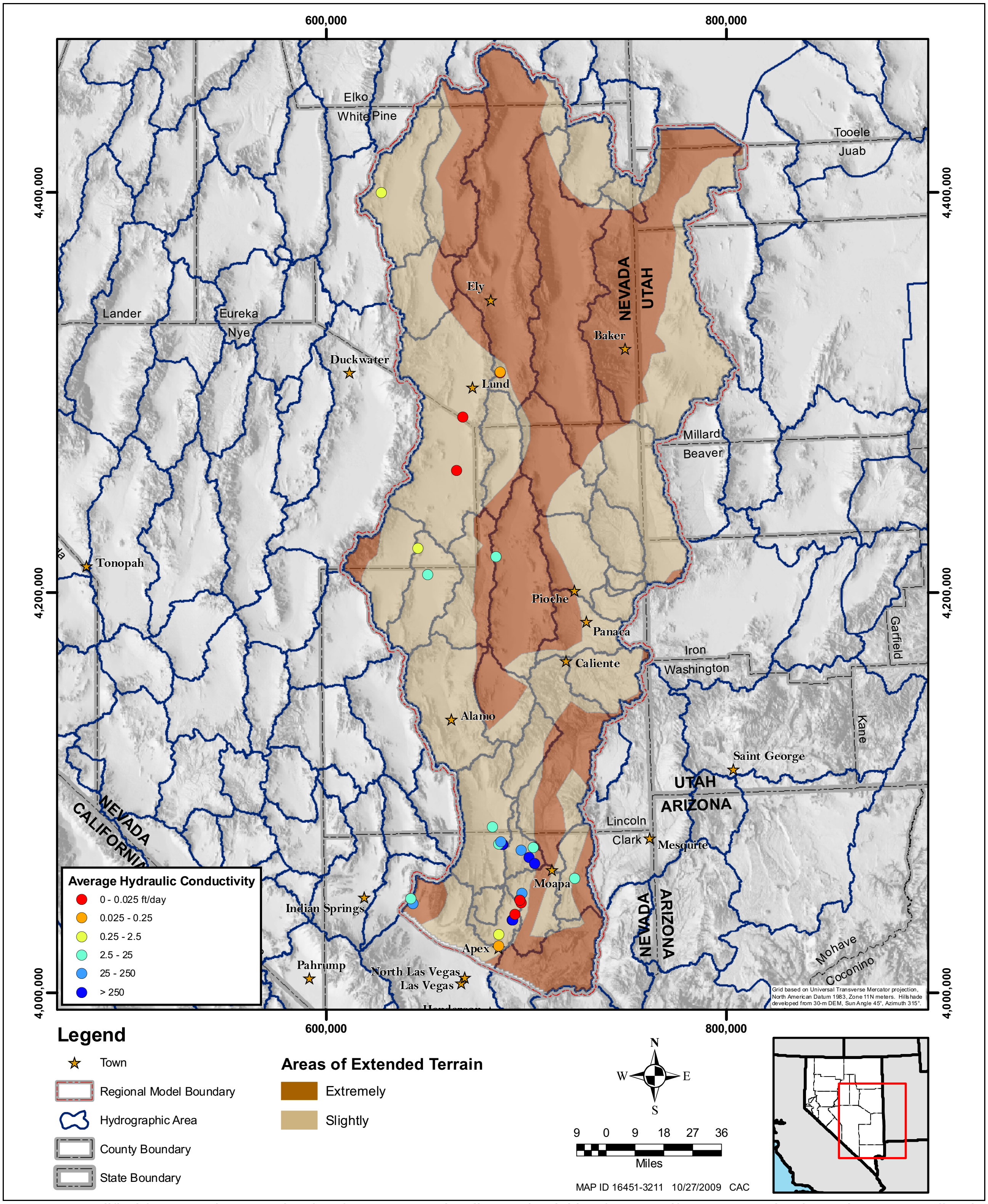

Source: Modified from Dettinger and Schaefer, 1996; Hydraulic conductivities from aquifer-property database (see Appendix C).

Figure 4-4
Extended Terrain Areas in the Region and Available Conductivity Data for the LC and UC RMUs

The study area was subdivided into three separate zones of extensional terrain: two areas of slight extension and one area of extreme extension. The resulting three zones are as follows (Figure 4-4):

- Centralized area of extreme extension
- Eastern area of slight extension
- Western area of slight extension

Structural Basins, Mountain Blocks, and Normal Faults

Mountain blocks, structural basins, moderate-displacement faults, and large-displacement normal faults are delineated in Figure 4-5. The faults not only serve as delineating lines but also constitute separate zones of hydraulic properties.

In general, the least disturbed materials are the mountain blocks. The structural basin materials in which alluvial fill accumulated are more disturbed than the mountain blocks. The moderate- and large-displacement faults (normal faults) are the most disturbed materials and generally form conduits to groundwater flow north or south along the hydraulic gradient. High-angle oblique-slip and local strike-slip faults that formed as accommodation zones during the same extensional deformation episode are also important. Normal faults are interpreted to be zones of increased hydraulic conductivity along the strike of the normal faults if the fault is parallel to the direction of flow. In areas where the fault zones are perpendicular to the direction of groundwater flow, the amount of flow across the fault zone may be limited but not completely inhibited by gouge (SNWA, 2008a). Some faults may act as conduits in the north-south direction but may also act as barriers to east or west groundwater flow. In some cases, a series of faults may be linked together to form a pathway for groundwater flow. Such is the case for a series of faults located in the southern part of the study area discussed in Section 4.2.3.

Sufficient hydraulic-property data are not available to prove or disprove the variability of hydraulic conductivity of the bedrock units from mountain blocks to structural basins. Data documenting the hydraulic conductivities along and across the major faults are also practically nonexistent. The zones delineated based on mountain blocks, structural basins, moderate-displacement faults, and large-displacement normal faults were incorporated into the numerical model. The zones' hydraulic properties were varied during calibration, if needed, based on the logic described above.

4.6.1.3 Hydrothermally and Thermally Altered Areas

As described by SNWA (2008a), plutonic rocks (PLUT RMU) are exposed throughout the study area. During their emplacement, the plutons were hot bodies of material that may have both thermally and hydrothermally altered surrounding rocks (SNWA, 2008a), creating metamorphic rocks. These contact-metamorphic rocks constitute regions of decreased hydraulic conductivity. These alteration aureoles (or halos) could extend to significant distances around the plutons. The size of the aureole depends primarily on the size of the pluton and probably increases with its size. This alteration is expected to affect all the RMUs except the UVF. Figure 4-6 illustrates the hydrothermally and thermally altered areas assumed to extend 1.2 mi (1.9 km) laterally around plutonic intrusions that are more than 3,281 ft (1 km) thick.

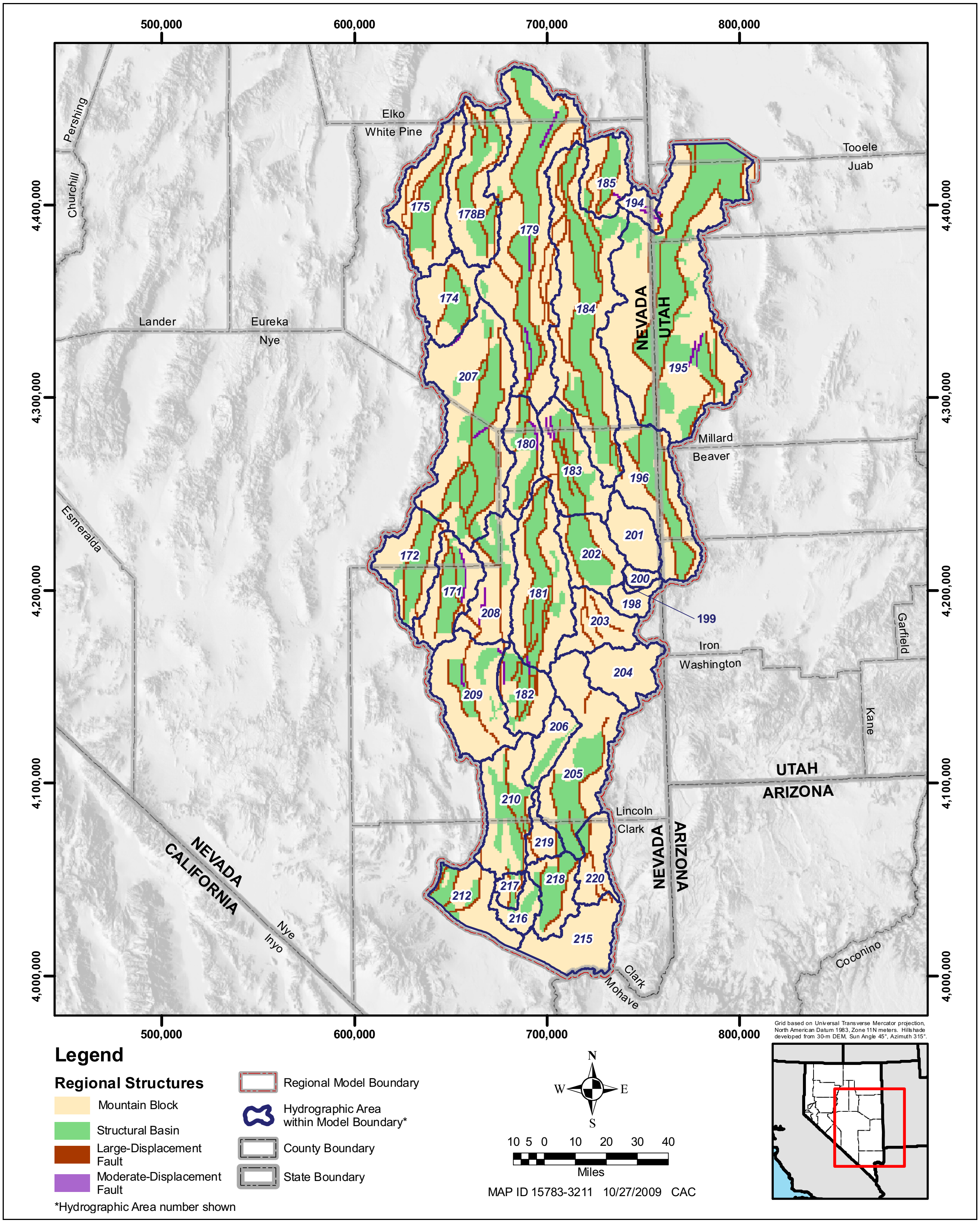

Figure 4-5
Mountain Blocks, Structural Basins, and Large- and Moderate-Displacement Normal Faults in the Study Area

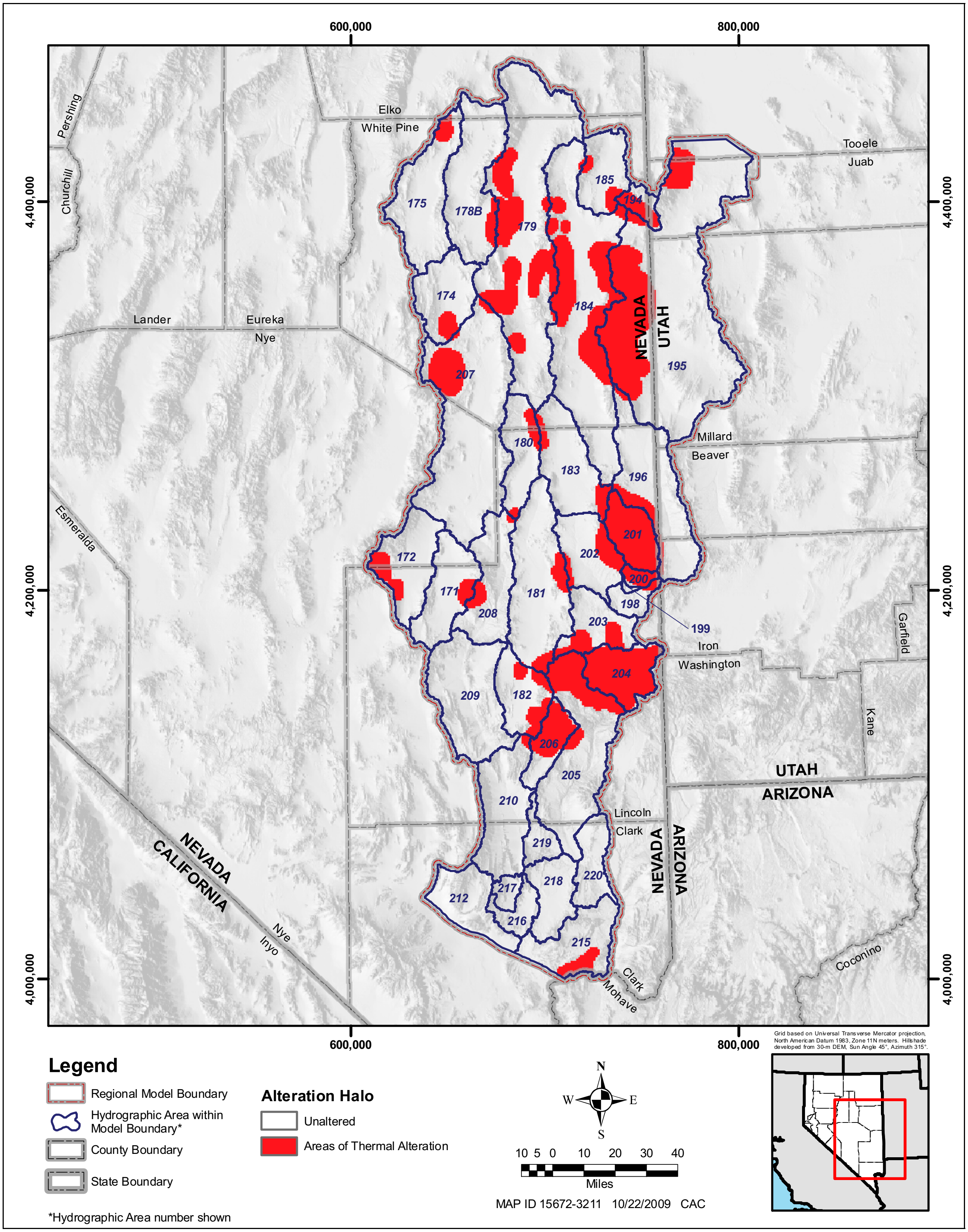

Figure 4-6
Thermally Altered PLUT RMU Areas in Study Area

4.6.2 Hydraulic Properties of RMUs

Hydraulic properties are important characteristics of an RMU, as they describe an RMU's ability to conduct and store water. Quantitative estimates of these properties are particularly important when a conceptual flow model is developed to form the basis of a numerical model. In numerical models, mean values derived from the statistical analysis of data serve as initial estimates of hydraulic-property parameters. The ranges derived from the data are used to gage the reasonableness of the simulated aquifer-property values. Estimates of hydraulic-property estimates were derived from the available aquifer-property data for the CCRP model. The data and the analysis are described in detail in Appendix C. A summary is presented in this section.

Except for preliminary data derived from the aquifer tests conducted by SNWA, reported data derived from aquifer testing were compiled from many sources and combined into a single aquifer-property database. The database was then queried to extract data for the eight RMUs listed in Table 4-1. The data set was reduced to a first subset of records, each representing a single tested interval. This was accomplished by sorting the data set by well and by interval. If an interval of a well had multiple records, the records were reduced to a single record as described in Section C.1.3.6.2 (Appendix C). The reduced data set was then statistically analyzed by RMU and by test type to derive geometric means and 95 percent confidence intervals for hydraulic conductivity. The range in values provides a measure of the uncertainty associated with the mean values. The results for all test types are provided in Section C.1.3.6.2. Statistics of the Log_{10} hydraulic conductivity derived from the constant-rate aquifer tests for most RMUs are presented in Table 4-2. The corresponding geometric means and associated 95 percent confidence intervals are also presented in Table 4-2. Constant-rate aquifer tests provide the most representative estimates of hydraulic properties for the scale of the CCRP model. For some RMUs, the estimates were derived from other test types or the literature because of a lack of constant-rate test data.

Table 4-2
Summary of Horizontal Hydraulic Conductivities for Regional Modeling Units

RMU	Log_{10} Hydraulic Conductivity (ft/day)				Hydraulic Conductivity (ft/day)				Source
	Mean	STD	95 percent CI[a]		Geometric Mean	STD	95 percent CI		
			Lower	Upper			Lower	Upper	
UVF	1.07	1.15	-1.18	3.32	11.75	14.13	0.066	2,089	Constant-rate test data in Table C-1.
LVF	0.29	1.04	-1.75	2.33	1.95	10.96	0.018	214	Constant-rate test data in Table C-1.
PLUT	-1.5	1.39	-4.22	1.22	0.032	24.55	6.03E-05	17	All test data in Table C-1.
Kps	-2.2	0.85	-3.87	-0.53	0.006	7.079	1.35E-04	0.30	Drill-Stem test data in Table C-1.
UC	0.73	1.24	-1.7	3.16	5.37	17.38	0.020	1,445	Constant-rate test data in Table C-1.
UA	-1.24	1.52	-4.22	1.74	0.058	33.11	6.03E-05	55	Constant-rate test data in Table C-1.
LC	0.73	1.24	-1.7	3.16	5.37	17.38	0.020	1,445	Constant-rate test data in Table C-1.
BASE	---	---	-7.2	0.11	---	---	6.6E-08	1.3	Reported by Belcher et al. (2001).

[a]CI = Confidence interval estimated as mean ± 1.96 x STD

Hydraulic conductivity is known to decrease with depth as a result of overburden pressures that compress sediments, fractures, and faults. The reduced data set described in the previous paragraph was used to investigate the relationship of hydraulic conductivity with depth for the UVF, LVF, and LC RMUs. The base-10 logarithmic values of hydraulic conductivity were plotted against the midpoint of the open interval of a given well for each aquifer RMU. The graphs were then visually examined for trends. Data from the constant-rate aquifer tests displayed the most consistent trends and were used to derive estimates of depth-decay constants through linear regressions (Figures C-9, C-10, and C-11). The reduced, first subset of records was also used to extract and summarize the few values of vertical anisotropy that are available. Depth-decay coefficients and vertical anisotropy factors derived from the available data are provided in Table 4-3. Because the available data on the vertical anisotropy of hydraulic conductivity are few, the BLM Hydrology Technical Group recommended that a vertical anisotropy ratio within the range of 10 to 100 be used in the numerical model. This range is within the range vertical anisotropy of 2 to 100 reported by Walton (1988).

Table 4-3
Summary of Depth Decay Coefficients and Vertical Anisotropy Ratios for Aquifer RMUs

RMU	Depth Decay Coefficients[a] (1/ft)	Vertical Anisotropy Ratio[b]
UVF	0.0019	3–333
LVF	0.0005	0.5–40
UC/LC	0.0004	2–137

[a]Based on Figures C-9, C-10, and C-11
[b]Ratio of horizontal-to-vertical hydraulic conductivity

Estimates of storage properties were only needed for the aquifer RMUs, i.e., the UVF, LVF, and UC/LC RMUs. Representative estimates of these aquifer properties can only be obtained from time-drawdown data collected from observation wells in multiple-well, constant-rate aquifer tests. Such tests also provide estimates of transmissivity values at the largest scale obtainable from all aquifer test types included in the database. Thus, a second subset of records was derived from the first one by extracting records corresponding to multiple-well, constant-rate aquifer tests for only the three aquifer RMUs. Aquifer-storage data were then statistically reduced. Estimates of transmissivities were also statistically reduced from this data set. The results are summarized in Table 4-4. The transmissivity range derived for the carbonate aquifer is on the larger side because the few available aquifer tests were conducted in fault zones.

The preliminary estimates of hydraulic properties derived from the aquifer tests conducted by SNWA, as provided in Section C.1.4 as supplemental information, helped guide the numerical model calibration in the basins where these tests were performed. These estimates were, however, used with caution, as they are preliminary and may represent localized rocks or features. The available data are not sufficient to estimate hydraulic-property ranges for the natural zones described in Section 4.6.1.

Table 4-4
Ranges of Transmissivity, Specific Yield, and Specific Storage Values for Aquifer RMUs

RMU	Transmissivity (ft^2/d)	Specific Yield (1/ft)	Specific Storage
UVF	39–72,719	0.0004–0.2870	1.72E-07–3.38E-03
LVF	43–34,432	0.0020–0.0030	1.03E-07–3.44E-05
UC/LC	963–1,000,000	0.0012–0.0309	4.67E-07–1.24E-05

4.6.2.1 Data Scaling

The hydraulic conductivity of geologic formations is highly variable as evident from Table 4-2. A substantial range in hydraulic conductivity with significant standard deviations is observed within each RMU. The tables also show that there is a difference in estimates based upon the method of analysis. This difference may be related to the scale of the test or to spatial differences in the tested medium.

Hydraulic properties, such as hydraulic conductivity and transmissivity, are thought to be functions of the scale at which they are determined (Neuman, 1990). The scaling concept stems from the idea that increasing the volume of material tested increases the amount of heterogeneity of the aquifer system encountered. For example, a laboratory measurement from a core sample may not contain the fractures that may be present and observable with a multi-well aquifer test (Belcher et al., 2001). In contrast, Zlotnik et al. (2000) have concluded that the apparent difference in hydraulic-conductivity values from laboratory to field-scale tests may be the result of sampling bias instead of scale dependence. They point out that there are very few data where the different methods were applied to the same spatial domain and that aquifer properties are highly spatially variable.

Most, if not all, of the data in the aquifer-property database have different spatial domains. This difference in domains would make the determination of any scaling factor problematic. The issue of scaling of hydrologic properties is difficult and even more difficult when developing models of fractured media (National Academy of Sciences, 1996). However, modeling is, by its nature, an iterative process whereby a conceptual model is developed and tested within a numerical flow model. As additional data are acquired, the assumptions that were made in the conceptual model are evaluated, and revisions to both the conceptual and numerical models are made, if necessary (National Academy of Sciences, 1996). This iterative process may also influence subsequent decisions on the types and locations of data to be collected to improve the overall understanding of the flow systems.

4.6.3 Hydraulic Properties of Major Structural Features

Faults play an important role in hydrogeology in that they provide pathways for fluid flow (National Academy of Sciences, 1996). Faults and fractures are a major target for many economically-significant petroleum, geothermal, and water supply reservoirs as a result of their transmissive abilities. For groundwater research, perhaps the most useful studies specific to fracture flow were those of Caine et al. (1996) and Sibson (1996) because they dealt primarily with the geology of fracture flow. For purposes of groundwater flow, Caine et al. (1996) broke faults into (1) a central core zone, which was generally of low permeability across it because of gouge and foliation in clay minerals formed along the axis of fault deformation, and (2) outer damage zones on each side of the core, which were likely to be of high permeability across and along them because they consist largely of joints and small faults that are generally parallel to the core zone. Both studies pointed out that the central core zones were in many places cut by synchronous or later faults and joints, so local flow was common across them. This heterogeneity in the composition of faults leads to heterogeneous hydraulic properties with faults that tend to retard flow across (perpendicular to) them and provide conduits to flow laterally along (parallel to) them. This heterogeneity has been described for Snake Valley by Kirby and Hurlow (2005).

Early hydrologic and geologic research, primarily by the USGS, on the role of faults with respect to groundwater flow resulted from Department of Energy (DOE)-funded studies on the NTS in order to trace movement of contaminated groundwater resulting from hundreds of above- and below-ground nuclear tests (Winograd and Thordarson, 1975; Laczniak et al., 1996; Leahy and Lyttle, 1998; Rowley and Dixon, 2006). These studies, which began in the 1950s, resulted in practical as opposed to academic research findings, and many were buried from the scientific community because they were published as limited-distribution USGS Open-File Reports, owing to the tight (yearly) deadlines required by DOE. The research led to the recognition of the Death Valley regional groundwater flow system (Harrill et al., 1988; Laczniak et al., 1996; Harrill and Prudic, 1998; D'Agnese et al., 2002; Belcher, 2004). In this flow system, recharge originated in the broad, high mountains of central Nevada, and the flow terminated at springs in Death Valley.

Among the early reports issued on the Death Valley Flow System (DVFS) was the early summary by Winograd and Thordarson (1975), who noted what had become general knowledge, that some major faults in the DVFS act as hydraulic barriers (groundwater dams) that compartmentalize the lower carbonate aquifer (LCA). One such barrier identified early is the east-northeast-trending Maynard Lake fault of the Pahranagat shear zone, at the southern end of Pahranagat Valley, where southward flow is dammed and deflected west-southwest along the fault (Eakin, 1966; Winograd and Thordarson, 1975; Ekren et al., 1977; Rowley, 1998; Rowley and Dixon, 2004; Johnson, 2007). Another example is the west-northwest-trending LVVSZ, which dammed southward flow sufficiently to create a water-level difference of 600 ft between two wells that are only 3 mi apart (Winograd and Thordarson, 1975; Prudic et al., 1995).

Research at the NTS also addressed lateral (horizontal) permeability along faults, in other words, conduit flow. Winograd and Thordarson (1975, p. C29) concluded from evidence from high yields in pump tests at the NTS and in the Eureka mining district of Nevada (Stuart, 1955) that "fault zones…are locally the principal water-bearing fractures in the lower carbonate aquifer." Highly permeable fracture zones in the NTS area were discussed in greater detail by Winograd and Thordarson (1975). Winograd and Thordarson (1975) and Dudley and Larson (1976) described pathways and springs that are along buried faults in the Ash Meadows area of the Amargosa Desert. Dettinger et al. (1995) suggested that some faults may act as conduits in the carbonate aquifer. Laczniak et al. (1996) summarized the literature of work at and near the NTS, including the role that high-angle faults had in directing the flow through, then south and southwest of the NTS. They detailed high groundwater yields in wells and high hydraulic conductivity along the Carpetbag-Yucca fault zone in the early nuclear-test areas of Yucca Flat and Frenchman Flat in the eastern part of the NTS. Winograd and Pearson (1976) discussed "megachannels" along faults in the lower carbonate aquifer in Frenchman Flat. Winograd and Thordarson (1975, Table 15) proposed flow rates between 600 and 60,000 ft/yr between Frenchman Flat and Ash Meadows, the former rate presumably by porous-media flow and the latter rate presumably by fracture-dominated flow. Laczniak et al. (1996) summarized these data on the topics of barriers versus conduits along faults in the Yucca and Frenchman Flat areas. They also described more complex, more deeply buried, and more poorly known flow directed toward Oasis Valley from the later areas of underground nuclear tests at Pahute Mesa, in the northwestern NTS, that are assumed to be also along faults and fractures formed along north-trending faults.

Faunt (1997), in studying the DVFS, noted that faults in that region may be conduits or barriers to flow and that large interbasin groundwater movements must be a result of regional structures. In Faunt (1997), faults were categorized as being either preferential conduits or barriers to flow, depending on their stress field, with faults in relative tension being more likely conduits to flow while those in shear or compression are more likely to be barriers to flow. Winograd and Thordarson (1975) stated that flow through the matrix is much less than flow through the secondary openings in carbonate aquifers, with secondary openings such as fractures, faults, and solution channels or cavities. Dettinger et al. (1995) found that hydraulic tests conducted in the carbonate aquifers of southeastern Nevada indicate much larger transmissivities (25 times or more) when faults are present. In areas where the carbonate rocks have been subjected to different types of secondary processes, the transmissivities may be even larger.

Dettinger et al. (1995) indicate that the most open faults found on carbonate rock outcrops are high-angle normal faults (range-front and basin-and-range faults). These faults tend to be the most permeable because they contain somewhat less gouge than flat-lying normal faults or compressional faults. Range-bounding faults also constitute large structures in the carbonate rocks of the study area. Other types of faults have been observed to have a tendency to contain more gouge and are, therefore, most likely not as permeable. Such faults include thrust faults and strike-slip faults (Dettinger et al., 1995).

A local example of the effects faults have on fluid flow was demonstrated during the ER-6-1 multiple well aquifer test-tracer test conducted on the NTS in Yucca Flat. This test was performed to investigate groundwater flow through the LCA (Bhark et al., 2006). The aquifer test in well ER-6-1#2 began on April 24, 2004, and ran for 90 days at an average pumping rate of 523.8 gpm. Several wells, principally those completed in the lower carbonate aquifer, were used as observation wells during the test. The observation wells were located anywhere from a couple hundred feet to as much as 8 mi away from the production well and were located both along and across the north-south-trending faults within the region (Figure 4-7). Responses to pumping varied with each observation well, including a lack of response at the UE-1h well located west of the ER-6-1 site and across the Yucca and Topgallant Fault systems, a 10-day lag in response at the ER-3-1 well located northeast of the production well and across at least three major faults, and an almost immediate response at the ER-7-1 well located approximately 6 mi north of the production well (Figure 4-7). The results of the test showed that the north-south faults impact flow through the aquifer by acting as east-west barriers to flow and north-south high-permeability conduits (Bhark et al., 2006).

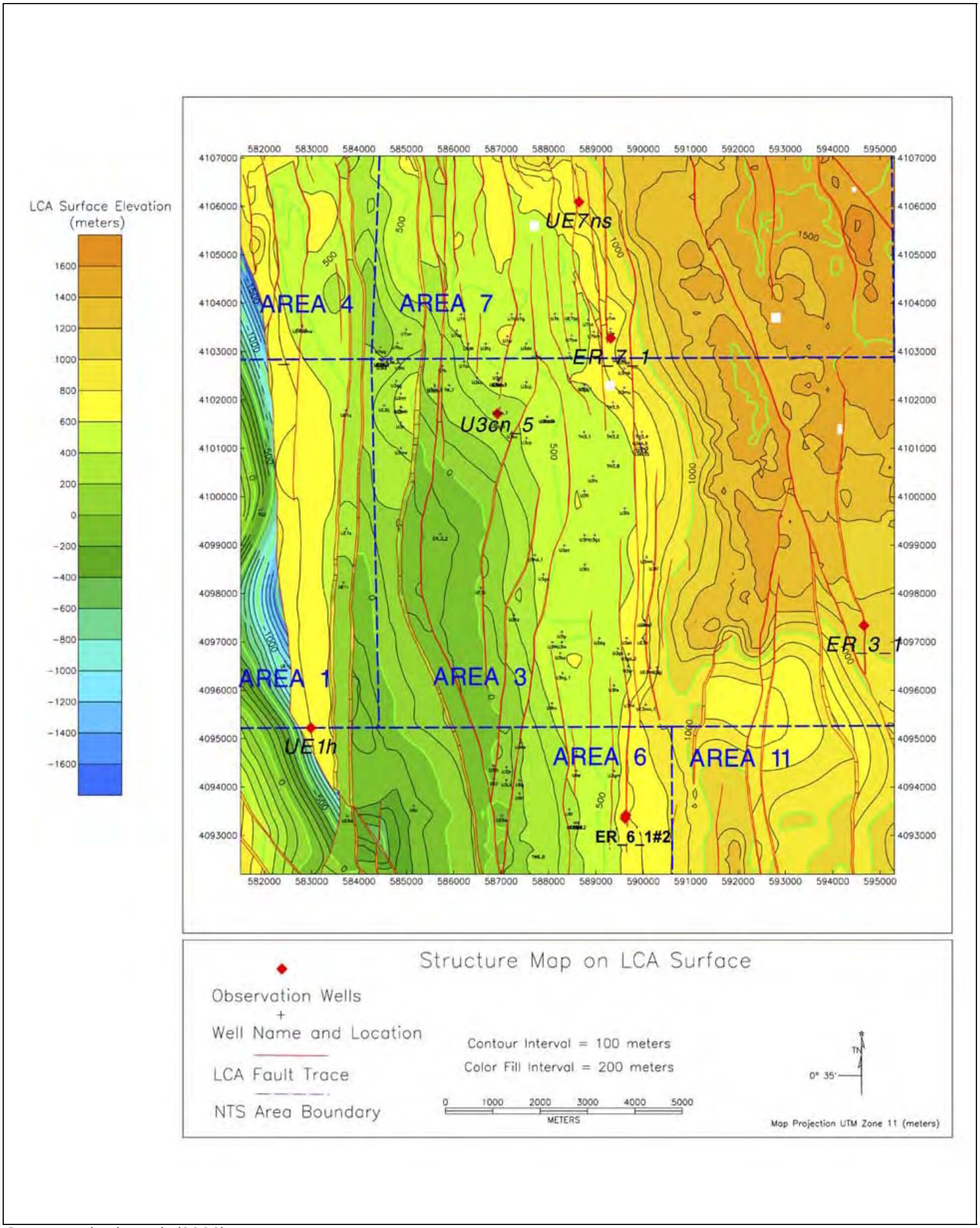

Source: Bhark et al. (2006)

Figure 4-7
Structural Features Impacting Groundwater Flow at the Nevada Test Site

This Page Intentionally Left Blank

5.0 Occurrence and Movement of Groundwater

In addition to the hydrogeologic framework, potentiometric data and locations of the major recharge and discharge areas are necessary to identify the occurrence and movement of groundwater within the flow systems of the study area. The compilation and analysis of potentiometric data are documented in Volume 4 of SNWA (2008a). The processes used to delineate the recharge and discharge areas and estimate the associated volumes are described in Sections 7.0 and 9.0, respectively. Relevant features are shown in Plate 1.

5.1 Groundwater Occurrence

Groundwater is known to occur within all the defined RMUs depending on their locations and volumes within the hydrogeologic framework model. However, only the saturated portions of the most expansive RMUs are considered to form major aquifers and to be relevant at the scale of this regional study. These RMUs include the UVF, LVF, UC, and LC. Groundwater occurring in both the UVF and LVF is termed the "basin-fill" aquifer, and groundwater occurring in the UC and LC is termed the "carbonate" or "regional" aquifer.

Although the basin-fill aquifer is discontinuous through the study area, it constitutes a major source of groundwater. This aquifer generally occurs within the valleys, between the mountain ranges, forming a series of aquifers. These basin-fill aquifers may be locally confined or semiconfined, but overall they are considered to form a major unconfined aquifer over most of the study area. Observed depth-to-water levels in the basin-fill aquifers are included in SNWA (2008a). Depth-to-water varies from above the ground surface in the discharge areas of some valleys to hundreds of feet beneath the floors of other valleys.

The carbonate aquifer is present everywhere in the study area, except where interrupted by calderas, and occurs under both confined and unconfined conditions. It is unconfined in areas where carbonate rocks crop out to the surface. The carbonate aquifer is confined in areas where a confining unit separates it from the basin-fill aquifer, as it is in the southern part of the study area where the Kps is present. In the northern part of the study area, the UC is separated from the LC by a confining unit, the UA. The LC is, therefore, under confined conditions in this area. Mean observed depth-to-water measurements in the carbonate aquifer are reported in SNWA (2008a).

5.2 Groundwater Movement

Although the general flow patterns in flow systems of the Great Basin region are understood, the flow patterns within the flow systems of the study area are subject to interpretation because of sparse data.

5.2.1 General Groundwater Flow Patterns

In general, a flow system can be subdivided into three subsystems as a function of their depth and the lengths of their flow paths. These are the so-called regional, intermediate, and local flow systems (Tóth, 1963; Freeze and Cherry, 1979) shown on Figure 5-1, as depicted by Welch et al. (2008). Welch et al. (2008, p. 38) describe the general flow patterns as follows:

> Local flow systems are characterized by relatively shallow and localized flow paths that terminate at upland springs. Local springs are low volume, tend to have temperatures similar to annual average ambient atmospheric conditions and have discharge that fluctuates according to the local precipitation. Intermediate flow systems include flow from upland recharge areas to discharge areas along the floor of the intermontane valley. Within intermediate-flow systems, springs typically discharge near the intersection of the alluvial fan and the valley floor near the range front. Intermediate-flow system springs often are of moderate volume and tend to have less-variable flow relative to local springs. Regional ground-water flow follows large-scale (tens to hundreds of miles) topographic gradients as water moves toward low altitudes in the region. Discharge from these regional flow systems manifests as large springs and, in some areas, extensive wetlands.

The maximum extent of a given regional flow system is defined by the longest flow paths between the most up-gradient recharge area and the most down-gradient discharge area. The flow system is usually named after this discharge area. The flow-system boundaries are usually selected to coincide with the hydrographic-area boundaries of the outer basins of the flow systems. The hydrographic-area boundaries coincide with the crests of the mountains, which provide most of the recharge to the flow system and typically form groundwater divides. A portion of the recharge from precipitation occurs in place on the mountain block. The remainder infiltrates through the beds of perennial and ephemeral streams located on the alluvial aprons from mountain-front runoff (Eakin, 1966; Frick, 1985). A portion of the recharge infiltrates in place within the mountain blocks, then moves through the subsurface to areas of lower groundwater potential located within the same basins (local and intermediate flow system) or other basins located down-gradient (regional flow systems). In some basins, this groundwater is forced to the surface by structural features in the form of large groundwater-discharge areas, which may include regional springs. Some of the recharge flows past the discharge areas and exits the basins via the subsurface. Water discharged from the regional springs exits the flow system through the process of ET in most basins. In some areas, however, spring discharge flows on the surface, and a portion of it exits the basins as stream discharge.

5.2.2 Groundwater Flow in Model Area

This section describes groundwater flow within the flow systems in the model area, including flow directions, flow system boundaries, and groundwater movement within each flow system.

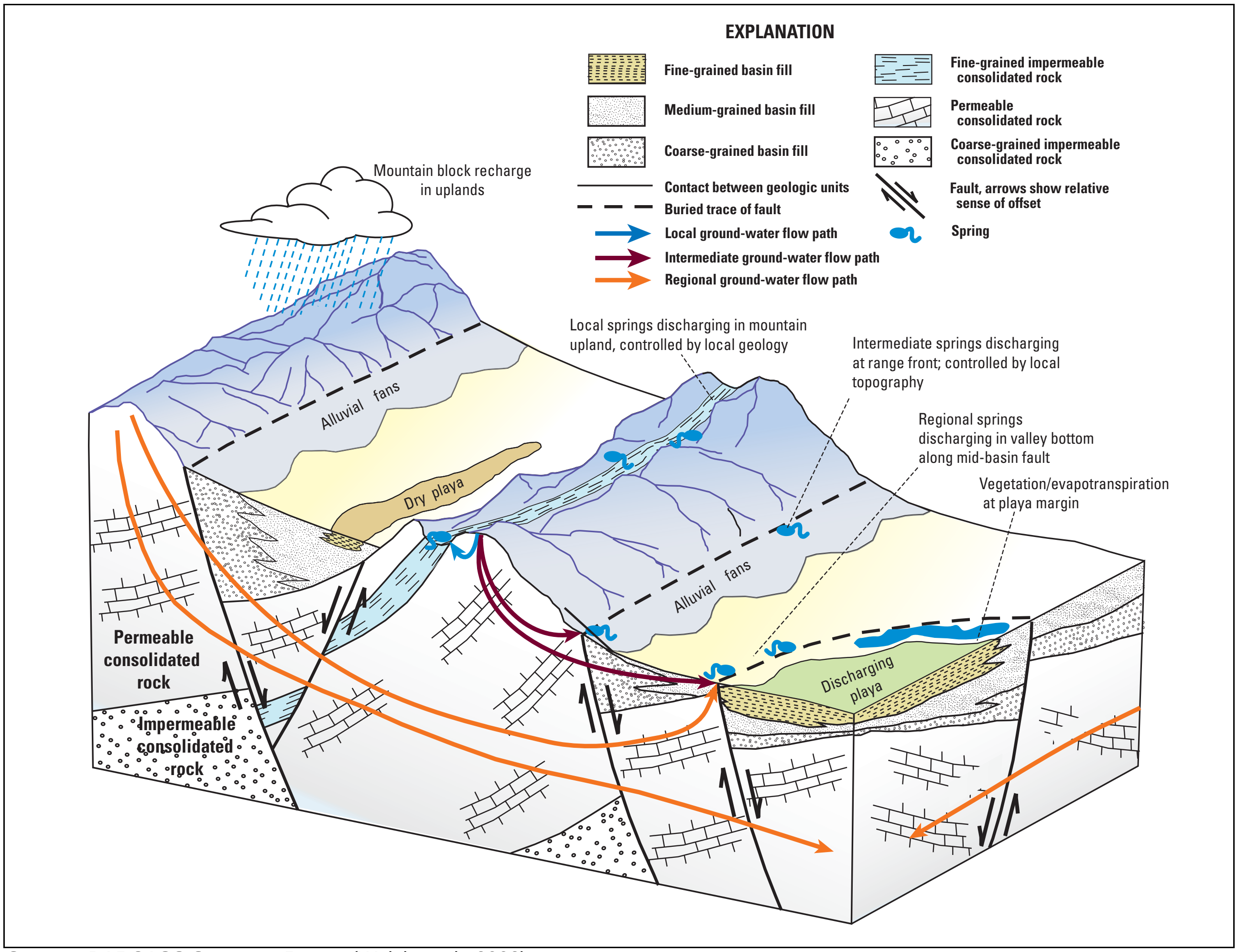

Source: BARCASS Summary Report (Welch et al., 2008).

Figure 5-1
General Conceptual Model of Groundwater Flow

5.2.2.1 Regional Groundwater Flow Directions

The northern part of the study area is higher in topography and precipitation than the southern area (Plate 1). Thus, wet valleys are found in the northern area, and dry valleys in the southern area. The study area is located in the central part of the Basin and Range Province where the extensional block faulting has produced the characteristic linear, northward-trending ranges and the intervening closed basins. The tectonic history has imprinted the rock mass with joints, faults, and fractures. Rock masses comprising such features are generally more permeable to groundwater than the rock matrix. The general direction of groundwater in the study area is from areas of both high precipitation and high topography to areas of low precipitation and topography.

Although data are available from a large number of wells in the study area, most wells are shallow and clustered in the central parts of the valleys where the water table is generally closest to the land surface. The current understanding of flow directions and quantities is constrained by the limited spatial distribution of the wells within the flow domain. The groundwater flow directions within the intermediate flow systems in the model area are interpreted to be from the mountains (zones of higher potential) to the bottoms of the valleys (zones of lower potential). Groundwater flow directions within the basin-fill aquifers were contoured from the water-level data available for wells completed in these aquifers. These maps may be found in Volume 4 of the Baseline Report (SNWA, 2008a). Groundwater flow directions within the deeper regional aquifer system are less obvious and subject to interpretation.

The available potentiometric data are insufficient to create detailed contour maps and identify definite regional flow directions. However, a simplified map of the potentiometric surface of the regional flow system was previously developed using a combination of the scarce available data, factors known to influence the potentiometric surface, and previous interpretations. This map was first presented in the Baseline Report (Figure E.1-1 in SNWA, 2008a). A modified version of that potentiometric map is presented in Figure 5-2. The available data used to develop this map (Figure 5-2) consisted of water-level elevations from 109 wells and 19 regional spring elevations. Factors influencing the potentiometric surface consist of geologic structures, topography, locations of recharge and discharge areas, and the extent of the carbonate-rock aquifer. Previous interpretations used to guide the construction of this map are those of Thomas et al. (1986), Prudic et al. (1995), Bedinger and Harrill (2004), and Wilson (2007). Due to the sparsity of the available point data, contour lines were hand-drawn at 500-ft intervals and were represented by dashed lines where uncertain or inferred. General regional flow directions have been depicted on this map by approximate arrows. Given the uncertainty associated with the regional potentiometric surface, the regional flow patterns cannot be identified with confidence in large portions of the model area (Figure 5-2). As a result, the boundaries of the flow systems are also uncertain and subject to interpretation.

5.2.2.2 Flow System Boundaries

The discussion of groundwater movement between and within the flow systems of the study area is supported by Plate 1, which depicts the five flow systems, their basins, and major groundwater features. Major features shown in Plate 1 consist of potential recharge areas (see Section 9.0), regional discharge areas including relevant springs and streams (see Section 7.0), and interbasin flow locations and directions (Section 8.0). Because of the sparsity of the available information, regional groundwater flow directions, and therefore, flow system boundaries, and interbasin flow are subject to interpretation. Thus, the initial configuration of interbasin flow used for this study (Section 8.0) was supplemented with previous interpretations. Major interpretations of interbasin flow locations and directions are shown on Plate 1 with arrows of different colors. These interpretations include those of Harrill et al. (1988) and Prudic et al. (1995) for the Great Basin; Belcher (2004) and San Juan et al. (2004) for the DVFS; SNWA (2007) for the WRFS; and Welch et al. (2008) for the BARCASS area (Plate 1). The interpretations contained in the Reconnaissance Series and those reported by Scott et al. (1971) are similar and have been incorporated and updated by Harrill et al. (1988) and were, therefore, not explicitly considered. More details about interpreted interbasin flow in the model area are provided in Section 5.2.2.2.2.

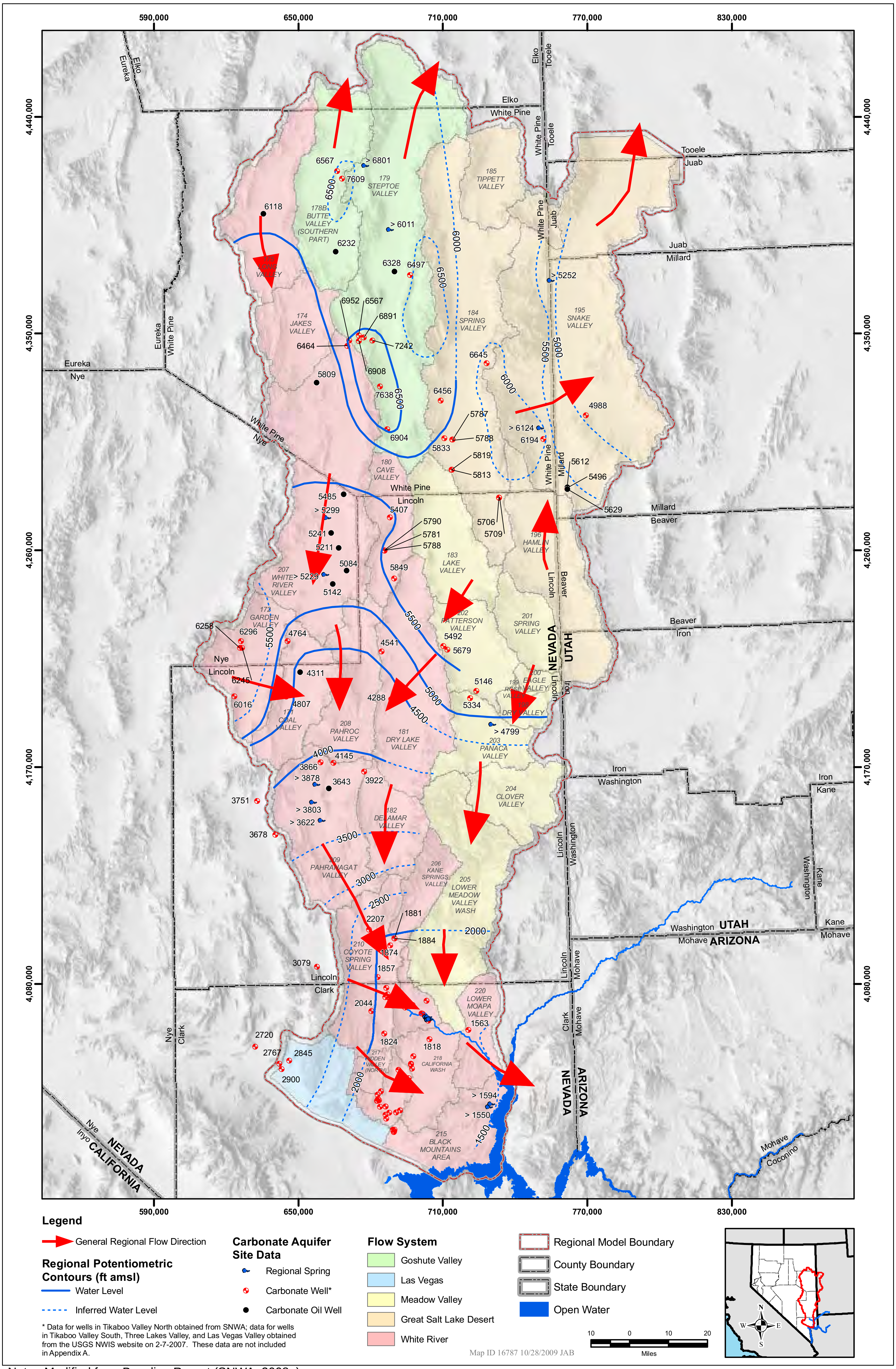

Note: Modified from Baseline Report (SNWA, 2008a).

Figure 5-2
Regional Potentiometric Map and General Regional Flow Directions

SE ROA 50418

JA_15819

5.2.2.2.1 Interpretations of Flow System Extents

As stated in Section 2.5, several flow systems have been delineated within the study area and vicinity. The primary flow systems of interest to this Project are the Meadow Valley and White River flow systems and portions of the Goshute Valley, Great Salt Lake Desert, and Las Vegas flow systems as generally depicted by Harrill et al. (1988) (Figure 2-2). A few major interpretations exist for the entire study area or substantial portions of it (Harrill et al., 1988; Prudic et al., 1995; Welch et al., 2008). The available data do not prove or disprove any of these interpretations. Summaries of the three main interpretations are presented in this section.

Harrill et al. (1988) developed an atlas of the major groundwater flow systems of the Great Basin region as part of the RASA program. The purpose of their atlas was to synthesize the information available at that time into a map report to include a discussion of regional groundwater flow and the delineation and description of major flow systems. Harrill et al. (1988) used general concepts of groundwater flow at the regional scale and the available information as of 1984. Such information included reported hydraulic heads and estimates of water budgets and interbasin flow. Their interpretations, therefore, incorporate the findings and estimates reported in the Reconnaissance Series and summarized by Eakin (1966) for the WRFS and by Scott et al. (1971) for Nevada. They combined the WRFS and MVFS into a single flow system referred to as the Colorado System. Harrill et al. state that “the Colorado and Virgin rivers act as drains at terminus of system, but most discharge occurs upgradient at discharge points of major regional subsystems” (1988, Table 1, Sheet 1). The interbasin flow directions posted on their map are shown in Plate 1 of this report.

Prudic et al. (1995) developed a conceptualization of groundwater flow within the flow system of the Central Carbonate-Rock Province of the Great Basin region, using a numerical flow model based on the USGS code MODFLOW (McDonald and Harbaugh, 1988). The model is focused on Nevada and Utah and has two layers representing the deep regional aquifer and the shallow aquifers, using equivalent porous-media aquifer properties. Based on the potentiometric levels simulated by their numerical flow model, they identified the groundwater flow directions in the two model layers (Plate 1). They also subdivided the Central Carbonate-Rock Province into several regions, which were further subdivided into subregions. The subregions approximately correspond to flow systems as defined by previous investigators. Their boundaries do not correspond everywhere. For example, the White River subregion does not include Long and Jakes valleys, ends at the Muddy River Springs Area, and extends into the classic DVFS to the west and into the MVFS to the east. Prudic et al. (1995) stress that their interpretation is conceptual in nature. They state that “although a fairly detailed analysis of ground-water will be discussed, it does not intend to indicate that the study results presented here are adequate…”(Prudic et al., 1995, p. D-15). The concept of the WRFS has been a classic example of regional flow systems.

Another interpretation of the flow systems within the study area was the one put forth during BARCASS. The volume of recharge estimated for Steptoe Valley by Welch et al. (2008) as part of BARCASS was first estimated at 168,600 afy for the period of 1971 to 2004. It was then adjusted to 154,068 afy for the period of 1898 to 2006 to represent long-term mean conditions (Flint and Flint, 2007). This adjusted estimate was used in the groundwater-budget estimates. The difference between recharge and groundwater ET, about 53,000 afy, was routed to neighboring valleys through the subsurface (Figure 5-3). About 22,000 afy of groundwater was routed from Steptoe Valley to the

WRFS (Jakes and White River valleys). About 24,000 afy of groundwater was routed from Steptoe Valley to the GSLDFS (Lake and Spring valleys) (Figure 5-3). This led to a redefinition of the boundaries of the three flow systems by placing portions of Steptoe Valley in the WRFS and the GSLDFS. This interpretation was incorporated into the current analysis through the uncertainty analysis.

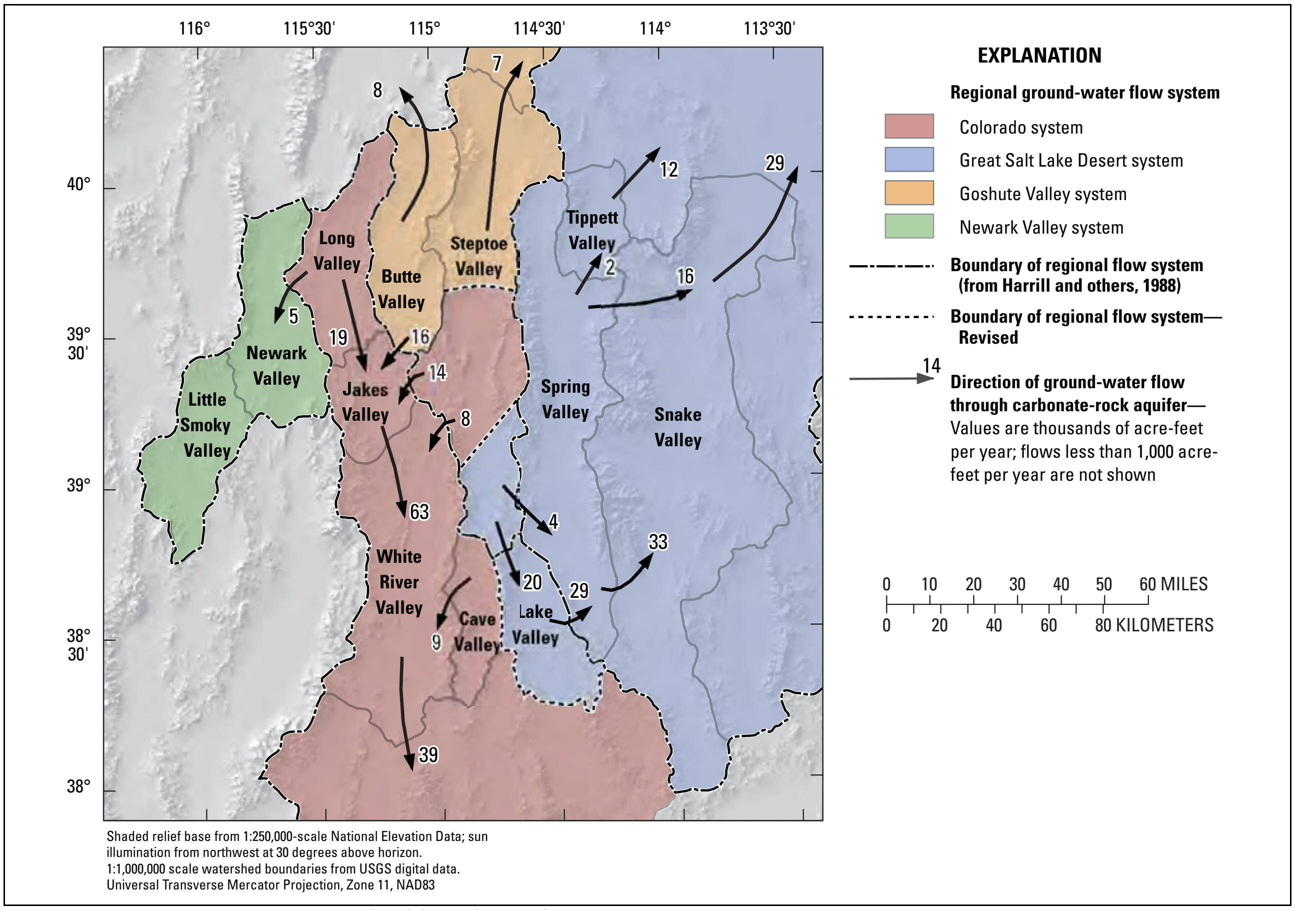

Source: BARCASS Summary Report (Welch et al., 2008).

Figure 5-3
BARCASS Interpretation of Flow Routing and System Boundaries

The flow systems delineated in the model area are approximately consistent with the interpretations of Harrill et al. (1988) (Figure 2-2). This interpretation of the flow systems is used here for illustration purposes and in Section 9.0 for purposes of deriving an initial estimate of the recharge distribution. However, because of the uncertainties associated with the available information, other interpretations of regional flow patterns, and therefore flow-system boundaries, are possible and were not dismissed in this study. They constitute alternate interpretations that were considered during the calibration of the numerical model.

5.2.2.2.2 Groundwater Movement by Flow System

Each of the flow systems in the study area is described with an emphasis on the available interpretations of interbasin flow. The discussion is supported by four maps showing the reported ranges of interbasin flow (Figures 5-4 through 5-7) and a table summarizing and providing the sources of the flow ranges (Table 5-1). Arrows of opposite directions are shown on Plate 1 and in the four figures in cases where the interpretations conflict. The detailed list of reported interbasin flow annual volumes is provided in Appendix H. Findings of selected major studies are discussed in the subsections.

Goshute Valley Flow System

Most previous investigators, such as Harrill et al. (1988), define the GVFS to include Southern Butte, Goshute, and Steptoe valleys. A portion of this flow system, as defined by Harrill et al. (1988), consisting of Southern Butte and Steptoe valleys is included within the study area (Plate 1 and Figure 5-4). Even though SNWA does not have groundwater applications in the GVFS, baseline conditions have been established to evaluate potential future changes in the groundwater system.

To the northwest, the GVFS is bounded by the Butte Mountains along the western side of Southern Butte Valley. To the southwest, the GVFS is bounded by the Egan Range along the western side of Steptoe Valley. The Schell Creek Range forms most of the eastern boundary of the flow system along the eastern side of Steptoe Valley (Plate 1). A small portion of this boundary coincides with the Antelope Range and is shared with Antelope Valley located outside of the study area. The Egan and Schell Creek ranges meet at the southern end of Steptoe Valley and form the southern boundary of this flow system. To the north, Southern Butte Valley is open to Northern Butte Valley, and Steptoe Valley is open to Goshute Valley.

The Egan and Schell Creek ranges constitute important recharge areas and are interpreted to coincide with groundwater divides along their crests (Plate 1). The available water-level data (SNWA, 2008a, Volume 4) indicate the presence of groundwater at a high altitude on the Egan Range between Steptoe Valley and Jakes and White River valleys. The data may represent perched conditions but are indicative of recharge occurrence.

Groundwater discharge by the ET process occurs in the central part of Steptoe Valley (Plate 1). Groundwater ET in this area is primarily by phreatophytes. No surface-water outflow of groundwater origin occurs from this flow system. Groundwater discharge may also occur through the subsurface. Given that the largest mountain ranges are located in the southern part of this flow system, a large amount of recharge creates a groundwater divide separating the GVFS from the other flow systems.

Regional flow directions are generally depicted from south to north (Eakin et al., 1967; Frick, 1985; Harrill et al., 1988; and Nichols, 2000) (Figure 5-2). However, significant amounts of groundwater have also been interpreted to flow to the south (Welch et al., 2008) for example. The available potentiometric data are insufficient in this area to identify definite regional flow directions. Given the uncertainty associated with the potentiometric surface, the regional flow patterns cannot be identified with certainty, and the interbasin flow for this flow system is uncertain as well. Several interpretations exist (Plate 1) and are discussed in the following text.

In a report describing a numerical flow model of the valley-fill aquifer of Steptoe Valley, Frick (1985) identified the potential locations of groundwater flow out of Steptoe Valley. They are a narrow canyon north of Currie, Connors Pass, McGill, an area 7 mi north of Gallagher Gap, Smith Valley,

Table 5-1
Ranges of Reported Interbasin Flow Volumes
(Page 1 of 2)

Location Index[a]	Interbasin Flow (afy)[b]	Sources of Extreme Values
1	22,500	Nichols (2000)
2	800 to 2,000	Scott et al. (1971); Nichols (2000)
3	M to 7,000	Harrill et al. (1988); Welch et al. (2008)
4	3,000 to 8,000	Glancy (1968); Welch et al. (2008)
5	3,000	Harrill et al. (1988)
6	2,000 to 12,000	Harrill et al. (1988); Welch et al. (2008)
7	3,500 to 29,000	Carlton (1985); Welch et al. (2008)
8	1,000 to 8,500	Harrill et al. (1988); Carlton (1985)
9	?	Harrill et al. (1988)
10	? to 18,500	Harrill et al. (1988); Carlton (1985)
11	? to 12,700	Harrill et al. (1988); Prudic et al. (1995)
12	3,600	Nichols (2000)
13	3,000	Scott et al. (1971)
14	-2,000 to 2,000	Welch et al. (2008); Harrill (1971); Harrill et al. (1988)
15	6,000	Carlton (1985)
16	25,500 to 27,000	Carlton (1985); Harrill et al. (1988)
17	4,000 to 16,000	Nichols (2000); Welch et al. (2008)
18	?	Harrill et al. (1988)
19	8,000 to 19,000	Eakin (1961); Welch et al. (2008)
20	16,000	Welch et al. (2008)
21	14,000	Welch et al. (2008)
22	5,500 to 9,000	Carlton (1985); Harrill et al. (1988)
23	8,000	Welch et al. (2008)
24	? to 700	Harrill et al. (1988); Nichols (2000)
25	15,000 to 42,000	Hood and Rush (1965); Harrill et al. (1988)
26	16,527 to 63,000	Kirk and Campana (1990); Welch et al. (2008)
27	30,000	Scott et al. (1971)
28	4,000	Welch et al. (2008)
29	-4,250 to 4,000	Harrill et al. (1988); Carlton (1985)
30	4,250 to 26,500	Harrill et al. (1988); Carlton (1985)
31	-5,500 to 16,500	Harrill et al. (1988); Carlton (1985)
32	20,000	Welch et al. (2008)
33	5,500 to 30,000	Harrill et al. (1988); Carlton (1985)
34	4,000 to 11,180	Thomas and Mihevc (2007); Kirk and Campana (1990)
35	4,000 to 33,000	Rusk and Kazmi (1965); Welch et al. (2008)
36	29,000	Welch et al. (2008)
37	10,000	Scott et al. (1971)
38	14,000 to 15,000	Eakin (1966); LVVWD (2001)
39	3,000 to 17,000	Rusk and Eakin (1963); Thomas et al. (2001)
40	9,400 to 15,000	Thomas and Mihevc (2007); Thomas et al. (2001)
41	6,400 to 40,000	Thomas and Mihevc (2007); Scott et al. (1971)
42	1,500	Carlton (1985)
43	2,000	Thomas and Mihevc (2007)
44	M to 15,000	Scott et al. (1971); Thomas et al. (2001)

Table 5-1
Ranges of Reported Interbasin Flow Volumes
(Page 2 of 2)

Location Index[a]	Interbasin Flow (afy)[b]	Sources of Extreme Values
45	20,000 to 27,000	LVVWD (2001); Thomas and Mihevc (2007)
46	8,000 to 23,100	Eakin (1966); Thomas and Mihevc (2007)
47	0 to 16,000	Scott et al. (1971); Thomas et al. (2001)
48	9,000 to 28,000	Harrill et al. (1988); Thomas et al. (2001)
49	0 to 16,000	Scott et al. (1971); Thomas et al. (2001)
50	7,400 to 16,000	Thomas and Mihevc (2007); Thomas et al. (2001)
51	1,216 to 3,758	San Juan et al. (2004); Faunt et al. (2004)
52	10,000 to 20,000	Eakin (1963b); Thomas et al. (2001)
53	1,330 to 59,000	Kirk and Campana (1990); LVVWD (2001)
54	M to 36,000	Harrill et al. (1988); Thomas et al. (2001)
55	M to 9,000	Scott et al. (1971); Thomas et al. (2001)
56	5,000 to 17,700	Eakin (1966); Thomas and Mihevc (2007)
57	9,000 to 9,700	LVVWD (2001); Thomas and Mihevc (2007)
58	6,000	Eakin (1966)
59	811 to 11,307	San Juan et al. (2004); Faunt et al. (2004)
60	16,000 to 24,100	Thomas et al. (2001); Thomas and Mihevc (2007)
61	22,300 to 35,000	Thomas and Mihevc (2007); Eakin (1966)
62	S	Scott et al. (1971)
63	M to 6,000	Scott et al. (1971); Thomas et al. (2001)
64	? to 14,023	Harrill et al. (1988); Faunt et al. (2004)
65	2,400 to 13,000	Buqo (2002); Prudic et al. (1995)
66	28,000 to 37,700	Thomas et al. (1996); Eakin (1966); Thomas and Mihevc (2007)
67	32,000	LVVWD (2001); Thomas et al. (2001)
68	M to 41,804	Rush (1968b); Kirk and Campana (1990)
69	5,300 to 7,000	Thomas and Mihevc (2007); Rush (1968b)
70	M to 41,000	Rush (1968b); LVVWD (2001)
71, 73, 74	15,000 to 16,000	Thomas and Mihevc (2007); Thomas et al. (2001)
72	?	Harrill et al. (1988)
75	5,000	Harrill et al. (1988)
76	1,100 to 49,000[c]	Scott et al. (1971); LVVWD (2001)
77	?,M to 15,000	LVVWD (2001); Harrill et al. (1988); Thomas and Mihevc (2007)
78	? to 17,000	LVVWD (2001); Thomas et al. (2001)
79	M to 4,000	Scott et al. (1971); Thomas et al. (2001)
80	1,378	San Juan et al. (2004)
81	600 to 1,000	Thomas and Mihevc (2007); LVVWD (2001)
82	400 to 1,200	Rush (1968b); Harrill et al. (1988)
83	M to 2,000	Scott et al. (1971); Thomas et al. (2001)
84	4,000	Kirk and Campana (1990)

[a]Location of interbasin flow is shown on Figures 5-4 through 5-7 and Figure H-1.
[b]A positive value signifies flow in same direction as arrow, and a negative value signifies flow in the opposite direction.
[c]This value includes 1,000 afy outflow from Black Mountains Area to Lake Mead.
? = Flow volume not specified.
M = Minor quantity. An amount which is either less than 500 afy, or small in comparison to other quantities in the particular hydrologic area (Scott et al., 1971).
S = Some quantity. Sufficient information is not available to make an estimate (Scott et al., 1971).

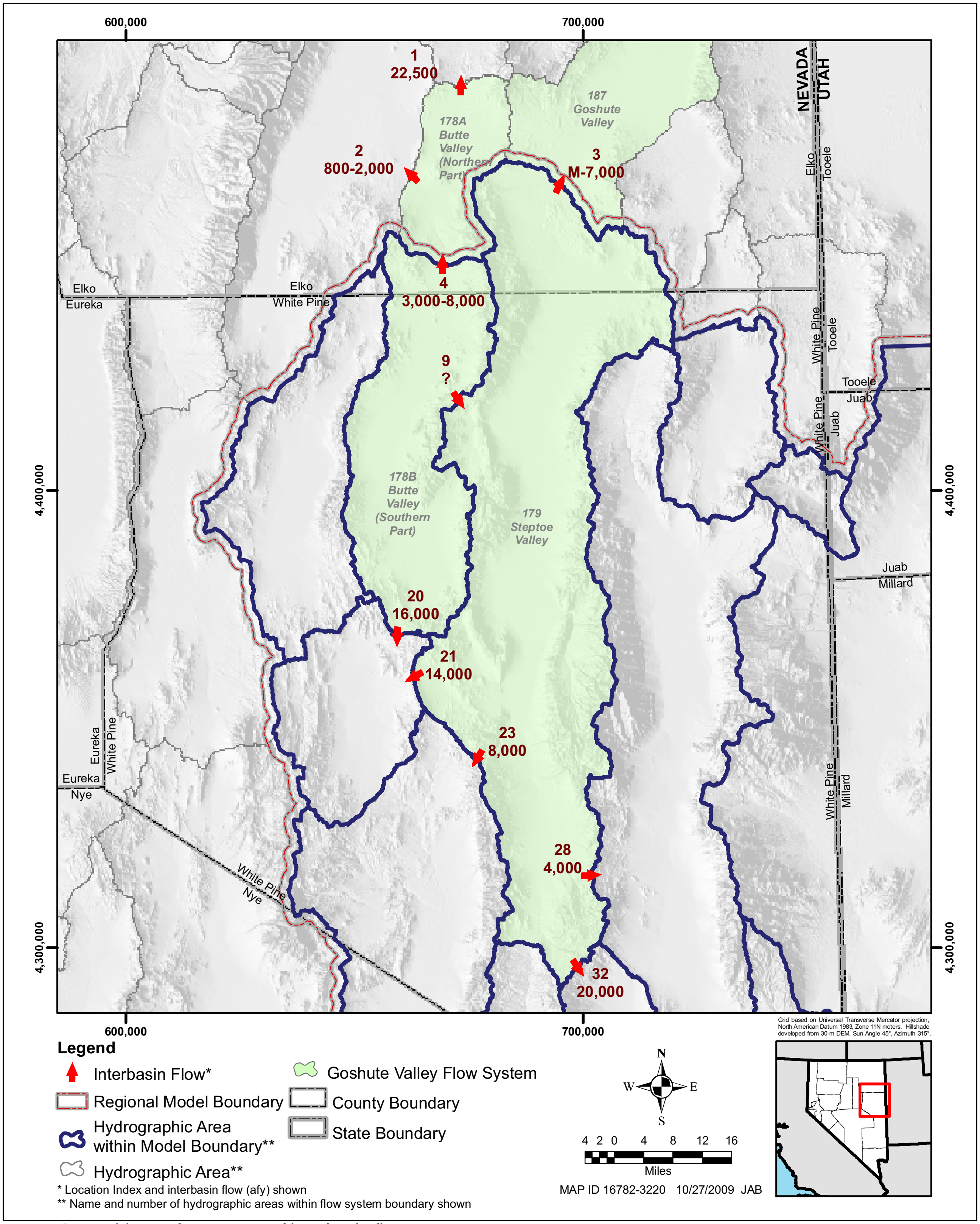

Note: See Table 5-1 for sources of interbasin flow ranges.

Figure 5-4
Locations and Ranges of Interbasin Flow in Goshute Valley Flow System

and the southernmost boundary of Steptoe Valley. The canyon north of Currie is the only location on the boundary of Steptoe Valley where a topographic divide is not present (Plate 1). According to Spengler et al. (1979), plutons occur in the subsurface at this location. Spengler et al. (1979, p. 184) state that "the Currie pluton and Dolly Varden stock may be connected at depth despite observed contrasts of mineralogic and petrologic composition." This interpretation implies that groundwater outflow from Steptoe Valley through this location is probably restricted. Outflow simulated by the calibrated model through this location is 2,510 afy or 2.5 percent of the total simulated inflow to the valley-fill groundwater (Frick, 1985).

A positive hydraulic gradient to valleys adjacent to Steptoe Valley exists across the other potential locations of interbasin flow (Plate 1). However, the hydrogeological characteristics, especially the structural and stratigraphic orientations at these locations, are not favorable to interbasin flow (Frick, 1985). Specifically, dips of hydrostratigraphic units are in opposite directions to hydraulic gradients between Steptoe Valley and White River Valley, Connors Pass of Spring Valley, and the Duck Creek Valley area of Spring Valley (Frick, 1985). Frick (1985) explains this concept:

> Altitude of hydrostratigraphic units is important where the original stratigraphic units remain roughly parallel. If the hydrostratigraphic units dip in the same direction as the groundwater gradient, then the more transmissive layers, such as limestone and dolomite, may act as conduits for flow. However, if the hydrostratigraphic units dip in the opposite direction to the gradient, then the interbedded layers with low transmissivities are more likely to act as aquicludes or aquitards. Dips of hydrostratigraphic units are in opposite directions of groundwater gradients between Steptoe Valley and the following valleys: White River Valley, Connors Pass area of Spring Valley, Duck Creek Valley area of Spring Valley, and the northern part of Southern Butte Valley.

Thus, interbasin groundwater flow through these locations, if any, is probably insignificant. In addition, north-south-trending stratigraphic units and/or faults may impede or prevent interbasin flow between Steptoe Valley and White River, northern Spring, Northern Butte and the northern end of Southern Butte and Jakes valleys (Frick, 1985).

Prudic et al. (1995) included Steptoe Valley and Butte Valley South into their Spring-Steptoe subregion of the Bonneville Region and simulated 3,000 afy of outflow into the White River subregion of the Colorado River Region (Plate 1). In southern Steptoe Valley, simulated flow is westward from the Schell Creek Range and eastward from the Egan and Cherry Creek ranges (Plate 1) (Prudic et al., 1995). Simulated flow in Butte Valley is westward from the Egan and Cherry Creek ranges and eastward from Butte Mountains (Plate 1) (Prudic et al., 1995). Potential deeper groundwater flow from Butte Valley to Steptoe Valley was simulated beneath the Egan Range (Prudic et al., 1995). This potential interbasin flow is supported by limited geochemical evidence (Prudic et al., 1995).

Based on his independent estimates of groundwater recharge and ET, Nichols (2000) calculated an annual outflow volume of 4,000 afy from Steptoe Valley to Goshute Valley (Plate 1). He estimated a total of 24,500 afy of subsurface outflow from Butte Valley (Butte Valley North and South). This total outflow consists of 22,500 afy to Clover Valley and 2,000 afy to Ruby Valley (Plate 1).

In BARCASS, however, a significant amount of underflow is interpreted to flow from the GVFS to the WRFS and the GSLDFS (Welch et al., 2008). The three referenced flow systems are not as delineated by BARCASS; they are as delineated in Figure 2-2. Underflow to the WRFS is from Butte Valley South and the southern portion of Steptoe Valley to Jakes Valley and the northern portion of White River Valley (Plate 1). Underflow to the GSLDFS is from the southern portion of Steptoe Valley to Lake Valley to Spring Valley (Plate 1).

Great Salt Lake Desert Flow System

The part of the GSLDFS located in the study area includes Spring Valley, Tippett Valley, and Big Snake Valley (Pleasant, Snake, and Hamlin valleys), and a small portion of Fish Springs Flat comprising Fish Springs. Major features of the flow system, including interpretations of interbasin flow, are discussed (Plate 1 and Figure 5-5).

This part of the GSLDFS is bounded on the west by the Schell Creek and Fortification ranges; on the east by the Confusion Ranges, Middle Range, and Fish Springs Flat; and on the north by Deep Creek Range and a portion of the Antelope Range (Plate 1). Other major mountain ranges throughout the area are the Snake Range and Wilson Creek Range. No perennial streams connect any of the valleys, and the only interbasin ephemeral drainage is Hamlin Valley Wash that is tributary to Snake Valley. The small portion of Fish Springs Flat containing the springs is included in the study area. Fish Springs Flat encompasses about 590 mi^2 in Tooele, Juab, and Millard counties in Utah. The valley is bounded by the Fish Springs Range on the west, the Dugway and Thomas ranges and Drum Mountains on the east, the Little Drum Mountains on the southeast, and a low divide between Swasey Mountain and the Little Drum Mountains on the southern boundary. Fish Springs Flat opens to the Great Salt Lake Desert to the north (Bolke and Sumsion, 1978). Callao, Utah, is located approximately 25 mi to the west of Fish Springs, and Delta, Utah, is approximately 78 mi to the southeast. The Fish Springs NWR, which contains the springs of interest, was founded in 1959 and is located in the northwest corner of Fish Springs Flat (USFWS, 2004).

Groundwater recharge occurs in the mountains and discharges in two large ET areas primarily by phreatophytes on the valley floors in Spring and Snake valleys (Plate 1). No surface-water outflow of groundwater origin occurs from this flow system. Groundwater discharge may also occur through the subsurface primarily across the northern and the eastern boundary of the portion of the GSLDFS considered in this study. As will be discussed later in this section, groundwater discharge from Fish Springs is believed to originate from the portion of the GSLDFS east of the model area. Hamlin Valley is hydrologically connected to Snake Valley and is typically considered part of Snake Valley. A portion of this recharge flows through the subsurface to the east and northeast and exits the portion of the GSLDFS in the study area, most likely through the northern boundary of Snake Valley. A portion of the recharge to this flow system may exit the system from the eastern boundary of Snake Valley (Plate 1) towards Fish Springs Flat.

General regional flow directions are south to north (Figure 5-2). However, because of sparse information, the detailed configuration of groundwater flow and therefore interbasin flow within the flow system is not well understood and is subject to interpretation. Various interpretations exist and are summarized in the following text.

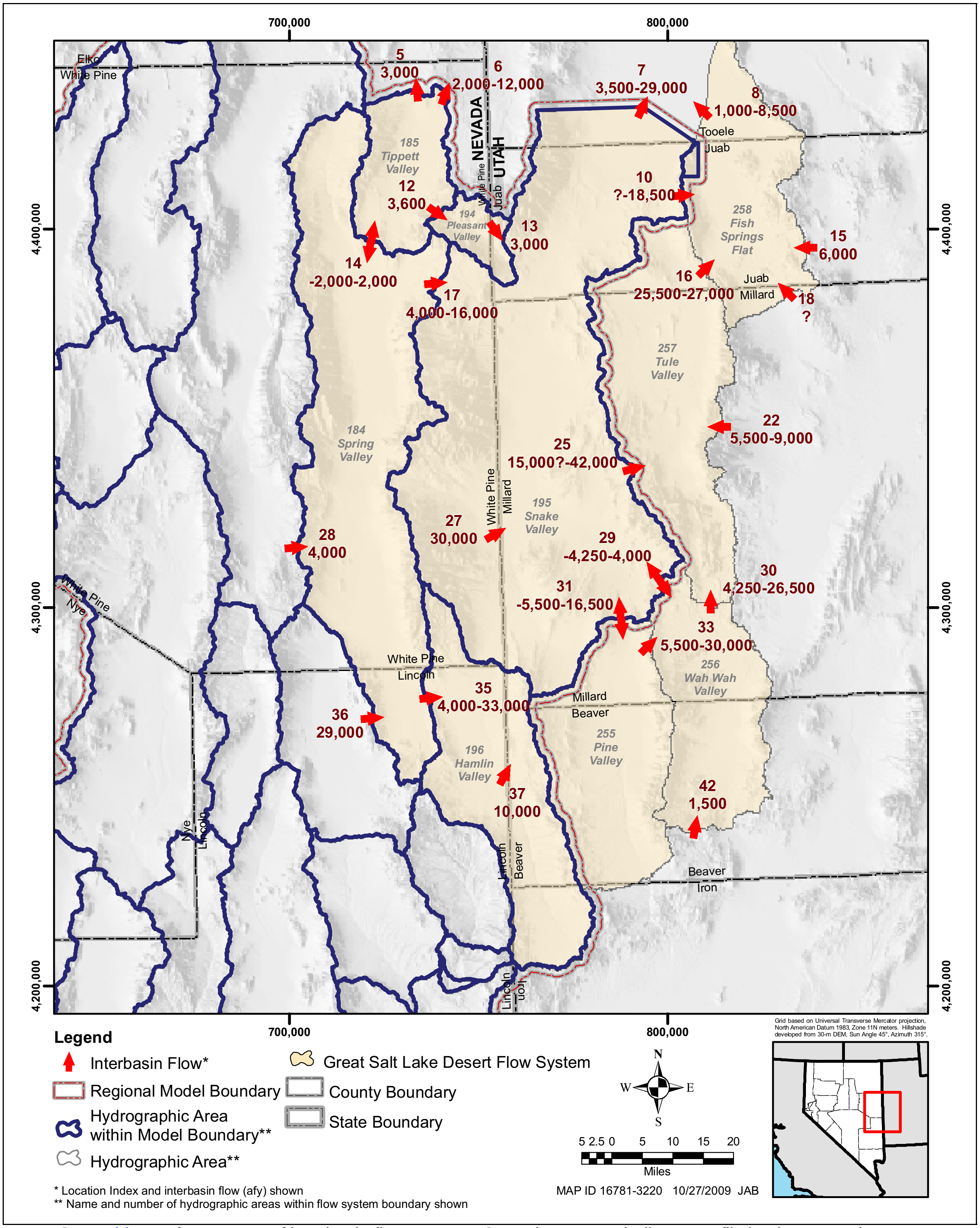

Note: See Table 5-1 for sources of interbasin flow ranges. Opposing arrows indicate conflicting interpretations.

Figure 5-5
Locations and Ranges of Interbasin Flow in Great Salt Lake Desert Flow System

SE ROA 50427

JA_15828

Rush and Kazmi (1965) estimated that 4,000 afy of subsurface outflow occurs from Spring Valley to Hamlin Valley through the Snake Range. Scott et al. (1971) estimated that 2,000 afy of inflow to Spring Valley originates in Tippett Valley. This inflow was accepted and used by Scott et al. (1971) and by Harrill et al. (1988). This interpretation of flow routing was also used by SNWA in the Spring Valley water-rights hearing (SNWA, 2006).

In the RASA model, Prudic et al. (1995) included the GSLDFS, as delineated in this study, in the Bonneville region. Prudic et al. (1995) state that simulated flow in the basins of this flow system is primarily in the upper layer, from recharge areas in the mountains to discharge areas on the adjacent valley floors. About 78 percent of the total inflow is simulated through the upper layer (Prudic et al., 1995). Simulated flow in northern Spring Valley is eastward from the Schell Creek Range and westward from the Snake Range to the valley floor. In southern Spring Valley, groundwater is simulated to flow into Hamlin Valley through the Limestone Hills. In Snake Valley, most of the simulated flow is toward the Great Salt Lake Desert.

Nichols (2000) estimated recharge in excess of groundwater ET in Tippett and Spring valleys. He routed the excess water (9,600 afy) in Tippett Valley as outflow toward the north (Plate 1). Recharge from precipitation in Spring Valley was estimated to be about 104,000 afy, whereas groundwater ET was estimated at 90,000 afy. The difference of 14,000 afy may be the result of an underestimation of groundwater ET, an overestimation of recharge, or a combination of both. However, much of the excess recharge is believed to leave the valley as interbasin flow to the east. Nichols (2000) routed 4,000 afy through the southern end of Spring Valley to Hamlin Valley and the remaining 10,000 afy to Snake Valley through a topographic low between the northern end of the Snake Range and the Kern Mountains.

As part of BARCASS, Welch et al. (2008) derived a new flow-routing configuration for the GSLDFS (Plate 1 and Figure 5-3). They routed groundwater from Steptoe Valley and Lake Valley to Spring Valley. The total volume of this interbasin flow is 33,000 afy, which accounts for more than one-third of the recharge of Spring Valley. All outflow from Snake Valley was routed through the northern boundary of Snake Valley, even though a high-potential interbasin flow segment was placed on their geological map along the eastern boundary of the valley (Figure 5-3). Welch et al. (2008) also estimated 2,000 afy of groundwater to flow from Spring Valley to Tippett Valley. This interbasin flow volume is the same as the volume estimated by Scott et al. (1971). However, the flow direction is reversed (i.e., flow is from Tippett Valley to Spring Valley).

As part of BARCASS, Hershey et al. (2007) evaluated data on dissolved gases, stable isotopes, and tritium from 15 wells and springs located in the BARCASS area. Using these data, they derived estimates of recharge ages, recharge altitudes, and flowpath directions. Hershey et al. (2007) also identified the major flow paths using water-rock reaction models. The paths they identified are as follows: (1) from north to south in White River Valley; (2) from south to north in Steptoe Valley; (3) from the central part of Spring Valley northward and then to northern Snake Valley; (4) from the central part of the valley southward and then to southern Snake Valley; and (5) from south to north in Snake Valley. Groundwater ages were calculated using dissolved organic ^{14}C and dissolved inorganic ^{14}C for groundwater flowing across the following basin boundaries: between Lake and Spring valleys, between Steptoe and Spring valleys, and between Spring and Snake valleys. The calculated groundwater ages ranged from less than 1,000 years to 16,000 years.

Lundmark (2007) developed a steady-state, mass-balance groundwater-accounting model, using the discrete-state compartment code and the Monte Carlo method, to evaluate basin and regional water budgets for the BARCASS area. The model was used to calculate annual interbasin flow volumes based on the fluxes of a conservative tracer (deuterium), using the independent estimates of recharge and groundwater ET reported by Welch et al. (2008). The model results consist of deterministic estimates and a limited analysis (Monte Carlo) of the uncertainty in the predicted interbasin flow volumes resulting from the uncertainty in recharge characteristics.

Gillespie (2008) conducted an analysis of flow paths in the GSLDFS using water chemistry, stable isotopes, measurable tritium, ^{14}C activities, and geochemical models. He concluded that (1) interbasin flow from southern Spring Valley to southern Snake Valley cannot be confirmed or rejected and (2) interbasin flow from northern Spring Valley to northern Snake Valley is unlikely.

The Utah Geological Survey (UGS) (2008) published a provisional project map on its website (http://geology.utah.gov/esp/snake_valley_project/pdf/projectmap.pdf). In that map, the UGS posted the volume of interbasin flow reported by Welch et al. (2008). The location of that interbasin flow is, however, different from that used in BARCASS. The UGS used a location of interbasin flow similar to that depicted by Harrill et al. (1988).

Of particular interest in this portion of the GSLDFS are the springs located in Fish Springs Flat (Plate 1). Although the total discharge from Fish Springs is known (described above), the source of the spring flow is much larger than the estimated recharge within Fish Springs Flat. Most groundwater in Fish Springs Flat is in the eastern parts of the north-flowing GSLDFS. Some groundwater is derived from the Sevier Desert area (Wilberg, 1991), moving northward along basin-range fault zones into Fish Springs Flat (Bolke and Sumsion, 1978; Harrill et al., 1988) (Figure 5-5). Most groundwater discharging from Fish Springs is probably derived from Tule Valley. Some of the Tule Valley groundwater is probably derived from local precipitation, but most of the groundwater in Tule Valley is probably derived from the ranges to the south and passes northward along basin-range faults through Wah Wah Valley, Pine Valley, and the southeastern Snake Valley (Figure 5-5) (Harrill et al., 1988). A portion of this northward-moving groundwater may be deflected eastward (Stephens, 1977; Bolke and Sumsion, 1978; Gates and Kruer, 1981; Harrill et al., 1988), from Tule Valley to Fish Springs Flat. Findings of the major existing interpretations are summarized in the following text.

Bolke and Sumsion (1978) estimated a recharge from precipitation of 4,000 afy, a discharge by ET of 8,000 afy, a total spring discharge of 27,000 afy, and subsurface inflow to Fish Springs Flat of about 31,000 afy. Groundwater discharge by subsurface outflow is negligible. Bolke and Sumsion (1978) argued that the high local relief of the eastern Fish Springs Range may contribute some recharge from surface water to the area around Fish Springs, but most of the spring discharge is groundwater. They state that this groundwater is from subsurface inflow from other basins, such as Tule Valley, and imply that the other contributing basins may be Snake, Wah Wah, and Pine valleys located to the south and west of Fish Springs Flat. However, no allocated volumes of underflow were provided in their report.

Gates and Kruer (1981) presented a theory to explain the source of spring flow to Fish Springs. They used the various types of data available at the time to conclude that:

> Although available evidence indicates that interbasin flows occurs to and within west-central Utah and that it likely occurs through solution-enhanced fracture openings in carbonate rocks of Paleozoic age, the exact source area of all this water is not known. Water budgets of Fish Springs Flat, Tule Valley, and the southern Great Salt Lake Desert require that large quantities of water move to these basins by subsurface flow; and water levels in west-central Utah (pl. 2) show that ground water potentially could move eastward from Snake Valley and northward from Pine and Wah Wah Valleys to Tule Valley and Fish Springs Flat. (p. 34)

Carlton (1985) developed a numerical groundwater flow model for the flow system comprising Fish Springs Flat. The flow system comprises Fish Springs Flat, Pine, Tule, Snake, and Wah Wah valleys. He constructed the model using the data available at the time. The model simulated subsurface inflow from external sources as follows: 25,500 afy from Tule Valley; 6,000 afy from the Sevier Desert; and 18,500 afy from Snake Valley. Simulated subsurface outflow was 8,500 afy to the southern Great Salt Lake Desert. The simulated discharge from Fish Springs was 28,000 afy. As indicated by Carlton (1985), about 50 percent of the water discharged by Fish Springs originates in Snake Valley. These modeling results are uncertain as the model was based on limited data and reconnaissance studies.

In Sheet 2 of 2 of HA-694-C, Harrill et al. (1988) presented estimates of recharge by precipitation and underflow to Fish Springs Flat as follows: (1) recharge from precipitation of 4,000 afy; (2) subsurface outflow of less than 1,000 afy; (3) 27,000 afy of subsurface inflow from Tule Valley; and (4) unknown amounts from Snake Valley (through the Fish Springs Range) and Wah Wah Valley. An unknown portion of the underflow from Tule Valley originates from Snake Valley by underflow through the Confusion Range. The uncertainty in the flow routing within these basins is most probably the reason why Harrill et al. (1988) reported three potential values for the subsurface outflow from Snake Valley to Tule Valley through the Confusion Range: 22,000, 33,000, and 42,000 afy.

Bedinger et al. (1990) pointed out that hydraulic gradients in the carbonate rocks are very low, creating relatively long groundwater travel times from potential host rocks to natural discharge points, such as springs. They estimated these travel times to be on the order of 10,000 to 100,000 years, not including movement in the unsaturated zone of the host rock (Bedinger et al., 1990). The age reported for water from Fish Springs ranges between 9,000 to 21,000 years (Gates and Kruer, 1981; Carlton, 1985).

Based on the results of the RASA model, Prudic et al. (1995, p. D-84) state that "at least half of the simulated flow to Fish Springs Flat from Tule Valley originates in the Snake Valley drainage basin. Of the 23,000 afy simulated as entering Tule Valley in the lower Interbasin Flow layer, 14,000 is underflow from Snake Valley through the Confusion Range and 9,000 is from Wah Wah Valley."

In summary, although Harrill et al. (1988) queried possible eastward movement of groundwater through the northern Fish Springs Range, presumably along the east-striking faults or basal parts of the lower carbonate aquifer (Plates 2 and 4), no evidence exists to support such flow. The hills and ranges, including the Confusion Range, that form the western side of Tule Valley are, like the Fish Springs Range, underlain by the basement-confining zone, so it appears unlikely that substantial groundwater is derived from west of Tule Valley. Furthermore, through-going easterly trending faults do not cut the Confusion Range (Plates 2 and 3). Thus, the source of groundwater flow to the springs must be from neighboring basins through the carbonate aquifer.

Meadow Valley Flow System

The MVFS is roughly parallel to the WRFS, starting in Lake Valley and ending as the Lower Meadow Valley Wash joins the Muddy River in Upper Moapa Valley. The MVFS (Plate 1 and Figure 5-6) is hydraulically connected to the WRFS in the south and is part of the Colorado River Region. A portion of the Muddy Springs discharge is believed to originate from the MVFS along Meadow Valley Wash.

The MVFS is bounded by the Schell Creek Range to the north; by the Fairview, Bristol, Highland, Chief, Burnt Spring ranges, and the Delamar and Meadow Valley mountains to the west; and by the Fortification and Wilson Creek ranges and the Clover and Mormon mountains to the east (Plate 1).

Recharge from precipitation occurs mostly on the mountains located in the northern and northwestern parts of this flow system (Plate 1). Groundwater discharges by the process of ET along the banks of Meadow Valley Wash, which has its headwaters in the Wilson Creek Range. The Meadow Valley Wash is perennial for much of its length with intermittent stream reaches occurring within the Lower Meadow Valley Wash. Clover Creek is a stream with an intermittent upper reach and perennial lower reach that headwaters in the Clover Mountains and is tributary to Meadow Valley Wash.

Regional flow directions are north to south, and flow out of this flow system is to the Muddy River Springs area and California Wash in the WRFS. The general regional flow directions are shown in Figure 5-2. The existing interpretations of interbasin flow are shown on Plate 1 and summarized in the following text.

The earliest and most detailed study of groundwater conditions for MVFS was conducted by Phoenix (1948). The basins included in MVFS, as defined by Phoenix (1948), are the same as in this study. Physiographic evidence indicates that the Meadow Valley Wash drainage pattern, with headwater starting from Spring Valley, possibly dates back well into the Pleistocene period (Phoenix, 1948).

Rush and Eakin (1963) constructed a cross section of the general topography and water table for Lake Valley. The cross section indicates that the general groundwater flow direction in Lake Valley is southward toward Patterson Wash (Patterson Valley in this study). Rush and Eakin (1963) estimated the annual volume of interbasin flow through this location at 3,000 afy.

Rush (1964) discussed groundwater conditions in basins of the MVFS that are connected by perennial or intermediate streams. This includes all basins of this flow system, except Lake Valley. During periods of spring snowmelt or flash floods, water of these streams flows to the mouth of Meadow Valley Wash and discharges into the Muddy River. However, most of the base flow in Meadow Valley Wash is from groundwater sources. Groundwater outflow from MVFS to the Muddy River Springs area occurs in two forms: underflow through the alluvium of lower Meadow Valley Wash and leakage through bedrock (Rush, 1964). The volume of this outflow was estimated as 7,000 afy based on the balance of recharge and discharge in the system.

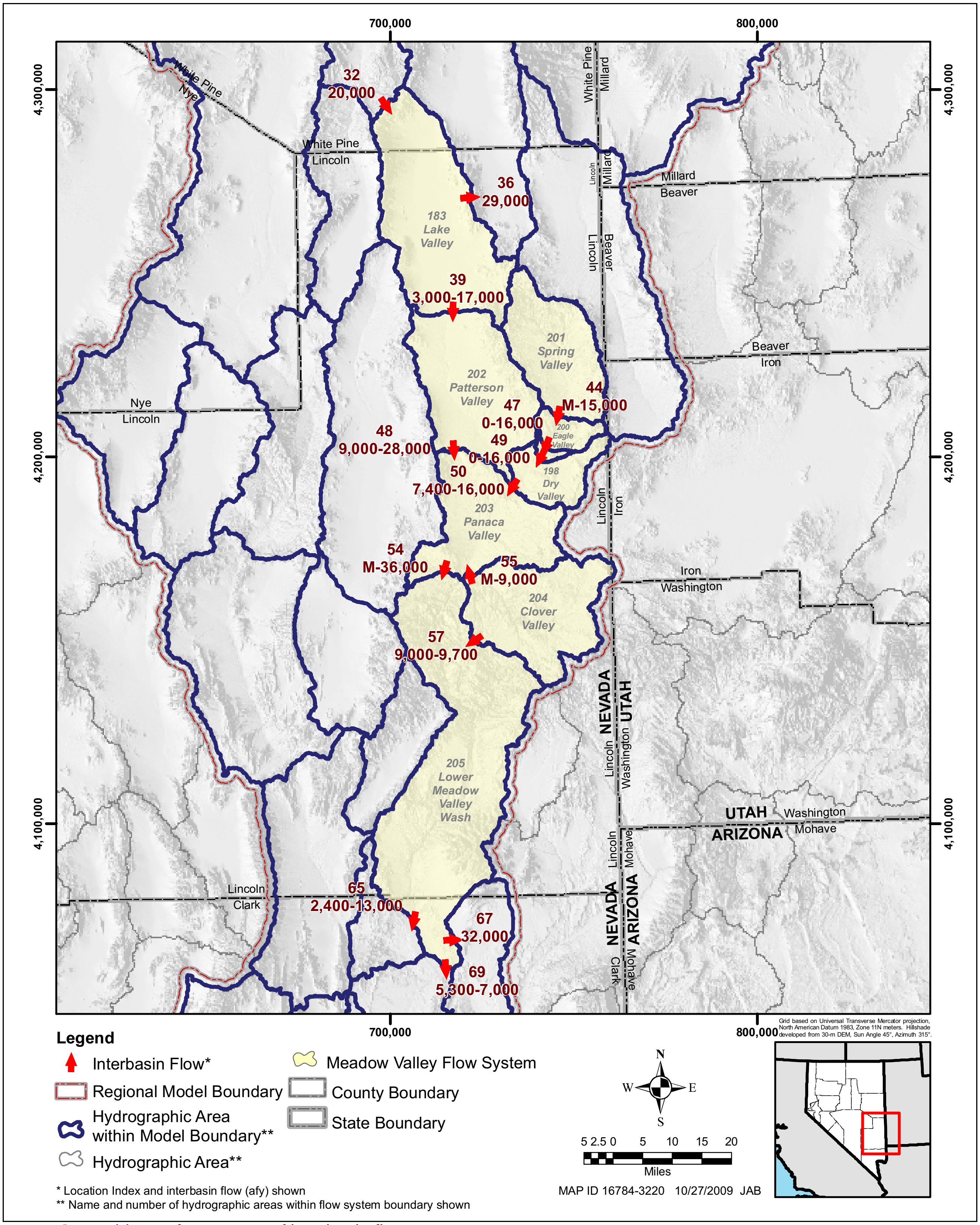

Note: See Table 5-1 for sources of interbasin flow ranges.

Figure 5-6
Locations and Ranges of Interbasin Flow in Meadow Valley Flow System

Based on a mass-balance model of deuterium, Kirk and Campana (1990) and Thomas et al. (1996) estimated that 5,500 to 9,000 afy and 8,000 afy of Muddy River Springs discharge is from the southern MVFS, respectively. The RASA model simulated the contribution of MVFS water to the Muddy River Springs area at 13,000 afy (Prudic et al., 1995).

LVVWD (2001) estimated a large flow rate of 32,000 afy from MVFS into Lower Moapa Valley based on the water balance of updated annual recharge and discharge volumes. Based on Darcy flux calculations, Buqo (2002) estimated an annual volume of flow from Lower Meadow Valley Wash to the Muddy River Springs area ranging from 2,400 to 7,200 afy.

Synoptic discharge measurements conducted by Beck and Wilson (2006) along the Muddy River indicate that a gain of about 4,200 afy occurs in the Muddy River flow from a gage near Moapa to the Muddy River below Anderson Wash near a Logandale gage. Based on these synoptic discharge measurements, Beck and Wilson (2006) and SNWA (2007) estimated an annual flow volume of 9,200 afy from the MVFS to the Muddy River Springs area.

The conceptual model of groundwater flow in MVFS had been about the same until 2008 when BARCASS was published (Welch et al., 2008). In BARCASS, Lake Valley is included in the GSLDFS. An annual volume of 20,000 afy of groundwater was routed from Steptoe Valley to Lake Valley, and an annual volume of 29,000 afy was routed from Lake Valley to Spring Valley.

White River Flow System

The WRFS (Plate 1 and Figure 5-7) used in this study is approximately as defined by Eakin (1966) and Harrill et al. (1988). It is the longest flow system in Nevada. Prudic et al. (1995) consider this flow system to be part of the Colorado River Region. Their interpretation excludes Long and northern Jakes valleys from the WRFS. As part of BARCASS, the USGS (Welch et al., 2008) first extended the boundary to include a portion of southern Butte Valley South and south-central Steptoe Valley in the WRFS.

The WRFS is bounded by the Maverick Springs, White Pine, Grant, Quinn Canyon, Pahranagat, and Sheep Mountain ranges to the west, and by the Egan, Schell Creek, Bristol, Highland, and Chief ranges and the Clover, Delamar, and Muddy mountains to the east (Plate 1). The southern boundary of this flow system is Lake Mead.

Based on the interpretation of Eakin (1966), all groundwater recharge to the WRFS is from precipitation on the bordering mountains, especially in its northern basins. However, according to other interpretations such as that of Welch et al. (2008), some recharge may also occur by interbasin flow from Steptoe Valley.

Major groundwater discharge areas occur in the White River and Pahranagat valleys and the Muddy River Springs area. Other minor discharge areas include Long, Cave, and Garden valleys and the Black Mountains Area. Numerous regional springs located in areas from southern White River Valley to the Muddy River Springs area discharge important volumes of groundwater, which is lost to ET for the most part (Plate 1). Except for White River Valley and the Muddy River Springs area, spring discharge is assumed to be completely consumed by the phreatophytes within the groundwater

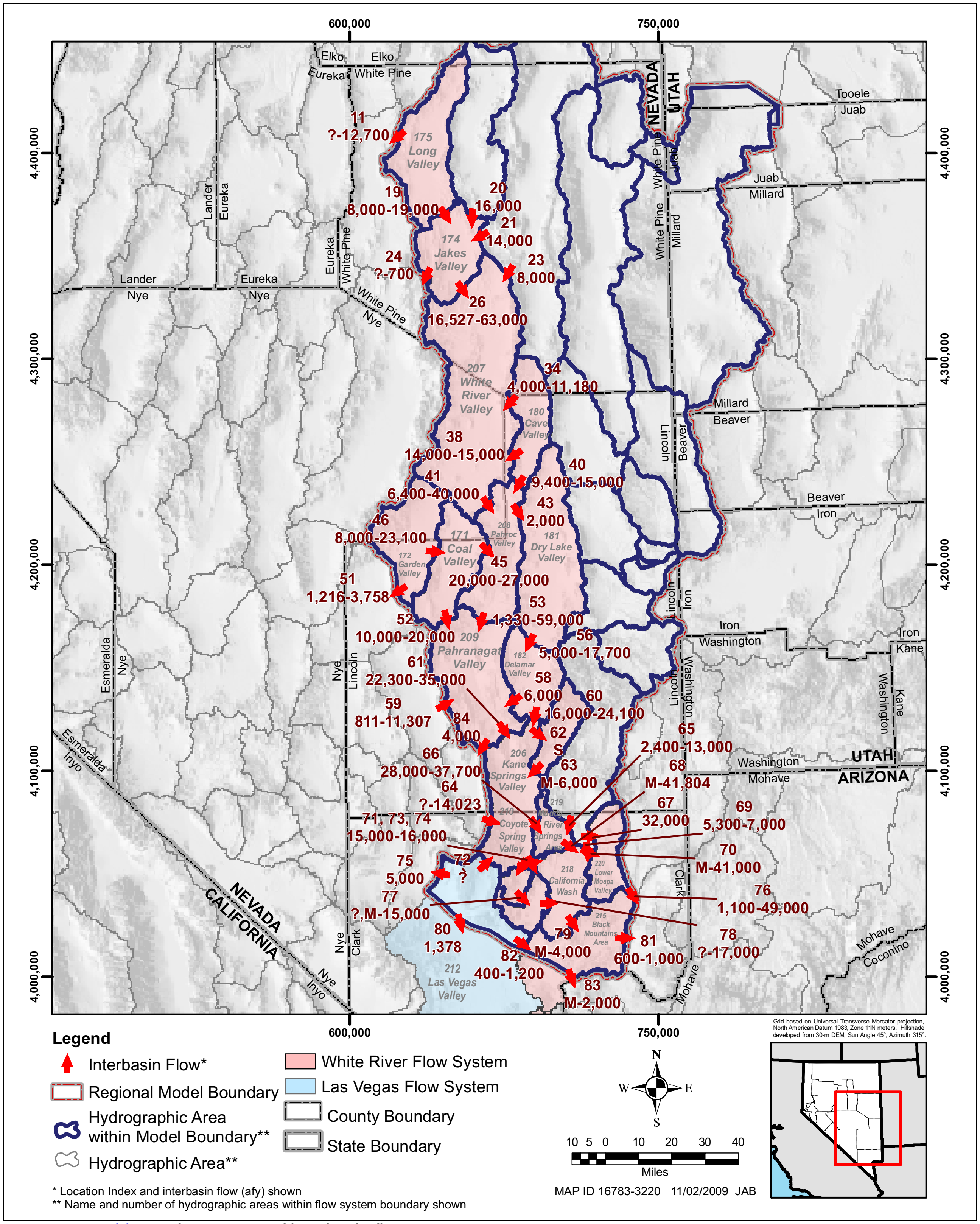

Note: See Table 5-1 for sources of interbasin flow ranges.

Figure 5-7
Locations and Ranges of Interbasin Flow in White River Flow System

ET areas. The discharge from the regional springs of southern White River is also mostly consumed by phreatophytes. However, a portion of the discharge contributes to the interbasin outflow to Pahroc Valley (Maxey and Eakin, 1949). The Muddy River Springs, which are the largest springs in the WRFS, are located in the central part of the Muddy River Springs area (Upper Moapa Valley). The Muddy River Springs form the headwaters of the Muddy River, a tributary to Lake Mead on the Colorado River (Plate 1). Water from the Muddy River Springs contributes to the riparian ET areas located along the Muddy River, down-gradient from the springs.

The general groundwater flow direction in the regional part of the flow system is from areas of major recharge (north) to major areas of discharge (south). Regional groundwater movement is through the carbonate aquifer, which occurs throughout the flow system. The regional flow through the carbonate aquifer of the WRFS is facilitated by north-south faults (Plate 2 and Figure 5-2). Although there is general agreement on the general direction of regional groundwater flow, interbasin flow locations and volumes are subject to interpretation.

Eakin (1966) proposed the first regional groundwater flow system and named it the White River System. The system is based on a regional gradient derived from elevation of springs, water levels of groundwater wells, playas, and water budgets of several basins in southeastern Nevada. The direction of the regional gradient was inferred from the elevation of water levels in adjacent basins; principal springs in White River, Pahranagat, and Upper Moapa valleys; and playas in Cave, Coal, Dry Lake, Delamar valleys. Eakin (1966) subtracted the annual discharge volume from the annual recharge volume and routed the residual to down-gradient basins. Because the water level of Jakes Valley is unknown, Eakin (1966) estimated it to be as much as 400 ft below the playa surface. The lowest known water-level elevation beneath the playa of Long Valley is about 6,000 ft. The elevation of the water level in a well in Jakes Wash of northern White River Valley is about 5,780 ft, whereas the elevation at Preston Springs, about 12 mi farther south, is about 5,680 ft. This indicates that a potential southward gradient apparently exists through the carbonate rocks toward White River Valley.

A synoptic view of regional groundwater potential based on inference of the regional head from the surface elevation of thermal springs was first offered by Mifflin (1968). Hydraulically forced thermal springs are expressions of movement of water from a depth heated by the natural geothermal gradient. The numerous thermal springs present in the Great Basin region indicate the inherent, permeable nature of a significant network of vertical faults associated with the extensional block faulting of this region.

Harrill et al. (1988) used previous estimates of basin-water budgets in their interpretation of groundwater flow in the Great Basin region. They also considered the topographic and shallow water-level differences between basins for interpreting the direction of interbasin flow and regional groundwater potential. Harrill et al. (1988) included an interbasin flow arrow on the western boundary of Long Valley, Jakes Valley and Pahranagat Valley, but without a flow volume. The western and southern boundary of Coyote Spring Valley was also marked with an interbasin flow arrow into the valley without a flow volume on the map prepared by Harrill et al. (1988). No volume of interbasin flow was estimated by Harrill et al. (1988) from the MVFS to WRFS. Rush (1964) interpreted an annual volume of 7,000 afy of interbasin flow from the MVFS into the Muddy River Springs area.

Nichols (2000) estimated about 10,000 afy and 13,000 afy of interbasin flow from Long Valley to Newark Valley and Long Valley to Railroad Valley, respectively. Nichols (2000) also estimated about 700 afy of interbasin flow from Jakes Valley to Newark Valley. In addition, he estimated a contribution of about 51,200 afy of interbasin flow from both Long and Jakes valleys to White River Valley.

The Muddy River Springs are the dominant hydrologic feature of the Muddy River Springs Area. Measurements of the discharge at a gaging station near Moapa have ranged from 43.5 cfs in 1930 to 49.6 cfs in 1958 (Eakin, 1964). Small variations in spring discharge exclude contributions of surface runoff that is highly variable and correlated to precipitation events. However, the exact sources of water discharging at the Muddy River Springs are not definitely known. Based on previous studies, the main source of water discharging from the Muddy River Springs is recharge occurring in the northern WRFS (Eakin, 1966; Harrill et al., 1988; Kirk and Campana, 1990; Thomas et al., 1996; and SNWA, 2007).

As part of a groundwater modeling study of the DVFS, which is located immediately to the west of the CCRP model area, estimated interbasin flow between the two flow systems was reported as (1) 811 afy to 11,307 afy from the DVFS into the WRFS at Pahranagat Valley; (2) 5,513 afy to 14,012 afy to Coyote Springs Valley from Tikaboo Valley South; and (3) 1,216 afy to 3,758 afy of interbasin flow from the WRFS to the DVFS at Garden Valley (San Juan et al., 2004; Faunt et al., 2004).

SNWA (2007) estimated the total outflow from the WRFS at 25,000 afy, which includes spring discharge from the Muddy Springs, Rogers Spring, and Blue Point Spring, and subsurface outflow from Lower Moapa Valley to the Colorado River.

In BARCASS, 16,000 afy of interbasin flow was routed into the WRFS from Butte Valley South and 22,000 afy was routed in from Steptoe Valley. About 5,000 afy interbasin flow was routed out of WRFS from Long Valley (Welch et al., 2008).

5.2.2.2.3 Las Vegas Flow System

The portion of Las Vegas Valley that includes the area located north of the LVVSZ is included in the model domain and is shown with the WRFS in Figure 5-7.

The LVVSZ is a west-northwest-striking fault with a traceable length of about 120 km. The western segment of the LVVSZ separates the highly extended Sheep Range detachment system to the north from the unextended Spring Mountain block to the south (Guth, 1981, 1990). The central segment of the LVVSZ forms the northern boundary of the Las Vegas Valley (Longwell, 1960; Campana and Levandowski, 1991). The eastern segment of the LVVSZ separates the highly extended Boulder Basin block to the south from the weakly extended Muddy Mountains block to the north (Duebendorfer and Black, 1992). The LVVSZ acts as not only a tectonic divide but also as a hydraulic barrier (SNWA, 2005).

The western hydrographic boundary of this portion of the Las Vegas Flow System consists of thick carbonate and alluvial deposits, so it is permeable. Harrill et al. (1988) routed 5,000 afy of

SE ROA 50436

JA_15837

groundwater through this boundary out of Las Vegas Valley. Harrill et al. (1988) also routed 1,200 afy of groundwater out of this portion along the LVVSZ to Black Mountains Area and an unknown amount of groundwater to Coyote Spring Valley.

San Juan et al. (2004) did not depict any interbasin flow arrows into this portion of Las Vegas Valley. Thus, the actual groundwater flow direction in this portion of the flow system is not known.

This Page Intentionally Left Blank

SE ROA 50438

6.0 PRECIPITATION

Precipitation is the main source of groundwater recharge to the flow systems of the study area. An estimate of the spatial distribution of precipitation is needed to estimate groundwater ET and the spatial distribution of recharge. The precipitation distribution needed for these estimates should represent long-term mean annual conditions, which are assumed to approximate predevelopment conditions. A brief review of the available methods and a description of the method selected for this analysis follow.

6.1 Available Methods

The available methods of deriving spatial distributions for precipitation are explained in this section, and previously reported volumes of precipitation are described.

Available methods used to derive precipitation distributions in Nevada include the Hardman maps (Hardman, 1936, 1962, 1965), PRISM (Daly et al., 1994, 1997, 1998, 2008), and precipitation-altitude regression models.

Hardman (1936) developed a hand-drawn precipitation contour map for Nevada using U.S. Weather Bureau records, USGS topographic maps, and Nevada Experiment Station forage-type maps. The Hardman map includes six precipitation zones, defined as follows: less than 5 in., 5 to 8 in., 8 to 12 in., 12 to 15 in., 15 to 20 in., and over 20 in. This map was also published in Hardman and Mason (1949) and was later updated by Hardman (1962 and 1965). This updated map was later revised by the Nevada State Engineer (Scott et al., 1971). The original Hardman (1936) precipitation map is used in the Maxey-Eakin recharge method (Maxey and Eakin, 1949).

PRISM is a mapping model of climate variables developed by the Natural Resources Conservation Service (NRCS) in partnership with the Climate Center and the PRISM Group at Oregon State University (Daly et al., 1994, 1997, 1998). Daly et al. (1997, p. 10) describe PRISM as "...a coordinated set of rules, decisions, and calculations, designed to approximate the decision-making process an expert climatologist would invoke when creating a climate map." The basic information used in PRISM consists of point measurements of a given climate variable (e.g., precipitation) and a DEM. PRISM incorporates rain shadows, coastal effects, and temperature inversions. PRISM products include grids of precipitation, temperature, and other climate variables for a given period of time and monthly, yearly, and event-based climatic parameters. PRISM has been used to estimate precipitation for each state of the United States, including Nevada (Daly et al., 1998).

Precipitation-altitude regression models have been developed for many areas of Nevada to derive precipitation distributions and to estimate precipitation volumes (Quiring, 1965; Daly et al., 1994;

SE ROA 50439

JA_15840

Maurer and Halford, 2004; SNWA, 2006). The regression models are defined by equations that express the relationship between precipitation and altitude based on station data compiled from various sources. The equation can be applied to DEMs to derive precipitation distributions. Typically, the regression models are developed for local-scale (e.g., hydrographic area) analyses where the data density is relatively high. For large areas with sparse precipitation data, the derived distribution of precipitation may not be representative of reality.

6.2 Selected Method

The main criterion for the selection of a precipitation map for use in the groundwater-budget estimate is an accurate spatial distribution of precipitation. The magnitude of the precipitation volume does not have a direct impact on the volume of recharge from precipitation. It does, however, affect it indirectly as will be explained in Section 6.3. The PRISM method (Daly et al., 1994, 1997, 1998, 2008), which incorporates important physical processes and uses state-of-the-art spatial methods, was selected for determining the precipitation distribution of the study area. The precipitation maps developed by Hardman (1936, 1962, 1965) were rejected simply because they were developed using the archaic methods and sparse station data available at the time. Development of a separate precipitation-altitude regression model was rejected because it would duplicate the PRISM work and would yield a product of lesser quality.

The PRISM data sets, including those of precipitation, represent state-of-the art distributions at the basin and regional scales and are recognized worldwide as the highest-quality spatial climate data sets currently available. The U.S. Department of Agriculture, for example, adopted PRISM as its official climatological data set (Daly et al., 2008). Precipitation distributions developed using the PRISM method use modern tools and incorporate more recent station data and information not reflected in previous mapping efforts. More recent data include additional stations and precipitation records. Additional information not reflected in previous mapping efforts includes the use of the DEM to represent the topography to simulate rain-shadow effects.

Several PRISM precipitation grids are available at many sites on the Internet (e.g., http://www.prism.oregonstate.edu/products/). The grids include precipitation distributions for various periods of time and different resolutions. All PRISM precipitation grids are based on the 1-degree DEM grid available at http://edc.usgs.gov/guides/dem.html. The station precipitation data used to generate the PRISM maps are not available to the public. The most recent normal grid (800-m 1971 to 2000 precipitation normals, Version 2, May 3, 2007) is considered to be the best-quality product to date and was deemed appropriate for the purposes of the conceptual model. One potential limitation of the use of this grid in the groundwater flow model is the limited period of record it represents, as this 30-year period may not exactly represent the desired long-term mean conditions that will be described in the next subsection. However, the historical precipitation record indicates that the overall variability of precipitation within the region is limited as discussed in the following paragraph.

The Climate Diagnostics Center/National Oceanic and Atmospheric Administration calculates historical precipitation indexes for the U.S. Climate Divisions. Climate Divisions intersecting the model area consist of Utah division 1 and Nevada divisions 2, 3, and 4 (Figure 6-1). The historical precipitation indexes were obtained for these four divisions and graphed (Figure 6-2). All four divisions exhibit an apparent slight increase starting in 1970. However, the difference between the

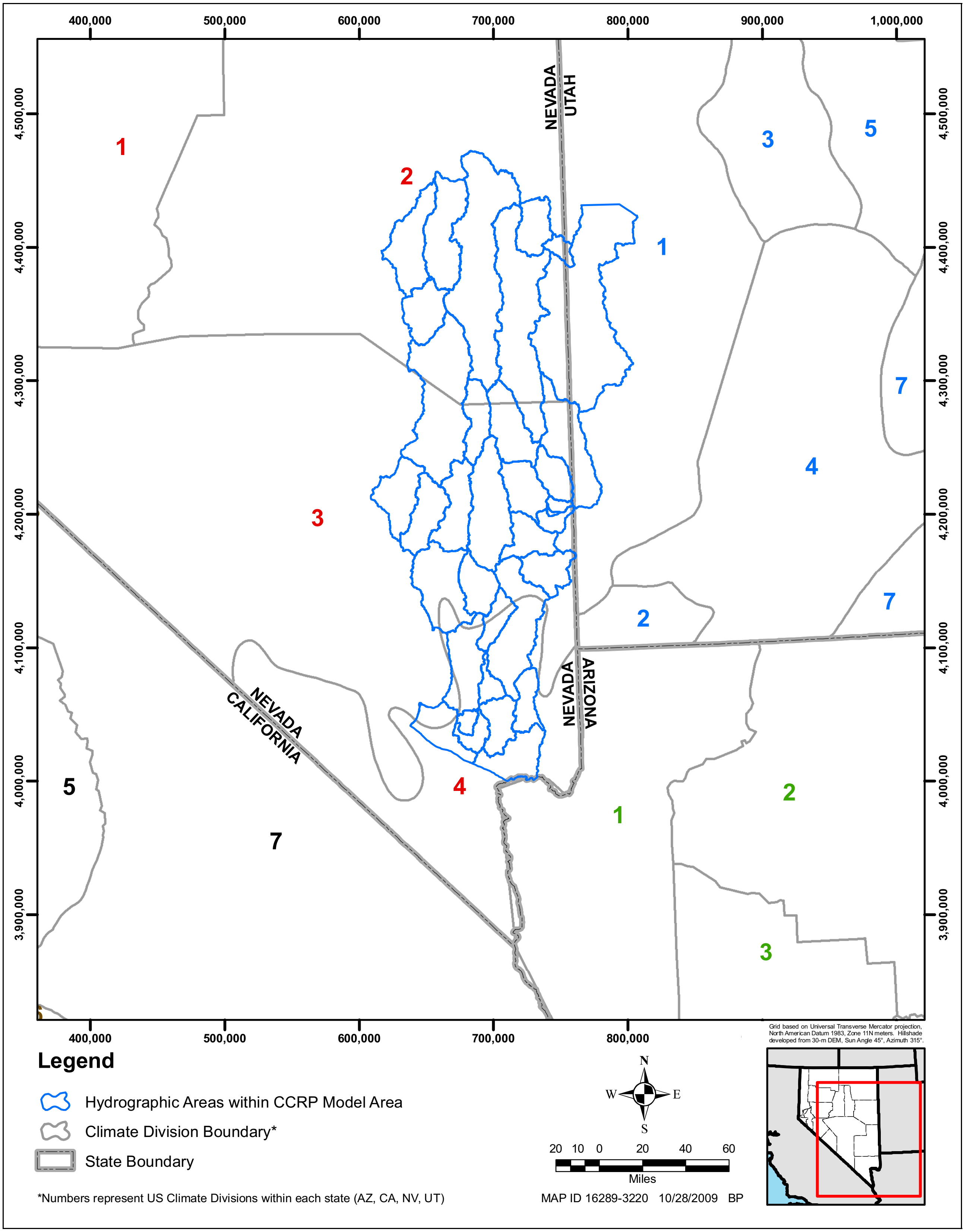

Figure 6-1
Location of U.S. Climate Divisions in Study Area and Vicinity

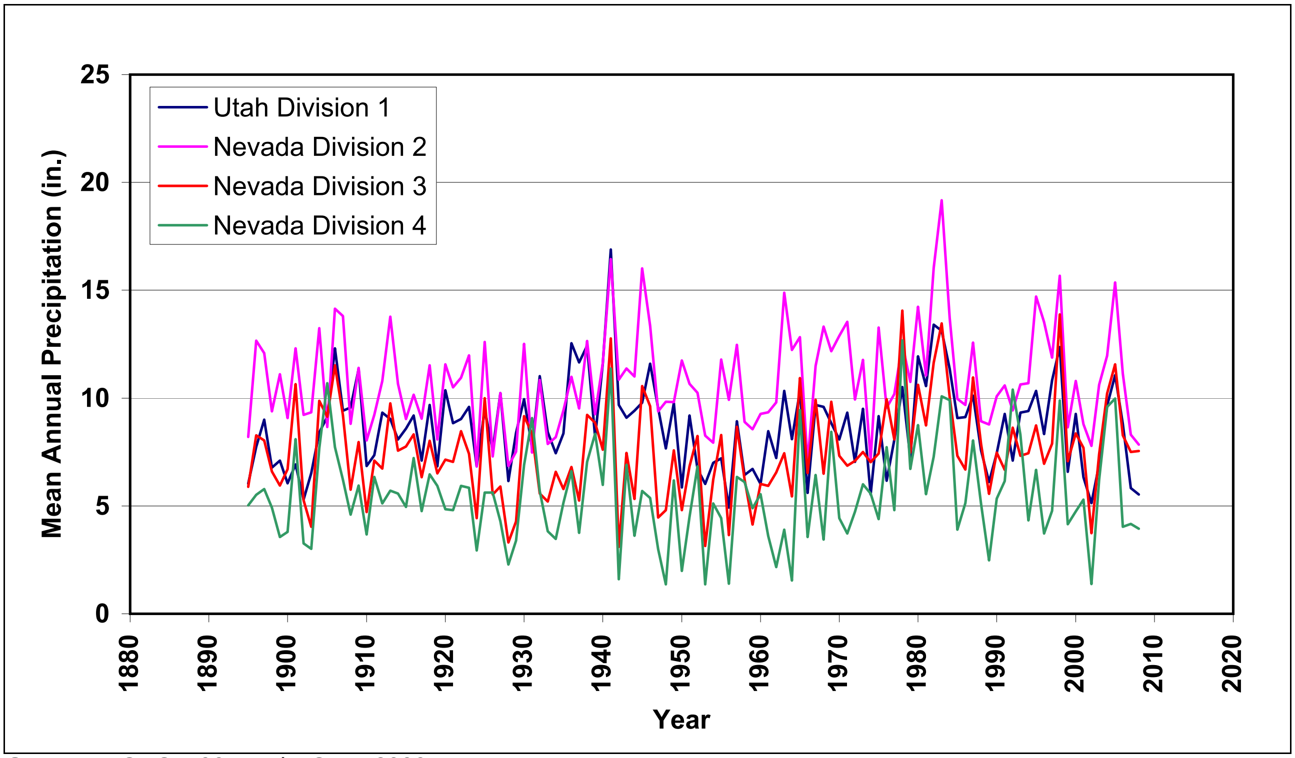

Source: NCDC, 1994 and NOAA, 2009

Figure 6-2
Historical Precipitation Variability in the Study Area and Vicinity

means for all four divisions for the periods of 1895 to 1970 and 1971 to 2008 is only 0.85 in. or about 10 percent of the overall mean. This uncertainty in the precipitation due to using the normal PRISM grid is negligible compared to the uncertainties associated with other components of the model.

In addition, precipitation is only used as a guide to estimate recharge in the groundwater-budget method used in this study, the volume of recharge is dictated by the estimated volume of discharge from the flow system. Thus, the magnitude of the precipitation is not important in estimating the total volume of recharge for a given flow system. The spatial distribution of precipitation, however, does affect the spatial distribution of recharge and therefore the individual basin's volume of recharge. This issue was addressed in the numerical model using additional constraints (water levels, spring flows, and other observations) to adjust the recharge volumes of the individual basins if necessary.

6.3 Estimated Precipitation Distribution and Comparison to Previous Estimates

The precipitation distribution over the study area was extracted from the 800-m PRISM grid, and the quality of this distribution was evaluated. The distribution was then integrated by hydrographic area to obtain yearly precipitation volumes for all basins in the study area. The resulting volumes were compared to previous estimates.

To ensure the selected PRISM precipitation grid approximated long-term mean conditions, it was compared to the period-of-record mean annual precipitation values of precipitation stations within the study area and vicinity. Precipitation station data were compiled, and the mean annual value for the

SE ROA 50442

JA_15843

period of record was derived for each station. Summary data for the stations located within and near the study area are listed in Appendix D and shown on Figure 6-3. Figure 6-4 depicts the PRISM precipitation distribution within the study area and a relative comparison of the model fit at the precipitation station locations. The comparison shows that the PRISM distribution slightly overestimated the period-of-record mean precipitation values for most stations. As precipitation is subtracted from ET to obtain groundwater ET, the larger estimates of precipitation derived from the PRISM grid will lead to smaller estimates of groundwater ET and, therefore, smaller recharge estimates. This demonstrates that the use of the PRISM precipitation distribution leads to conservative estimates of recharge and is appropriate in this study.

The derived precipitation volumes for all basins in the study area are listed in Table 6-1. Estimates derived for other studies (Scott et al., 1971; Nichols, 2000; LVVWD, 2001; Flint and Flint, 2007) are also listed in this table for comparison. The estimates reported by Scott et al. (1971) are those derived during the NDWR/USGS Reconnaissance investigations and are based on the Hardman (1936) map or subsequent updates. The estimates derived by Nichols (2000) are based on the 4-km PRISM grid for the normal period of 1961 to 1990. The estimates derived by LVVWD (2001) are based on linear relationships between the precipitation station data available at the time and land-surface elevation. The estimates derived by this study are generally larger than those estimated during the Reconnaissance investigations (Scott et al., 1971) but are very similar to the estimates derived for BARCASS (Flint and Flint, 2007).

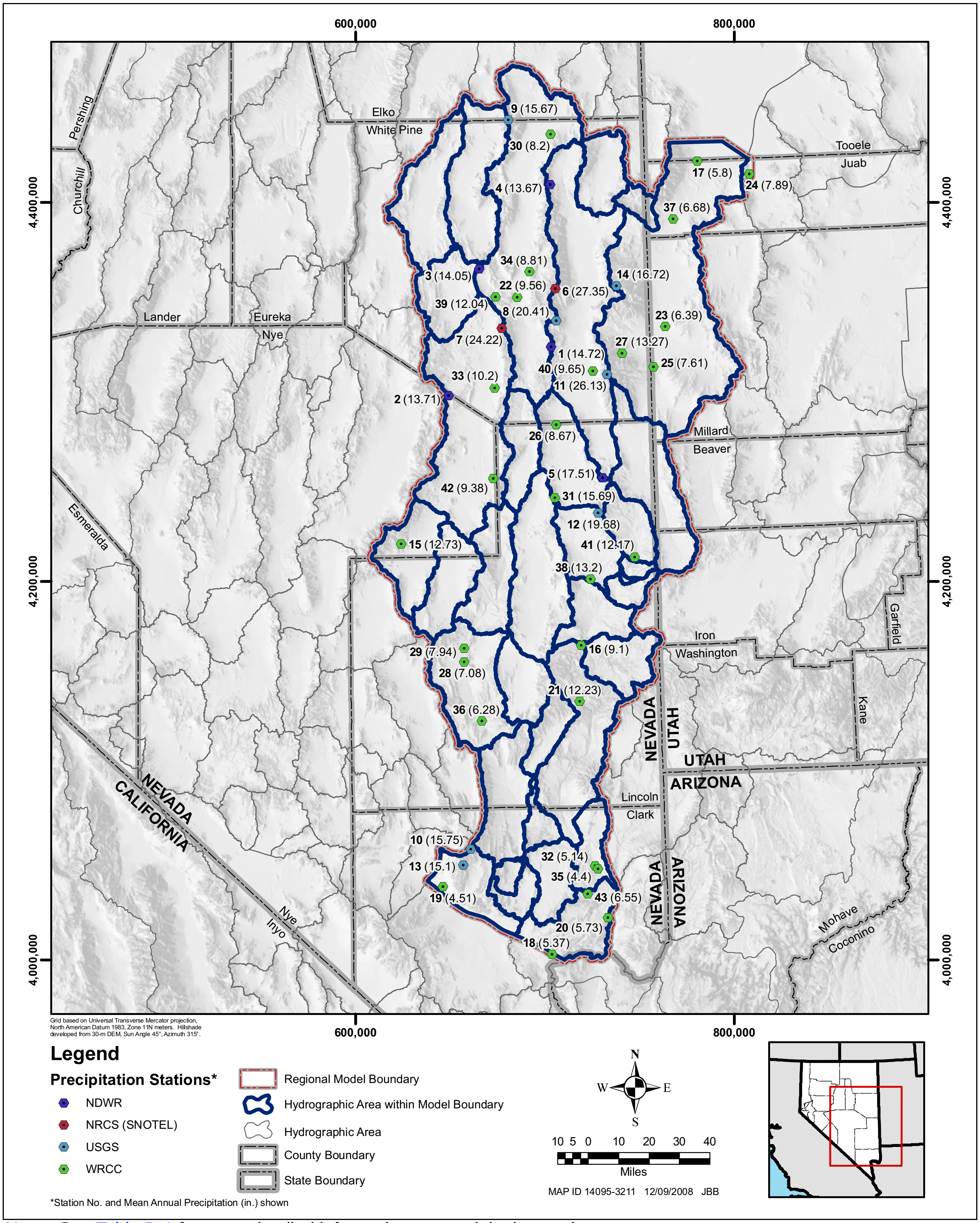

Note: See Table D-1 for more detailed information on precipitation stations.

Figure 6-3
Location of Precipitation Stations and Mean Annual Precipitation within Study Area

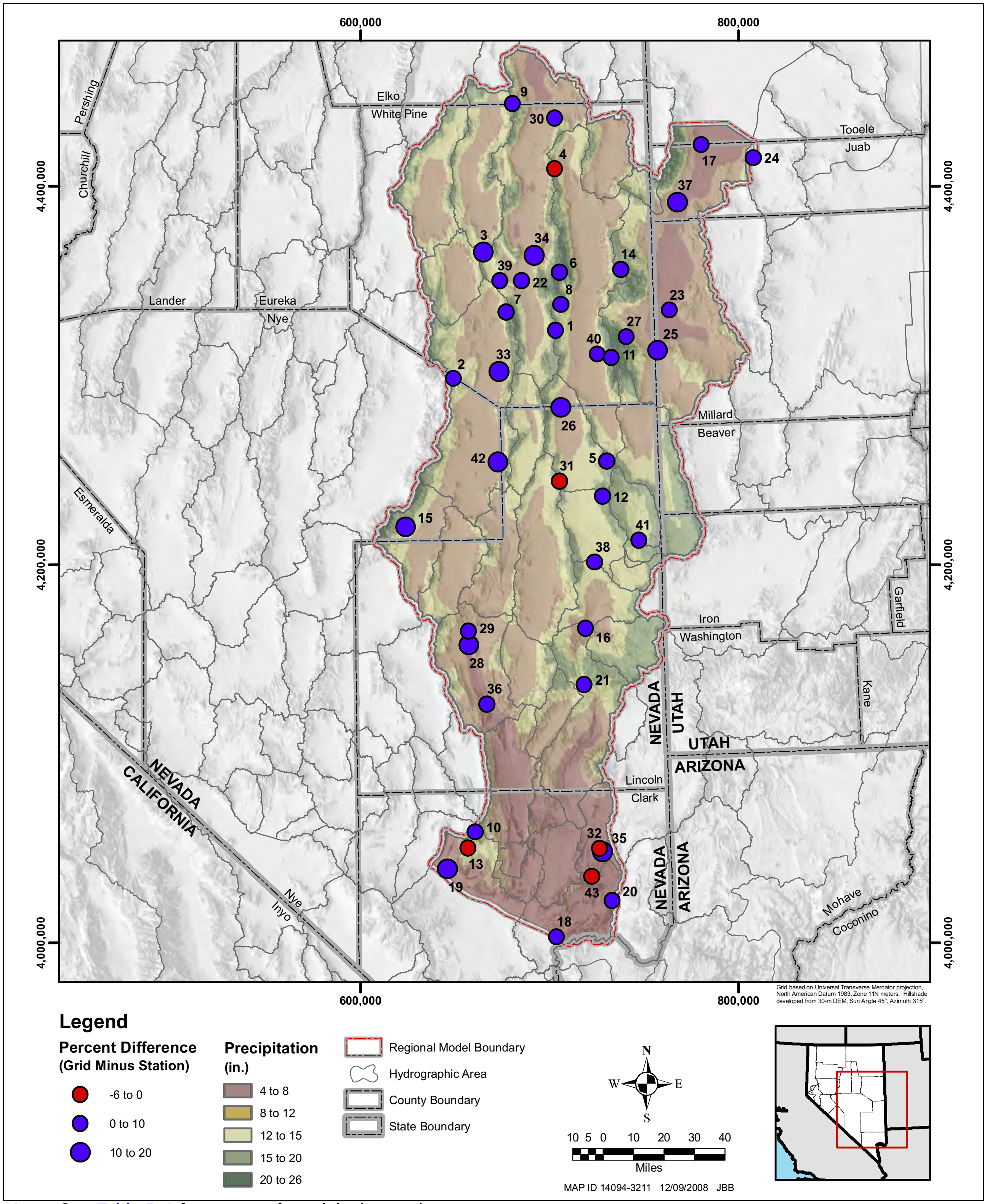

Note: See Table D-1 for names of precipitation stations.

Figure 6-4
PRISM Precipitation Distribution within Study Area and Percent Difference between PRISM and Precipitation Station Data

SE ROA 50445

JA_15846

Table 6-1
Precipitation Volumes in afy for Basins in Study Area

HA Number	HA Name	800-m PRISM (This Study)	Scott et al. (1971)	Nichols (2000)	LVVWD (2001)	Flint and Flint (2007)
Goshute Valley Flow System						
178B	Butte Valley South	502,000	420,000	NE	NE	470,000
179	Steptoe Valley	1,271,000	1,200,000	1,344,191	NE	1,303,000
	Total	**1,773,000**	**1,620,000**	**NE**	**NE**	**1,773,000**
Great Salt Lake Desert Flow System						
184	Spring Valley	1,116,000	960,000	1,141,444	NE	1,131,000
185	Tippett Valley	213,000	160,000	211,905	NE	209,000
254	Big Snake	2,321,000	2,000,000[a]	NE	NE	2,159,000
	Total	**3,650,000**	**3,120,000**	**NE**	**NE**	**3,499,000**
Meadow Valley Flow System						
183	Lake Valley	401,000	290,000	NE	437,000	380,000
202	Patterson Valley	318,000	190,000	NE	275,000	NE
201	Spring Valley	243,000	180,000	NE	212,000	NE
200	Eagle Valley	46,000	28,000	NE	37,000	NE
199	Rose Valley	9,000	5,100	NE	7,000	NE
198	Dry Valley	92,000	50,000	NE	77,000	NE
203	Panaca Valley	234,000	180,000	NE	224,000	NE
204	Clover Valley	307,000	140,000	NE	205,000	NE
205	Lower Meadow Valley Wash	552,000	320,000	NE	523,000	NE
	Total	**2,201,000**	**1,383,100**	**NE**	**1,998,000**	**NE**
White River Flow System						
175	Long Valley	450,000	250,000	452,367	460,000	407,000
174	Jakes Valley	289,000	240,000	289,477	312,000	261,000
207	White River Valley	1,011,000	750,000	NE	1,032,000	892,000
180	Cave Valley	265,000	220,000	NE	258,000	245,000
172	Garden Valley	351,000	230,000	NE	320,000	NE
171	Coal Valley	267,000	170,000	NE	234,000	NE
208	Pahroc Valley	310,000	190,000	NE	260,000	NE
181	Dry Lake Valley	571,000	340,000	NE	455,000	NE
182	Delamar Valley	236,000	140,000	NE	176,000	NE
209	Pahranagat Valley	418,000	270,000	NE	344,000	NE
206	Kane Springs Valley	146,000	80,000	NE	140,000	NE
210	Coyote Spring Valley	272,000	220,000	NE	224,000	NE
219	Muddy River Springs Area	54,000	33,000	NE	38,000	NE
217	Hidden Valley	33,000	28,000	NE	28,000	NE
216	Garnet Valley	55,000	58,000	NE	45,000	NE
218	California Wash	106,000	100,000	NE	76,000	NE
215	Black Mountains Area	169,000	200,000	NE	132,000	NE
220	Lower Moapa Valley	95,000	76,000	NE	101,000	NE
	Total	**5,097,000**	**3,595,000**	**NE**	**4,638,000**	**NE**

NE = Not Estimated
[a] Reported in Hood and Rush (1965)

7.0 GROUNDWATER DISCHARGE TO THE SURFACE

Within the CCRP model area, groundwater discharges to the surface primarily through the process of ET and spring flow. Groundwater may also discharge to the surface directly into streams through the process of upward leakage. At the regional scale, discharge to streams is considered important only for a few of the streams located in the model area, including the Muddy River. Thus, this section includes descriptions of groundwater ET, discharge from major springs, and information supporting groundwater discharge into these streams.

7.1 Groundwater Discharge by ET

The objective of this work was to develop estimates of groundwater ET for relevant basins of the study area using the information available to date. Groundwater ET is a portion of the ET observed at the surface of a given basin. Other sources of water to the ET process include surface water and precipitation. Furthermore, the portion of groundwater ET of interest to this project is from the connected portion of the flow system. In the following discussion, the term "net ET" will refer to total ET less the contribution by precipitation. Depending on the assumption of a given ET study, the difference between ET and precipitation will be termed "net ET" and may represent ET from groundwater or ET from groundwater and surface water. The following items are described: (1) ET process, (2) methodology, (3) compilation of ET and PET rates, (4) deterministic groundwater ET estimates derived for this study, and (5) stochastic groundwater ET estimates.

7.1.1 Evapotranspiration Process

ET is the process whereby water is returned to the atmosphere through evaporation from soil, wet plant surfaces, and open water bodies and through transpiration from plants. The portion of ET that was of interest to this study is groundwater ET, more specifically, ET from plants, open water bodies, and wet playas that are linked to the main groundwater system (regional and intermediate). Groundwater ET is an important component of discharge when conducting basinwide water-resource budgeting in arid and semiarid areas. It is the only budget component that can be observed and estimated with some level of confidence. In general, estimates of groundwater ET may be derived using the basic simplifying assumption that the volume of groundwater ET discharging from a given ET area is equal to the volume of total ET reduced by the volume of precipitation on that area. When added to estimates of underflow for a given groundwater flow system, estimates of groundwater ET can be used with the groundwater-balance method to derive estimates of groundwater recharge.

7.1.1.1 Evapotranspiration by Plants

Evapotranspiration by plants consists of two basic processes: evaporation and transpiration. In the evaporation process, water on the plants and in the soils surrounding the plants is removed by conversion from the liquid phase to the vapor phase. Transpiration is similar to evaporation, but the water is removed from the plant tissues, mostly through small openings on the plant leaves called stomata. The resulting vapor is lost to the surrounding atmosphere (Allen et al., 1998).

The type of plants that use groundwater as a source of water are called phreatophytes. Phreatophytes were first defined by Meinzer (1927, p. 1) as "plants that habitually grow where they can send their roots down to the water table or the capillary fringe immediately overlying the water table and are thus able to obtain a perennial and secure supply of water." Phreatophytes occur in many basins within the study area. However, phreatophytes tapping the water table occur mostly in the northern part of the study area. The phreatophytic plant assemblage present in the study area is composed primarily of greasewood (*Sarcobatus vermiculatus*), saltgrass (*Distichlis spicata*), rabbitbrush (*Chrysothamnus nauseosus*), saltbush (*Atriplex canescens*), spiny hopsage (*Grayia spinosa*), shadscale (*Atriplex confertifolia*), and big sagebrush (*Artemisia tridentata*).

A riparian plant assemblage also occurs within the study area and includes cottonwood (*Populus fremontii*), willow (*Chilopsis linearis*), saltcedar (*Tamarix ramosissima*), mesquite (*Prosopis glandulosa*), cattails (*Typha sp.*) and tules (*Scirpus sp.*). Most riparian vegetation occurs in basins located in the southern part of the study area.

7.1.1.2 Open-Water Evaporation

Evaporation from water bodies is a major component of the hydrologic cycle and a primary process of water loss from open water bodies. As such, it has important implications on water-resource management. Open-water evaporation takes place during energy transfer from an evaporating surface when the vapor pressure in the air is less than the saturated pressure (Rosenberry et al., 2007). Some of the meteorological factors that influence evaporation from water bodies are solar radiation, wind speed, air humidity, and air temperature (Allen et al., 1998). The quantity of evaporated water from open water bodies, such as lakes, reservoirs, and streams and springs, is dependent on the quantity of open water.

Evaporation from water surfaces is rarely measured directly. Rather, it is usually measured by proxy (Kirono and Jones, 2007). A widely used proxy method to calculate evaporation rates from open water bodies is the pan-evaporation method (measuring rates of evaporation from pans filled with water). The decrease in water depth in the pan during a given period equals the amount of water evaporated during that period, provided that no precipitation occurred. The measured evaporation rate implicitly incorporates the effects of radiation, wind, temperature, and humidity prevailing during that period (Allen et al., 1998). If precipitation occurs during that period and is measured nearby, the net amount of evaporated water is derived by subtracting the amount of precipitation from the measured amount of evaporated water. An empirical method is used to derive estimates of evaporation rates from pan-evaporation measurements, applying a coefficient that relates pan evaporation to open-water-body evaporation (Allen et al., 1998).

Basins having major open water bodies in the study area are Jakes Valley, Butte Valley (southern part), Steptoe Valley, Lake Valley, Spring Valley, Snake Valley, Hamlin Valley, Dry Valley, Lower Meadow Valley Wash, White River Valley, Pahranagat Valley, and Lower Moapa Valley. When estimating groundwater ET, it makes sense to include evaporation from open water bodies in the estimate if the surface water is known to originate from groundwater. However, the main source of water to open water bodies is not always known with certainty.

7.1.1.3 Wet-Playa Evaporation

Wet playas are defined here as playas located above a water table shallow enough for groundwater evaporation to occur. Quantitative estimates of groundwater evaporation from wet playas is important to the estimation of a basin’s ET volumes.

The process and magnitude of groundwater evaporation through wet playas yield essential information regarding the relationship of mass and energy fluxes between the ground and the atmosphere (Bittelli et al., 2008). The quantity of evaporated water is influenced by the hydrology and climatic factors of the area. The amount of evaporation depends on the local depth of the water table below the ground surface (Menking et al., 2000). The process is carried out through vapor pressure gradient between soil water and the atmosphere, and this phenomenon is directly related to groundwater depth (Deverel et al., 2005). When the water table is at or near the ground surface, the rate of water loss is equivalent to molecular diffusion of open water bodies driven by the vapor pressure gradient. As the water table gets deeper, the rate of water loss declines, and additional factors, such as the soil’s physical and chemical properties and the meteorological conditions, play an important role in driving ET rates. Deverel et al. (2005) further explain that evaporation from playas with shallow groundwater is affected by the spatial and temporal patterns of physical and chemical properties of the soil. The salinity of wet-playa groundwater also has a great impact on the rate of evaporation (Kampf et al., 2005).

In this study, the largest wet playas occur in Steptoe, Snake, Cave, and White River valleys. Wet playas of lesser extent occur in Lake, Spring, and Tippett valleys.

7.1.2 Methodology

The general method for developing groundwater ET estimates for a given area is described, followed by a description of the methodology used in this study.

7.1.2.1 General Methodology

The general methodology of estimating groundwater ET is described followed by a brief mention of other methods.

In general, estimates of groundwater ET can be made using the simplifying assumption that the volume of groundwater ET discharging from a given ET area is equal to the volume of total ET reduced by the volume of precipitation on that area, expressed by:

$$ET_{gw} = ET_T - P \qquad \text{(Eq. 7-1)}$$

SE ROA 50449

JA_15850

where,

ET_{gw} = Volume of groundwater ET from a given ET unit
ET_T = Volume of total ET from the same given ET unit
P = Volume of precipitation over the same given ET unit

All three terms of Equation 7-1 represent a rate multiplied by the same area (the potential groundwater area). Thus, information needed to derive estimates of groundwater ET volumes for a given period of time are:

- ET rates (total)
- Precipitation rates
- Areas of potential groundwater ET

ET rates can be derived from field measurements or from remote-sensing data. Field measurements of energy variations are made using eddy covariance towers (ET towers). ET rates from remote-sensing data may be derived using the Surface Energy Balance Algorithm for Land (SEBAL) remote-sensing model (Bastiaanssen et al., 2005). Precipitation rates may be obtained as described in the previous section. Areas of potential groundwater ET may be derived from field mapping or from a combination of satellite imagery and field data. To obtain more detailed and accurate groundwater ET volumes, the potential groundwater ET areas are subdivided into classes or units using vegetation type and density, and sometimes soil characteristics, depending on the classification method.

Another methodology of estimating groundwater ET is similar to the one expressed by Equation 7-1 but consists of removing only a portion of the precipitation volume, called effective precipitation. Effective precipitation represents the volume of precipitation residing in the root zone that is actually used by the plants. In this method, ET areas and ET and precipitation rates may be measured as described above. Note that this method generally yields larger estimates of groundwater ET, as less precipitation is assumed to be available to the plants.

Similar methods for estimating groundwater ET were applied by Nichols (1993, 1994) and Nichols et al. (1997). In these methods, groundwater ET rates are estimated separately and integrated over the period when plants transpire groundwater only. Furthermore, the groundwater ET rates are related to the leaf area index and the depth to water to derive estimates of annual groundwater ET volumes for areas covered by specific plants. Nichols (2000) used ET information collected by Nichols (1994), Nichols et al. (1997), and Duell (1990) to estimate groundwater ET for basins in Nevada. Nichols (2000) developed two equations, one relating groundwater ET to plant cover and the other one relating groundwater ET to depth to water. He found that the correlation between groundwater ET and plant density is much stronger and used it together with satellite imagery to derive estimates of annual groundwater ET volumes for the basins in the study area. This method of groundwater ET estimation generally yields larger estimates of groundwater ET volumes. The larger estimates may be because the groundwater ET rates derived by this method contain some precipitation or because other methods remove some of the groundwater contribution by assuming it is precipitation.

7.1.2.2 Methodology Used in this Study

The groundwater ET estimates for this study had to include ranges of uncertainty. Thus, deterministic and stochastic estimates were derived.

To derive one set of deterministic estimates, two methods were considered, compared, and combined. The first method (Method 1) was developed as part of this study for the whole study area. The second method (Method 2) is that used by Welch et al. (2008) in BARCASS and by DeMeo et al. (2008) in the southern part of the Colorado Regional Ground-Water Flow System. The combination of these two methods constitutes the deterministic method adopted for this study. The BARCASS estimates (Method 2) required simplification that will be explained in Section 7.1.8. Estimates made by DeMeo et al. (2008) (Method 2) were not fully incorporated in the analysis. Rather, estimates for selected basins were later incorporated in the deterministic estimates for the CCRP model.

In Method 1, potential areas of groundwater ET are delineated and classified, and published ET rates are compiled and evaluated. Appropriate rates are selected, adjusted to local PET conditions, and applied to the delineated potential groundwater ET areas in each basin. The 800-m PRISM precipitation grid is then used to remove the ET volume associated with precipitation as the source.

In Method 2, potential areas of groundwater ET are delineated and classified similarly to Method 1 but with more detail. Welch et al. (2008) and DeMeo et al. (2008) handled the ET rates differently. Welch et al. (2008) derived mean ET rates from the literature and adjusted them to local conditions using the Modified Soil Adjusted Vegetation Index (MSAVI) method (Qi et al., 1994). DeMeo et al. (2008) estimated annual ET rates from measurements or used published ET rates for similar environments. The ET rates were then multiplied by the corresponding potential groundwater ET areas and adjusted for precipitation. DeMeo et al. (2008) reported that their estimates of ET included ET from groundwater and surface water.

Stochastic estimates of mean annual groundwater ET volumes were derived using the information in the deterministic estimates and other available information as necessary. This stochastic analysis was implemented using the Monte Carlo method via Crystal Ball software.

The information needed to derive the groundwater ET estimates by the methods described above includes previous interpretations and historical data, as well as the most recent data, including ET rate measurements, remote-sensing data, and field verification. The overall process consists of the following steps: (1) compilation of ET rate data, (2) derivation of groundwater ET estimates by Method 1, (3) derivation of groundwater ET estimates by Method 2, (4) derivation of groundwater ET estimates for the groundwater flow model by combining Method 1 with a simplified Method 2, and (5) calculation of stochastic estimates of groundwater ET volumes. Each of these steps is described in the following text.

7.1.3 ET Rates and Related Information

The available measurements of total ET rates, groundwater ET rates, and related information were compiled from the literature and are presented in Appendix E. The ET process and the variables that affect it are discussed in this section.

ET rates vary greatly spatially and temporally and are affected by a number of factors including air temperature, relative humidity, wind, water availability, plant type and coverage, and soil type. The rates generally increase with temperature (during the growing season), wind, and water availability within limits and with plant density and leaf area. The rates generally decrease as the relative humidity of the air increases.

Phreatophytes extract water from both the unsaturated and saturated zones through the process of ET. Different phreatophytic species, however, use the available water at different rates. Groundwater ET emanating exclusively from the saturated zone is difficult, if not impossible, to measure separately. ET rates derived from field data (using ET towers) represent the total ET rates from the plants and the soils under and around the plants. The measured ET rates may include several sources of water: groundwater and soil moisture uptake by the plants, groundwater and soil moisture lost by evaporation, and water on the plant leaves lost by evaporation. The following simplifying assumption is usually made to derive mean annual groundwater ET rates: all sources of water, other than groundwater, can be attributed to the mean annual precipitation. Estimates of groundwater ET rates can then be obtained by subtracting the local mean annual precipitation rate from the measured annual ET rate.

ET rates are at their maximum when the water table is at the land surface and are approximated by measurements of PET. They decrease with increasing depth to water and reach zero at the extinction depth (Shah et al., 2007). The depth at which ET ceases is called the ET-extinction depth. This depth is important because it affects the magnitude of groundwater ET rates. Phreatophytes, in essence, pump groundwater from the water table to the atmosphere through their root systems. Thus, rooting depths of phreatophytes are good indicators of the extinction depths of groundwater ET.

Groundwater-ET-extinction depths are influenced by several physical characteristics. Soil characteristics, for example, can have an impact on the maximum rooting depth. For instance, a phreatophyte in a sandy clay soil can have a greater extinction depth than in sandy loam (Shah et al., 2007). Conventionally, it was believed that the relationship between depth and groundwater ET is linear, but as mentioned above, different soil characteristics with different phreatophytes could generate different relationships. For example, Shah et al. (2007) found an exponential decline of groundwater ET with increasing depth to water.

A literature survey for annual ET rates measured in the study area and vicinity was conducted and the rates were compiled into the data set presented in Table E-1 (Appendix E). Additionally, selected ET data derived from on-going SNWA studies were used. A description of the SNWA field ET sites is presented in Appendix A. Annual ET rates measured by DeMeo et al. (2008) are not included in Table E-1 because they did not become available until the data analysis was completed. They are, however, comparable to the rates listed in Table E-1 for similar vegetation types.

A literature survey was conducted to compile the available phreatophyte rooting depths for the phreatophytes present in the study area. Together with the depth-to-water data (see SNWA, 2008a), rooting depths help identify ET-extinction depths (Appendix E, Table E-2).

The PET rates were calculated using a regression equation derived from PET data compiled by McCurdy and Albright (2004). The PET calculation details are provided in Appendix E. The spatial distribution is provided on Figure E-1 (Appendix E).

7.1.4 Method 1 - Groundwater ET Estimates

The groundwater ET estimates were developed as follows: (1) delineation of groundwater ET areas, (2) identification of mean annual ET rates, and (3) calculation of groundwater ET volumes. Each of these steps is described in the following subsections.

7.1.4.1 Delineation of Groundwater ET Areas

The groundwater ET areas of interest were identified in three steps: (1) a "current-condition" map was developed using satellite imagery and other information; (2) this map was then converted to predevelopment conditions; and (3) groundwater ET areas delineated in the predevelopment map were evaluated to interpret the source of the water.

Method 1 - "Current-Condition" ET Map

SNWA defined the outer boundaries of the groundwater ET areas, subdivided them into classes, and assessed the accuracy of this classification through field investigations. This work is summarized in the following text.

The SNWA current-condition ET map (Figure 7-1) was derived using 2002 satellite imagery together with the USGS 1:100,000 scale topographic maps and phreatophytic areas mapped by previous studies. The 2002 image was used to confirm and/or refine the phreatophytic areas and define any additional areas where no previous remote-sensing analysis had been conducted. Phreatophytic communities are typically located on the relatively flat areas of a basin between mountain blocks. To ensure that all potential groundwater ET areas were identified, flat areas were defined as land expanses in the basin where the land-surface slope is less than or equal to 10 percent. These areas were initially defined by performing a slope analysis in ArcGIS®, using USGS 30-m National Elevation Dataset (NED) seamless DEMs and masking out any land-cover features that fell on slopes greater than 10 percent.

The groundwater ET areas were delineated based on a compilation of earlier work described in the Reconnaissance Series, LVVWD et al. (1994), LVVWD (2001), and Nichols (2000). Occasionally, the Southwest Regional Gap Analysis Project (SWReGAP) data (USGS, 2004) and the National Land Cover Data (NLCD, 1992) were used if there was great uncertainty over the location of a boundary. Boundaries of many, but not all, of the phreatophytic areas were checked in the field during the summer of 2004 by SNWA and modified as needed using high-resolution global positioning system equipment.

Areas of groundwater ET representing current conditions were then classified using Normalized Difference Vegetation Index (NDVI) and Landsat 7 Thematic Mapper 2002 satellite imagery. To represent current conditions, the areas of groundwater ET were classified into six categories: Open Water, Bare Soil/Low Vegetation, Phreatophyte/Medium Vegetation, Wetland/Meadow, Agriculture,

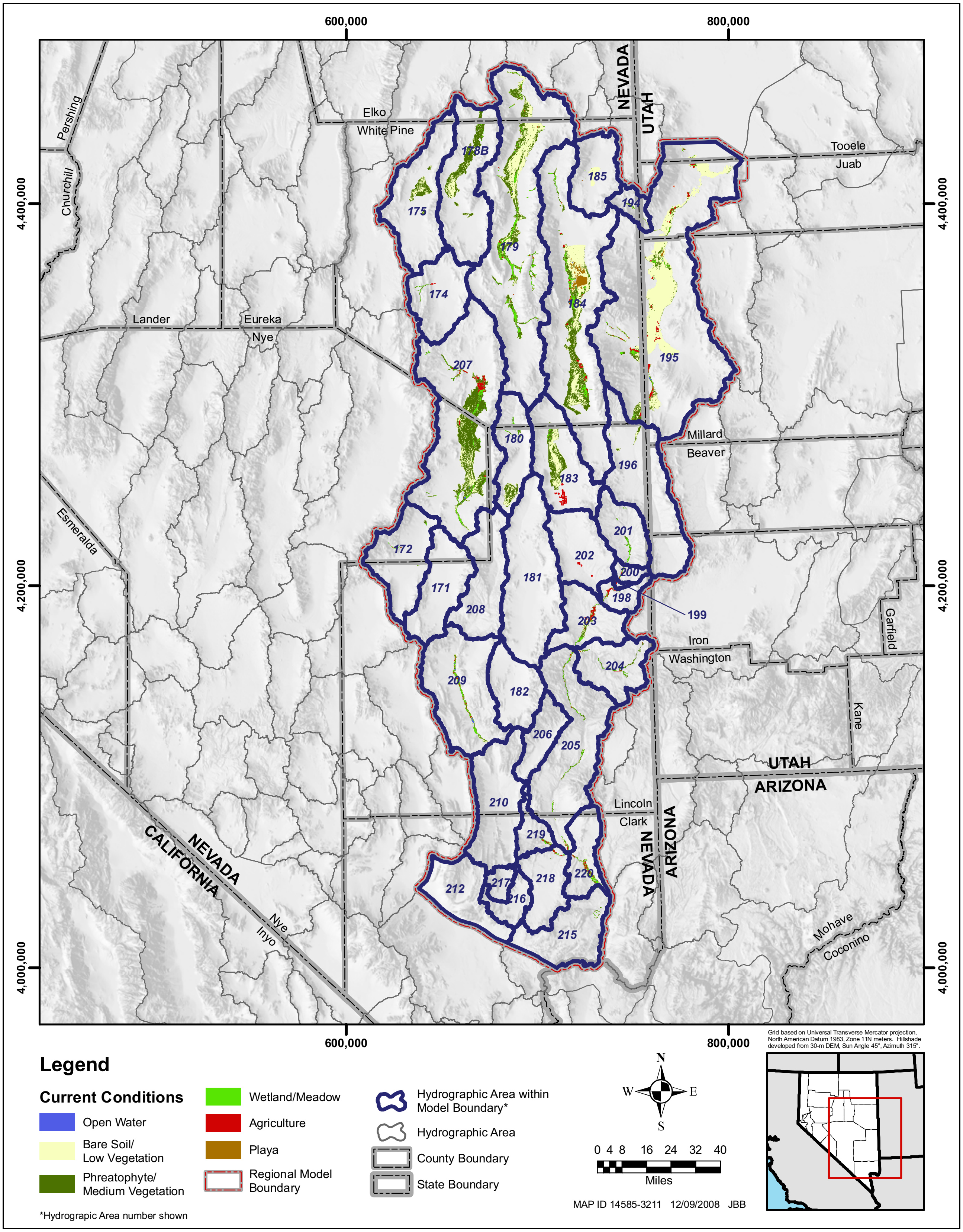

Figure 7-1
Method 1 - "Current-Condition" Groundwater ET Map

SE ROA 50454

JA_15855

and Playa (Table 7-1). A number of transects were generated to supplement the remote-sensing techniques in defining phreatophytic-area boundaries across the landscape. Transects are strips of land across the groundwater ET areas along which estimates of the percent cover and density of the vegetation community were made and recorded. Percent cover was estimated as the fraction of the line that is covered by each species, and density estimates were calculated using strip transects as described in Barbour et al. (1987).

An assessment was completed to evaluate the accuracy of the land classification using accepted protocols as outlined in Congalton and Green (1999). A total of 249 randomly selected points representing each classification were field checked. This assessment returned an overall accuracy of 88 percent. The detailed results are presented by ET class in Table F-4 (Appendix F). This value is above the generally accepted value of 85 percent as established by Anderson et al. (1976). These accuracies suggest that the error on the areas of the delineated classes is approximately 12 percent on average.

Table 7-1
Method 1 - Land-Cover Classification

ET Class	Classification	Description	Depth-to-Water Range (ft bgs)
1	Open Water	Bodies of open water fed by groundwater sources (direct hydraulic connection, springs, seeps, etc.)	Above ground surface
2	Bare Soil/Low Vegetation	Shrubland less than or equal to 20% plant cover - Areas dominated by bare soil and low- to moderate-density desert shrubland, including greasewood, rabbit brush, and other phreatophytic species	Mostly 10 to >30 ft bgs (Roots have been observed at depths up to 175 ft bgs)
3	Phreatophyte/ Medium Vegetation	Shrubland with plant cover greater than 20% - Areas dominated by desert shrubland, including mixed stands of medium-density greasewood, rabbit brush, and other phreatophytic species	2 to 60
4	Wetland/Meadow	Area of shallow groundwater near bodies of open water consisting of wetland vegetation, marshland, woodland, and dense meadows - additionally includes riparian corridors in the southern part of study area, consisting of saltcedar, desert willows, cottonwood, and mesquite trees with underlying shrubs and grasses	0 to 20
5	Agriculture	Agricultural lands identified from 2002 satellite image and field observations	NA
6	Playa	Bare-soil flat areas located in the bottoms of some basins. Classified as potential groundwater ET areas in basins where the water table is within 10 ft of the land surface	0 to 10

Method 1 - Predevelopment Map

The SNWA current-condition groundwater ET map was converted to predevelopment conditions by removing the agricultural areas from the map. For agricultural areas located within phreatophytic areas, it was assumed that these areas had displaced what otherwise would have been phreatophytes prior to development. It was also assumed that the majority of water being used for agricultural purposes originated within the phreatophytic areas prior to development. This seems to be an appropriate assumption for the regional conceptual evaluation described in this report. These agricultural areas were reclassified to represent the phreatophytes they apparently displaced, which in most cases were Wetland/Meadow. Agricultural areas located outside of phreatophytic areas were simply deleted from the groundwater ET map.

In addition, all playa areas represented on the current-condition map were changed to reflect, as closely as possible, playa areas as documented in the NDWR/USGS Reconnaissance Series. These changes were particular to Spring Valley and Snake Valley. Rush and Kazmi (1965) describe two playas totaling 11,600 acres in Spring Valley. Hood and Rush (1965) describe a series of playas from Trout Creek southward to Bishop Springs totaling 3,200 acres in Snake Valley. In addition, 60,000 acres were added to include the Great Salt Lake Playa (the portion occurring within the hydrographic boundary of Snake Valley) as delineated in Hood and Rush (1965). Eakin (1962) defines a playa for Cave Valley but does not identify it as a discharging playa. This area, located in the southern portion of Cave Valley, is vegetated with a large greasewood community and is likely contributing to the total ET in the Basin. This area is illustrated on the steady-state map but is represented as a combination of Bare Soil/Low Vegetation and Phreatophyte/Medium Vegetation. An inherent challenge in all geographic information system (GIS) applications is attempting to create polygons of the exact acreage. Therefore, the acreages reflected on the steady-state map do not exactly match one-to-one with the NDWR/USGS reconnaissance maps. Polygons were created as accurately as possible to reflect the acreages reported. The predevelopment map developed by SNWA is shown on Figure 7-2.

Method 1 - Evaluation of Groundwater ET Areas

The predevelopment ET map developed by Method 1 (Figure 7-2) most likely includes all major groundwater ET areas. However, the type of aquifer that feeds each of the groundwater ET areas, whether local and disconnected or part of the main groundwater system, still remains unknown. The main groundwater system is defined here as the union of the regional and intermediate flow systems, which are generally hydraulically connected to each other. The main groundwater system is the only part of the flow system that may be included in a regional numerical model, such as the one constructed for this study. Perched or local groundwater is definitely not part of this main flow system. Semi-perched groundwater within the valley fill is part of the main flow system but may not be included in the numerical flow model.

The groundwater ET areas were evaluated for their level of connectivity to the main flow system. Three categories of groundwater ET areas were created based on the following criteria:

- Size of the groundwater ET area
- Topography of the groundwater ET area and its relative location within the basin

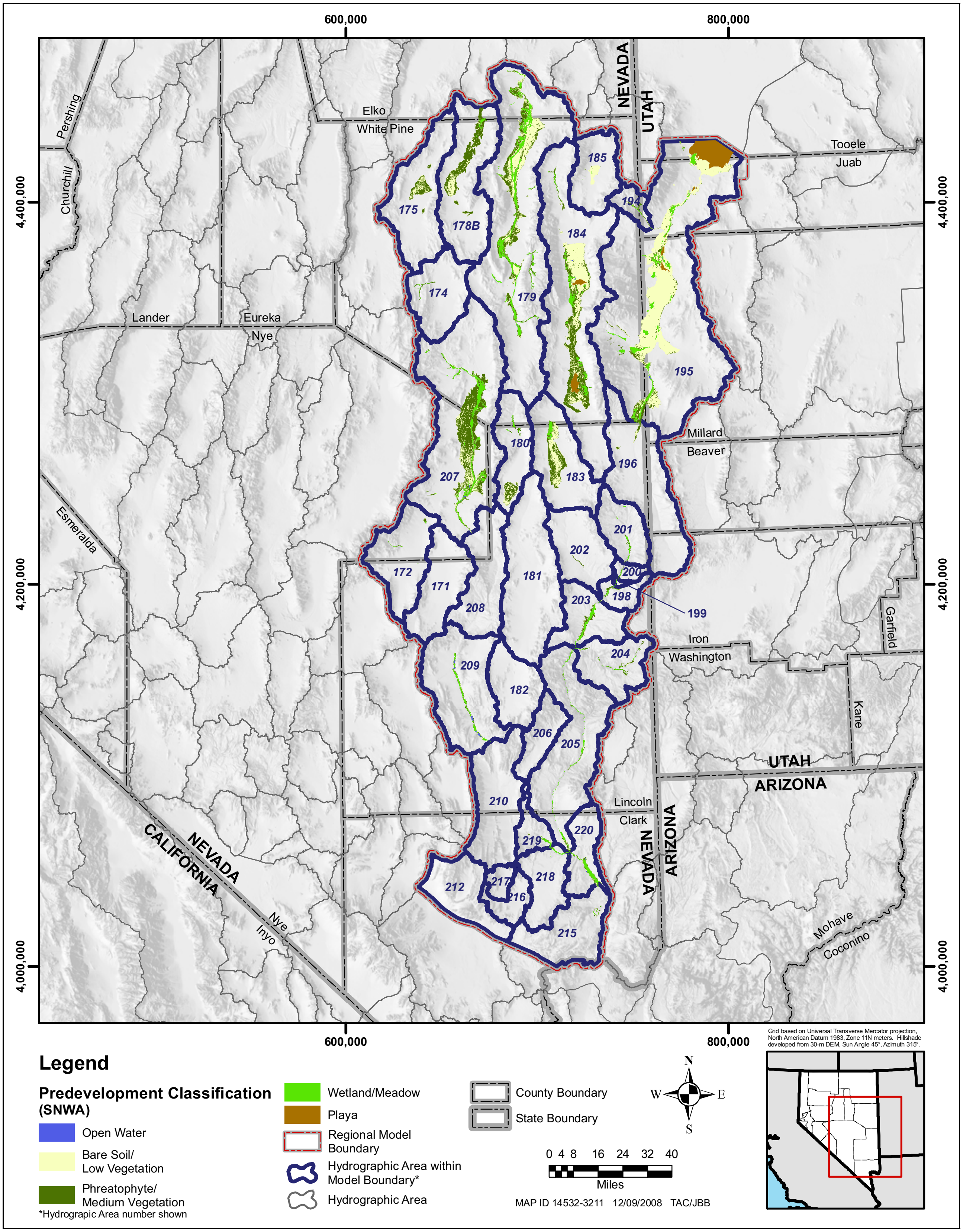

Figure 7-2
Method 1 - Predevelopment Groundwater ET Map

- Estimated depth to main groundwater flow system within the groundwater ET area
- Apparent source of water sustaining the groundwater ET area
- Previous classification of groundwater ET area

The depth to water on the valley floors was used as an indicator of groundwater-ET-extinction depths. A maximum extinction depth of 100 ft was selected as the cutoff value beyond which significant amounts of phreatophytes could not occur. Thus, the 100-ft depth-to-water contour was only used as a guide to identify the approximate location of the outermost (maximum) boundary of groundwater ET areas on the valley floors. An examination of the ET map superposed onto depth-to-water data including contours shows that most of the ET areas are located within the 50-ft contour line (SNWA, 2008a). The contours represent the depth to the main groundwater system. Some of the large ET areas extend outside of the 50-ft contour line. They, however, are within the 100-ft contour line. The main groundwater ET areas were assumed to occur where the depth to the main groundwater system is within 100 ft of the ground surface. These areas were assigned a category of 1 or 2 depending on the other criteria. A few isolated phreatophyte "islands" exist away from the main phreatophytic areas (Categories 1 and 2). A closer look at the depth-to-water data indicates that semi-perched or perched conditions may exist in these groundwater ET areas (categorized as 2 or 3, depending on their conditions).

The results of this evaluation are summarized in Table 7-2. The available depth-to-water information is sparse and provides an uncertain understanding of the water table. Thus, this information was only used as a guide. In addition, phreatophytes in areas where the water table is rather deep (about 50 to 100 ft bgs) may be facultative. This condition applies to the groundwater ET areas flagged as Category 2 (Table 7-2). Each category is further discussed in the following text.

Table 7-2
Categorization of Groundwater ET Areas

Category	Size of Groundwater ET Area	Location of Groundwater ET Area	Depth to Main Groundwater Flow System	Source of Water
1	Area > 1 km^2 or length > 1 km	Valley floor	< 100 ft	Shallow water table, or regional springs
2	Area > 1 km^2 or length > 1 km	Valley floor or alluvial fans	50 to 100 ft	Not fed by a spring
3	Area may be < 1 km^2 or length may be < 1 km	Alluvial fans or mountain block	> 100 ft	Ephemeral spring or stream

Category 1 - These groundwater ET areas are most likely either in complete hydraulic connection with the main groundwater system or known to be sustained by regional springs. These areas were considered appropriate for inclusion in numerical models at the regional scale.

Category 2 - These groundwater ET areas may have a complete or partial (semi-perched) hydraulic connection with the main groundwater system, but actual conditions are uncertain.

Category 3 - These groundwater ET areas are typically smaller than 1 km^2 (the resolution of the numerical model) or have no hydraulic connection with the main groundwater system (perched). These areas were not included in the numerical model.

The total areas categorized as 2 and 3 are small compared to the area categorized as 1. To allow calculation and evaluation of the associated ET volumes, groundwater ET areas categorized as 2 and 3 were not removed from the map (Table 7-3). Although the areas categorized as 2 or 3 may not have been appropriate for inclusion in the numerical groundwater flow model, they must be included in groundwater budgets designed to evaluate water resources because the groundwater supporting the associated phreatophytes is part of the water yield for the valley. The three categories of groundwater ET areas were superposed onto the extents of the predevelopment groundwater ET areas and are depicted on Figure 7-3.

7.1.4.2 Method 1 - ET Rates

To derive ET rates for use in the calculations of groundwater ET for Method 1, appropriate ET rates were selected from those available in the literature and were scaled by PET. The literature ET rates, the PET rates, and the data selected are described in the following text.

Available annual ET rates were compiled from the literature for the study area and the region surrounding it. The resulting data set comprises both field measurements and average rates estimated from basin ET volumes and is presented in Table E-1 (Appendix E).

The PET rates were calculated using a regression equation derived from PET data compiled by McCurdy and Albright (2004). The PET calculation details are provided in Appendix E. The spatial distribution is presented on Figure E-1 (Appendix E).

The available ET rates (Table E-1) were reviewed to select the most appropriate rates for each of the five ET classes defined for this analysis. The rates selected for each class were based on the similarities between the vegetation types and the climate, and the availability of supporting data, such as site coordinates, precipitation, and depth to water. The selected ET rates are presented in Table F-1 (Appendix F).

ET-rate measurements for a given ET class were adjusted before being applied to the basins in the study area. The adjustment was performed using PET rates and consisted of scaling the measurements by the ratio of the PET of ET class to that of the ET site (PET of ET class/PET of ET site). The final adjusted ET rates for all classes in all basins are also presented in Table F-2 (Appendix F).

7.1.4.3 Method 1 - Groundwater ET Volumes

Groundwater ET volumes for a given area were calculated as the difference between the total ET volume and the precipitation volume on the area. The volumes were calculated for each class in each basin by multiplying the rates by the groundwater ET area and were summed to derive a volume for the basin. The groundwater ET areas are based on the predevelopment ET map (Figure 7-3).

Total ET volumes were calculated for each ET class for each basin where groundwater ET occurs by multiplying the appropriate PET-scaled ET rate by the area of the ET class.

Table 7-3
Method 1 - Area of Groundwater ET Areas By Category

HA Number	HA Name	Category 1 Area	Category 2 Area	Category 3 Area
		(acres)		
Goshute Valley Flow System				
178B	Butte Valley South	51,100	0	0
179	Steptoe Valley	157,900	1,200	4,400
	Total	**209,000**	**1,200**	**4,400**
Great Salt Lake Desert Flow System				
184	Spring Valley	171,400	100	600
185	Tippett Valley	7,800	0	0
194	Pleasant Valley	0	0	2,100
195	Snake Valley	307,200	2,300	2,400
196	Hamlin Valley	2,900	400	100
	Total	**489,200**	**2,800**	**5,300**
Meadow Valley Flow System				
183	Lake Valley	47,400	0	0
198	Dry Valley	2,100	0	0
199	Rose Valley	300	0	0
200	Eagle Valley	600	0	0
201	Spring Valley	2,200	100	100
202	Patterson Valley	800	0	0
203	Panaca Valley	9,100	0	0
204	Clover Valley	500	0	3,000
205	Lower Meadow Valley Wash	7,800	0	0
	Total	**70,900**	**100**	**3,100**
White River Flow System				
172	Garden Valley	600	0	300
174	Jakes Valley	0	0	1,000
175	Long Valley	17,000	600	0
180	Cave Valley	1,800	14,700	200
207	White River Valley	140,800	3,300	700
209	Pahranagat Valley	8,700	0	0
215	Black Mountains Area	500	0	0
218	California Wash	1,400	0	0
219	Muddy River Springs Area	2,000	0	0
220	Lower Moapa Valley	7,500	0	0
	Total	**180,200**	**18,500**	**2,200**
	Grand Total	**949,300**	**22,600**	**15,000**

Note: Values are rounded to the nearest hundred (see Table F-2). Totals are rounded from the totals reported in Table F-2.

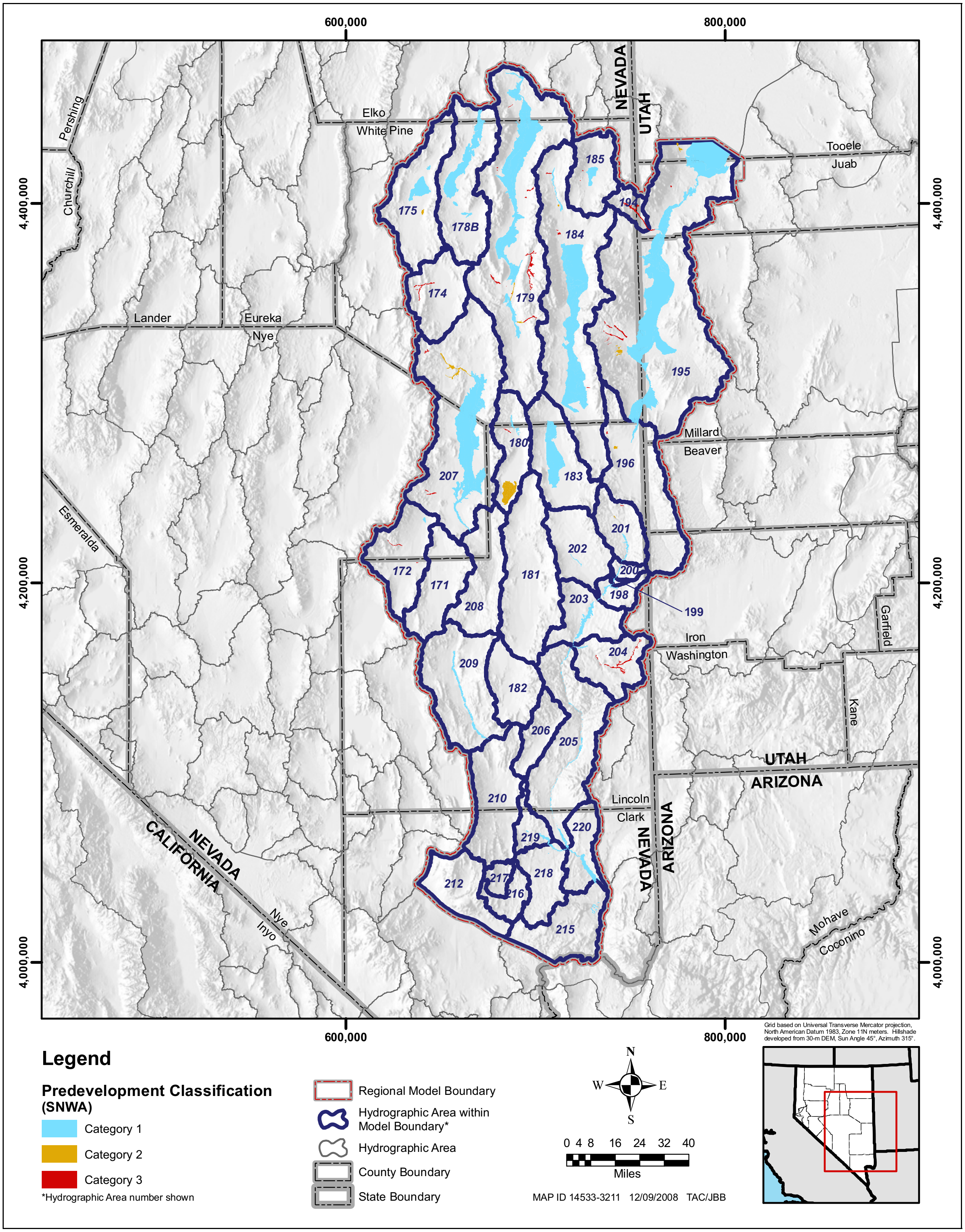

Figure 7-3
Method 1 - Predevelopment Groundwater ET Map Showing Categories

The precipitation rates were obtained from the 800-m PRISM grid by averaging the grid cell values for each ET class within basins where groundwater ET occurs. This is consistent with the simplifying assumption that the observed vegetation within the potential groundwater ET area uses both groundwater and soil moisture (from precipitation) as sources. The precipitation rates are presented in Table F-2 (Appendix F).

The groundwater ET volumes were calculated for each class by subtracting the corresponding precipitation volume (from the 800-m PRISM grid) from the total ET volumes. The groundwater ET volumes were then summed to derive the total volume for the basin. The ET areas and their ET, precipitation, and groundwater ET volumes are presented in Table F-2 (Appendix F). The groundwater ET volumes are summarized by category in Table 7-4. As can be seen from this table, most of the groundwater ET is from areas categorized as 1. The groundwater ET volumes from areas categorized as 2 and 3 constitute less than 5 percent of the total groundwater ET in the study area.

7.1.5 Method 2 (USGS) - Groundwater ET Estimates

The groundwater ET estimates derived for BARCASS (Welch et al., 2008) and for the southern part of the Colorado Regional Ground-Water Flow System (DeMeo et al., 2008) deserve further consideration in this study because they are more detailed than the estimates derived using Method 1. In fact, for BARCASS, Smith et al. (2007) used and refined SNWA's interpretation of the extent of the groundwater ET areas (described under Method 1). Summary descriptions of the methods and results of Welch et al. (2008) and DeMeo et al. (2008) follow.

7.1.5.1 Method 2 - Groundwater ET Areas

Smith et al. (2007) (BARCASS) and DeMeo et al. (2008) used similar methods to identify the ET units within their respective study area. The USGS identifies ET units as areas of similar plant type, density, and vigor (DeMeo et al., 2008). The two methods are summarized below.

BARCAS Study

Smith et al. (2007) used the boundaries delineated by Harrill et al. (1988), Nichols (2000), and SNWA (2008a) to refine the outer limits of the potential groundwater discharge areas located within the BARCASS area. They combined and compared these existing boundaries and resolved the discrepancies they found during field verification trips in mid-July 2005.

Smith et al. (2007) subdivided the potential groundwater ET areas into 11 units using data from SWReGAP ecological systems, interpreted Landsat data from multiple dates (2005), and Landsat MSAVI and Tasseled Cap products. The eleven ET units are as follows:

- Xerophytic
- Open water
- Marshland
- Meadowland
- Grassland
- Moist bare soil

Table 7-4
Method 1 - Groundwater ET Volumes by Category

HA Number	HA Name	Groundwater ET Volumes (afy)			
		Category 1	**Category 2**	**Category 3**	**Total**
	Goshute Valley Flow System				
178B	Butte Valley South	11,300	0	0	11,300
179	Steptoe Valley	103,500	1,600	5,300	110,400
	GVFS Total	**114,800**	**1,600**	**5,300**	**121,700**
	Great Salt Lake Desert Flow System				
184	Spring Valley	71,700	0	300	72,100
185	Tippett Valley	1,900	0	100	2,000
194	Pleasant Valley	0	0	1,000	1,000
195	Snake Valley	131,700	2,700	2,700	137,200
196	Hamlin Valley	1,300	200	100	1,500
	GSLDFS Total	**206,600**	**2,900**	**4,100**	**213,600**
	Meadow Valley Flow System				
183	Lake Valley	6,800	0	0	6,800
198	Dry Valley	3,700	0	0	3,700
199	Rose Valley	600	0	0	600
200	Eagle Valley	1,000	0	0	1,000
201	Spring Valley	3,700	100	100	3,900
202	Patterson Valley	1,300	0	0	1,300
203	Panaca Valley	18,900	0	0	18,900
204	Clover Valley	800	0	4,400	5,200
205	Lower Meadow Valley Wash	21,900	0	0	21,900
	MVFS Total	**58,700**	**100**	**4,600**	**63,400**
	White River Flow System				
172	Garden Valley	1,100	0	600	1,700
174	Jakes Valley	0	0	400	400
175	Long Valley	2,800	100	0	3,000
180	Cave Valley	1,100	0	200	1,300
207	White River Valley	63,200	3,900	500	67,600
209	Pahranagat Valley	28,500	0	0	28,500
215	Black Mountains Area	1,400	0	0	1,400
218	California Wash	4,500	0	0	4,500
219	Muddy River Springs Area	6,000	0	0	6,000
220	Lower Moapa Valley	25,300	0	0	25,300
	WRFS Total	**134,000**	**4,100**	**1,600**	**139,700**
	Grand Total	**514,100**	**8,700**	**15,600**	**538,400**

Note: Values are rounded to the nearest hundred (see Table F-2). Totals are rounded from the totals reported in Table F-2.

- Dense desert shrubland
- Moderately dense desert shrubland
- Sparse desert shrubland
- Dry playa
- Recently irrigated cropland—historically mixed phreatophyte

Except for the xerophytic areas, which consist of bare dry soil and/or sparse, non-phreatophytic vegetation, all other identified ET units may contribute to the volume of ET from groundwater. The derived distribution of potential groundwater ET areas is presented in Figure 7-4. The 10 areas of potential groundwater ET were used to estimate groundwater discharge for predevelopment conditions (Welch et al., 2008). The potential groundwater ET areas were further subdivided by sub-basins (Figure 7-4).

DeMeo et al. (2008)

DeMeo et al. (2008) delineated and classified the study area into eight ET units primarily based on information from multispectral satellite imagery and SWReGAP data. Similarly to BARCASS, the MSAVI method was used to classify the ET units. The eight ET units identified are as follows:

- Dense meadowland vegetation (DMV)
- Dense woodland vegetation (DWV)
- Moderate woodland vegetation (MWV)
- Dense shrubland vegetation (DSV)
- Moderate shrubland vegetation (MSV)
- Agricultural unit (AGU)
- Open water unit (OWU)
- Non-phreatophytic unit (NPU)

More than 99 percent of the study area is occupied by xerophytes (non-phreatophytic unit). Areas covered with xerophytes do not contribute to the volume of ET from surface water and groundwater. The distribution of the groundwater and surface-water ET areas delineated by DeMeo et al. (2008) are shown in their Plate 1 (DeMeo et al., 2008).

7.1.5.2 Method 2 - ET Rates

Welch et al. (2008) (BARCASS) and DeMeo et al. (2008) used different methods to identify the ET rates for the ET units they identified. The two methods are summarized below.

Welch et al. (2008) BARCASS

Welch et al. (2008) derived a range of ET rates for each of the ET units they identified from the literature. They state that:

> ET rates reported in the more recent literature (Nichols, 2000; Berger et al., 2001; Reiner et al., 2002; Cooper et al., 2006) were used to develop a range of average annual ET for each ET unit inclusive of the variations associated with the different vegetation and soil-moisture conditions making up the ET units delineated for the

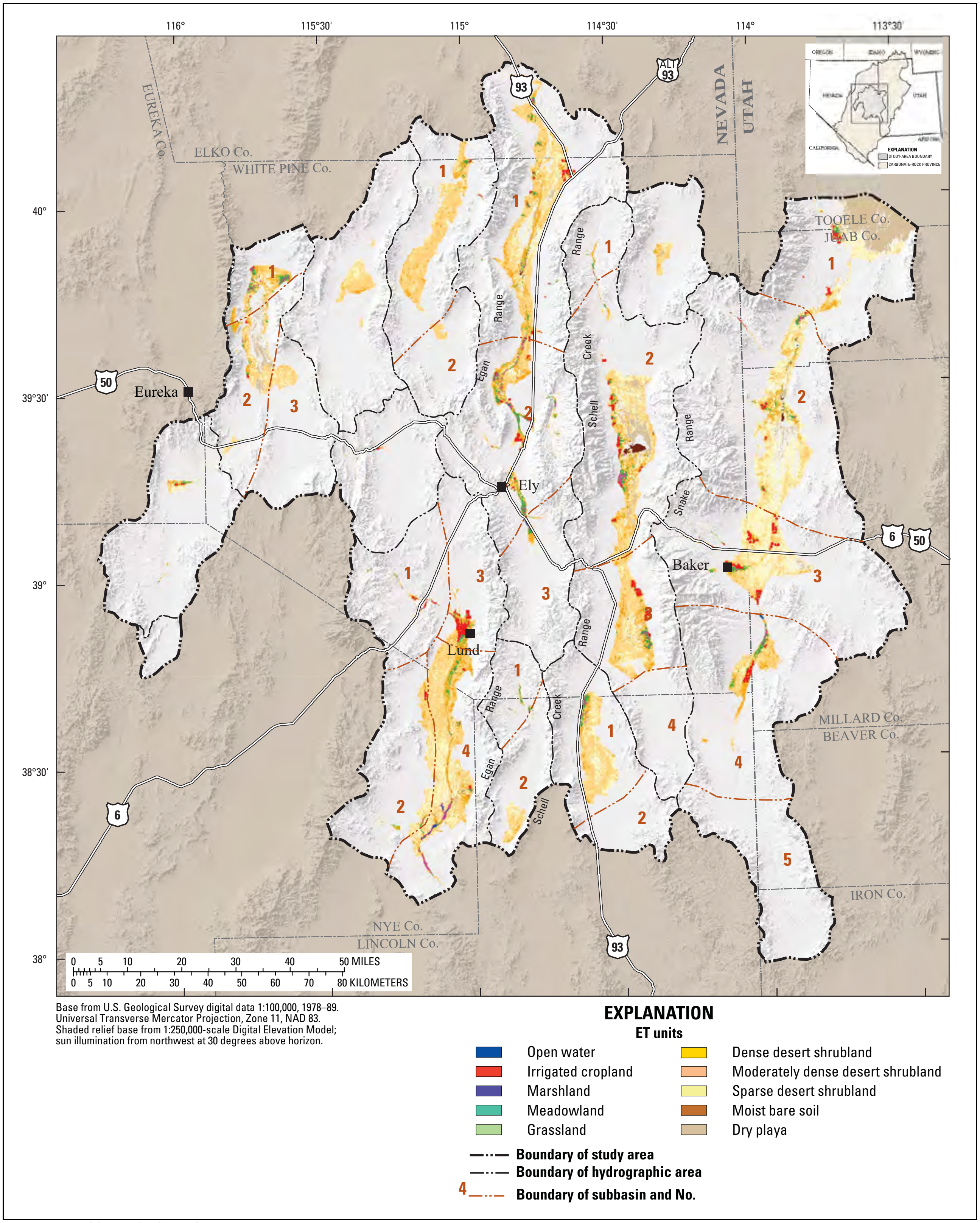

Source: Smith et al. (2007)

Figure 7-4
BARCASS Spatial Distribution of Evapotranspiration Units

study area. Annual ET estimates developed from reported values vary from less than 1 ft over playa and sparse shrubland units to more than 5 ft from open water areas. (p. 56)

The derived literature rates are shown on Figure 7-5. Observed ET rates derived from field data collected for BARCASS are also shown in this figure. They all fall within the literature ranges. The ET rates applied to the ET units were derived by adjusting the literature range of ET of a given zone in a given basin by the range of MSAVI grid values occurring within that zone. A mixed vegetation with a constant mean ET rate of 1.4 ft/yr was assumed for irrigated lands (Welch et al., 2008).

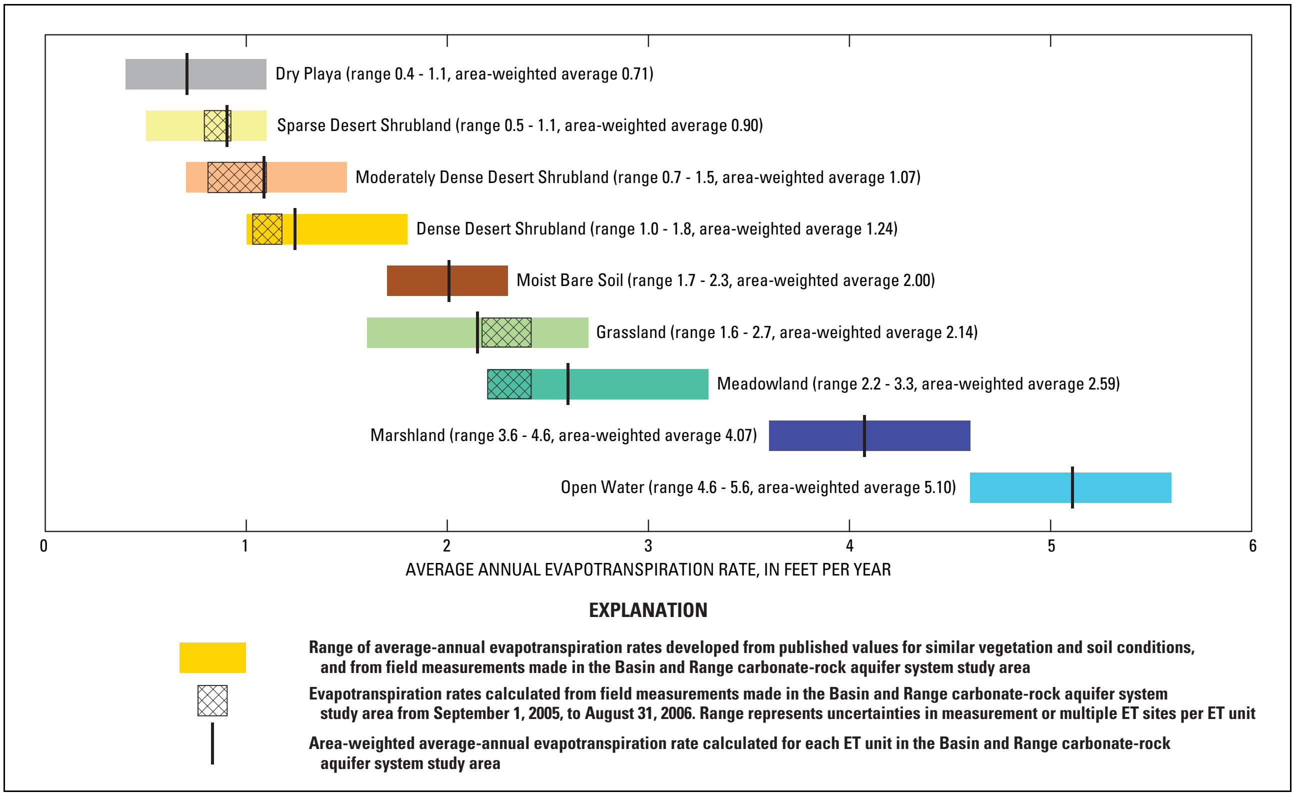

Source: Welch et al. (2008)

Figure 7-5
BARCASS Range of ET Rates from Literature and Measured Values

DeMeo et al. (2008)

ET rates were estimated using data collected at four micrometeorological stations located in ET units or using published ET rates for similar environments. The overall period of data collection extends from 2003 to 2006.

ET sites were installed in four types of ET units: DWV, MWV, DSV, and MSV. Two sites (dense grove of saltcedar trees along the Virgin River floodplain and a dense grove of mesquite trees along the Muddy River) were set up to collect data for analysis with the Bowen-ratio ET method. Two other sites (one in Rainbow Canyon just south of Caliente and one just north of Moapa in Lower Meadow Valley Wash) were set up for analysis with the eddy covariance ET method. A variant of the

Bowen-ratio method was also applied at two sites using data collected for the eddy covariance method. The data collected at these sites were analyzed and used to derive annual estimates of ET (Table 7-5).

Table 7-5
Annual ET Rates Estimated by DeMeo et al. (2008)

Site Name	ET-Unit Name	ET-Unit Identifier	Annual ET_T Rate (ft)
Virgin River	Dense woodland vegetation	DWV	3.9
Muddy River	Moderate woodland vegetation	MWV	3.6
Lower Meadow Valley Wash	Dense shrubland vegetation	DSV	2.8
Rainbow Canyon	Moderate shrubland vegetation	MSV	1.5

7.1.5.3 Method 2 - Precipitation

The precipitation estimates used by Welch et al. (2008) and DeMeo et al. (2008) to adjust the ET rates are presented.

Welch et al. (2008)

The precipitation distribution used in BARCASS is described by Welch et al. (2008) and by Flint and Flint (2007). Welch et al. (2008, p. 60-61) state:

> The average annual precipitation falling directly on ET units was estimated from a map of mean annual precipitation generated from model simulations of monthly precipitation distributions used to estimate average annual recharge for the BARCAS study area over the period 1970–2004 (Flint and Flint, 2007). Estimates of the average annual precipitation to discharge areas delineated within HAs range from about 6 in. in Little Smoky Valley to about 13 in. in Cave Valley (fig. 33, appendix A). In general, precipitation to discharge areas decreases from north to south. Contrarily, the highest annual precipitation occurs in Cave and Lake Valleys in the southern part of the study area. This anomaly is attributed to orographic effects that also contribute to higher annual precipitation in the southern subbasins of Snake and Steptoe Valleys.

Flint and Flint (2007, p. 10-11) describe the process they followed to generate the precipitation distribution they used in their recharge model:

> PRISM precipitation and temperature model results are available as monthly averages from 1895 to 2006 for a 1.8-mi (4-km) grid (Daly and others, 2004). The 1.8-mi grids were interpolated to 866-ft (270-m) grids for 1970–2004 by using spatial gradient and inverse distance squared weighting (Nalder and Wein, 1998)…A search radius of 4.5 mi (10,000 m) was used to limit the influence of distant data. Approximately 25 PRISM grid cells were used to estimate temperature and precipitation for each cell, with the closest cell having the most influence.

DeMeo et al. (2008)

DeMeo et al. (2008) installed a volumetric precipitation gage at each site to collect bulk rainfall during the ET data collection activities. The annual precipitation rates used to adjust ET are 6.0 in. for the Virgin River site, 4.8 in. for the Muddy River site, 6.0 in. for the Rainbow Canyon site, and 7.2 in. for the Lower Meadow Valley Wash site.

7.1.5.4 Method 2 - Groundwater ET Volumes

Welch et al. (2008) and DeMeo et al. (2008) used the general method described in Section 7.1.2.1 to calculate yearly net ET volumes for most of the ET areas they studied.

In the general method of groundwater/surface-water ET volume calculation, the yearly volume from a given ET area is calculated as the yearly groundwater ET rate (Welch et al., 2008) or groundwater/surface-water ET rate (DeMeo et al., 2008) (i.e., ET rate reduced by precipitation) times the ET area. However, DeMeo et al. (2008) did not have sufficient information from their ET sites. Thus, they obtained published rates of ET_{gs} (ET from both groundwater and surface water) from the literature. DeMeo et al. (2008) obtained rates from Laczniak et al. (1999) for the DMV unit (3.4 ft) and the OWU unit (4.9 ft) and from the Bureau of Reclamation (2005) for the AGU unit (5.2 ft). The OWU unit's annual ET_{gs} rate estimate is a mean value of open-water evaporation from the Lower Colorado River. The AGU unit's annual ET_{gs} rate is the ET consumptive-use rate for alfalfa.

For BARCASS, the groundwater ET volumes were calculated by ET unit (for each of the ten ET units) and each sub-basin. The basins were subdivided into sub-basins to account for the spatial variability of the precipitation. The groundwater net ET volumes calculated for BARCASS are included in Table 7-6.

For the southern CRFS ET study (DeMeo et al., 2008), the yearly ET volumes from both groundwater and surface water were calculated for each ET unit by (1) subtracting the local precipitation from the annual ET rate for that ET unit and (2) multiplying the resulting ET rate, ET_{gs}, by the acreage of the ET units. The annual ET_{gs} rate is the combined ET rate associated with groundwater and surface water.

7.1.6 Comparison of Method 1 and Method 2

The areas of potential ET and their classification are compared, followed by a comparison of estimated annual volumes of net ET.

7.1.6.1 ET Areas and Classifications

Areas of potential groundwater ET identified by SNWA for this study (Method 1) (Figure 7-2) and by the USGS for BARCASS and the southern CRFS (Method 2) (Welch et al., 2008 and DeMeo et al., 2008, respectively) were compared for common basins.

Table 7-6
Net ET Volumes Obtained by Method 2

HA Number	HA Name	Welch et al. (2008)[a]	DeMeo et al. (2008)
Goshute Valley Flow System			
179	Steptoe Valley	101,500	NE
178B	Butte Valley South	11,900	NE
Great Salt Lake Desert Flow System			
184	Spring Valley	75,600	NE
185	Tippett Valley	1,700	NE
254	Big Snake[b]	132,300	NE
Meadow Valley Flow System			
183	Lake Valley	6,100	NE
204	Clover Valley	NE	5,840
205	Lower Meadow Valley Wash	NE	16,168
White River Flow System			
174	Jakes Valley	900	NE
175	Long Valley	1,200	NE
180	Cave Valley	1,600	NE
207	White River Valley	76,700	NE
215	Black Mountains Area	NE	1,952
218	California Wash	NE	6,080
219	Muddy River Springs Area	NE	4,090
220	Lower Moapa Valley	NE	11,510

NE = Not Estimated
[a]Values are rounded to the nearest hundred
[b]Big Snake includes Pleasant, Snake, and Hamlin valleys.

Welch et al. (2008)

The acreages for Method 1 and Method 2 (BARCASS) and the differences are presented in Table 7-7. For the most part, total acreages of polygons were quite similar, but BARCASS acreages were generally larger. The average difference as a percent of the mean acreage is about 13 percent. For further comparison between the two groundwater ET maps, the BARCASS ET units were correlated to the ET units identified in this study based on similarities in species composition and percent cover. The correlation of the two units is shown in Table 7-8. The ET units from the two studies did not, however, correlate well spatially.

DeMeo et al. (2008)

A comparison of the ET acreages estimated by SNWA for Method 1 and by DeMeo et al. (2008) for Method 2 is presented in Table 7-9. Note that the table does not include the basins common to the two studies that do not have any groundwater/surface-water ET. Except for Lower Moapa, the ET acreages derived by Method 1 are generally less than those derived by Method 2 (DeMeo et al.,

Table 7-7
Basin ET Acreage Comparison between Method 1 and Method 2 (BARCASS)

HA Number	HA Name	ET Acreage		Absolute Difference as Percent of Mean Area
		Method 1	Method 2/ BARCASS[a]	
Goshute Valley Flow System				
179	Steptoe Valley	163,521	174,540	7
178B	Butte Valley South	51,132	69,671	31
Great Salt Lake Desert Flow System				
184	Spring Valley	172,154	177,698	3
185	Tippett Valley	7,819	7,775	1
254	Big Snake[b]	317,395	325,440	3
White River Flow System				
175	Long Valley	17,595	18,283	4
174	Jakes Valley	971	1,224	23
207	White River Valley	144,692	178,096	21
180	Cave Valley	16,649	13,348	22
Meadow Valley Flow System				
183	Lake Valley	47,445	55,472	16

[a]Smith et al. (2007, Table 4)
[b]Includes Pleasant (194), Snake (195), and Hamlin (196) valleys

Table 7-8
Correlation of Method 1 ET Class and Method 2 (BARCASS) ET Units

Method 1 - ET Class	Method 2-ET Unit Welch et al. (2008)
Open Water	Open Water
Bare Soil/Low Vegetation	Sparse to Moderate Desert Shrubland
Phreatophyte/Medium Vegetation	Dense Desert Shrubland
	Moderately Dense Desert Shrubland
	Recently Irrigated Cropland
Wetland/Meadow	Marshland
	Meadowland
	Grassland
Playa	Moist Bare Soil
	Playa

SE ROA 50470

JA_15871

Table 7-9
Basin ET Acreage Comparison between
Method 1 and Method 2 (DeMeo et al., 2008)

HA Number	HA Name	Method 1[a]	Method 2 DeMeo et al. (2008)	Absolute Difference as Percent of Mean Area
204	Clover Valley	3,500	3,500	0
205	Lower Meadow Valley Wash	7,800	9,410	19
215	Black Mountains Area	500	1,340	91
218	California Wash	1,400	2,400	53
219	Muddy River Springs Area	2,000	2,350	16
220	Lower Moapa Valley	7,500	4,250	55

[a]Values are rounded to the nearest hundred.

2008). The average difference as a percent of the mean acreage is about 39 percent. However, when these same percent differences are weighted by the mean ET areas, the mean percent error is only 5 percent. The correlation of ET units is shown in Table 7-10. A major difference in the ET classification is that in Method 1, the agricultural areas were converted back to their likely natural state, whereas in Method 2 they were not.

Table 7-10
Correlation of Method 1 ET Class and
Method 2 (DeMeo et al., 2008) ET Units

Method 1 - ET Class	Method 2 - ET Unit DeMeo et al. (2008)
Open Water	Open water unit
Phreatophyte/Medium Vegetation	Dense shrubland vegetation
	Moderate shrubland vegetation
Wetland/Meadow	Dense woodland vegetation
	Moderate woodland vegetation
	Dense meadowland vegetation
	Agricultural unit

Differences

The differences between the acreages and the classes identified for Method 1 and Method 2 stem from three differences between the two methods:

- The satellite imagery used was from two different years: 2005 imagery for BARCASS and southern CRFS (DeMeo et al., 2008; Welch et al., 2008, respectively) and 2002 imagery for SNWA. Whereas the year 2005 is considered to be a wet year, the year 2002 is considered to be a dry year. The potential ET areas may be more extensive during wet years.

- For BARCASS, USGS conducted field visits in areas that SNWA did not visit, identifying additional phreatophytic areas.

- Whereas DeMeo et al. (2008) and Welch et al. (2008) used the MSAVI method to derive their classifications of the phreatophytic areas, SNWA used the NDVI method. Although the two methods are quite similar, the MSAVI method accounts for the presence of soils and therefore may yield different classes than the NDVI method.

7.1.7 Comparison of Net ET Volumes

As stated in Section 7.1, net ET volumes are total ET minus precipitation. The net ET volumes obtained by Method 1 and Method 2 are listed in Table 7-11. The differences, when significant, and their causes are discussed in this section.

Despite the differences between the extent of the ET areas and the differences in the ET classes, the ET rates, and the precipitation distributions, the basin groundwater ET volumes derived for Method 2 (BARCASS) compare closely to those derived by Method 1.

The comparison between Method 1 and Method 2 (DeMeo et al., 2008) depends on the basin and the extent of the potential ET area. The differences in the net ET volumes for some of the basins are relatively large, but the areas themselves are small (less than 2,500 acres). This is the case for Black Mountains Area, California Wash, and Muddy River Springs Area. All three areas have annual net ET volumes of less than 10,000 afy (Table 7-11).

The comparison is more complicated for Lower Meadow Valley Wash and Lower Moapa Valley. The amounts are large and different. For Lower Meadow Valley Wash, the annual volume of net ET is 21,900 afy for Method 1 and 16,168 afy for Method 2. For Lower Moapa Valley, the annual volume of net ET is 25,300 afy for Method 1 and 11,510 afy for Method 2. Whereas DeMeo et al. (2008) state that their estimates of ET include both groundwater and surface water, SNWA (Method 1) assumed that the surface water flowing in Meadow Valley Wash was of groundwater origin. Thus, the Method 1 estimates of net ET are estimates of groundwater ET. Nonetheless, uncertainty in the source of water that evapotranspirates is acknowledged for all ET areas and may be larger in ET areas when open water bodies are present. For Lower Moapa Valley, the estimate derived by DeMeo et al. (2008) appears to be too low. The estimate of net ET derived by Method 1 is more consistent with the decrease in stream flow between two stream gages located on the Muddy River as described in Section 7.3.1.1.3.

7.1.8 Conceptual Model Groundwater ET Estimates

The groundwater ET estimates used in the conceptual model of the groundwater flow system of the model area are a combination of Method 1 and Method 2. The specifics are as follows:

- Northern basins: Method 2/BARCASS estimates (Welch et al., 2008).

Table 7-11
Net ET Volumes Obtained by Method 1 and Method 2

HA Number	HA Name	Method 1	Method 2	
		SNWA (This Study)[a]	Welch et al. (2008)[a]	DeMeo et al. (2008)
Goshute Valley Flow System				
179	Steptoe Valley	101,700	101,500	NE
178B	Butte Valley South	11,900	11,900	NE
Great Salt Lake Desert Flow System				
184	Spring Valley	75,400	75,600	NE
185	Tippett Valley	1,700	1,700	NE
254	Big Snake[b]	132,000	132,300	NE
Meadow Valley Flow System				
183	Lake Valley	5,900	6,100	NE
198	Dry Valley	3,700	NE	NE
199	Rose Valley	600	NE	NE
200	Eagle Valley	1,000	NE	NE
201	Spring Valley	3,900	NE	NE
202	Patterson Valley	1,300	NE	NE
203	Panaca Valley	18,900	NE	NE
204	Clover Valley	5,200	NE	5,840
205	Lower Meadow Valley Wash	21,900	NE	16,168
White River Flow System				
172	Garden Valley	1,700	NE	NE
174	Jakes Valley	900	900	NE
175	Long Valley	2,300	1,200	NE
180	Cave Valley	1,700	1,600	NE
207	White River Valley	76,400	76,700	NE
209	Pahranagat Valley	28,500	NE	NE
215	Black Mountains Area	1,400	NE	1,952
218	California Wash	4,500	NE	6,080
219	Muddy River Springs Area	6,000	NE	4,090
220	Lower Moapa Valley	25,300	NE	11,510

NE = Not Estimated
[a]Values are rounded to the nearest hundred.
[b]Big Snake includes Pleasant, Snake, and Hamlin valleys.

- Southern basins other than Lower Meadow Valley Wash and Clover Valley: Method 1/SNWA estimates.

- Lower Meadow Valley Wash and Clover Valley: Method 2/southern. CRFS estimates (DeMeo et al., 2008) adjusted to remove ET by surface water.

The BARCASS estimates (Welch et al., 2008) and Method 1 estimates were initially combined to produce a consistent set of estimates for the CCRP model. The southern CRFS estimates (DeMeo et al., 2008) were added later. The process is described below.

7.1.8.1 Combination of Method 1 and BARCASS (Method 2)

The use of the BARCASS estimates for the northern basins was deemed most appropriate based on the following considerations:

- BARCASS ET area extents are a refinement of SNWA extents.
- BARCASS ET mapping is more detailed: 10 units for BARCASS versus 5 classes for SNWA.
- Total ET rates were allowed to vary spatially (adjusted by MSAVI).

In order to use both Method 1 and Method 2 (BARCASS), the Method 2 data required simplification. The simplification was performed because the two methods are incompatible with respect to their ET unit classifications and different rates of ET and precipitation. The simplification was also performed to simplify ET in the numerical model. A consistent groundwater ET data set was derived by reducing the BARCASS data set to five ET classes and combining the two data sets. The Method 2 data set was modified as follows:

- The 10 BARCASS ET units were grouped into 5 ET classes that are similar to the 5 ET classes defined in Method 1.

- Mean ET rates were calculated for each of the 5 ET classes in each basin by averaging the ET rates associated with the 10 BARCASS ET units of each basin. These mean rates were weighted by the areas of the BARCASS ET units.

- Mean precipitation rates were calculated for each of the five ET classes in each basin by averaging the precipitation rates used by Welch et al. (2008) for the BARCASS ET units. These means were also weighted by the areas of the BARCASS ET units.

7.1.8.2 Resulting ET Estimates

The resulting ET areas and annual volumes of groundwater ET for the five ET classes for the basins of the study area are listed in Table 7-12 by category as previously described in Table 7-2. The simplification of Method 2 results in volumes that are slightly different from those reported by Welch et al. (2008). The combined ET data set was used to accomplish the following:

- Directly compare the ET rates and volumes derived using Methods 1 and 2.

Table 7-12
Groundwater ET Areas and Volumes by Basin Using Combined Data Set

HA Number	HA Name	Groundwater ET Area (acre)				Groundwater ET Volume (afy)			
		Categories			Total[a]	Categories			Total[a]
		1	2	3		1	2	3	
Goshute Valley Flow System									
178B	Butte Valley (South)	69,400	0	300	69,700	11,800	0	100	11,900
179	Steptoe Valley	169,000	400	5,200	174,600	96,600	200	4,900	101,700
	Total	**238,400**	**400**	**5,500**	**244,300**	**108,400**	**200**	**5,000**	**113,600**
Great Salt Lake Desert Flow System									
184	Spring Valley	176,800	300	700	177,800	74,900	100	400	75,400
185	Tippett Valley	7,700	0	0	7,800	1,700	0	0	1,700
194	Pleasant Valley	0	0	1,100	1,100	0	0	1,000	1,000
195	Snake Valley	316,600	1,400	2,300	320,300	126,500	1,100	1,800	129,400
196	Hamlin Valley	3,800	400	0	4,200	1,800	200	0	2,100
	Total	**504,900**	**2,100**	**4,100**	**511,200**	**204,900**	**1,400**	**3,200**	**209,600**
Meadow Valley Flow System									
183	Lake Valley	55,500	0	0	55,500	5,900	0	0	5,900
198	Dry Valley	2,100	0	0	2,100	3,700	0	0	3,700
199	Rose Valley	300	0	0	300	600	0	0	600
200	Eagle Valley	600	0	0	600	1,000	0	0	1,000
201	Spring Valley	2,200	100	100	2,300	3,700	100	100	3,900
202	Patterson Valley	800	0	0	800	1,300	0	0	1,300
203	Panaca Valley	9,100	0	0	9,100	18,900	0	0	18,900
204	Clover Valley	500	0	3,000	3,500	900	0	4,900	5,800
205	Lower Meadow Valley Wash	7,800	0	0	7,800	9,700	0	0	9,700
	Total	**78,900**	**100**	**3,100**	**82,000**	**45,700**	**100**	**5,000**	**50,800**
White River Flow System									
172	Garden Valley	600	0	300	900	1,100	0	600	1,700
174	Jakes Valley	0	0	1,200	1,200	0	0	900	900
175	Long Valley	17,800	500	0	18,300	2,200	100	0	2,300
180	Cave Valley	1,900	11,300	200	13,400	1,200	400	100	1,700
207	White River Valley	174,000	2,900	1,300	178,200	73,700	1,600	1,100	76,400
209	Pahranagat Valley	8,700	0	0	8,700	28,500	0	0	28,500
215	Black Mountain Area	500	0	0	500	1,400	0	0	1,400
218	California Wash	1,400	0	0	1,400	4,500	0	0	4,500
219	Muddy River Springs Area	2,000	0	0	2,000	6,000	0	0	6,000
220	Lower Moapa Valley	7,500	0	0	7,500	25,300	0	0	25,300
	Total	**214,400**	**14,700**	**3,000**	**232,100**	**143,900**	**2,100**	**2,700**	**148,700**

Note: Values are rounded to the nearest hundred.
[a]Hydrographic area totals are rounded from the totals reported in Table F-3.

SE ROA 50475

JA_15876

- Calculate and compare groundwater ET volumes for each category of ET area in each basin.
- Derive stochastic estimates of groundwater ET volumes using a single ET data set.

The combined data set permits comparisons between the ET rates and the annual groundwater ET volumes. The rates derived using the two methods were found to be comparable (Appendix F, Figure F-1), particularly at the lower rates (less than 2 ft/yr). For mid-range ET rates (between 2 and 3 ft/yr), most rates derived by BARCASS are slightly larger than those used in Method 1. However, at the higher rates (larger than 4.5 ft/yr), the Method-1 ET rates are larger than those derived by BARCASS. These rates, which represent open water, differ by about 1 ft/yr or about 20 percent of the average between the two values. This difference is due to the fact that in BARCASS, the open-water evaporation rates were set at 5.2 ft/yr, whereas in Method 1, they were varied to account for spatial climate variations.

The combined groundwater ET map is shown on Figure 7-6. After the two maps were combined, the categories previously defined (Table 7-2) were applied to the ET areas. The groundwater ET map showing the three categories is shown on Figure 7-7. The areas of potential groundwater ET are presented in Table 7-13 by category. The combined groundwater ET volumes by ET class, by category, and by basin are also presented in Table 7-13.

To allow more flexibility in the selection of calibration targets for the numerical model, an additional subdivision of the groundwater ET areas was implemented. Sub-areas of similar topography and depth to water were identified and used to subdivide the potential groundwater ET areas of selected basins (highlighted in light blue in Figure 7-6).

7.1.8.3 Addition of Method 2 (DeMeo et al., 2008)

The BLM Hydrology Technical Group recommended that the estimates of groundwater ET obtained by Method 1 for Lower Meadow Valley Wash be updated with estimates derived by DeMeo et al. (2008) and adjusted for surface water.

DeMeo et al. (2008) estimated a total of 16,168 afy of ET from both groundwater and surface-water for Lower Meadow Valley Wash. The BLM Hydrology Technical Group recommended that a volume equal to stream flow loss of 6,500 afy along the Meadow Valley Wash in Lower Meadow Valley Wash be removed from the estimate of net ET. The remainder of 9,668 afy is assumed to be from groundwater ET. The mean volume of stream flow loss along the Meadow Valley Wash for predevelopment conditions cannot be accurately calculated because of the lack of complete stream-gaging records for appropriate gages. It is, however, possible to estimate the amount of loss from the information reported by Rush (1964) and from stream-gaging records reported by the USGS (2005, 2008).

Rush (1964) reported a mean annual stream flow of 9,400 afy at a gage located 4.5 mi south of Caliente for the period of 1952 to 1959. Rush (1964) also reported a mean stream flow of 8,620 afy from 1951 to 1960. Based on stream flow measurements made on February 17, 1955, by the USGS, stream flow in Meadow Valley Wash near Rox, Nevada, was 2.5 cfs or 2,800 afy. The difference is 6,600 or 5,820 afy, depending on the Caliente measurement used (USGS, 2005).

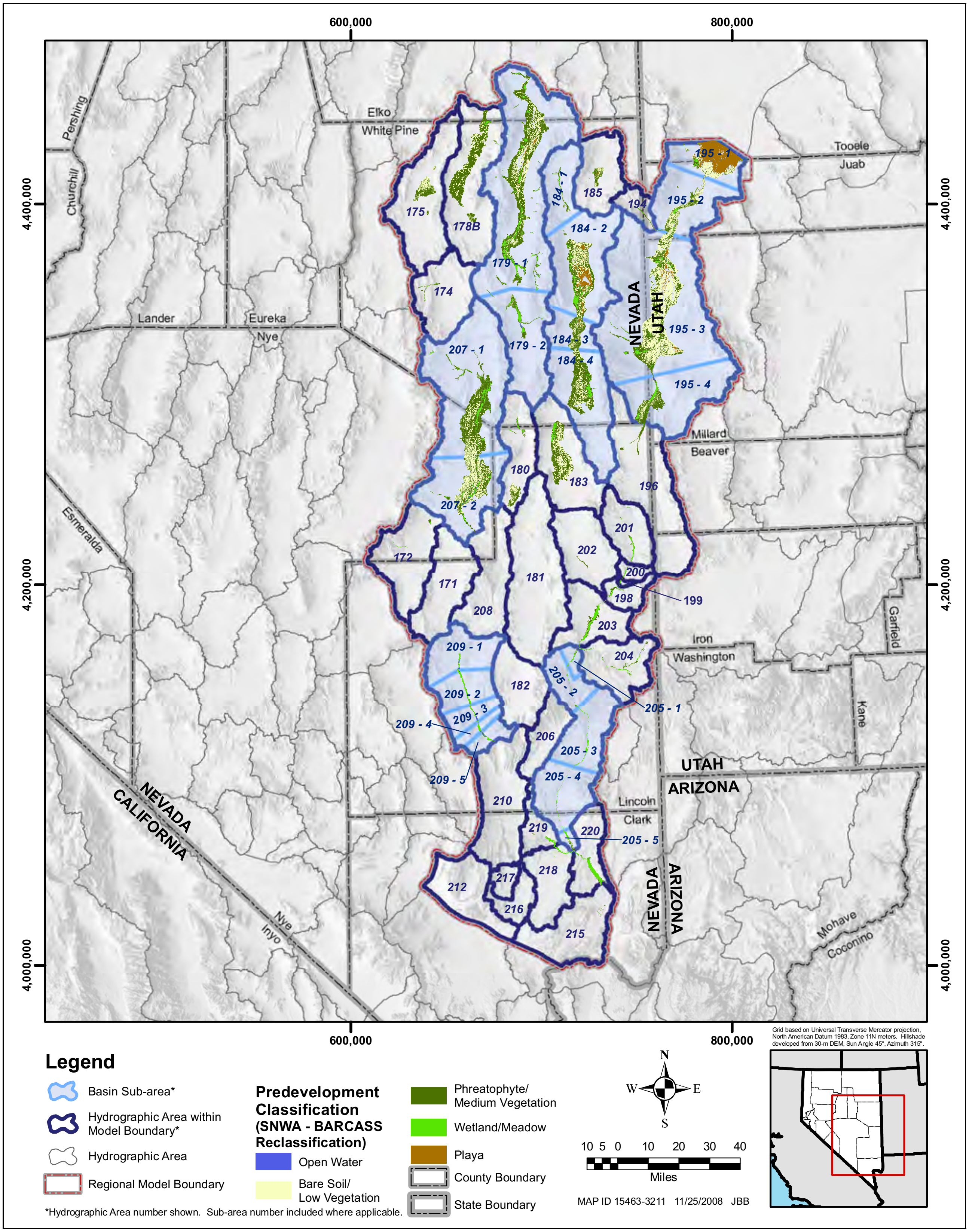

Figure 7-6
Project Predevelopment Groundwater ET Map Showing Basin Sub-Areas

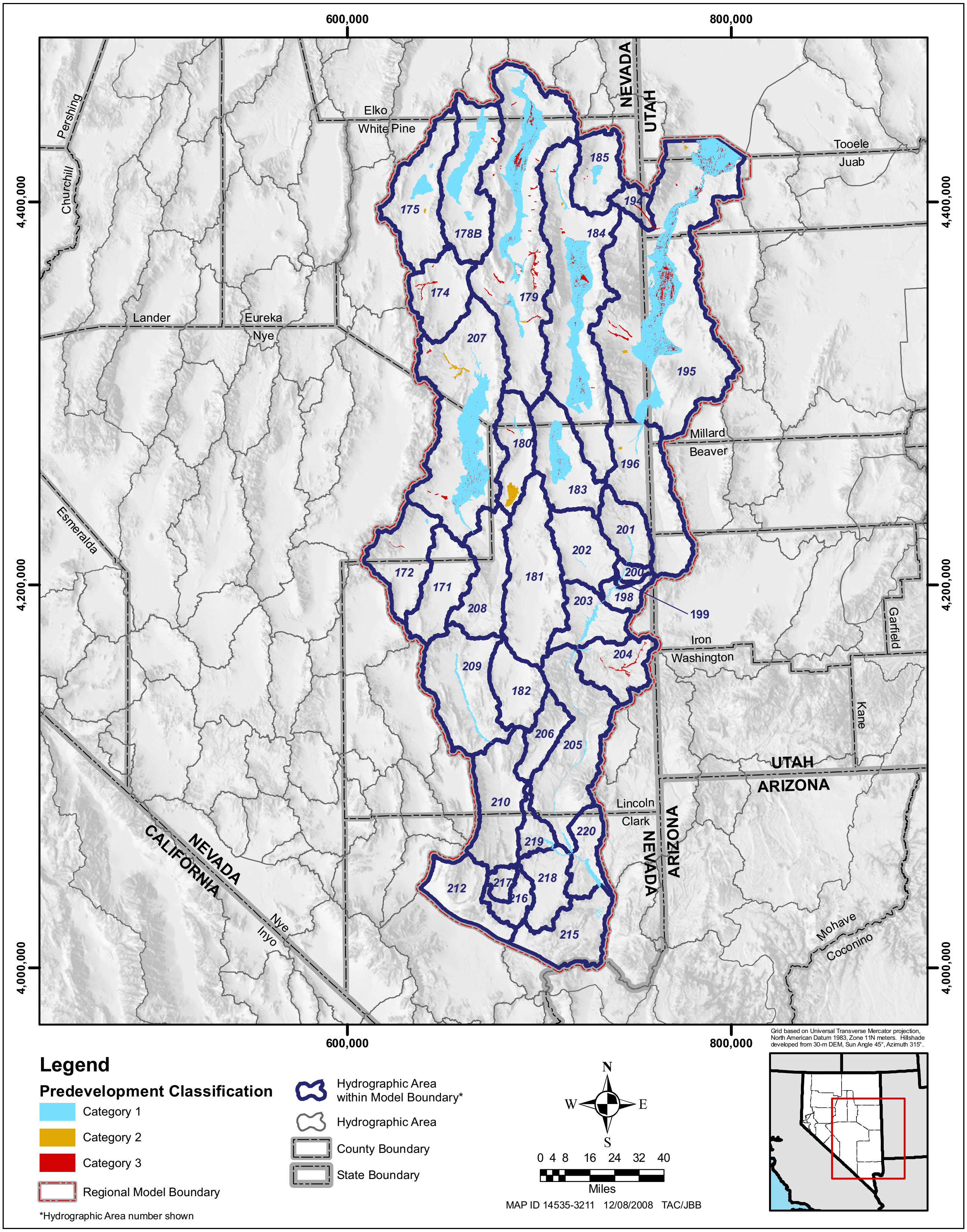

Figure 7-7
Project Predevelopment Groundwater ET Map Showing Categories

Table 7-13
CCRP Model Groundwater ET Volumes Estimates and Comparison to Reported Estimates in afy

HA Number	HA Name	CCRP Model	SNWA (This Study)[a]	Welch et al. (2008)[a]	Nichols (2000)	LVVWD (2001)	SNWA (2007)	DeMeo et al. (2008)	Reconnaissance Studies
Goshute Valley Flow System									
179	Steptoe Valley	101,500	101,700	101,500	128,000	NE	NE	NE	70,000
178B	Butte Valley South	11,900	11,900	11,900	44,500[b]	NE	NE	NE	1,200
Great Salt Lake Desert Flow System									
184	Spring Valley	75,600	75,400	75,600	90,000	NE	NE	NE	70,000
185	Tippett Valley	1,700	1,700	1,700	2,900	NE	NE	NE	NE
254	Big Snake[c]	132,300	132,000	132,300	NE	NE	NE	NE	80,000
Meadow Valley Flow System									
183	Lake Valley	6,100	5,900	6,100	NE	24,000	NE	NE	8,500
198	Dry Valley	3,700	3,700	NE	NE	4,000	NE	NE	3,600
199	Rose Valley	600	600	NE	NE	700	NE	NE	
200	Eagle Valley	1,000	1,000	NE	NE	1,000	NE	NE	
201	Spring Valley	3,900	3,900	NE	NE	1,000	NE	NE	
202	Patterson Valley	1,300	1,300	NE	NE	5,000	NE	NE	
203	Panaca Valley	18,900	18,900	NE	NE	26,000	NE	NE	
204	Clover Valley	5,840	5,200	NE	NE	2,000	NE	5,840	
205	Lower Meadow Valley Wash	9,668	21,900	NE	NE	27,000	NE	16,168	
White River Flow System									
172	Garden Valley	1,700	1,700	NE	NE	5,000	1,696	NE	2,000
174	Jakes Valley	900	900	900	600	600	392	NE	NE
175	Long Valley	2,300	2,300	1,200	11,000	11,000	2,952	NE	2,200
180	Cave Valley	1,700	1,700	1,600	NE	5,000	1,285	NE	200
207	White River Valley	76,400	76,400	76,700	NE	80,000	67,342	NE	37,000
209	Pahranagat Valley	28,500	28,500	NE	NE	38,000	28,516	NE	25,000
215	Black Mountains Area	1,400	1,400	NE	NE	0	1,432	1,952	1,200
218	California Wash	4,500	4,500	NE	NE	6,000	4,505	6,080	6,700[d]
219	Muddy River Springs Area	6,000	6,000	NE	NE	5,000	5,989	4,090	2,300
220	Lower Moapa Valley	25,300	25,300	NE	NE	26,000	25,311	11,510	24,000[d]

NE = Not Estimated
[a]Values are rounded to the nearest hundred.
[b]The reported value is the total ET for Butte Valley North and South.
[c]Big Snake includes Pleasant, Snake, and Hamlin valleys.
[d]The reported discharge value is a combination of water used by natural plants and crops.

Historical stream flow records are available for two gaging stations bracketing almost the entire length of the Meadow Valley Wash in the Meadow Valley Wash hydrographic area (USGS, 2005, 2008). Meadow Valley Wash near Caliente, Nevada (09418500) gaging station is located at the northern end of the hydrographic area, and Meadow Valley Wash near Rox, Nevada (09418700) gaging station is located at the southern end of the hydrographic area. The upstream gage near Caliente has stream flow records from 1951 to 2008 that reflect a mean annual flow of 9.94 cfs (USGS, 2008). The downstream gage near Rox, Nevada, was operated from 1987 to 2005 and has a mean annual flow of 2.37 cfs (USGS, 2005). The difference in stream flow between the two gages is 7.57 cfs or 5,481 afy.

The estimated flow loss along Meadow Valley Wash was derived from information provided by Rush (1964) and USGS (2005) and ranges between 5,481 and 6,600 afy. The amount used to adjust ET (6,500 afy) falls in that range. The adjusted ET estimate of 9,668 afy is assumed to represent groundwater ET in the CCRP model. The estimate of net ET derived by DeMeo et al. (2008) for Clover Valley (5,840 afy) was also used in the CCRP model.

The changes to the groundwater ET estimates of Clover Valley and Lower Meadow Valley Wash, although important for the MVFS, are minor at the regional scale. Therefore, the comparison of rates and the Monte Carlo simulations of groundwater ET described later in this section were not updated. The results would be essentially the same. It was, however, important to incorporate the new estimates in the deterministic estimates of groundwater ET prior to revising the groundwater-budget solutions.

To incorporate the updated estimates of groundwater ET into the CCRP estimates described in the previous section, the ET areas and the five ET classes were assumed to be the same as in Method 1. The total ET volume for Clover Valley and Lower Meadow Valley Wash were adjusted to represent those estimated by DeMeo et al. (2008). The ET volumes of each class and each category were adjusted by the ratio of the new ET volume (Method 2 - DeMeo et al., 2008) over the old ET volume (Method 1) for the basin.

7.1.8.4 Comparison to Other Studies

The volumes of groundwater ET estimated for the conceptual model were compared to volumes estimated by previous investigators (Table 7-13). These include SNWA (2007), Nichols (2000), and LVVWD (2001), and those related to the Reconnaissance studies conducted by the USGS. Each ET study is summarized and then compared to the CCRP estimates.

- Welch et al. (2008) and DeMeo et al. (2008) reflect the numbers that were used in Method 2.

- Nichols (2000) estimated groundwater ET for 16 valleys in central and eastern Nevada. For some basins, the annual groundwater ET volume estimates are substantially larger than estimates made by others.

- LVVWD (2001) estimated groundwater ET for all basins in the White River and Meadow Valley flow systems. Potential groundwater ET areas were delineated using satellite imagery and previous mapping efforts available at that time. ET rates were based on the work of

Devitt et al. (1998) on the Virgin River and on published rates by USGS and the NRCS (formerly the Soil Conservation Service).

- SNWA (2007) estimated groundwater ET for the basins of the WRFS in support of the water-rights hearing for SNWA's groundwater applications in Cave, Dry Lake, and Delamar valleys. The information used to derive the estimates was very similar to that used in Method 1 of this study.

- In the NDWR/USGS reconnaissance studies (1940s–1970s), the areas of groundwater ET were mapped in the field. Groundwater ET rates were derived from ET tank experiments conducted by Lee (1912), White (1932), Young and Blaney (1942), Gatewood et al. (1950) and Robinson (1970).

The volumes derived by this study are generally comparable to the literature values (Table 7-13). Some significant differences do exist, however, and may be due to two reasons:

- The estimates of ET derived for this study are based on conditions observed in 2002 (Method 1) and 2005 (Method 2). The previous estimates were made for earlier years when natural and anthropogenic conditions were different. The conditions prevailing at the time of the estimates affect the extent of the phreatophytic areas and the plant makeup of these areas.

- The method of groundwater ET estimation affects the estimated volumes. For example, the volume of groundwater ET (101,500 afy) estimated for Steptoe Valley (HA 179) by BARCASS (Welch et al., 2008) and adopted in this study is much less than the 128,000 afy estimated by Nichols (2000). The reason may be that the groundwater ET rates used by Nichols (2000) actually contain some precipitation, whereas all contributions of precipitation to ET were removed from the estimates of this study.

7.1.9 Stochastic Estimates

Stochastic estimates of groundwater ET were derived for the study area. In addition to mean values of groundwater ET, the stochastic method provides estimates of the range of uncertainty. Uncertainty in the groundwater ET estimates is due to uncertainty in the areas, the ET rates, and the precipitation estimates. The magnitude of the uncertainty in the calculated volumes of groundwater ET was estimated using Monte Carlo simulations implemented in the Crystal Ball software.

The Monte Carlo analysis requires estimates of the uncertainty on each of the input variables: potential ET area, ET rate, and precipitation rate. The uncertainty ranges for each input variable were estimated and are presented in Section F.1.2.1 (Appendix F).

Statistics describing the uncertainty in the groundwater volumes of each ET class in each area of each basin were derived from 10,000 realizations. Realizations resulting in a negative value of groundwater ET were removed from the resulting set of estimates. Statistics derived include stochastic means, coefficient of variation (COV), and ranges of uncertainty by ET class and by basin. Even though the Monte Carlo simulations were conducted for the five ET classes, the results are reported for four major ET classes, as two of the five classes were grouped. The two grouped classes, Bare Soil/Low Vegetation and Phreatophyte/Medium Vegetation, are not easily distinguishable at the regional scale. The results by sub-area are presented in Table 7-14. The detailed results for the four ET classes in each sub-area of each basin are provided in Table F-8 (Appendix F).

The results were compared with those similar to an uncertainty analysis conducted by DRI (Zhu et al., 2007) as part of BARCASS. Stochastic groundwater ET volumes were derived for the BARCASS basins using the Monte Carlo method. Zhu et al. (2007) calculated the groundwater ET volume as the difference between the total ET volume and the local precipitation volume. They used estimates of the uncertainties associated with the three input parameters, i.e., potential groundwater ET areas, the total ET rates, and the precipitation rates, to quantify the level of uncertainty associated with their groundwater discharge estimates.

Ten thousand Monte Carlo simulations were conducted for each ET unit found within each sub-basin of the BARCASS area. The input parameters, potential groundwater ET areas, ET rates, and precipitation rates, were assumed to follow normal distributions (Laczniak et al., 2001). The mean values of each parameter for each ET class of each sub-basin were set equal to the mean values derived from the deterministic analysis of groundwater ET (Welch et al., 2008).

The uncertainties associated with the three input parameters were characterized by COV estimated from the available information. The mean and COV values are provided by Zhu et al. (2007) in their Tables 2 and 3 for the ET rates, Table 4 for mean acreage, and Table 5 for mean precipitation and COVs. The COV for the area of each ET unit was assumed to be 10 percent. To derive COVs for the ET rates, the literature ranges were assumed to represent ±2 standard deviations of a normal distribution.

The COV values derived by the Monte Carlo analysis (Zhu et al., 2007) are highly variable depending on the sub-basin and the ET unit. However, the COV values of basin groundwater discharge volumes are moderate. This indicates that the overall uncertainty of total groundwater discharge estimate is moderate even if uncertainties on the volumes of smaller areas may be large.

As was the case for the COV values derived by Zhu et al. (2007) for BARCASS, the COVs derived in this study vary greatly depending on the sub-area and the ET unit. The variability in the COVs, however, is much less at the basin level.

The estimates of variances derived from this uncertainty analysis were used in the numerical model to derive appropriate weights for the groundwater ET values. The weighted values were incorporated in the objective function during the model calibration process. The estimates of standard deviations were used to derive a range of potential groundwater ET values.

7.2 Major Springs and Muddy River

Surface-water features located in the study area are discussed in SNWA (2008a). The spring data set is included in Volume 3, and the stream data set is in Volume 2. The springs and streams that have a connection to the main flow system were of interest to the development of the groundwater flow model. An evaluation of the available surface-water features was conducted to identify such features at the regional scale.

SE ROA 50482

JA_15883

Table 7-14
Uncertainty on Annual Volumes of Groundwater ET by Sub-Area
(Page 1 of 2)

Forecast Name	HA Name	Groundwater ET Volume (afy)		Standard Deviation (afy)	COV	Groundwater ET Volume Confidence Interval (afy)			
		Deterministic Mean	Monte Carlo Mean			95 Percent Lower	95 Percent Upper	99 Percent Lower	99 Percent Upper
172-Basin	Garden Valley	1,696	1,703	466	0.27	946	2,477	659	2,800
174-Basin	Jakes Valley	864	885	308	0.35	430	1,424	323	1,667
175-Basin	Long Valley	2,321	3,608	3,331	0.92	14	10,076	10	13,309
178B-Basin	Butte Valley South	11,893	16,522	14,728	0.89	1,484	44,955	1,050	59,165
179-Sub-basin 1	Steptoe Valley	90,297	90,991	26,840	0.29	47,225	136,309	33,968	155,064
179-Sub-basin 2		11,418	11,477	2,200	0.19	7,958	15,186	6,801	16,759
180-Basin	Cave Valley	1,710	3,113	2,192	0.70	869	7,546	553	9,900
183-Basin	Lake Valley	5,944	13,333	9,464	0.71	3,668	32,459	2,660	43,515
184-Sub-basin 1	Spring Valley	2,870	2,881	605	0.21	1,903	3,894	1,556	4,369
184-Sub-basin 2		38,374	38,705	9,532	0.25	23,329	54,854	18,293	62,734
184-Sub-basin 3		8,111	8,234	3,875	0.47	1,872	14,813	762	17,802
184-Sub-basin 4		26,080	26,324	10,394	0.39	9,573	44,045	6,799	51,455
184-Basin		75,435	76,144	14,769	0.19	52,692	100,910	43,837	112,581
185-Basin	Tippett Valley	1,727	1,992	1,355	0.68	202	4,480	91	5,655
194-Basin	Pleasant Valley	1,023	1,027	154	0.15	782	1,291	696	1,402
195-Sub-basin 1	Snake Valley	12,304	13,885	6,418	0.46	5,724	25,971	4,621	31,481
195-Sub-basin 2		15,124	15,217	3,819	0.25	9,282	21,859	7,077	24,764
195-Sub-basin 3		82,324	82,484	26,155	0.32	44,159	129,427	32,139	153,115
195-Sub-basin 4		19,600	19,704	4,957	0.25	11,637	28,094	8,748	31,586
195-Basin		129,352	131,290	27,694	0.21	89,731	179,926	75,669	203,818
196-Basin	Hamlin Valley	2,054	2,063	792	0.38	789	3,405	266	3,959
198-Basin	Dry Valley	3,710	3,716	996	0.27	2,120	5,382	1,481	6,120
199-Basin	Rose Valley	594	596	193	0.32	285	919	170	1,062
200-Basin	Eagle Valley	1,033	1,033	361	0.35	443	1,654	258	1,927
201-Basin	Spring Valley	3,912	3,925	1,232	0.31	1,915	6,002	1,183	6,918
202-Basin	Patterson Valley	1,346	1,350	525	0.39	500	2,226	158	2,635
203-Basin	Panaca Valley	18,895	18,868	4,740	0.25	11,174	26,912	8,297	30,499
204-Basin	Clover Valley	5,840	5,244	1,745	0.33	2,405	8,099	1,338	9,509
205-Sub-basin 1	Lower Meadow Valley Wash	1,293	2,935	796	0.27	1,658	4,276	1,174	4,885
205-Sub-basin 2		959	2,182	737	0.34	1,016	3,438	533	3,978
205-Sub-basin 3		3,194	7,252	2,207	0.30	3,786	11,074	2,340	12,663
205-Sub-basin 4		1,216	2,756	763	0.28	1,556	4,051	1,074	4,647
205-Sub-basin 5		3,006	6,801	1,404	0.21	4,548	9,151	3,681	10,168
205-Basin		9,668	21,927	2,932	0.13	17,186	26,831	15,286	29,020
207-Sub-basin	White River Valley	41,558	43,656	23,682	0.54	10,562	86,243	7,265	105,241
207-Sub-basin		34,888	37,497	15,824	0.42	16,217	67,315	13,213	86,725
207-Basin		76,446	81,154	28,633	0.35	38,792	132,373	28,736	156,913

SE ROA 50483

JA_15884

Table 7-14
Uncertainty on Annual Volumes of Groundwater ET by Sub-Area
(Page 2 of 2)

Forecast Name	HA Name	Groundwater ET Volume (afy)		Standard Deviation (afy)	COV	Groundwater ET Volume Confidence Interval (afy)			
		Deterministic Mean	Monte Carlo Mean			95 Percent Lower	95 Percent Upper	99 Percent Lower	99 Percent Upper
209-Sub-basin 1	Pahranagat Valley	5,683	5,677	836	0.15	4,334	7,076	3,817	7,728
209-Sub-basin 2		8,701	8,682	2,402	0.28	4,912	12,746	3,382	14,580
209-Sub-basin 3		5,865	5,874	829	0.14	4,560	7,267	4,022	7,886
209-Sub-basin 4		3,203	3,193	738	0.23	2,024	4,439	1,544	5,045
209-Sub-basin 5		5,070	5,073	708	0.14	3,923	6,259	3,496	6,796
209-Basin		28,522	28,499	2,840	0.10	23,937	33,298	22,130	35,423
215-Basin	Black Mountains Area	1,432	1,435	290	0.20	970	1,926	782	2,142
218-Basin	California Wash	4,505	4,505	1,126	0.25	2,698	6,415	2,035	7,270
219-Basin	Muddy River Springs Area	5,988	5,998	1,497	0.25	3,613	8,517	2,725	9,780
220-Basin	Lower Moapa Valley	25,311	25,242	5,878	0.23	15,720	35,148	12,379	39,461
All Basins		**521,940**	**557,638**	**54,984**	**0.10**	**469,806**	**650,950**	**437,930**	**689,576**

7.2.1 Major Springs

An evaluation of the springs present within the study area was conducted to identify and document those that play an important role in the regional groundwater flow system. The purpose of the spring evaluation was to derive information to support the water-budget calculations and the conceptual model of groundwater flow. The specific objectives of the spring evaluation were to (1) classify the springs of the study area by the type of groundwater system and identify springs that are important to the main groundwater system; (2) estimate long-term flow rates; and (3) identify the source depths of regional springs when enough data are available.

7.2.1.1 Spring Classification

The spring data set compiled in SNWA (2008a) was evaluated for completeness. A few springs were found to be missing and were added to the data set. All springs in the new data set were then classified following the classification postulated by Mifflin (1968). His classification is based on the groundwater system from which the springs originate. Groundwater systems were classified as local, intermediate, and regional. Springs may be classified as local, intermediate, or regional based on the following criteria:

- Location within basin
- Water temperature
- Spring flow rate
- Magnitude of fluctuations of spring flow rate
- Geologic and topographic settings

- Geochemical and isotopic data relative to recharge source areas

Regional Springs

A regional spring is defined as a spring that discharges from the carbonate-rock aquifer system. Therefore, regional springs provide an invaluable source of information on the carbonate flow system of the study area. Regional springs have the following characteristics:

- Location on the valley floor
- Water temperatures greater than 20°C
- Significant flow rates (greater than 100 gpm [Thomas et, al., 1986])
- Perennial flow not reflective of seasonal variation in precipitation
- Evidence of hydraulic connection with the regional carbonate-rock aquifer
- Evidence of long travel times based on geochemical and isotopic data

Previous investigations, including the following selected references, were used to identify all known regional springs present in the study area:

- Meinzer (1942)
- Mifflin (1968)
- Thomas et al. (1986)
- Prudic et al. (1995)

The annual flow volumes of all identified regional springs were included either explicitly or implicitly in the groundwater budget of the conceptual model. Their locations are plotted on Plate 1.

Intermediate Springs

Intermediate springs are also important at the regional scale because they represent a part of the flow system that connects the basin's recharge areas to the regional flow system. Characteristics of intermediate springs are as follows:

- Location on the valley floor or valley margins
- Water temperatures between 55°F and 80°F (13°C and 27°C)
- Variable flow rates
- Perennial flow that correlates with seasonal variation in precipitation
- Little or no hydraulic connection with the regional carbonate-rock aquifer
- Evidence of short travel times (basin-scale) based on geochemical and isotopic data

Groundwater flowing out of all identified intermediate springs was implicitly accounted for in the groundwater budget of the conceptual model. Their locations are plotted on Plate 1.

Local Springs (Perched)

Local springs are not important at the regional scale because they represent perched parts of the flow system, which are not hydraulically connected to the main flow system (regional and intermediate). Characteristics of local springs are as follows:

- Location typically on mountain block above the bedrock-basin-fill interface but may reside on valley margins or floors.

- Temperature less than 55°F (13°C) (Mifflin, 1968).

- Small and highly variable flow rates. Spring may be dry at times.

The locations of local springs are not shown on Plate 1 because of the large number of springs.

7.2.1.2 Spring Description

Regional and intermediate springs of interest in the basins of the study area are shown in Plate 1. Long-term mean annual spring flows were derived from USGS yearly mean values when available. Otherwise, they were derived from the available spring discharge records. The mean flow rates and standard deviations are presented in Table G-1 (Appendix G). A summary discussion of the regional springs and the intermediate springs selected as flow observation targets are discussed below.

Regional Springs

Regional springs in the study are concentrated within the regional groundwater discharge areas of White River and Pahranagat valleys, the Muddy River Springs area, and Fish Springs Flat.

White River Valley - The groundwater discharge area in White River Valley contains a number of regional springs. Spring discharge measurements for the regional springs are listed in Table G-1. The most significant of these springs are Hot Creek Spring, Preston Big Spring, Moorman Spring, and Moon River Spring. The total average annual discharge measured at these springs is approximately 24 cfs or approximately 17,000 afy.

Pahranagat Valley - The groundwater discharge area in Pahranagat Valley contains a number of springs. Most notable are the Hiko Springs, Crystal Springs, and Ash Springs. Other smaller springs and seeps occur in the southern portion of the discharge area. Hiko, Crystal, and Ash springs have the most significant discharge (Table G-1) and, when combined, produce a total spring discharge of about 36 cfs or about 26,000 afy (Eakin, 1963b). This discharge flows along the Pahranagat Wash and sustains the riparian vegetation located along the wash.

Muddy River Springs Area - The Muddy Springs are located in the eastern part of the Muddy River Springs Area and consist of numerous springs and seeps, including several large thermal spring groups. The springs and seeps are spread over an area of approximately 3 mi^2. The Muddy Springs represent the principal source of groundwater discharge in the southern portion of the WRFS and form the headwaters of the Muddy River. The Muddy River near Moapa gage (09416000) measures the combined spring discharge from the Muddy River Springs Area minus the diversions for municipal and industrial water use.

Fish Springs Flat - Several groups of springs are located in Fish Springs Flat. The largest group is located on and near the NWR and is described by Mundorff (1970) as the Fish Springs Group, which consists of Wilson Hot Springs (aka Wilson Health Springs), Cold Spring, (C-11-14) 4bbb-S1, Big

Spring (aka North Spring), Deadman Spring, Walter Spring and Fish Springs (includes House, Mirror, Thomas, Middle, Lost, Crater, South, and Percy springs). The total discharge from the Fish Springs Group of springs is about 21,000 afy or 29 cfs (USFWS, 2004). Bolke and Sumsion (1978) estimated the total spring discharge at about 27,000 afy. Although the total discharge from Fish Springs is known (described above), the source of the spring flow is much larger than the estimated recharge within Fish Springs Flat. Thus, the source of groundwater flow to the springs must be from neighboring basins through the regional carbonate aquifer. However, the actual flow patterns and individual basin contributions are subject to interpretation.

Intermediate Springs

Significant intermediate springs located in Snake Valley, White River Valley, Steptoe Valley, and the Black Mountains area were included as such in the conceptual model. These intermediate springs were selected because of their relatively large discharge rates, their importance as natural resources, or their geographic locations. For the intermediate springs, the spring pool elevation is used to approximate the spring head potential. The selected intermediate springs include Rogers, Blue Point, McGill, Gandy Warm, Big, and Lund springs. These springs are discussed in greater detail in the following paragraphs.

Rogers and Blue Point Springs - Rogers and Blue Point springs are located in the Black Mountains area hydrographic basin (Plate 1). They are located in the far southern portion of the study area near the terminal end of the WRFS. The source of their water is believed to be a mixture of water from the carbonate aquifer and water from intermediate aquifers (Pohlmann et al., 1998). These springs were selected for inclusion in the conceptual model because of the importance of their geographic location near several important fault structures and their proximity to Lake Mead.

McGill Spring - McGill Spring is located in Steptoe Valley in the northern portion of the study area (Plate 1). It is located near the town of McGill, Nevada. The spring discharges water from alluvial materials between two parallel faults on the valley floor of Steptoe Valley. It is classified intermediate because the source of its water is within Steptoe Valley (Frick, 1985) and because it has a relatively large discharge. The average spring discharge is approximately 10.6 cfs.

Gandy Warm Springs - Gandy Warm Springs is located on the western edge of Snake Valley in the northern portion of the study area (Plate 1). It discharges water from alluvial materials approximately 1.6 mi west of a normal fault. The spring was selected for inclusion in the conceptual model because of its large discharge. The average spring discharge is approximately 17 cfs.

Big Springs - Big Springs is located on the western edge of Snake Valley in the far southern portion of Snake Valley (Plate 1). It discharges from a scarp, in alluvium, 0.6 mi east of a normal fault. The spring is also located 1 mi east of a carbonate-rock outcrop. The spring was selected for inclusion in the conceptual model because of its large discharge of approximately 10 cfs. The spring discharge flows into Big Spring Creek and feeds Lake Pruess.

Lund Spring - Lund Spring is located in the northern portion of White River Valley near the town of Lund, Nevada (Plate 1). It discharges water from a contact between alluvial materials and carbonate bedrock. The deuterium content of Lund Spring water is -113.0‰ and is similar to the deuterium content of local recharge water (Thomas and Mihevc, 2007). The spring is included in the conceptual model because of its relatively large discharge of approximately 8 cfs.

7.2.1.3 *Estimated Depths of Spring Sources*

Spring source depths cannot be measured directly. However, they can be estimated using various methods, including the geothermal-gradient method, which is the most straightforward. In this method, the depth of the groundwater source of a given spring is estimated using the temperature of the spring flow and the prevailing temperature-depth relationship (geothermal gradient). The available estimates of the geothermal gradients in Nevada are described in Appendix G. A summary is provided in this section, followed by the estimates of the depths of the source aquifers of major springs in the study area.

Estimates of the geothermal gradients for the study area were obtained from a study by Mifflin (1968) from data and estimates made by the UNR Great Basin Center for Geothermal Energy and from thermal logs obtained from monitor wells drilled by SNWA (Appendix A). Three temperature-depth relationships (presented as red, black, and purple lines on Figure 7-8) were derived from the information discussed by Mifflin (1968). Two relationships were derived from the information obtained from the UNR Great Basin Center. The blue line and blue diamonds on Figure 7-8 represent temperature-depth data compiled by the UNR Great Basin Center for deep wells in Nevada. The brown symbols represent the mean temperature-depth values derived from the thermal logs obtained from monitor wells drilled by SNWA. The thermal logs were conducted before the temperature in the wells stabilized and therefore are not fully representative of formation conditions.

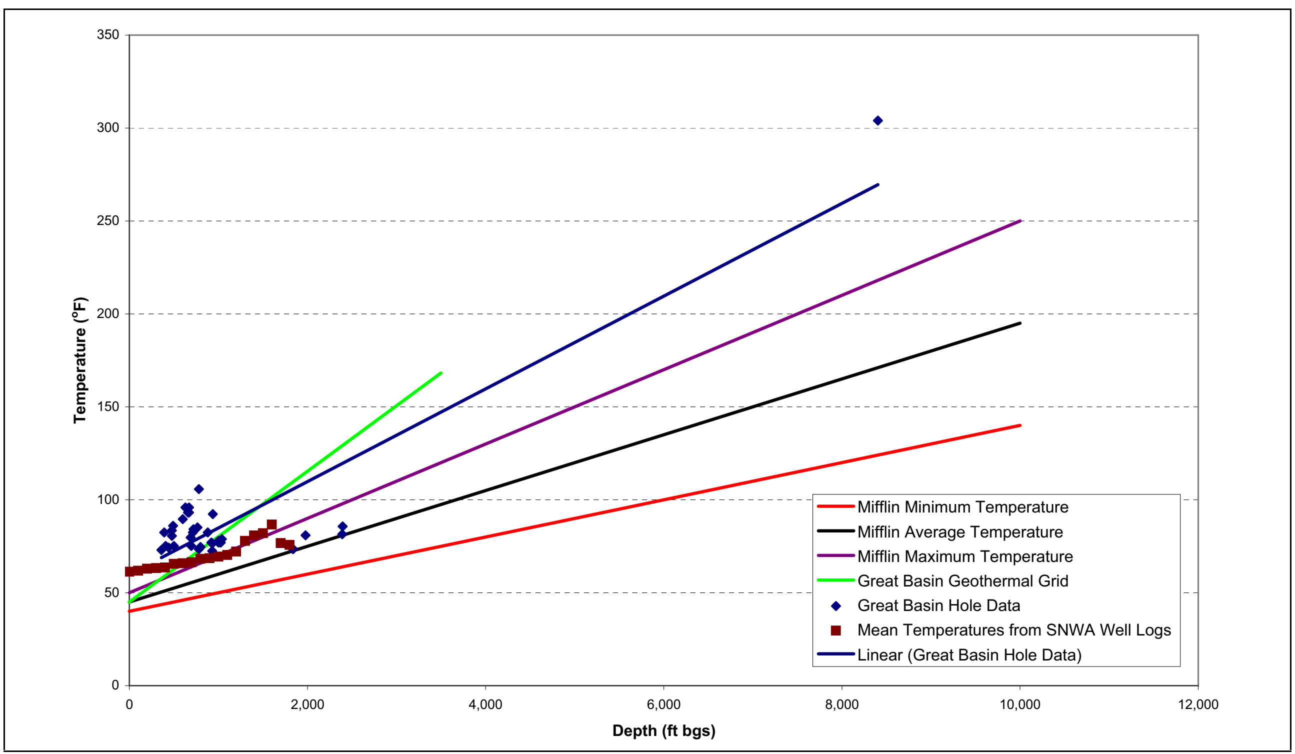

Figure 7-8
Geothermal-Gradient Trends for Nevada

The mean thermal gradient derived from the middle temperature-depth relationship interpreted by Mifflin (1968) was selected to estimate the depth of the source aquifer of major springs in the study area. These estimated depths are listed in Table G-5 (Appendix G). The estimated spring depths range from 81 to 8,422 ft bgs. The depth estimated for one intermediary spring (Stonehouse Spring) was negative because the temperature was too low for the thermal-gradient relationship to be applicable. These source depths are only estimates and do not necessarily represent the only source of water to the springs. Spring flow may originate from an aquifer at a given depth but mix with waters of differing temperatures from overlying aquifers on its way to the surface.

7.3 Streams

Streams of importance to the simulation of the groundwater flow system of the model area include the Muddy River and other smaller spring-fed streams located in Pahranagat and Snake valleys.

7.3.1 Muddy River

The Muddy River is an important hydrologic feature in the model area for several reasons (Figure 7-9). It receives the water discharged from the Muddy Springs and forms a flow path from the Muddy Springs area to the Colorado River (now Lake Mead). In addition, the Muddy River interacts with the aquifer system along its path. The stream aquifer interactions of the Muddy River are not fully understood. However, stream-gaging data acquired at surface sites located along the river channel were evaluated to provide some information (Figure 7-9). The purpose of this evaluation was (1) to derive estimates of predevelopment mean annual stream flow rates at selected stream gages with long periods of records and (2) to estimate the amount of seepage into the stream from groundwater, where possible, from the available synoptic discharge measurements.

7.3.1.1 Estimates of Predevelopment Mean Annual Stream Flow Rates

Estimates of mean annual predevelopment stream flow rates were made at three major gages located along the Muddy River: Muddy River near Moapa, Muddy River near Glendale, and Muddy River at St. Thomas (Figure 7-9). Data on stream flow are included in SNWA (2008a). Mean annual stream flow measurements for the Muddy River near Moapa gage and the Muddy River near Glendale gage are provided in Appendix G.

7.3.1.1.1 Muddy River near Moapa Gage

The Muddy River near Moapa gage (09416000) is located at White Narrows near the intersection of the Muddy River with the boundary of the Muddy River Springs Area hydrographic area (Figure 7-9). It is located downstream from all regional springs and seeps in the Muddy River Springs area. Therefore, stream flow rates measured at this gage represent the total discharge from the springs and seeps located upstream. This gage has a long record starting in 1913. The record of mean annual stream flow rates used in this study is from 1913 to 2004 (Table G-6 in Appendix G). However, records from 1918 to 1943 are missing, and records for 1913 and 1915 are low and constitute outliers.

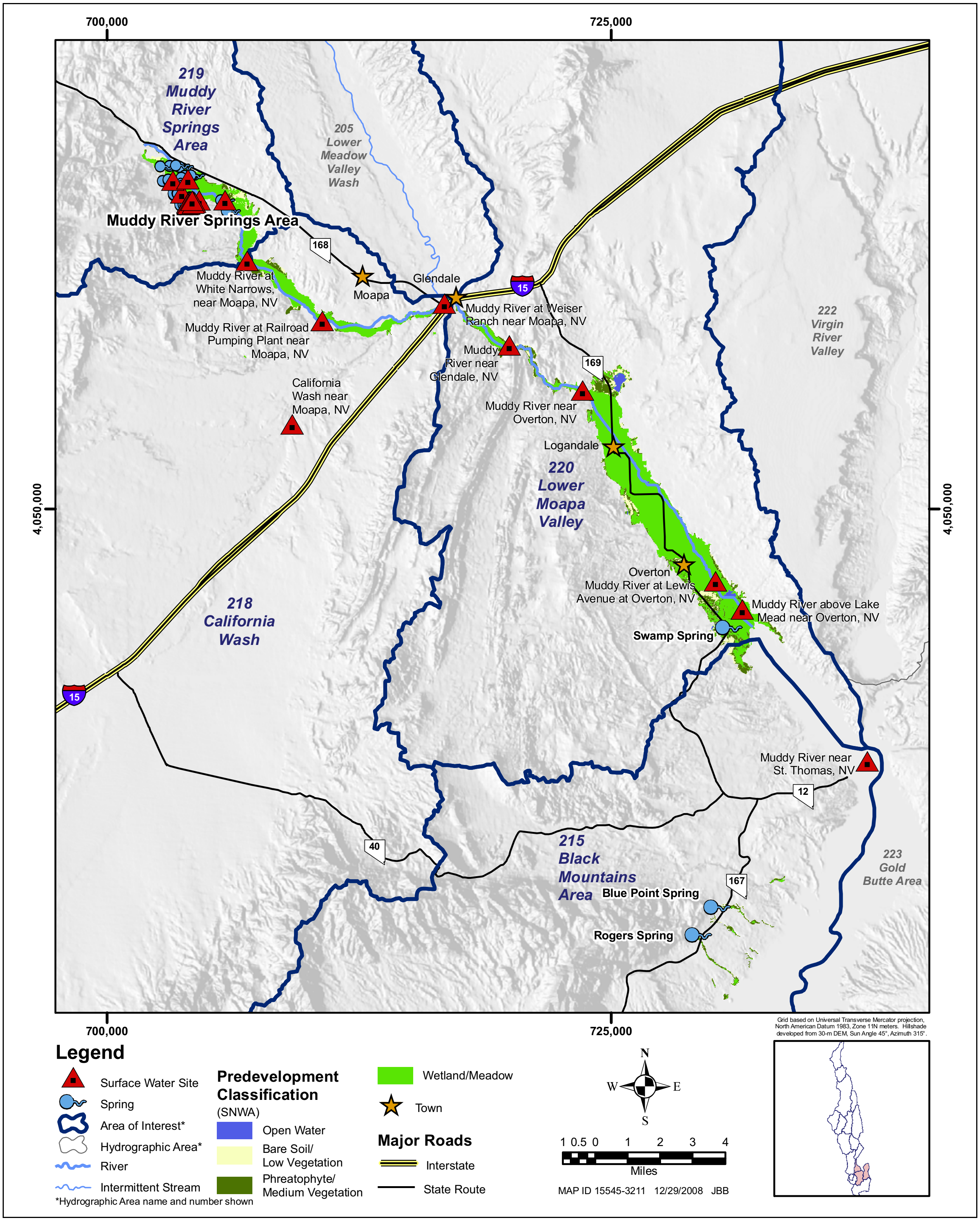

Figure 7-9
Important Hydrologic Features in Muddy River Springs Area and Vicinity under Predevelopment Conditions and Locations of Surface-Water Sites

This gage currently measures the combined spring discharge from the Muddy River Springs area minus the diversions for municipal and industrial water use. Prior to 1962, the measurements represented predevelopment conditions, as no significant diversions were made. From 1913 to 1918, the mean annual discharge at this location was about 34,000 afy (47 cfs). From 1914 to 1962, the mean annual discharge was reported as 33,700 afy (46.5 cfs) (Eakin, 1964). These measurements account for the flow observed at the gage but not the consumptive uses by the riparian vegetation along the spring channels and river corridor or by the phreatophytes that likely existed in the area during predevelopment conditions (Figure 7-9). Eakin (1964) estimated 2,000 to 3,000 afy were being consumed by phreatophytes between the spring area and the gaging station. The discharge from the springs flows into the Muddy River and is believed to support the phreatophytic areas in down-gradient basins, at least in part.

The predevelopment stream flow at the Muddy River near Moapa gage is assumed to be equal to the average annual flow of 33,700 afy (adjusted for precipitation runoff events) (Eakin, 1964). This value corresponds to approximately the same as the value measured in 1945, the assumed end of predevelopment conditions in this study. An estimate of the variability of this estimate may be derived from the historical record up to 1962. The COV of stream flow at that location prior to 1962 was about 0.13 for the raw record (unadjusted) and about 0.02 for the adjusted record, not including suspect measurements.

7.3.1.1.2 Muddy River near Glendale Gage

The Muddy River near Glendale gage is located downstream from the gage near Moapa, within California Wash, and near its hydrographic boundary with Lower Meadow Valley Wash (Figure 7-9). The historical record for the Muddy River near Glendale gage begins in 1951 (Table G-6 in Appendix G). The record of mean annual stream flow rates used in this study is from 1951 to 2004 with the 1984 record missing. Therefore, no data are available for this gage prior to 1945. However, estimates may be derived from the available record using the similarities of this gage with the gage near Moapa discussed in the previous subsection.

An estimate of the correlation between stream flow rates at the Glendale gage and the Moapa gage was derived using the mean annual stream flow rates of the two gages for the period of 1951 to 2004, not including 1984 (Appendix G). The derived correlation coefficient is 0.92, indicating a high degree of correlation between stream flow at the two gages. Considering this high degree of correlation with the gage near Moapa, it is assumed that the gage near Glendale is subject to the same stress conditions as the gage near Moapa. Thus, based on the fact that the stream flow rates measured at the gage near Moapa were relatively stable up to 1962, it is assumed that the stream flow rates measured at the gage near Glendale were also relatively stable up to 1962. Therefore, the predevelopment stream flow at the Muddy River near Glendale gage is assumed to be equal to the average annual flow recorded in 1951, the first recorded year, adjusted for precipitation runoff events, or 31,500 afy. Using the 1951 to 1962 record for this gage, a COV of about 0.11 was derived from the unadjusted measurements and 0.03 for the adjusted measurements. Given the high correlation with the Moapa gage record and the shorter record available for this station, it can be assumed that the variability of stream flow at both locations was similar prior to 1962.

The predevelopment stream flow in the Muddy River decreases from 33,700 afy at the Muddy River near Moapa gage to 31,500 afy at the Muddy River near Glendale gage. Most of the difference of 2,200 afy is lost to ET by riparian vegetation located along the stream in California Wash.

7.3.1.1.3 Muddy River near St. Thomas Gage

The Muddy River near the St. Thomas gaging station was located just upstream from the confluence of the Muddy and Virgin rivers (Figure 7-9). This gaging station was flooded and destroyed when Lake Mead was created. Because of its early record and location with respect to the Colorado River, the gage records for this station were most representative of predevelopment conditions of flow from the Muddy River to the Colorado River. Gage records are available for Water Years (WY) 1913 through 1916 (Wells, 1954).

The gage records began in June of WY 1913 and ended in September of WY 1916, during which time there was a 7-month period of missing records from June of WY 1915 to December of WY 1916 (Wells, 1954). The mean annual flow for the only complete year (WY 1914) was 19.3 cfs, or about 14,000 afy (Wells, 1954). This measurement includes contributions from both groundwater and storm runoff. The period of record mean annual flow was calculated to be 19.6 cfs based on the mean monthly values; however, this value reflects large flood events during February of WY 1914 (136 cfs). Given the limitations of the available records, it is impossible to determine the magnitude of the groundwater component. Rush (1968b) estimated this flow to be 10,000 afy but qualified the estimate as a rough approximation based on few data gathered in 1967. This flow most likely represented agricultural return flows.

For this analysis, it is estimated that about half of the stream flow measured in WY 1914 was groundwater discharge, or 7,000 afy. Furthermore, this value is assumed to represent the portion of stream flow of groundwater origin reaching the Colorado River (pre-lake) or Lake Mead under predevelopment conditions. No data are available to derive COVs for this gage; however, they can be assumed to be at least as large as the COV estimated for the other two gages. Considering the lack of information, they are probably larger.

Stream flow in the Muddy River between the Glendale gage and the St. Thomas gage (Figure 7-9) decreases from 31,500 afy to 7,000 afy, or a difference of about 24,500 afy. This amount is very close to the annual volume of groundwater ET estimated by Method 1 for Lower Moapa Valley. This amount, when reduced by the amount of ET located above the gage near Glendale (2,200 afy), is equal to about 23,100 afy. Therefore, stream flow between the two gages is most probably infiltrating into the groundwater flow system and sustaining the riparian vegetation located along the banks of the Muddy River in Lower Moapa Valley.

7.3.1.2 Seepage into the Muddy River

Two synoptic discharge measurement studies of the Muddy River stream flow (Rush, 1968b, Beck and Wilson, 2006) provide evidence of groundwater seepage into the Muddy River (Figure 7-10). Although these two studies were conducted after 1945, they provide valuable information about the interactions of the Muddy River with the aquifer system.

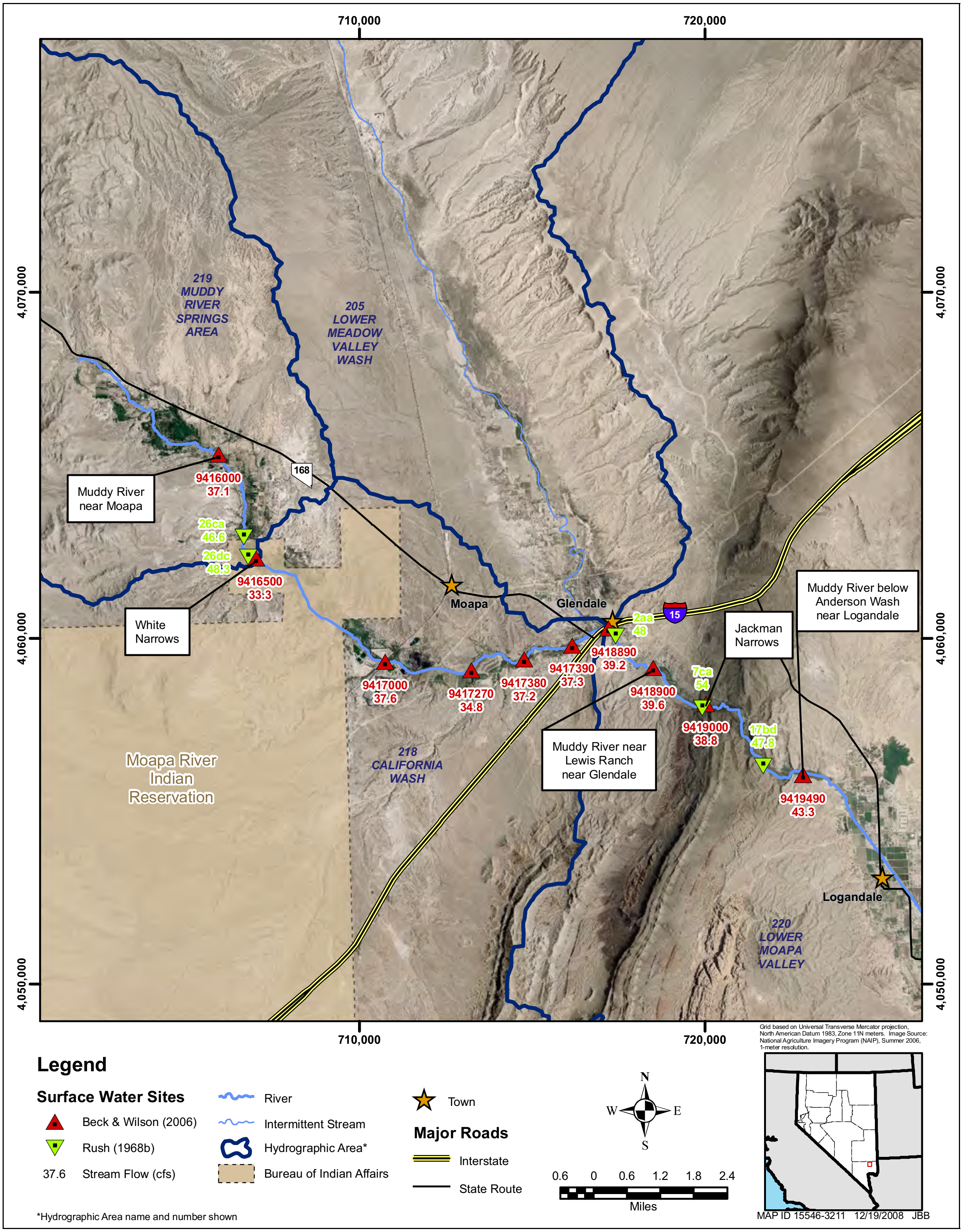

Figure 7-10
Two Sets of Synoptic Discharge Measurements along Muddy River

Rush (1968b) reports measurements from a February 5, 1968, study in which the gage flow above White Narrows was 46.6 cfs, while a measurement made minutes later above Jackman Narrows near Glendale was 48.3 cfs (Figure 7-10). On February 6, 1968, measurements were made at three sites: near Glendale, at Jackman Narrows, and at a site about 1 mi below Jackman Narrows. Flow rates of 48, 54, and 47.8 cfs, respectively, were recorded at these sites. Based on this study, the net gain from above White Narrows to Jackman Narrows is about 7.4 cfs, or 5,360 afy. Rush (1968b) suggests that the observed increase in flow is likely due to inflow from alluvial sediments and/or underlying consolidated rocks, namely the carbonate-rock aquifer.

The second and more recent study (Beck and Wilson, 2006) corroborates the findings of Rush (1968b). Beck and Wilson (2006) describe the results of a synoptic discharge study for approximately the same river reaches described by Rush (1968b) (Figure 7-10). This study was conducted on February 7, 2001, and involved many of the measurement sections. For essentially the same reach, from White Narrows to Jackman Narrows near Glendale, the river gained about 2.5 cfs (about 1,800 afy) based on the maximum values of the gage record for the Muddy River near Moapa gage (09416000) and the measurement section at Muddy River near Lewis Ranch near Glendale (09418900). Maximum flow rates at these sites were measured at 37.1 cfs and 39.6 cfs, respectively (Beck and Wilson, 2006, p. 9). From the gage near Glendale (09418900) to the Muddy River below Anderson Wash near Logandale gage (09419490), an apparent increase in flow of 3.7 cfs (about 2,700 afy) was observed. In total, from the Muddy River near Moapa gage to the Muddy River below Anderson Wash near Logandale gage, an apparent increase in flow of 6.2 cfs, or about 4,500 afy, was observed.

7.3.2 Other Streams Related to Groundwater

Other streams sustained by regional or intermediate springs include the Pahranagat Wash in Pahranagat Valley and Big Spring Creek in Snake Valley (Plate 1). Detailed descriptions of the areas in which these springs and associated streams are located are provided in Volumes 2 and 3 of the Baseline Report (SNWA, 2008a).

The Pahranagat Wash flows south along the central axis of Pahranagat Valley and is sustained by groundwater discharge from three regional springs located in the northwestern part of Pahranagat Valley: Hiko, Crystal, and Ash springs (Plate 1). Spring flow moving down the Pahranagat Wash sustains a significant extent of riparian vegetation along the wash. Spring flow recharges a shallow alluvial aquifer that sustains the phreatophytes. No flow is present in the Pahranagat Wash at the hydrographic-area boundary with Coyote Spring Valley.

In southern Snake Valley, Big Springs discharges into Big Springs Creek, which flows to the northeast toward the Nevada-Utah boundary. In Utah, stream flow occurs in Lake Creek and then Pruess Lake where the water accumulates. Some flow continues slightly after the lake toward Baker before ending (Plate 1). Several other springs (other than Big Springs) contribute additional water to the stream. The gain in the stream below Big Springs has been measured to be approximately 10 cfs (Walker, 1972).

8.0 SELECTED INTERBASIN FLOW LOCATIONS

As stated in Section 5.0, locations, directions, and rates of interbasin flow in the model area are uncertain in many locations. However, it was necessary to quantify interbasin flow at specific locations for two reasons: (1) to use them as constraints in the groundwater-balance method of calculating recharge, and (2) to define boundary conditions for the numerical model. The implementation of the groundwater-budget-method described in Section 9.0 required the selection of specific flow-routing patterns. The groundwater-budget method calculations yielded a recharge distribution, more refined estimates on interbasin flow at selected locations, and groundwater budgets for the model area. Boundary conditions were defined in the numerical model for sufficiently transmissive portions of the model external boundary.

8.1 Location Selection

Potential, regional groundwater flow within the flow systems of the study area occurs through the geologic units present along basin boundaries. Potential locations of boundary segments where interbasin flow could occur within the study area were identified based on the three-dimensional hydrogeologic framework described in SNWA (2008a). The lithology and structure along each of the basin boundaries were examined to assess the likelihood of interbasin groundwater flow across them. Each basin boundary was classified, based on its potential for flow, as likely, permissible, or unlikely (SNWA, 2008a, Volume 1, Figure 4-10).

The basin boundaries through which flow was deemed likely or permissible were further examined for their likelihood to transmit groundwater flow, using the available potentiometric data (SNWA, 2008a, Volume 2).

Arrows in the direction of flow potential were posted on basin boundaries across which a hydraulic potential exists to represent locations where interbasin flow likely occurs under natural conditions (Plate 1).

Thus, some interbasin flow directions were selected over others in areas of conflicting interpretations. However, no single interpretation was dismissed from this study. Rather, interpretations not used to derive initial recharge distributions and groundwater budgets were included in the uncertainty envelope of the conceptual model. The final interbasin flow directions and volumes were derived from the calibrated numerical model.

8.2 Estimates of Interbasin Flow Rates

A subset of the interbasin flow locations shown on Plate 1 were selected for the purpose of estimating flow rates. The selected flow-routing configuration (Figure 8-1) matches the interpretation of Harrill

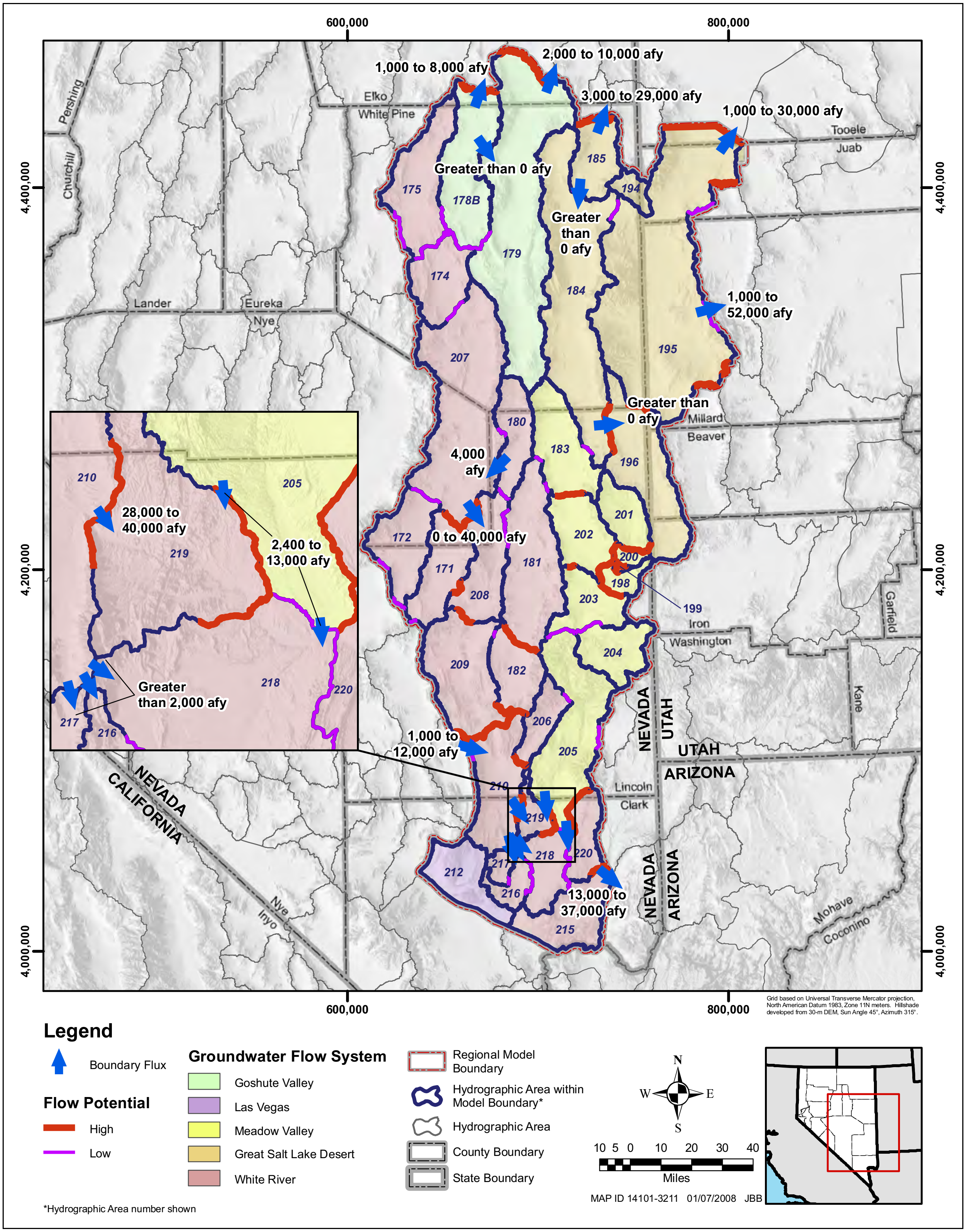

Figure 8-1
Interbasin Flow Locations and Volume Ranges Used in Solver

et al. (1988) for the most part. Interbasin flow volumes across the external boundaries of the model area were estimated using Darcy's equation and Monte Carlo simulations. Others were estimated using available information from the literature. These methods are presented within this section.

8.2.1 Estimates of Interbasin Flow by Monte Carlo Method

Flux through each RMU present across a flow-boundary segment was calculated using Darcy's equation:

$$Q = T \times I \times W \qquad \text{(Eq. 8-1)}$$

where,

Q = Flow rate (ft^3/day)
T = Transmissivity (ft^2/day)
I = Hydraulic gradient
W = Flow width (ft)

Data requirements are as follows:

- Identification of potential flux boundaries
- Identification of RMUs present across each flux boundary
- Probability distributions of transmissivity (T) data for each RMU present
- Probability distributions of hydraulic gradient (I) across each flow-boundary segment
- Probability distributions of flow widths (W) along each flow-boundary segment

The method consisted of conducting multiple calculations of flux across a given flow-boundary segment to derive stochastic estimates of the flux. Each flux calculation is a Monte Carlo realization. A group of realizations constitutes a Monte Carlo simulation, and the simulations were implemented using the Crystal Ball software. A Monte Carlo simulation consisting of 10,000 realizations was conducted for each flow-boundary segment.

8.2.2 Description of Input Data

Estimates of lateral interbasin flow were derived for all external boundaries, except Las Vegas Valley, using the available information.

Probability distributions of transmissivities were derived from the hydraulic-property database described in Appendix C. For RMUs with sufficient data records, the probability distributions were confirmed to be log-normal. The statistics, means, and standard deviations were as calculated. For others, the probability distributions were assumed to also be log-normal.

Hydraulic gradients across permeable-basin boundary segments were derived from a combination of water-level data and previous interpretations of the potentiometric surface. Water-level data were used to calculate the hydraulic gradients. Potentiometric contours for the region (Prudic et al., 1995) were used to identify the approximate directions of groundwater flow. To approximate the regional hydraulic gradient between basins, water levels from the central parts of the basins were used rather than water levels on the mountain blocks. Because carbonate wells are scarce, water levels in the central parts of the basins were assumed to represent regional potentiometric levels, i.e., carbonate aquifer is connected to alluvial aquifers. Also, water levels from groups of wells, rather than single-well measurements, were preferred to capture the magnitude of the mean gradient. The probability distribution was assumed to be normal with COVs between 0.5 and 1. The input data are provided in Appendix H.

The flow widths across permeable segments of the model boundary were identified from a combination of information: (1) the map of permissible flow segments, (2) the regional potentiometric map (Prudic et al., 1995), and (3) the hydrogeologic map including the locations of major structural features. The probability distribution was assumed to be normal with COVs between 0.5 and 1.

8.2.3 Results

The estimates derived for each boundary segment using Darcy flux calculations coupled with Monte Carlo simulations are presented in Table 8-1. The table lists the simulated mean values and 95 percent confidence intervals.

Table 8-1
Estimates of Boundary Fluxes by the Monte Carlo Method

External Flow-Boundary Description	Flow Direction	Annual Volume (afy)			COV
		Mean	5th Percentile	95th Percentile	
Snake Valley to Tule Valley	Out	19,082	1,101	51,576	0.86
Long Valley to Newark Valley	Out	3,670	135	11,002	0.97
Butte Valley South to Butte Valley North	Out	4,006	768	8,426	0.60
Steptoe Valley to Goshute Valley	Out	5,861	2,297	10,152	0.41
Tippett Valley to Antelope Valley	Out	13,718	2,528	29,087	0.60
Snake Valley to Great Salt Lake Desert	Out	11,526	1,138	29,241	0.79
Tikaboo Valley South to Coyote Springs Valley	In	5,042	664	11,544	0.68
Lower Moapa Valley to Colorado River (pre-Lake Mead)	Out	14,727	4,771	27,109	0.48
Lower Moapa Valley to Lake Mead	Out	10,808	3,362	20,144	0.48

8.3 Estimates of Interbasin Flow for Other Boundary Segments

Interbasin flow for selected basin boundaries located on the outer boundaries of the flow systems, or internal to the flow system, was also estimated using the available information to be used in the groundwater-balance method calculations to derive a recharge distribution and groundwater budgets.

Descriptions of these estimates, including the information used to derive them, are provided in this section by flow system.

8.3.1 Goshute Valley Flow System

Interbasin flow may occur at one location within the GVFS (Figure 8-1): from Butte Valley South to Steptoe Valley. Prudic et al. (1995) simulated about 2,100 afy of interbasin flow from Butte Valley South to Steptoe Valley. In the solver, the annual volume of flow across this basin boundary was treated as a constrained unknown greater than zero.

8.3.2 Great Salt Lake Desert Flow System

Interbasin flow may occur at two locations within the GSLDFS (Figure 8-1): from Spring Valley to Hamlin Valley and from Tippett Valley to Spring Valley.

The amount of outflow from Spring Valley to Hamlin Valley has been estimated at 4,000 afy by Rush and Kazmi (1965) and Nichols (2000) and at 51,000 afy by Welch et al. (2008). For flow between North Spring Valley and South Tippet Valley, Scott et al. (1971) estimated 2,000 afy of inflow from Tippett Valley to Spring Valley. This estimate was also used by Harrill et al. (1988). In short, previous investigators estimated small volumes of flow in the same direction for both interbasin boundaries. Thus, the annual volume of flow across these basin boundaries was treated as constrained unknowns greater than zero in the solver.

8.3.3 White River Flow System

Reasonable ranges of flow may be derived from the available information for several interbasin flow locations internal to the WRFS. They are as follows, from north to south: (1) outflow from Cave Valley to White River Valley and Pahroc Valley, (2) outflow from White River Valley to Pahroc Valley, (3) outflow from Coyote Spring Valley to the Muddy River Springs area and other basins, and (4) inflow from Lower Meadow Valley Wash (Figure 8-1). Estimates of these interbasin flow volumes are summarized in this section.

1. Outflow from Cave Valley is most probably to the west and south. Outflow to the west is through Shingle Pass to White River Valley and has been estimated at 4,000 afy (SNWA, 2007). A detailed estimate is provided by SNWA (2007, Appendix D). The interbasin flow at this location was treated as a fixed constraint in the solver. Potentiometric contours also support flow from Cave Valley to the south to Pahroc Valley (Plate 1). The quantity of interbasin flow in this case was derived from the solution.

2. Outflow from Pahroc Valley is most probably to Dry Lake and Pahranagat valleys. Outflow to Dry Lake Valley has been estimated to be small at 2,000 afy (SNWA, 2007). A detailed estimate is provided by SNWA (2007, Appendix D). The interbasin flow at this location was treated as a fixed constraint in the solver. Potentiometric contours also support flow from Pahroc Valley to Pahranagat Valley (Plate 1). The quantity of interbasin flow in this case was derived from the solution.

3. Maxey and Eakin (1949) estimate the groundwater outflow from White River Valley to Pahroc Valley to be between about 6,300 and 19,000 afy. Their minimum estimate is based on the assumption that the outflow consists of spring flow. No evidence exists to substantiate this assumption. Thus, this flow was set to be unknown in the solver with a flow range constrained to vary between 0 and 40,000 afy.

4. Outflow from Coyote Spring Valley is likely to occur within the carbonate-rock aquifer. Most of this outflow probably enters the Muddy River Springs area. The rest of it probably moves into California Wash, Garnet Valley, and Hidden Valley (Plate 1). These quantities were set as constrained unknowns in the solver. The outflow from Coyote Spring Valley to Muddy River Springs area was constrained to be between 28,000 and 40,000 afy. The 28,000 afy is the difference between the spring discharge (34,000 afy) and the inflow from Lower Meadow Valley Wash (6,000 afy). The 40,000 afy is the sum of the spring discharge and the volume of groundwater ET from the Muddy River Springs area. The outflow to the other three basins was constrained to be greater than 2,000 afy, based on the discharge of Rogers and Blue Point springs. A hydraulic link between the Muddy River and Rogers springs is uncertain because of the difference in the geochemistry of their waters. This outflow was then subdivided equally among the three basins.

5. A portion of the flow into the WRFS originates from the MVFS. This inflow is from Lower Meadow Valley Wash to the Muddy River Springs Area and California Wash. The two annual inflow volumes were treated as constrained unknowns in the solver. The total flow volume was constrained to be between 2,400 and 13,000 afy. Buqo (2002) estimated the interbasin flow from Lower Meadow Valley Wash to the Lewis Farm area (California Wash) to range between 2,400 and 7,200 afy. In the same report, Buqo (2002) also suggested that, if the groundwater fluxes through the deep Tertiary units and the thick upper carbonate aquifer are taken into consideration, appreciably more subsurface flow through the area could occur at depth. Based on the RASA model, Prudic et al. (1995) found that 13,000 afy of Muddy River Springs area water may originate from the MVFS. Using isotope-balance models, Thomas et al. (1996) and Kirk and Campana (1990) derived an estimate of interbasin flow from the MVFS that falls within the 2,400–13,000-afy range. LVVWD (2001) estimated an interbasin flow rate of 32,000 afy from the MVFS to Lower Moapa Valley.

8.3.4 Las Vegas Valley

No consensus exists about flow across the boundary between the model area and the rest of the Las Vegas Valley. To account for the diverging interpretations, the flow is assumed to be zero with an uncertainty range of ±3,000 afy. The magnitude of the uncertainty range is based on the recharge volume estimated for the portion of the Las Vegas Valley located in the model area.

8.4 Flow Summary

The interbasin flow volumes described above are summarized in Table 8-2. For comparison purposes, the estimates reported in the literature are also listed in this table. The ranges of lateral flow across the external boundaries of the four flow systems along with selected internal locations of internal basin flow were used in the Excel® Solver to derive the solutions described in Section 9.0. The interbasin flow locations and constraints on the annual flow volumes are shown in Figure 8-1. The estimated ranges of lateral flow along the external boundary of the model area were used in the numerical model. Their locations are shown in Figure 8-2. The corresponding estimated fluxes are listed in Table 8-3.

Table 8-2
Estimated Interbasin Flow Volumes and Reported Values
(Page 1 of 2)

Flow Section	This Study	Reported	Source
Goshute Valley Flow System			
Outflow (afy)			
Butte Valley South to Butte Valley North	1,000 to 8,000	8,000	Welch et al. (2008)
		~3,000[a]	Glancy (1968)
		~1,000[b]	Harrill et al. (1988)
Steptoe Valley to Goshute Valley	2,000 to 10,000	7,000	Welch et al. (2008)
		4,000	Nichols (2000)
		~1,000	Eakin et al. (1967)
		Minor (1,000)	Harrill et al. (1988)
		~1,000 (some)	Scott et al. (1971)
		2,130 to 5,330	Frick (1985)
Butte Valley South to Jakes Valley	NE	16,000	Welch et al. (2008)
Steptoe Valley to Jakes Valley	NE	14,000	
Steptoe Valley to White River Valley	NE	8,000	
Steptoe Valley to Lake Valley	NE	20,000	
Steptoe Valley to Spring Valley	NE	4,000	
Inflow (afy)			
NA	NA	NA	NA
Great Salt Lake Desert Flow System			
Outflow (afy)			
Snake Valley to Great Salt Lake Desert	1,000 to 30,000	29,000	Welch et al. (2008)
		10,000	Hood and Rush (1965)
		10,000	Gates and Kruer (1981)
		10,000	Harrill et al. (1988)
Tippett Valley to Antelope Valley	3,000 to 29,000	12,000	Welch et al. (2008)
		5,000	Scott et al. (1971)
		5,000	Harrill et al. (1988)
		5,000	Harrill (1971)
Snake Valley to Tule Valley	1,000 to 52,000	22,000 to 42,000 (33,000)	Harrill et al. (1988)
		15,000	Hood and Rush (1965)
		15,000[c]	Gates and Kruer (1981)
Inflow (afy)			
Steptoe Valley to Spring Valley	NE	4,000	Welch et al. (2008)
Lake Valley to Spring Valley	NE	29,000	
Wah Wah Valley to Snake Valley	NE	9,750[d]	Harrill et al. (1988)
Pine Valley to Snake Valley	NE		
Lower Meadow Valley Flow System			
Outflow (afy)			
Lake Valley to Spring Valley	NE	29,000	Welch et al. (2008)
Lower Meadow Valley Wash to WRFS	2,400 to 13,000	13,000	Prudic et al. (1995)
		2,400 to 7,200	Buqo (2002)
		7,000	Rush (1964)
		8,000	Thomas et al. (1996)
		5,500 to 9,000	Kirk and Campana (1990) as reported by Thomas et al. (1996)
		32,000	LVVWD (2001)
Inflow (afy)			
Steptoe Valley to Lake Valley	NE	20,000	Welch et al. (2008)

Table 8-2
Estimated Interbasin Flow Volumes and Reported Values
(Page 2 of 2)

Flow Section	This Study	Reported	Source
White River Flow System			
Outflow (afy)			
Long Valley to Newark Valley or Railroad Valley	0 to 12,000	NE	Harrill et al. (1988)
		10,000	Nichols (2000)
		13,000	
		5,000	Welch et al. (2008)
		12,700	Prudic et al. (1995)
Garden Valley to Three Lakes Valley	-1,000 to 1,000	1,226	San Juan et al. (2004)
Pahranagat Valley to Tikaboo Valley South	NE	7,000	Thomas et al. (1996)
		0	Thomas et al. (2001) and Thomas et al. (2006)
		6,000	D'Agnese et al. (1997)
		3,700 to 4,600	Kirk and Campana (1990)
Lower Moapa Valley and Black Mountain to Colorado River	5,000 to 28,000	NE	Harrill et al. (1988)
		1,100	Scott et al. (1971)
		1,100	Rush (1968b)
		3,000	Prudic et al. (1995)
Groundwater Components in the stream	6,600 to 7,400	10,000	Scott et al. (1971)
		10,000	Rush (1968b)
Rogers and Blue Point Springs	1,500 to 1,700	---	---
Total outflow (Lower Moapa and Black Mt.)	13,000 to 37,000	49,000	LVVWD (2001)
Inflow (afy)			
Lower Meadow Valley Wash to WRFS	2,400 to 13,000	7,000	Harrill et al. (1988)
		7,000	Scott et al. (1971)
		7,000	Rush (1968b)
		8,000	Welch (1988) as reported by Thomas et al. (1996)
		13,000	Prudic et al. (1995)
		2,400 to 7,200	Buqo (2002)
		32,000	LVVWD (2001)
		8,000	Thomas et al. (1996)
		5,500 to 9,000	Kirk and Campana (1990) as reported by Thomas et al. (1996)
Tikaboo Valley North to Pahranagat Valley	NE	824	San Juan et al. (2004)
Tikaboo Valley South to Coyote Springs Valley	1,000 to 12,000	5,551	
Muddy River Spring Discharge			
Inflow to Muddy River Spring Area	28,000 to 40,000	37,000	Harrill et al. (1988)
		37,000	Scott et al. (1971)
		28,000	Thomas et al. (1996)
		37,000	Thomas et al. (2001)
		35,000	Eakin (1966)
		16,500 to 19,100	Kirk and Campana (1990) as reported by Thomas et al. (1996)
Las Vegas Flow System			
Outflow (afy)			
Las Vegas to Three Lakes	-3,000 to 3,000	5,000	Harrill et al. (1988)
		5,000	Scott et al. (1971)
Inflow (afy)			
Three Lakes to Las Vegas	NA	1,355	San Juan et al. (2004)

NA = Not applicable, NE = Not estimated
[a]Value estimated as recharge minus discharge.
[b]Reported value is the flow volume out of Butte Valley North.
[c]Reported value is for flow from Snake Valley to possibly Fish Springs Flat.
[d]Reported value is half of the total flow volume into Snake Valley from Pine and Wah Wah valleys (19,500 afy).

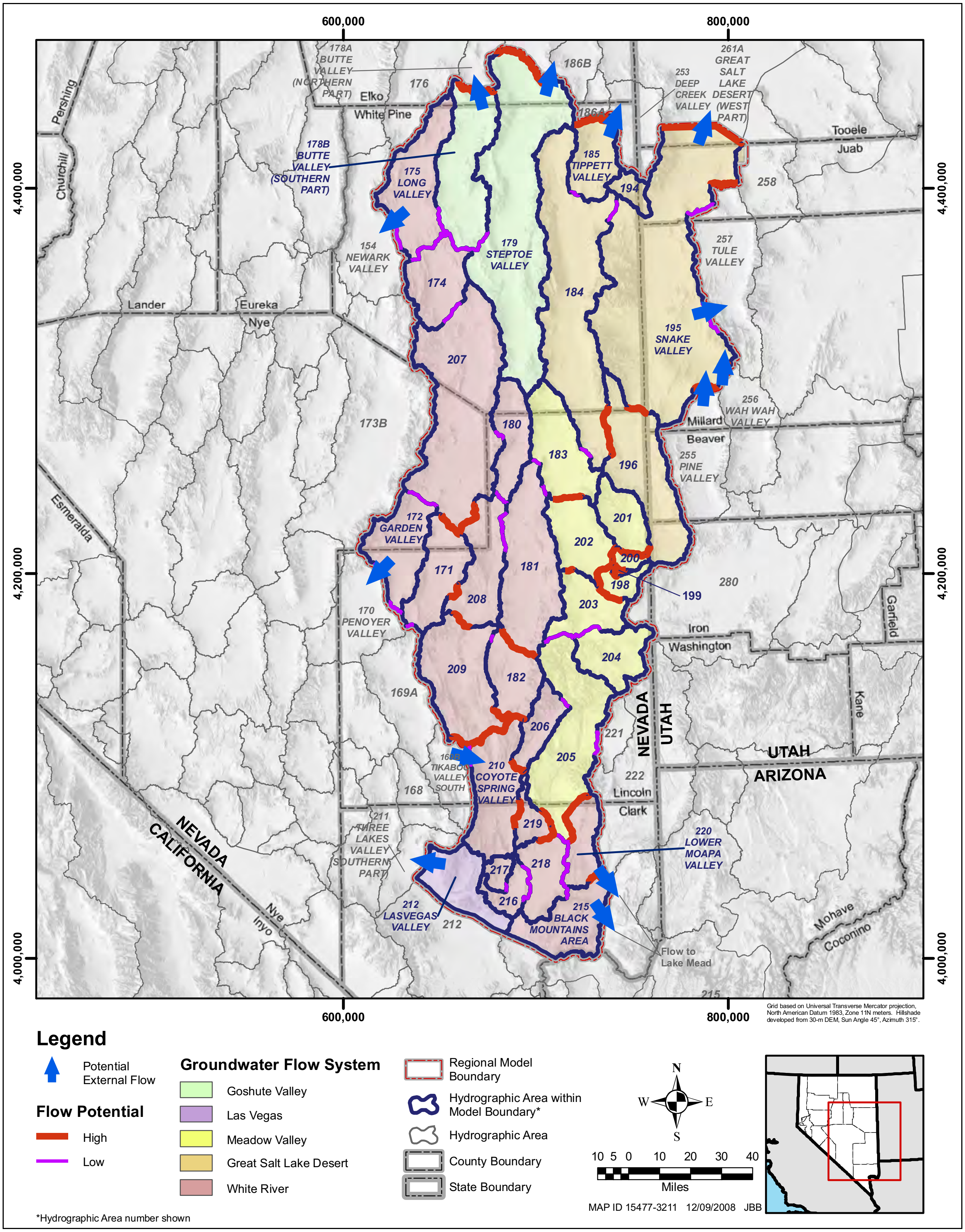

Figure 8-2
Initial Configuration of Flow Information Used in Numerical Model

Table 8-3
External Boundary Flux Estimates for Numerical Model

Lateral Flow-Boundary Description	Flow Direction	Estimated Flux (afy)			Comment
		Expected	Minimum[a]	Maximum	
Pine Valley to south Snake Valley	In/Out	0	-5,000	5,000	Boundary permeable but no hydraulic gradient across, under predevelopment conditions. Flux is estimated.
Wah Wah Valley to south Snake Valley	In/Out	0	-5,000	5,000	
Snake Valley to Tule Valley	Out	21,000	1,000	52,000	Expected value from solver solution. Range rounded from Monte Carlo analysis results.
Long Valley to Newark Valley	Out	0	0	12,000	
Butte Valley South to Butte Valley North	Out	1,000	1,000	8,000	
Steptoe Valley to Goshute Valley	Out	2,000	2,000	10,000	
Tippett Valley to Antelope Valley	Out	3,300	3,000	29,000	
Snake Valley to Great Salt Lake Desert	Out	13,000	1,000	30,000	
Tikaboo Valley South to Coyote Springs Valley	In	5,000	1,000	12,000	
Garden Valley to Three Lakes Valley	In/Out	0	-1,000	1,000	Boundary permeable but no hydraulic gradient across, under predevelopment conditions. Flux is estimated.
Las Vegas Valley to Three Lakes Valley	In/Out	0	-3,000	3,000	Based on recharge volume estimated for portion of Las Vegas Valley in model area.
Lower Moapa Valley to Colorado River (pre-Lake Mead)	Out	16,000	5,000	28,000	Range rounded from Monte Carlo analysis results. Hydraulic gradient observed between wells in Lower Moapa Valley and St. Thomas Well. Includes spring flow of 2,000 afy and stream flow of 7,000 afy.
Black Mountain to Colorado River (pre-Lake Mead)	Out	0	0	2,000	Flux is estimated.
Lower Moapa Valley to Colorado River (post-Lake Mead)	Out	11,000	3,000	20,000	Expected value, range rounded from Monte Carlo analysis results. Does not include spring flow and stream flow. Hydraulic gradient observed between wells in Lower Moapa Valley and mean Lake Mead water level.
Black Mountain to Colorado River (post-Lake Mead)	Out	0	0	1,000	Flux is estimated.

[a]Negative values are shown where flow direction may be in or out at the same volume.

This Page Intentionally Left Blank

9.0 POTENTIAL RECHARGE

Given that precipitation recharge cannot be measured directly, it must be estimated by some other means. In this section, relevant methods to estimate groundwater recharge, previous recharge studies, the use of the groundwater-balance method to estimate recharge distributions for this study, the resulting estimates, and a discussion of uncertainty analysis are presented.

9.1 Review of Relevant Recharge Methods

Recharge methods that have been used to estimate basin-scale groundwater recharge in the study area and vicinity are based on the law of conservation of mass and may be categorized as follows:

- Groundwater-balance methods
- Soil-water-balance methods
- Chloride mass-balance method

Brief descriptions of the three methods and their implementation by various authors are provided in the following sections.

9.1.1 Groundwater-Balance Methods

The groundwater-balance method is applied to a groundwater basin, usually under estimated predevelopment steady-state conditions, to derive an estimate of the basin's recharge volume. This volume is calculated as the difference between the total volume of groundwater discharge (i.e., groundwater ET plus subsurface outflow) and the volume of subsurface inflow. A prominent groundwater-balance method developed and applied to basins in Nevada is the Maxey-Eakin method (Maxey and Eakin, 1949). This method and its derivatives are summarized, followed by brief descriptions of other selected groundwater-balance methods used elsewhere.

9.1.1.1 Maxey-Eakin Method and Derivatives

The Maxey-Eakin method (Maxey and Eakin, 1949; Eakin et al., 1951) was designed to estimate groundwater recharge from precipitation for hydrographic areas of Nevada. Estimates of groundwater recharge based on the Maxey-Eakin method were published in the NDWR/USGS Reconnaissance Series from the late-1940s through the mid-1970s. Maxey-Eakin methods include the "standard" method and modified versions.

The standard Maxey-Eakin method (Maxey and Eakin, 1949) is based on a precipitation map developed by Hardman (1936). This map delineates six precipitation zones, ranging from 0 to over 20 in. of precipitation per year. Using this map, the five precipitation zones above 8 in. in a given hydrographic area are identified as recharge areas. The acreage for each precipitation zone is then measured and multiplied by its average precipitation rate. The resulting precipitation volume is then multiplied by the recharge efficiency for the zone (i.e., the percentage of precipitation that becomes groundwater recharge). The resulting recharge volumes are then summed to yield an estimate of the total recharge volume from precipitation for that hydrographic area, including recharge by direct infiltration and infiltration of runoff. The standard Maxey-Eakin efficiencies were derived by balancing the recharge volume to estimates of discharge volume for 13 basins in Nevada (Maxey and Eakin, 1949). The standard Maxey-Eakin method is not designed to provide a realistic spatial distribution of recharge rates. It does, however, provide first-order approximations of basin recharge volumes (Avon and Durbin, 1994).

One major modification of the standard Maxey-Eakin method involves the use of altitude zones on a topographic map to approximate the precipitation zones and calculate their areas. Examples of this variation of the Maxey-Eakin (1949) method are presented by Eakin (1962, 1963a) for Cave, Dry Lake, and Delamar valleys. Other investigators used variations of the standard Maxey-Eakin method by modifying the precipitation and the recharge efficiencies (D’Agnese et al., 1997; Berger, 2000; Donovan and Katzer, 2000; LVVWD, 2001; Dixon and Katzer, 2002; Hevesi et al., 2002; and Katzer and Donovan, 2003). Of particular interest are Donovan and Katzer (2000), Hevesi et al. (2002), and Wilson and Guan (2004) who converted the recharge efficiency step function, defined in the standard Maxey-Eakin method, to similar power functions expressing recharge as a continuous function of precipitation.

9.1.1.2 Other Groundwater-Balance-Based Methods

Other selected methods of estimating recharge from precipitation using power functions to describe the relationship between recharge and precipitation were applied in Idaho (Contor, 2004), India (Kumar and Seethapathi, 2002), and Arizona (Anderson et al., 1992).

In support of the Eastern Snake Plain Aquifer Model Enhancement Project in Idaho, Contor (2004) adapted a relationship used by Rich (1951) to describe a basin’s total yield. Contor (2004) simplified the relationship to represent recharge on nonirrigated lands as a function of precipitation as follows:

$$\text{Recharge} = K \times \text{Precipitation}^N \qquad \text{(Eq. 9-1)}$$

where,

K = Empirical slope parameter
N = Empirical exponent

Because recharge cannot physically be greater than precipitation, the slope of the recharge-precipitation relationship should never be greater than 1. At the point at which recharge equals precipitation, the exponential relationship is replaced by a straight line with a slope of 1. Furthermore, for a given relationship, the area between the 1 to 1 straight line extends to zero, and the exponential curve represents the portion of precipitation that does not become recharge. This represents the water that is stored in the soil or lost to ET.

SE ROA 50508

JA_15909

Kumar and Seethapathi (2002) derived an empirical relationship to estimate groundwater recharge from rainfall for the Upper Ganga Canal command area using a seasonal groundwater balance spanning over several seasons during 1972 to 1973 and 1983 to 1984. They found that recharge increases with rainfall in a nonlinear fashion. The recharge efficiencies they calculated for the monsoon season ranged between 0.05 to 0.19. Kumar and Seethapathi (2002) then derived an empirical relationship between recharge and rainfall by fitting the estimated values of recharge and the values of rainfall using the nonlinear regression method. The corresponding equation is as follows:

$$R = 0.63(P - 15.28)^{0.76} \qquad \text{(Eq. 9-2)}$$

where,

R = Groundwater recharge from rainfall in monsoon season (in.)
P = Mean rainfall in monsoon season (in.)

The term 15.28 in. represents the magnitude of rainfall below which recharge does not occur. This equation is similar to that of Contor (2004), except it assumes that recharge only occurs above a certain level of precipitation (15.28 in.).

As part of a RASA study for alluvial basins located in southwest Arizona and vicinity, Anderson et al. (1992) developed an equation for estimating mountain-front recharge as a function of precipitation using the water-budget method. Their approach consisted of developing a relationship between the mean annual mountain-front recharge volume and the total annual volume of precipitation for several watersheds when the precipitation is greater than 8 in./yr. They initiated the equation starting with the available data points and adjusted its coefficients until both the individual basin budgets and the total budget for all basins balanced. Their data points included recharge values derived from models and a few basin estimates. Two forms of the equation were developed, one using the total precipitation volume for the basins and one using only the precipitation volume for precipitation rates larger than 8 in. The 8-in. cutoff was arbitrary but yielded better fits to the data and therefore was used to estimate recharge for the study area. The volume of precipitation below 8 in. was attributed to losses to soil-moisture deficits and ET. The resulting equation is as follows:

$$Log\ R = -1.40 + 0.98 \times Log\ P \qquad \text{(Eq. 9-3)}$$

where,

R = Mean direct mountain-front recharge volume (afy)
P = Mean annual precipitation (afy) for $P > 8$ in./yr

Taking the inverse of each side of the equation yields a power function similar to that of Contor (2004):

$$R = 0.042P^{0.98} \qquad \text{(Eq. 9-4)}$$

where,

R = Mean direct mountain-front recharge volume (afy)
P = Mean annual precipitation (afy) for $P > 8$ in./yr

9.1.2 Soil-Water-Balance Methods

The soil-water-balance method focuses on the processes that control net infiltration through the uppermost layers of surficial materials in a given area. These processes include precipitation, snow melt, snow accumulation, and soil-water storage. The soil-water balance must be successively applied to relatively short time periods for the method to yield reasonable estimates of recharge over long periods of time. This method is used to calculate the amount of water available at each time step, for potential recharge and/or runoff, or water to be carried to the next time step. The soil-water-balance method has been implemented to estimate basin recharge in Nevada using two models: the INFIL code and the BCM. Brief descriptions of these two models follow.

9.1.2.1 INFIL Code

The INFIL code (Scanlon et al., 2006) calculates potential groundwater recharge, including volume and distribution. INFIL uses a 24-hour (daily) time step to allow for an accurate simulation of the snow accumulation and melting processes. INFIL calculates runoff and distributes it to a stream network and simulates recharge through the streambeds. An INFIL model may be calibrated to the available stream flow data or measurements of soil-moisture content. INFIL has been extensively used to estimate recharge for the Yucca Mountain Project (Flint et al., 2002; BSC, 2004). The INFIL code is the most detailed and refined of all the methods discussed here. However, this method requires a tremendous amount of data and intensive computational resources.

9.1.2.2 Basin Characterization Model

BCM is a GIS-based, distributed-parameter, water-balance method of estimating basin recharge using monthly climatic boundary conditions (Flint and Flint, 2007). BCM is, in essence, a simplification of the INFIL code. BCM differs from the INFIL code in that monthly climate data are used, only one soil layer is used, and surface water is not an explicit parameter. BCM simulates total potential recharge, which is a combination of in-place recharge and runoff. One major shortcoming is the noninclusion of streams in the code, which renders calibration very difficult, if not impossible. Despite its more simplified form, BCM also requires large amounts of data and significant computational resources. The BCM code has been used by Flint et al. (2004) to derive recharge estimates for basins in the Desert Southwest and by Flint and Flint (2007) for basins in the BARCASS area.

9.1.3 Chloride Mass-Balance Method

The chloride mass-balance method is used to estimate groundwater recharge in arid and semiarid environments. Given estimates of annual precipitation and known chloride concentrations of bulk precipitation (wet and dry deposition of chloride) and groundwater in targeted aquifers, groundwater recharge can be estimated with the following assumptions: (1) atmospheric deposition is the only source for chloride in groundwater in the targeted aquifer; (2) direct runoff to discharge areas is insignificant or is known; and (3) the recharge sources for the basin are correctly delineated (Dettinger, 1989). This method has been used in several studies to derive reconnaissance estimates of natural recharge for desert basins in Nevada, including those by Dettinger (1989), Maurer and Berger (1997), Russell and Minor (2002), and Mizell et al. (2007).

9.2 Previous Recharge Estimates

Annual volumes of recharge from precipitation and their uncertainty have been estimated for basins of the study area by several investigators. Short descriptions of their work on recharge follow.

- Scott et al. (1971) compiled annual recharge estimates derived for Nevada as part of the NDWR/USGS Reconnaissance Series. These estimates are based on the Maxey-Eakin method (Maxey and Eakin, 1949) or one of its variants.

- Watson et al. (1976) conducted a study to evaluate the statistical validity of the Maxey-Eakin method. Using a set of criteria, they identified 63 adequate basin estimates from the NDWR/USGS Reconnaissance Series and developed regressions of recharge estimates versus precipitation to derive estimates of recharge efficiencies and the associated uncertainties.

- Gates and Kruer (1981) estimated recharge for hydrographic areas in west-central Utah using a method similar to the Maxey-Eakin method but with different precipitation interval zones and recharge efficiencies. Gates and Kruer (1981) also tried to incorporate the effect of geology on their recharge estimates. Big Snake Valley (Snake, Pleasant, and Hamlin valleys) was included in this study. The total recharge estimated for Big Snake Valley is 100,000 afy, which is the same as the value estimated by Hood and Rush (1965).

- Frick (1985) used an initial recharge distribution based on the Maxey-Eakin method in her numerical flow model of Steptoe Valley. The Maxey-Eakin recharge efficiencies were applied to Maxey-Eakin elevation zones. The precipitation rate for each elevation zone was estimated using available precipitation station data. An annual recharge volume of 98,900 afy was derived from the calibrated model. Based on the model's sensitivity analysis, Frick (1985) concluded that the annual ET volume estimated by Eakin et al. (1967) is grossly inaccurate.

- Carlton (1985) derived an initial recharge distribution using a method developed by Hood and Waddell (1968) in his groundwater flow model for the Fish Springs flow system. This is the same method as the one described by Gates and Kruer (1981). The annual recharge volume estimated by Carlton (1985) for Big Snake Valley was 104,000 afy, which is almost identical to the value estimated by Hood and Rush (1965). Carlton (1985) assumed that the estimated precipitation recharge was correct and did not vary it during model calibration.

- Dettinger (1989) estimated recharge using the chloride mass-balance method. Because it is difficult to find a groundwater system to meet all of the assumptions associated with this method, the resulting recharge estimates are often underestimated for basins with large precipitation volumes and overestimated for basins with small precipitation volumes.

- Kirk and Campana (1990) estimated recharge for the WRFS using a simple mixing cell model calibrated with the environmentally stable isotope deuterium. The simulated total recharge for the WRFS is almost the same as the one estimated by Eakin (1966). However, the resulting spatial recharge distribution is slightly different. Because the solution of the model is nonunique, the recharge volumes estimated by this method have large uncertainties.

- Avon and Durbin (1994) compared recharge estimates derived using the Maxey-Eakin method with independent estimates for basins located in Nevada. They found that the standard Maxey-Eakin method provides reasonable first-order approximations of basin recharge volumes. They concluded that the upper bound on the standard deviation for an individual basin is 4,800 afy, and the corresponding coefficient of variation of the Maxey-Eakin estimate is no greater than 44 percent for the group of 40 water-budget estimates they considered.

- Brothers et al. (1993, 1994, 1996) are part of the CWP report series containing hydrologic assessments and steady-state groundwater flow models of selected basins in Nevada. The data and information used in these models are mainly from the NDWR/USGS Reconnaissance Series and information reported by Harrill et al. (1988). The simulated groundwater budgets are essentially the same as the ones reported in the NDWR/USGS Reconnaissance Series.

- Nichols (2000) estimated recharge from precipitation for several basins of Nevada. He reevaluated the Maxey-Eakin recharge efficiencies using new estimates of groundwater discharge and the PRISM normal precipitation map (1961 to 1990). The recharge efficiencies were calculated using a multi-linear regression model. The efficiencies derived from the regression model were used to estimate groundwater recharge. Initial groundwater recharge was estimated using estimates of groundwater ET from this study and estimates of groundwater ET modified by interbasin groundwater flow from this study or previous studies.

- LVVWD (2001) estimated annual recharge from precipitation for hydrographic areas of the WRFS and MVFS using a modified version of the Maxey-Eakin method (Donovan and Katzer, 2000). The recharge efficiencies were represented as a continuous function of precipitation. The precipitation distribution was derived by linear regression of measured precipitation and altitude data for precipitation stations located within the flow systems and vicinity. Thomas et al. (2001) evaluated the water budget and flow routing derived by LVVWD (2001) using a deuterium mass-balance model.

- Epstein (2004) used an inverse method to evaluate and find optimal sets of recharge efficiencies for the Maxey-Eakin method and the regression method developed by Nichols (2000). Epstein (2004) also used his method to derive an optimal solution using a set of recharge estimates reported for basins in Nevada. He found that generally the recalculated Maxey-Eakin recharge efficiencies yielded the lowest basin recharge volumes, and the recalculated Nichols (2000) recharge efficiencies yielded the high end of the range.

- Flint et al. (2004) used the BCM code to derive potential recharge estimates for basins in the Desert Southwest.

- SNWA (2006) estimated recharge for Spring Valley by applying the standard Maxey-Eakin method to an updated spatial precipitation distribution. Linear regression was performed on precipitation station data that consisted of measured precipitation rates and altitudes. The regression equation was used to derive the precipitation distribution for the area, assuming that no recharge occurs in areas where precipitation is less than 8 in. or altitude is less than 6,000 ft.

- SNWA (2007) derived recharge estimates for the WRFS using the groundwater-balance method and the Excel® Solver. The latest 800-m PRISM grid was used for the precipitation distribution. The annual volumes of subsurface inflow and outflow to and from the flow system were independently estimated. New estimates of groundwater ET were derived using satellite imagery and other information.

- As part of BARCASS, Welch et al. (2008) reported recharge estimates derived by Flint and Flint (2007) using the BCM code. The precipitation distribution used in this model was based on an adjusted version of the 4-km PRISM (1971 to 2000) grid. Mizell et al. (2007) also estimated recharge for basins in the BARCASS area using the chloride mass-balance method. The recharge estimates reported by Mizzell et al. (2007) carry an uncertainty that is similar to the estimates reported by Dettinger (1989).

- Halford (2008) estimated annual recharge volumes for the entire study area using the groundwater-balance method. Different recharge efficiencies were derived for carbonate and noncarbonate areas using an optimization technique implemented with a customized solver. Halford found that most of the uncertainty associated with this method is due to the large uncertainties associated with locations and volumes of interbasin flow.

9.3 Rationale for Selected Recharge Method

The groundwater-balance method was selected as the approach for estimating natural recharge for the flow systems of the study area because it provides the best means of deriving a calibrated recharge estimate by incorporating measurable budget components, namely groundwater ET. The PRISM precipitation distribution was used and a trial-and-error approach taken to solve for a relationship between recharge efficiencies and precipitation to produce a total recharge estimate that balances with the total groundwater discharge estimate for each flow system. This method also provided an initial spatial distribution of recharge based on the spatial distribution of precipitation.

For this study, it was concluded that a nonlinear equation would best reflect the relationship between recharge efficiency and precipitation. Many investigators have expressed this relationship as a nonlinear function rather than a linear relationship or a step-wise function such as that defined by the standard Maxey-Eakin method. Hevesi et al. (2002) modified the standard Maxey-Eakin method by developing an exponential curve to define recharge as a continuous function of precipitation. This approach was also used by Donovan and Katzer (2000) and Wilson and Guan (2004). Contor (2004) adapted a relationship used by Rich (1951) to describe a basin’s total yield and simplified the relationship to represent recharge on nonirrigated lands as a nonlinear function of precipitation.

Application of the standard Maxey-Eakin efficiencies to the PRISM precipitation distribution was rejected because this would result in an overestimation of the natural recharge. As the Maxey-Eakin method is an empirically derived solution calibrated to the NDWR/USGS Reconnaissance Series estimates of groundwater discharge using the Hardman (1936) precipitation map, it was concluded that the standard Maxey-Eakin recharge efficiencies should only be applied to the Hardman precipitation map (Nevada State Engineer, 2007a and b). If new recharge estimates are to be derived based on updated precipitation maps, the appropriate recharge efficiencies should be obtained using the groundwater-balance method and updated estimates of groundwater discharge.

The BCM method offers the best approach for distributing recharge, as it uses spatial distributions for the parameter data sets considered in the model. However, the recharge values derived by this method are unconstrained by observed data. In addition, BCM-based models have never been calibrated to the groundwater-budget components for a basin. For this reason, the BCM method was not used in this analysis.

The chloride mass-balance method offers an alternative method of deriving recharge estimates, but the method was rejected, as it was concluded that the chloride concentration observations for precipitation and groundwater are too few to represent the spatial variability of these input parameters for the flow systems of the study area.

9.4 Technical Approach Using the Groundwater-Balance Method

The groundwater-balance method is based on fundamental concepts of hydrology and is a standard approach for estimating unknown groundwater-budget components (e.g., recharge) using estimates of other budget components that can be measured within the bounds of reasonable uncertainty (e.g., precipitation, ET). This method is more reliable for closed groundwater basins (i.e., basins with no boundary flow). It can, however, yield reasonable results when applied to a basin or flow system where the amount of boundary flow is known to be small relative to the total budget for that basin or flow system. For this study, the groundwater-balance method was used to derive a relationship (e.g., a power function) between recharge efficiencies and precipitation that yielded a balanced groundwater budget for the flow systems. A different set of efficiencies was derived for each of the four flow systems in the study area. The annual recharge volume for the portion of Las Vegas Valley contained within the model area was calculated using the recharge efficiencies derived for the WRFS. This was completed using a spatial distribution of precipitation (Section 6.0) and estimates of groundwater ET (Section 7.0) and outflow (Section 8.0).

The Excel® Solver was used to calculate estimates of basin recharge volumes and boundary fluxes across predefined boundary segments for each flow system. Input data consisted of the following:

1. Groundwater ET volume estimates for each basin
2. One-inch precipitation bands within predefined potential recharge areas extracted from the 800-m PRISM grid
3. Flow ranges for each permeable boundary segment for the four flow systems

SE ROA 50514

JA_15915

4. Additional estimates of interbasin flow at selected locations to further constrain the WRFS solution

The detailed analysis, including the solver setup, targets, parameters, constraints, and results, are described in detail in Appendix I. Analysis results relevant to the flow systems, including recharge-precipitation relationships and recharge efficiencies, and spatial recharge distribution are discussed within this section.

9.4.1 Recharge-Precipitation Relationships and Recharge Efficiencies

The power functions computed by the solver are recharge-precipitation relationships requiring two coefficients (see Appendix I). A graph of these relationships is presented on Figure 9-1, which also includes the relationship for Maxey-Eakin (1949) and other sources for comparison. As shown on Figure 9-1, all relationships have the expected general trend of increasing recharge with increasing precipitation, and the relationships developed by this study (WRFS, MVFS, GVFS and GSLDFS) fall within the range defined by the others. All relationships shown are similar to each other at the lower precipitation rates but diverge at larger rates.

The relationships derived by this analysis for the four flow systems fall significantly above the Maxey-Eakin line (black triangles) at higher precipitation rates. However, they are similar at middle to lower precipitation rates, i.e., for precipitation rates up to 25 in./yr (curves outside of the gray zone in Figure 9-1). The recharge-precipitation relationships derived by this study are considered to be more representative than the Maxey-Eakin relationships because this study bases its relationships on more accurate estimates of precipitation and groundwater ET.

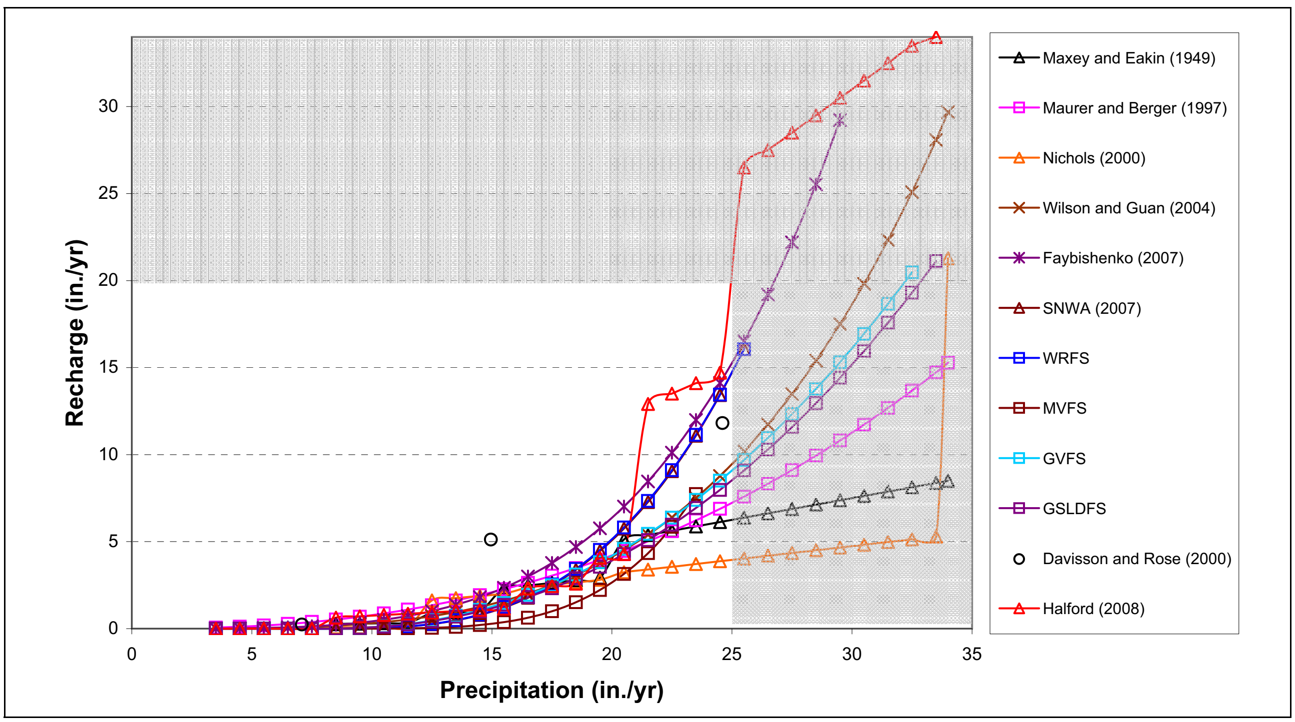

Figure 9-1
Recharge-Precipitation Relationship for the Flow Systems of the Study Area

SE ROA 50515

JA_15916

The recharge efficiencies derived by this analysis are presented in Table 9-1 along with the standard Maxey-Eakin precipitation zones and efficiencies for comparison. For all flow systems, except the MVFS, the efficiencies for the >20 in./yr zone are much greater than the Maxey-Eakin efficiency for the same interval. However, they are very similar for the middle to lower zones. This places greater volumes of recharge at the higher altitudes, where the precipitation is greater. For the MVFS, all efficiencies, except the one for the maximum precipitation zone, are well below the Maxey-Eakin efficiencies.

A test was conducted to evaluate the relative importance of the higher portions of the curves derived in this study. The volume of recharge was calculated for each Maxey-Eakin precipitation band for the entire study area, and area-weighted recharge efficiencies (Table 9-1) were applied to the appropriate band. The resulting recharge volumes are shown in Figure 9-2. The majority of the recharge corresponds to precipitation bands of less than or equal to 25 in./yr. Actually, only less than 12 percent of the total recharge calculated for the study area corresponds to areas where precipitation rates are greater than 25 in./yr. The areas where precipitation rates are larger than 25 in./yr are small because they are located only at the tops of mountains or along the crests of mountain ranges.

Table 9-1
Mean Recharge Efficiencies as Percentage of Precipitation

Precipitation Zone (in.)	WRFS	MVFS	GVFS	GSLDFS	Maxey-Eakin
<8	0	0	0	0	0
8 to 12	0.61	0.06	1.41	1.05	3
12 to 15	3.47	0.89	5.30	4.47	7
15 to 20	11.86	4.92	12.66	9.86	15
>20	37.28	17.55	31.65	30.97	25

Note: Recharge efficiencies are weighted by the areas of the corresponding precipitation zone.

9.4.2 Spatial Recharge Distribution

Recharge efficiencies derived for 1-in. precipitation bands were used to calculate recharge rates and depict the spatial distribution of recharge from precipitation over the study area. The same information was used to compute recharge volumes for the individual basins composing the four flow systems.

The derived spatial recharge distribution is presented on Figure 9-3. The calculated groundwater recharge rates are largest in the northern part of the study area, which coincides with the highest mountain ranges of the GSLDFS and GVFS (Figure 9-3). Groundwater recharge rates are generally lower in the middle of the study area. No groundwater recharge occurs in most of the southern basins. It must be noted that this spatial distribution only accounts for variation of recharge rates with altitude. It does not explicitly account for the geology of the units through which precipitation infiltrates to recharge the flow system, and it does not explicitly distribute the recharge from runoff to the actual locations where it occurs. The quantity of recharge from infiltration is, however, implicitly included in the recharge estimated using the groundwater-balance method. Although the recharge

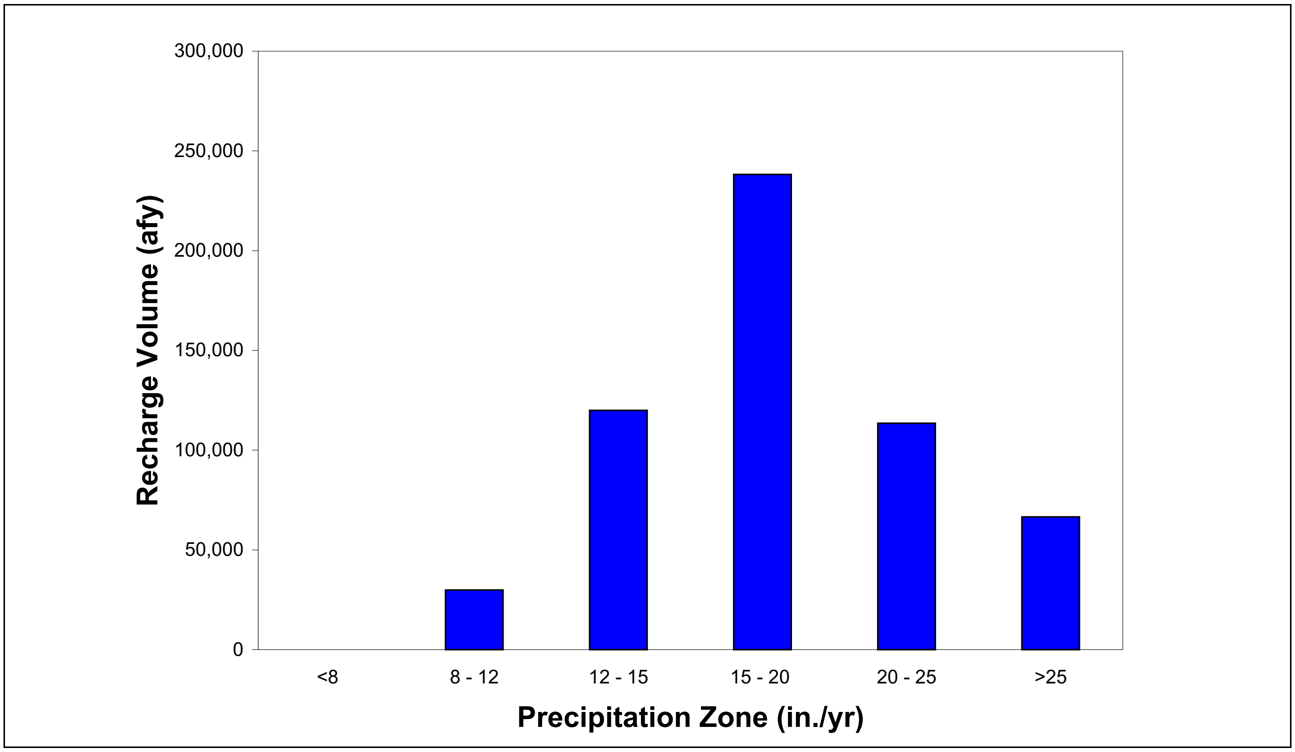

Figure 9-2
Recharge Volume Distribution by Maxey-Eakin Precipitation Zone for Study Area

map shown on Figure 9-3 does not accurately depict the spatial distribution of recharge, it does provide an approximate distribution on a basin-by-basin basis.

The recharge volumes were calculated by multiplying the recharge efficiency by the volume of precipitation calculated for each band. The recharge values were then summed for each basin and compared to previously reported estimates (Section 9.2). Table 9-2 lists the calculated annual recharge volumes as compared to the ranges of recharge estimates from previous studies. Two detailed tables listing each of the reported estimates are located in Appendix I. As shown in Table 9-2, all calculated basin recharge volumes fall within the ranges of previous estimates.

The total recharge estimated for the entire study area is 570,933 afy. This value falls within the overall range derived from the estimates reported in the literature: 396,029 to 1,264,363 afy (Epstein, 2004). The extreme values defining the range of total annual recharge volume correspond to estimates derived by Epstein (2004) in his reevaluation of previous methods using his model. The minimum value corresponds to the numerical version of the Maxey-Eakin (1949) Method (N-ME), and the maximum value corresponds to the numerical version of the Nichols (2000) Method (N-N).

The annual recharge volume for each basin was also calculated as a percentage of the annual precipitation volume of that basin (Table 9-3). The basin recharge volumes range between 0 and 7 percent of the corresponding basin's precipitation volumes. This range is similar to the percentage of 3 to 7 percent reported by Eakin et al. (1976) for the Great Basin region. Similar numbers were generated for each of the flow systems and for the whole study area. The largest annual recharge volume as a percentage of precipitation volume was calculated for the GVFS (7 percent) and

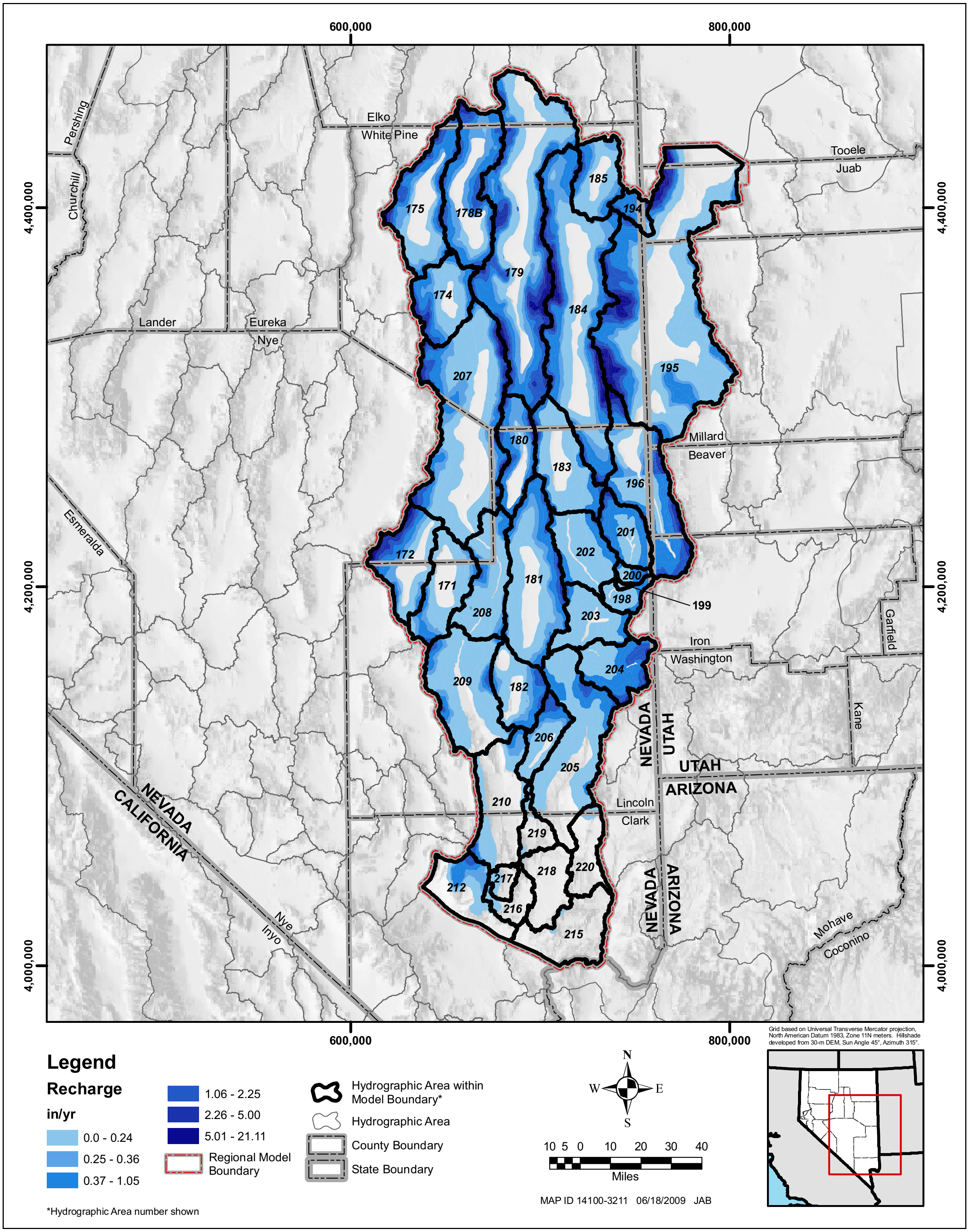

Figure 9-3
Recharge Distribution for Study Area

SE ROA 50518

JA_15919

Table 9-2
Comparison of Recharge Estimates to Reported Ranges in afy

HA Number	HA Name	This Study	Reported Value		Source
			Minimum	Maximum	
	Goshute Valley Flow System				
178B	Butte Valley South	24,688	12,165	55,029	Dettinger (1989); Epstein (2004)[a]
179	Steptoe Valley	91,685	84,885	171,952	Epstein (2004)[b]; Epstein (2004)[a]
	Total (Flow System)	**116,373**	**100,000**	**226,981**	Scott et al. (1971); Epstein (2004)[a]
	Great Salt Lake Desert Flow System				
184	Spring Valley	81,339	53,335	139,194	Epstein (2004)[b]; Epstein (2004)[a]
185	Tippett Valley	5,616	4,282	18,418	Halford (2008); Epstein (2004)[a]
194	Pleasant Valley	5,388	2,931	10,756	Epstein (2004)[c]; Epstein (2004)[a]
195	Snake Valley	104,210	34,697	106,556	Epstein (2004)[b]; Halford (2008)
196	Hamlin Valley	41,358	6,451	50,269	Epstein (2004)[b]; Halford (2008)
	Total (Flow System)	**237,911**	**104,502**	**295,884**	Epstein (2004)[b]; Epstein (2004)[a]
	Meadow Valley Flow System				
183	Lake Valley	9,861	10,875	62,123	Epstein (2004)[b]; Epstein (2004)[a]
202	Patterson Valley	5,656	6,000	51,852	Scott et al. (1971); Epstein (2004)[a]
201	Spring Valley	9,644	8,892	43,969	Epstein (2004)[b]; Epstein (2004)[a]
200	Eagle Valley	1,465	890	7,509	Flint et al. (2004) (Mean year); Epstein (2004)[a]
199	Rose Valley	79	43	1,541	Flint et al. (2004) (Time series); Epstein (2004)[a]
198	Dry Valley	1,953	1,300	14,055	Scott et al. (1971); Epstein (2004)[a]
203	Panaca Valley	2,381	1,500	28,408	Scott et al. (1971); Epstein (2004)[a]
204	Clover Valley	15,110	1,700	46,946	Scott et al. (1971); Epstein (2004)[a]
205	Lower Meadow Valley Wash	8,078	1,300	44,841	Scott et al. (1971); Epstein (2004)[a]
	Total (Flow System)	**54,227**	**35,900**	**301,244**	Scott et al. (1971); Epstein (2004)[a]
	White River Flow System				
175	Long Valley	20,496	5,011	52,736	Kirk and Campana (1990); Epstein (2004)[a]
174	Jakes Valley	12,658	7,242	39,000	Mizell et al. (2007); Halford (2008)
207	White River Valley	42,037	30,759	89,570	Flint et al. (2004) (time series); Epstein (2004)[a]
180	Cave Valley	15,044	8,964	45,913	Halford (2008); Epstein (2004)[a]
172	Garden Valley	25,292	5,331	32,223	Epstein (2004)[b]; Epstein (2004)[a]
171	Coal Valley	4,020	2,000	12,107	Scott et al. (1971); Epstein (2004)[a]
208	Pahroc Valley	4,705	1,994	19,362	Kirk and Campana (1990); Epstein (2004)[a]
181	Dry Lake Valley	16,208	5,000	50,389	Scott et al. (1971); Epstein (2004)[a]
182	Delamar Valley	6,627	1,000	21,442	Scott et al. (1971); Epstein (2004)[a]
209	Pahranagat Valley	5,726	1,508	15,979	Kirk and Campana (1990); Epstein (2004)[a]
206	Kane Springs Valley	4,329	460	13,864	Epstein (2004)[d]; Epstein (2004)[a]
210	Coyote Spring Valley	2,215	535	8,331	Epstein (2004)[d]; Epstein (2004)[a]
219	Muddy River Springs Area	41	0	509	Epstein (2004)[d, e]; Epstein (2004)[c]
217	Hidden Valley	45	0	571	Epstein (2004)[d]; Flint et al. (2004) (Time series)
216	Garnet Valley	101	0	1,000	Epstein (2004)[d]; Flint et al. (2004) (Time series)
218	California Wash	0	0	1,738	SNWA (2006, 2007); Epstein (2004)[c]
215	Black Mountains Area	0	0	3,644	SNWA (2006, 2007); Epstein (2004)[b]
220	Lower Moapa Valley	35	0	1,454	Flint et al. (2004) (Mean year); Epstein (2004)[c]
	Total (Flow System)	**159,580**	**104,500**	**396,389**	Scott et al. (1971); Epstein (2004)[a]
	Las Vegas Flow System				
212	Las Vegas Valley (Partial)	2,843	---	---	---
	Total (Project Study Area)	**570,933**	**396,029**	**1,264,363**	Epstein (2004)[b]; Epstein (2004)[a]

[a]Numeric Nichols Method
[b]Numeric Maxey-Eakin Method
[c]Bootstrap Brute-Force Model
[d]Maxey-Eakin Method Evaluation
[e]Nichols Method Evaluation

Table 9-3
Recharge as a Percentage of Precipitation

HA Number	HA Name	Precipitation[a] (afy)	Recharge (afy)	Recharge as Percentage of Precipitation
Goshute Valley Flow System				
178B	Butte Valley South	502,030	24,688	5%
179	Steptoe Valley	1,271,360	91,685	7%
	Total (Flow System)	**1,773,390**	**116,373**	**7%**
Great Salt Lake Desert Flow System				
184	Spring Valley	1,115,613	81,339	7%
185	Tippett Valley	212,996	5,616	3%
194	Pleasant Valley	79,362	5,388	7%
195	Snake Valley	1,592,560	104,210	7%
196	Hamlin Valley	649,174	41,358	6%
	Total (Flow System)	**3,649,705**	**237,911**	**7%**
Meadow Valley Flow System				
183	Lake Valley	400,964	9,861	2%
202	Patterson Valley	317,671	5,656	2%
201	Spring Valley	242,839	9,644	4%
200	Eagle Valley	46,367	1,465	3%
199	Rose Valley	8,738	79	1%
198	Dry Valley	91,900	1,953	2%
203	Panaca Valley	233,956	2,381	1%
204	Clover Valley	306,717	15,110	5%
205	Lower Meadow Valley Wash	551,874	8,078	1%
	Total (Flow System)	**2,201,026**	**54,227**	**2%**
White River Flow System				
175	Long Valley	449,902	20,496	5%
174	Jakes Valley	289,002	12,658	4%
207	White River Valley	1,010,761	42,037	4%
180	Cave Valley	265,033	15,044	6%
172	Garden Valley	350,969	25,292	7%
171	Coal Valley	267,397	4,020	2%
208	Pahroc Valley	309,740	4,705	2%
181	Dry Lake Valley	571,040	16,208	3%
182	Delamar Valley	235,967	6,627	3%
209	Pahranagat Valley	418,495	5,726	1%
206	Kane Springs Valley	145,587	4,329	3%
210	Coyote Spring Valley	272,214	2,215	1%
219	Muddy River Springs Area	53,504	41	0%
217	Hidden Valley	33,040	45	0%
216	Garnet Valley	54,873	101	0%
218	California Wash	106,283	0	0%
215	Black Mountains Area	168,683	0	0%
220	Lower Moapa Valley	94,697	35	0%
	Total (Flow System)	**5,097,186**	**159,580**	**3%**
Las Vegas Flow System				
212	Las Vegas Valley (Partial)	193,145	2,843	1%
	Total	**193,145**	**2,843**	**1%**
	Total (Project Study Area)	**12,914,452**	**570,933**	**4%**

[a]Total precipitation volume derived from 800-m PRISM grid, Version 2.

GSLDFS (7 percent); percentages are only 2 and 3 percent for the MVFS and WRFS, respectively. For the entire study area, recharge represents 4 percent of precipitation. The range of percentages are comparable to those reported in the NDWR/USGS Reconnaissance Series.

9.5 Uncertainty Analysis

An uncertainty analysis was conducted to identify the potential ranges of recharge for basins of the study area. The uncertainty associated with the solutions was examined from multiple angles as follows:

- Evaluation of uncertainty in solver solutions
- Evaluation of the BARCASS groundwater budgets

9.5.1 Evaluation of Uncertainty in Solver Solutions

The uncertainty of recharge estimates derived by the groundwater-balance method is directly related to the uncertainty associated with the estimates of precipitation and groundwater ET and lateral boundary flow volumes. The uncertainty in the precipitation distribution is not included in this analysis. Only the errors associated with the estimates of groundwater ET and lateral boundary flow are propagated to the derived estimate of recharge.

Given that the recharge volume of each flow system was calculated as the algebraic sum of the groundwater ET volumes and the lateral boundary flow volumes, the error propagation is expressed through the variances as follows:

$$VAR_R = VAR_{ET} + VAR_{BF} \qquad \text{(Eq. 9-5)}$$

where,

VAR_R = Variance of recharge volume estimate (afy^2)
VAR_{ET} = Variance of groundwater ET volume estimate (afy^2)
VAR_{BF} = Variance of lateral boundary flow volume (afy^2)

The resulting recharge variances were then used to calculate a standard deviation and a coefficient of variation for each flow system as follows:

$$COV = \frac{STD}{R} \qquad \text{(Eq. 9-6)}$$

where,

COV = Coefficient of variation (-)
STD = Standard deviation (afy) [STD = VAR$^{1/2}$]
R = Recharge volume for flow system (afy)

SE ROA 50521

JA_15922

The uncertainties associated with groundwater ET and lateral boundary fluxes are as described in Section 7.0 and processed as follows:

- The variances of each component of the groundwater discharge were compiled for each flow system.
- They were then summed to yield a variance for the total recharge volume of each flow system (Equation 9-5).
- The square root of this variance was calculated and divided by the recharge volume of the flow system to yield a coefficient of variability.

The calculations and results are shown in Table 9-4. The coefficients of variation for flow system recharge volumes vary between 0.13 and 0.25. Assuming that the recharge probability distributions are normal, a range of recharge volume can be derived using the value derived from the solution and the standard deviations listed in Table 9-4. The resulting recharge ranges are listed in Table 9-5. The listed ranges represent the 95 percent confidence range, i.e., the mean value plus or minus two standard deviations.

Assuming that the uncertainty associated with recharge is dominant, it can be transferred to the recharge efficiencies (Table 9-6). The uncertainty in the actual recharge efficiencies may in reality be larger due to the uncertainty associated with precipitation. However, for the purpose of the numerical model, it is assumed that precipitation is invariable, as its magnitude has no effect on the estimates of recharge derived by the groundwater-balance method. Thus, the uncertainty of the recharge volumes is only dependent on the uncertainty associated with the discharge estimates.

9.5.2 Evaluation of BARCASS Groundwater Budgets

The BARCASS interpretations of groundwater flow in the basins common to the two studies were evaluated. The purpose of this evaluation was two-fold: (1) to derive recharge efficiencies that correspond to the groundwater budgets interpreted by Welch et al. (2008) for the BARCASS basins and compare them with the recharge efficiencies derived for this study and (2) to apply the derived recharge efficiencies to the four flow systems and evaluate the impact on the flow system's budget components.

The basins, flow-routing patterns, and discharge components of the groundwater budgets reported for BARCASS were entered into the solvers. The precipitation distribution used in the solvers was unchanged. The grid used in BARCASS is not available. Comparison of the results are summarized in Table 9-7 for recharge efficiencies and in Table 9-8 for annual recharge volumes. The solvers were initially run for each flow system in the study area. If a solution could not be found for the flow system, solutions were derived for each of the basins separately. The solver runs are described by flow system in the following sections.

Table 9-4
Calculations of Recharge Uncertainty

Budget Component	Groundwater Volume (afy)	Coefficient of Variation	Standard Deviation (afy)	Variance (afy^2)
Goshute Valley Flow System				
Groundwater ET from Butte Valley South	**11,876**	0.89	10,586	112,073,878
Groundwater ET from Steptoe Valley	**101,497**	0.26	26,698	712,765,121
Outflow from Butte Valley South	**1,000**	0.60	597	356,559
Outflow from Steptoe Valley	**2,000**	0.41	825	681,141
Total Recharge	**116,373**	**0.25**	**28,738**	**825,876,699**
Great Salt Lake Desert Flow System				
Groundwater ET from Spring Valley	**75,615**	0.19	14,666	215,099,235
Groundwater ET from Tippett Valley	**1,742**	0.68	1,185	1,403,368
Groundwater ET from Pleasant Valley	**912**	0.15	137	18,770
Groundwater ET from Snake Valley	**129,041**	0.21	27,219	740,892,465
Groundwater ET from Hamlin Valley	**2,333**	0.38	896	802,068
Outflow from Snake Valley to Tule Valley	**15,000**	0.86	12,900	166,410,000
Outflow from Tippett Valley	**3,874**	0.60	2,325	5,403,524
Outflow from Snake Valley to Great Salt Lake Desert	**9,374**	0.79	7,417	55,016,423
Total Recharge	**237,891**	**0.14**	**34,424**	**1,185,045,853**
Meadow Valley Flow System				
Groundwater ET from Lake Valley	**6,134**	0.71	4,354	18,958,543
Groundwater ET from Dry Valley	**3,709**	0.27	995	989,282
Groundwater ET from Rose Valley	**594**	0.32	192	36,895
Groundwater ET from Eagle Valley	**1,034**	0.35	361	130,583
Groundwater ET from Spring Valley	**3,913**	0.31	1,228	1,508,369
Groundwater ET from Patterson Valley	**1,346**	0.39	523	273,481
Groundwater ET from Panaca Valley	**18,895**	0.25	4,747	22,533,926
Groundwater ET from Clover Valley	**5,840**	0.33	1,943	3,774,922
Groundwater ET from Lower Meadow Valley Wash	**9,668**	0.13	1,293	1,670,766
Outflow to WRFS	**3,095**	0.44	1,362	1,854,499
Total Recharge	**54,228**	**0.13**	**7,192**	**51,731,266**
White River Flow System				
Groundwater ET from Garden Valley	**1,696**	0.27	464	215,150
Groundwater ET from Jakes Valley	**858**	0.35	298	89,006
Groundwater ET from Long Valley	**1,233**	0.92	1,138	1,296,024
Groundwater ET from Cave Valley	**1,550**	0.70	1,091	1,191,051
Groundwater ET from White River Valley	**76,701**	0.35	27,062	732,374,506
Groundwater ET from Pahranagat Valley	**28,516**	0.10	2,842	8,075,260
Groundwater ET from Muddy River Springs Area	**5,989**	0.25	1,495	2,234,441
Groundwater ET from California Wash	**4,505**	0.25	1,126	1,267,469
Groundwater ET from Lower Moapa Valley	**25,311**	0.23	5,894	34,737,000
Groundwater ET from Black Mountain Area	**1,432**	0.20	289	83,715
Inflow from Tikaboo Valley	**7,200**	0.68	4,896	23,970,816
Inflow from Meadow Valley Flow System	**3,095**	0.44	1,362	1,854,499
Outflow via Muddy River (at Overton)	**7,000**	0.05	350	122,500
Discharge from Rogers and Blue Point Springs	**1,600**	0.05	80	6,400
Outflow from Lower Moapa Valley	**13,482**	0.48	6,471	41,878,500
Total Recharge	**159,578**	**0.18**	**29,144**	**849,396,336**

Table 9-5
Flow System Ranges of Annual Recharge Volumes in afy

Flow System	Mean	95 Percent Confidence Interval[a]	
		Lower	Upper
Goshute Valley	116,373	58,897	173,849
Great Salt Lake Desert	237,891	169,042	306,740
Meadow Valley	54,228	39,843	68,613
White River	159,578	101,289	217,867
Total[b]	**568,070**	**369,072**	**767,069**

[a]95 percent confidence interval estimated as mean ±2 x STD.
[b]Not including portion of Las Vegas Valley in the model area.

Table 9-6
Flow System Recharge Efficiency Uncertainty by Maxey-Eakin Zone

Maxey-Eakin Precipitation Zone (in.)	Area (acres)	Precipitation Volume (afy)	Mean Recharge Efficiency (percent)	Mean Recharge Volume (afy)	COV	Recharge Efficiency (percent)		Recharge Volume (afy)	
						Minimum	Maximum	Minimum	Maximum
Goshute Valley Flow System									
<8	51,243	32,027	0.00	0	0.25	0.00	0.00	0	0
8 to 12	550,537	475,031	1.41	6,705	0.25	0.71	2.12	3,353	10,058
12 to 15	464,543	515,331	5.30	27,327	0.25	2.65	7.95	13,664	40,991
15 to 20	278,696	388,510	12.66	49,195	0.25	6.33	18.99	24,598	73,793
>20	54,258	104,739	31.65	33,146	0.25	15.82	47.47	16,573	49,718
Total or Mean	**1,399,277**	**1,515,637**	**7.68**	**116,373**	**0.25**	**3.84**	**11.52**	**58,186**	**174,559**
Great Salt Lake Desert Flow System									
<8	156,131	95,960	0.00	0	0.14	0.00	0.00	---	---
8 to 12	1,388,238	1,171,173	1.05	12,328	0.14	0.76	1.35	8,876	15,780
12 to 15	705,995	788,183	4.47	35,221	0.14	3.22	5.72	25,359	45,082
15 to 20	549,652	773,466	9.86	76,253	0.14	7.10	12.62	54,902	97,604
>20	187,463	368,440	30.97	114,110	0.14	22.30	39.64	82,159	146,061
Total or Mean	**2,987,479**	**3,197,222**	**7.44**	**237,912**	**0.14**	**5.36**	**9.52**	**171,296**	**304,527**
Meadow Valley Flow System									
<8	144,584	79,040	0.00	0	0.13	0.00	0.00	---	---
8 to 12	380,970	330,228	0.06	210	0.13	0.05	0.08	155	264
12 to 15	756,932	857,470	0.89	7,665	0.13	0.66	1.13	5,672	9,658
15 - 20	569,180	795,638	4.92	39,157	0.13	3.64	6.20	28,976	49,338
>20	23,536	40,996	17.55	7,196	0.13	12.99	22.12	5,325	9,067
Total or Mean	**1,875,202**	**2,103,372**	**2.58**	**54,228**	**0.13**	**1.91**	**3.25**	**40,129**	**68,327**
White River Flow System									
<8	1,072,005	572,741	0.00	0	0.18	0.00	0.00	---	---
8 to 12	1,988,199	1,741,618	0.61	10,660	0.18	0.39	0.83	6,822	14,498
12 to 15	1,295,142	1,433,007	3.47	49,720	0.18	2.22	4.72	31,821	67,619
15 to 20	449,876	620,595	11.86	73,608	0.18	7.59	16.13	47,109	100,106
>20	37,702	68,647	37.28	25,591	0.18	23.86	50.70	16,378	34,804
Total or Mean	**4,842,924**	**4,436,607**	**3.60**	**159,579**	**0.18**	**2.30**	**4.89**	**102,130**	**217,027**
Total or Mean	**11,104,883**	**11,252,839**	**5.05**	**568,091**	---	**3.30**	**6.79**	**371,742**	**764,440**

Table 9-7
Recharge Efficiencies Derived from BARCASS Discharge Estimates

Goshute Valley Flow System						
Precipitation (in.)	BARCASS[a]			This Study[a]		
	Steptoe Valley	Butte Valley South	Mean[b]	Mean	95 Percent CI[c] Lower	Upper
<8	0	0	0	0.00	0.00	0.00
8 to 12	3.57	3.72	3.65	1.41	0.71	2.12
12 to 15	11.59	8.03	9.81	5.30	2.65	7.95
15 to 20	21.71	15.66	18.69	12.66	6.33	18.99
≥20	39.83	33.62	36.73	31.65	15.82	47.47
Great Salt Lake Desert Flow System						
Precipitation (in.)	BARCASS[a]			This Study[a]		
	Big Snake Valley	Spring Valley	Mean[b]	Mean	95 Percent CI[c] Lower	Upper
<8	0	0	0	0.00	0.00	0.00
8 to 12	0.25	1.82	1.04	1.05	0.76	1.35
12 to 15	2.21	6.30	4.25	4.47	3.22	5.72
15 to 20	7.05	13.93	10.49	9.86	7.10	12.62
≥20	24.15	35.49	29.82	30.97	22.30	39.64
Meadow Valley Flow System						
Precipitation (in.)	BARCASS[a]			This Study[a]		
	Lake Valley	---	---	Mean	95 Percent CI[c] Lower	Upper
<8	0	---	---	0.00	0.00	0.00
8 to 12	0.07	---	---	0.06	0.05	0.08
12 to 15	1.11	---	---	0.89	0.66	1.13
15 to 20	6.46	---	---	4.92	3.64	6.20
≥20	23.94	---	---	17.55	12.99	22.12
White River Flow System						
Precipitation (in.)	BARCASS[a]			This Study[a]		
	BARCASS Basins Only	---	---	Mean	95 Percent CI[c] Lower	Upper
<8	0	---	---	0.00	0.00	0.00
8 to 12	0.66	---	---	0.61	0.39	0.83
12 to 15	3.29	---	---	3.47	2.22	4.72
15 to 20	11.73	---	---	11.86	7.59	16.13
≥20	37.51	---	---	37.28	23.86	50.70

[a]Value shown as percentage.
[b]Average of Steptoe Valley and Butte Valley South for the Goshute Valley Flow System and Big Snake Valley and Spring Valley for the Great Salt Lake Desert Flow System.
[c] 95 percent confidence interval (CI) estimated as mean ±2 x STD.

SE ROA 50525

JA_15926

Table 9-8
Flow System Annual Groundwater Budgets Based on BARCASS Discharge Estimates in afy

Goshute Valley Flow System			
		BARCASS	
Budget Component	This Study	Steptoe Valley	Butte Valley South
Recharge	116,373	203,880	35,876
Boundary Inflow	0	0	0
Groundwater ET	113,373	113,373	11,876
Boundary Outflow	3,000	90,507	24,000
Great Salt Lake Desert Flow System			
		BARCASS	
Budget Component	This Study	Big Snake Valley	Spring Valley
Recharge	237,912	166,568	301,634
Boundary Inflow	0	33,000	33,000
Groundwater ET	209,642	209,642	209,642
Boundary Outflow	28,270	-10,074	124,992
Meadow Valley Flow System			
		BARCASS	
Budget Component	This Study	Lake Valley	---
Recharge	54,228	82,326	---
Boundary Inflow	0	20,000	---
Groundwater ET	51,133	62,730	---
Boundary Outflow	3,095	39,596	---
White River Flow System			
		BARCASS	
Budget Component	This Study	All Basins	---
Recharge	159,579	152,198	---
Boundary Inflow	10,295	48,295	---
Groundwater ET	147,792	147,792	---
Boundary Outflow	22,082	52,702	---

9.5.2.1 Goshute Valley Flow System

The BARCASS area includes the same portion of the GVFS as in the study area, which consists of Butte Valley South and Steptoe Valley. The groundwater ET volumes are unchanged. However, boundary flow locations and volumes estimated by Welch et al. (2008) for these two basins are different. This information was entered into the solver to derive a single solution; however, the solver yielded no solution. Solutions were then derived for each basin separately. The derived efficiencies for the two lower precipitation zones are larger than those derived by this study (Table 9-7). However, the derived recharge volumes for the flow system (Table 9-7), as a whole, fall within the range of uncertainty derived by this study (Table 9-8).

9.5.2.2 Great Salt Lake Desert Flow System

The BARCASS area includes the same portion of the GSLDFS as in the study area, which consists of Spring, Tippett, Snake, Pleasant and Hamlin valleys. Two solver configurations were attempted. In the first configuration, all basins were included. The groundwater ET volumes for all basins and the boundary flow locations and volumes were assigned as interpreted by Welch et al. (2008). The solver yielded no solution in this case. Two separate solutions were then derived: one for Spring Valley and one for Big Snake Valley. The resulting recharge efficiencies are listed in Table 9-7. Overall groundwater budgets were then developed by entering the efficiencies derived for each case in all other basins (Table 9-8). The total outflow from the GSLDFS was 124,992 afy in the Spring Valley case and -10,074 afy in the Big Snake Valley case as compared to this study's volume of 28,270 afy. In the Spring Valley case, the negative volume means that groundwater would need to flow into the flow system to satisfy the mass balance. This is because the BARCASS Spring Valley recharge efficiencies yield less recharge than necessary as compared to the other two cases (Table 9-8).

9.5.2.3 Meadow Valley Flow System

The BARCASS area only includes one of the basins composing the MVFS: Lake Valley. A solver configuration consisting of only Lake Valley was set up. Groundwater ET and lateral boundary flows were set to represent the BARCASS results (Welch et al., 2008). The solver was executed to identify the recharge efficiencies associated with this flow configuration. The other basins of the MVFS were then added to Lake Valley, as configured by BARCASS, and the recharge efficiencies derived for Lake Valley were assigned to the other valleys. The resulting groundwater budget for the entire MVFS is presented in Table 9-8.

9.5.2.4 White River Flow System

The BARCASS area includes a portion of the WRFS, which consists of Long, Jakes, Cave, and White River valleys. Three test cases were examined.

- Test Case 1: The solver configuration was limited to the four BARCASS basins listed above, and all discharge volumes and interbasin flow directions were modified to match the flow routing used in the BARCASS interpretation (Welch et al., 2008). Modifications were then made to flow routing from Cave to White River and Pahroc valleys. The solver was executed, and a solution was found.

- Test Case 2: The remainder of the WRFS basins were added to the Test Case 1 solver setup. Groundwater ET and interbasin flow were as they were in the main solution for this flow system. However, the recharge efficiencies derived from Test Case 1 were applied to the additional basins. The solver was not run in this case. However, interbasin flow volumes were calculated.

- Test Case 3: The solver was setup as in the Test Case 2 solver setup, and a solution was sought for the whole flow system. The solver did not converge to a solution.

The recharge efficiencies derived for Test Case 1 are listed in Table 9-7. They are very close to the efficiencies derived for this study (Section 9.4.1). A remarkable result of the second test case is the amount of total outflow from the WRFS. The total outflow in this case is 47,702 afy, an amount more than double the one derived from the main solution: 22,082 afy (Table 9-8). This amount of outflow (47,702 afy) is similar to that simulated by LVVWD (2001).

10.0 PREDEVELOPMENT GROUNDWATER BUDGET

Analyses of the available hydrologic data were conducted and described in the previous sections of this report to derive independent estimates of groundwater discharge to the surface, interbasin groundwater flow, and recharge using Version 2 of the 800-m PRISM precipitation grid. This information was used to estimate the predevelopment groundwater budgets for the flow systems of the study area.

The resulting combined groundwater budget for the study area is presented in Table 10-1. The recharge and groundwater ET volumes reflect the total for all flow systems in the model area. The annual recharge volume for the portion of Las Vegas Valley contained within the model area was calculated using the recharge efficiencies derived for the WRFS and is included in the groundwater budgets presented in Table 10-1. The boundary flow only reflects flow into and out of the external boundaries of the study area. Discharge from Fish Springs is not explicitly included in the budget. Contributions of Snake Valley to Fish Springs, if any, would be through interbasin flow from Snake Valley.

These estimates for the groundwater-budget components as well as the uncertainty analyses were used to develop the numerical groundwater flow model.

Table 10-1
Predevelopment Groundwater Budget for Study Area

HA Name	Recharge (afy)	Groundwater ET (afy)	Inflow (afy)	Inflow From	Outflow (afy)	Outflow To
Goshute Valley Flow System[a]	116,373	113,373	0	---	3,000	Out of model boundary
Great Salt Lake Desert Flow System[a]	237,912	209,642	0	---	28,270	Out of model boundary
Meadow Valley Flow System	54,228	51,133	0	---	3,095	Out of MVFS
White River Flow System	159,579	147,792	10,295	MVFS and Tikaboo Valley	22,082	Out of model boundary
Las Vegas[a]	2,843	0	0	---	2,843	Out of model boundary
Project Model	570,933	521,940	7,200	Tikaboo Valley	56,193	Out of model boundary

[a]These flow systems are only partially represented in the Project model.

This Page Intentionally Left Blank

11.0 SUMMARY

A conceptual model of the groundwater flow system underlying the project study area of Southern Nevada Water Authority's Clark, Lincoln, and White Pine Counties Groundwater Development Project was developed. The conceptual model was used to develop a regional three-dimensional numerical flow model of the flow system underlying the study area (SNWA, 2009b). The numerical model was used to perform preliminary regional-scale simulations of the effects of SNWA-proposed groundwater pumping under alternate scenarios (SNWA, 2009a). The simulation results, in turn, will be used to assist in evaluations of the potential water-related effects on the environment. A summary of the conceptual model is presented in this section, followed by a list of the specific products used to develop the numerical model (SNWA, 2009b).

11.1 Conceptual Model

The conceptual model was developed for an area extending over portions of Clark, Lincoln, and White Pine counties in Nevada and a small portion of western Utah. The flow system underlying the study area is within the Central Carbonate-Rock Province in the Great Basin Region, and includes five flow systems: the MVFS and WRFS and portions of the GVFS, GSLDFS, and Las Vegas Flow System. See Plate 1 for the locations of many of the features of the conceptual model under predevelopment conditions.

Components of the conceptual model include (1) a simplified hydrogeologic framework, (2) a description of groundwater occurrence and movement under natural conditions, (3) estimates of a predevelopment groundwater budget, and (4) anthropogenic stresses and their effects included in (SNWA, 2009b). Each of these components is summarized below. Estimates of predevelopment groundwater budgets were derived using the groundwater-balance method. In the groundwater-balance method, recharge from precipitation is equated to the net discharge from the flow system (groundwater ET + subsurface outflow - subsurface inflow). Recharge from precipitation is derived as a function of the other estimated budget components. Information needed to implement this method consists of a precipitation distribution, estimates of groundwater ET, and estimated ranges of interbasin flow, where possible.

A simplified hydrogeologic framework was developed for the flow system underlying the study area. The simplified framework consists of several RMUs, which are groups of HGUs. Among the RMUs, two are classified as major aquifers: the basin-fill aquifer (composed of the upper and lower valley fill) and the carbonate-rock aquifer. Other RMUs include basement rocks that compose the base of the flow system (clastic rocks), plutons, plateau sediments, and an upper aquitard that separates the carbonate aquifer into upper and lower carbonate aquifers throughout much of the northern study area. The available aquifer-property data were compiled and analyzed, and ranges of properties were assigned to each of the RMUs.

The groundwater flow system is a finite three-dimensional body, bounded by the saturated zone at the top, low hydraulic-conductivity geologic units at the bottom, and variable hydrogeologic features on the sides corresponding to the hydrographic-area boundaries of the peripheral basins. Flow into or out of the flow system may occur through permeable segments of the boundaries. The regional flow model comprises two full flow systems—WRFS and MVFS—and two partial flow systems—GVFS and GSLDFS. In addition, a small portion of Las Vegas Valley located north of the LVVSZ is included in the conceptual model area. Most of the groundwater recharge occurs in the mountain ranges present across the northern part of the study area. Regional groundwater discharge occurs by ET through major springs and associated streams or through the subsurface. General regional groundwater flow directions are north to south in the WRFS and MVFS, mostly south to north in GVFS, and to the north and potentially to the east in the GSLDFS.

Groundwater ET was estimated using two methods. Method 1 was developed as part of this study and was applied to the southern basins of the study area. Method 2 was developed by the USGS and was used by Welch et al. (2008) (BARCASS) and by DeMeo et al. (2008) (southern CRFS ET study). Method 2 estimates of ET were applied to selected basins of the study area. Spring data including locations, land-surface elevations, and flow rates were compiled and evaluated. All regional springs and selected intermediate springs were included in the conceptual model as such. Estimated ranges of external and selected internal interbasin flow volumes were derived independently using either the Monte Carlo method or the available information. These estimates of interbasin flow were used to constrain the groundwater-budget solutions and to support the definition of boundary conditions in the numerical flow model.

The spatial distribution of precipitation was represented by the PRISM grids. Estimates of predevelopment groundwater budgets were derived for each of the main flow systems using the groundwater-balance method. The budgets were then combined and simplified to express an overall budget for the entire regional flow system composing the study area. First, recharge from precipitation was derived as a function of estimates of the other budget components (summarized above). Second, to distribute the precipitation recharge, recharge efficiencies were expressed as a power function of precipitation, and the function's coefficients were derived through an optimization process. The optimization process was implemented using the Excel® Solver and consisted of solving for parameter values (i.e., unknowns), including the power function coefficients, under a set of constraints (i.e., estimated ranges of interbasin flow at selected locations). The optimization process also yielded estimates of selected interbasin flow annual volumes and groundwater budgets for each basin in the study area.

A combined groundwater budget representing predevelopment conditions was developed for the entire groundwater flow system (Table 10-1). The budget components are as follows, rounded to the nearest 1,000 afy:

- Precipitation recharge totaling about 571,000 afy
- Groundwater discharge from ET areas totaling about 522,000 afy
- Net boundary outflow totaling about 56,000 afy, outflow totaling 63,000 afy, and inflow totaling 7,000 afy

Anthropogenic stresses, including historical consumptive groundwater-use rates and their effects on water levels, and spring and stream flows were evaluated and are presented within the numerical model report (SNWA, 2008b).

11.2 Products for Numerical Model

Several specific products describe the four main components of the conceptual model that were used to construct the numerical model. These products are listed along with their locations in the reports.

- Simplified hydrogeologic framework
  - A list of simplified hydrogeologic units (Table 4-1)
  - A surficial map of the simplified hydrogelogic units (Plate 2)
  - A map of major structural features affecting groundwater flow (Plate 2)
  - Simplified hydrogeologic cross sections (Plate 3)
  - Maps depicting the extent and topography of each simplified HGU (Figures B-1 to B-12)
  - Hydraulic properties for the simplified HGUs and major structural features (Section 4.6)
- Groundwater occurrence and movement under natural conditions
  - Locations of head measurements and mean predevelopment heads and uncertainty (SNWA, 2008a)
  - Contours of regional potentiometric head (Plate 1)
  - Delineated areas of groundwater ET under predevelopment conditions (Plate 1)
  - Locations of major springs, their elevations, and source depths (Plate 1, and Tables G-1 and G-2)
  - Locations of interbasin flow segments (Plate 1)
  - Approximate locations of recharge from precipitation (Plate 1)
  - Location of streams (Plate 1)
- Estimates of a predevelopment groundwater budget
  - Mean annual volumes and uncertainty of groundwater ET (Tables F-3 and 7-14)

- Mean annual flow rates and uncertainty of regional and selected intermediate springs (Table G-1)

- Mean annual rates of interbasin flow and range of uncertainty (Tables 8-2 and 8-3)

- Spatial distribution of precipitation (Figure 6-4)

- Recharge efficiencies and uncertainty range by recharge zones for each flow system (Table 9-6)

- Approximate spatial distribution of potential recharge from precipitation (Figure 9-3)

- Annual potential recharge volumes by basin (Table 9-2) and uncertainty ranges by flow system (Table 9-4)

• Anthropogenic stresses and their effects on flow system (SNWA, 2009b)

12.0 References

Allen, R.G., Pereira, L.S., Raes, D., and Smith, M., 1998, Crop evapotranspiration—guidelines for computing crop water requirements: Food and Agriculture Organization of the United Nations, Rome, Italy, FAO Irrigation and Drainage Paper No. 56.

American Society for Testing and Materials, 1996, Standard guide for conceptualization and characterization of ground-water systems, ASTM D-5979-96, American Society for Testing and Materials, West Conshohocken, PA, 7 p.

Anderson, J.R., Hardy, E.E., Roach, J.T., and Witmer, R.E., 1976, A land use and land cover classification system for use with remote sensor data: U.S. Geological Survey Professional Paper 964, 33 p.

Anderson, T.W., Freethey, G.W., and Tucci, P., 1992, Geohydrology and water resources of alluvial basins in south-central Arizona and parts of adjacent states: U.S. Geological Survey Professional Paper 1406-B, 77 p.

ASTM, see American Society for Testing and Materials.

Avon, L., and Durbin, T.J., 1994, Evaluation of the Maxey-Eakin method for estimating recharge to groundwater basins in Nevada: American Water Resources Association, Water Resources Bulletin, Vol. 30, No. 1, p. 99–111.

Barbour, M.G., Burk, J.H., and Pitts, W.D., 1987, Terrestrial plant ecology. Second edition: Menlo Park, California, Benjamin/Cummings Publishing Company, Inc.

Bastiaanssen, W.G.M., Noordman, E.J.M., Pelgrum, H., Davids, G., Thoreson, B.P., and Allen, R.G., 2005, SEBAL model with remotely sensed data to improve water-resources management under actual field conditions: Journal of Irrigation and Drainage Engineering, ASCE 131(1), p. 85-93.

Bechtel SAIC Company, LLC, 2004, Technical Basis Document No. 1—Climate and infiltration: U.S. Department of Energy, Office of Civilian Radioactive Waste Management, DE-AC28-01RW12101, Rev. 1, 206 p.

Beck, D.A., and Wilson, J.W., 2006, Synoptic discharge, water-property, and pH measurements for Muddy River Springs Area and Muddy River, Nevada, February 7, 2001: U.S. Geological Survey Scientific Investigations Report 2006-5237, 19 p.

Bedinger, M.S., Sargent, K.A., and Langer, W.H., eds., 1990, Studies of geology and hydrology in the Basin and Range Province, southwestern United States, for isolation of high-level radioactive waste—Characterization of the Bonneville region, Utah and Nevada: U.S. Geological Survey Professional Paper 1370-G, 49 p, seven plates.

Bedinger, M.S., Harrill, J.R., 2004, Appendix 1—Regional potential for interbasin flow of ground water, *in* Belcher, W.R., ed., 2004, Death Valley Regional Ground-water Flow System, Nevada and California—Hydrogeologic framework and transient ground-water flow model: U.S. Geological Survey Scientific Investigations Report 2004-5205.

Belcher, W.R., ed., 2004, Death Valley Regional Ground-Water Flow System, Nevada and California—Hydrogeologic framework and transient ground-water flow model: U.S. Geological Survey Scientific Investigations Report 2004-5205, 402 p.

Belcher, W.R., Elliott, P.E., and Geldon, A.L., 2001, Hydraulic-property estimates for use with a transient ground-water flow model of the Death Valley Regional Ground-Water Flow System, Nevada and California: U.S. Geological Survey Water-Resources Investigations Report 2001-4210 (revised August 1, 2002), 33 p.

Berger, D.L., 2000, Water budgets for Pine Valley, Carico Lake Valley, and Upper Reese River Valley hydrographic areas, middle Humboldt River basin, north-central Nevada—Methods for estimation and results: U.S. Geological Survey Water-Resources Investigations Report 99-4272, 45 p.

Berger, D.L., Johnson, M.J., Tumbusch, M.L., and Mackay, J., 2001, Estimates of evapotranspiration from the Ruby Lake National Wildlife Refuge area, Ruby Valley, northeastern Nevada, May 1999–October 2000: U.S. Geological Survey Water-Resources Investigations Report 01-4234, 38 p.

Bhark, E., Kelley, V., Pickens, J., Ruskauff, G., Gable, C., Reimus, P., Vesselinov, V., 2006, Well ER-6-1 tracer test analysis: Yucca Flat, Nevada Test Site, Nye County, Nevada: Stoller-Navarro Joint Venture, Las Vegas, Nevada, S-N/99205--084, 177 p.

Bittelli M., Ventura, F., Campbell, G.S., Snyder, R.L., Gallegati, F., and Pisa, P.R., 2008, Coupling of heat, water vapor, and liquid water fluxes to compute evaporation in bare soils: Journal of Hydrology, Vol. 362, p. 191-205.

Black, B.D., Hecker, S., Hylland, M.D., Christenson, G.L., and McDonald, G.N., 2003, Quaternary fault and fold database and map of Utah: Utah Geological Survey Map 193DM (CD-ROM).

Blakely, R.J., 1995, Potential theory in gravity and magnetic applications: New York, Cambridge University Press, 441 p.

Bolke, E.L., and Sumsion, C.T., 1978, Hydrologic reconnaissance of the Fish Springs Flat area, Tooele, Juab, and Millard counties, Utah: Utah Department of Natural Resources, Technical Publication No. 64, 36 p.

Brothers, K., Bernholtz, A.J., Buqo, T.S., and Tracy, J.V., 1994, Hydrology and steady state ground-water model of Spring Valley, Lincoln and White Pine counties, Nevada: Las Vegas Valley Water District, Cooperative Water Project, Report No. 13, 111 p.

Brothers, K., Buqo, T.S., and Tracy, J.V., 1993, Hydrology and steady state ground-water model of Snake Valley, east-central Nevada, and west-central Utah: Las Vegas Valley Water District, Cooperative Water Project, Report No. 9, 97 p.

Brothers, K., Katzer, T., and Johnson, M., 1996, Hydrology and steady state ground-water model of Dry Lake and Delamar valleys, Lincoln County, Nevada: Las Vegas Valley Water District, Cooperative Water Project Report No. 16, 71 p.

BSC, see Bechtel SAIC Company.

Bunch, R.L., and Harrill J.R., 1984, Compilation of selected hydrologic data from the MX missile-siting investigation, east-central Nevada and western Utah: U.S. Geological Survey Open-File Report 84-702, 128 p.

Buqo, T.S., 2002, Hydrogeologic and water supply assessment - Lewis Farm Area Lower Meadow Valley Wash Hydrographic Basin (Basin 205): Pahrump, Nevada, 48 p.

Cablk, M.E., and Kratt, C., 2007, A methodology for mapping shrub canopy cover in the Great Basin Desert using high spatial resolution satellite imagery: Desert Research Institute, Publication No. 41236, 28 p.

Caine, J.S., Evans, J.P., and Forster, C.B., 1996, Fault zone architecture and permeability structure: Geology, Vol. 24, No. 11, p. 1025–1028.

Campana, D.J., and Levandowski, D.W., 1991, The recognition of strike-slip fault systems using imagery, gravity, and topographic data sets: Photogrammetric Engineering and Remote Sensing, v. 57, n. 9, p. 1195-1201.

Carlton, S.M., 1985, Fish Springs Multibasin Flow System, Nevada and Utah [Master's thesis]: University of Nevada, Reno, 112 p.

Carpenter, E., 1915, Ground water in southeastern Nevada: U.S. Geological Survey Water-Supply Paper 365, 92 p.

Chidsey, T.C., Jr., 1978, Intrusions, alteration, and economic implications in the northern House Range, Utah: Brigham Young University Geology Studies, v. 25, pt. 3, p. 47-65.

Christiansen, W.J., 1977, Geology of the Fish Springs mining district, Juab County, Utah [M.S.thesis]: University of Utah, Salt Lake City, 66 p.

Clark, D.L., Oviatt, C.G., and Page, D., 2007, Progress report geologic map of Dugway Proving Ground and adjacent areas, parts of the Wildcat Mountain, Rush Valley, and Fish Springs 30' × 60' quadrangles, Toole County, Utah (year 1 and 2): Utah Geological Survey Open-File Report 501, scale 1:62,500.

Coats, R.R., 1987, Geology of Elko County, Nevada: Nevada Bureau of Mines and Geology Bulletin 101, 112 p., scale 1:250,000.

Congalton, R.G., and Green, K., 1999, Assessing the accuracy of remotely sensed data—Principles and practices: Boca Raton, Florida, CRC Press.

Contor, B.A., 2004, Recharge on non-irrigated lands: University of Idaho, Idaho Water Resources Research Institute, Technical Report 04-006, 19 p.

Cooper, D.J., Sanderson, J.S., Stannard, D.I., and Groeneveld, D.P., 2006, Effects of long-term water table drawdown on evapotranspiration and vegetation in an arid region phreatophyte community: Journal of Hydrology, Vol. 325, p. 21–34.

D'Agnese, F.A., Faunt, C.C., Turner, A.K., and Hill, M.C., 1997, Hydrogeologic evaluation and numerical simulation of the Death Valley Regional Ground-Water Flow System, Nevada and California: U.S. Geological Survey Water-Resources Investigations Report 96-4300, 131 p.

D'Agnese, F.A., O'Brien, G.M., Faunt, C.C., Belcher, W.R., and San Juan, C., 2002, A three-dimensional numerical model of predevelopment conditions in the Death Valley Regional Ground-Water Flow System, Nevada and California: U.S. Geological Survey Water-Resources Investigations Report 2002-4102, 122 p.

Daly, C., Gibson, W.P., Doggett, M., Smith, J., and Taylor, G., 2004, Up-to-date monthly climate maps for the conterminous United States, *in* Proceedings of the 14th American Meteorological Society Conference on Applied Climatology, Seattle, Washington, January 13–16, 2004, Paper P5.1, 8 p.

Daly, C., Halbleib, M., Smith, J.I., Gibson, W.P., Doggett, M.K., Taylor, G.H., Curtis, J., and Pasteris, P.A, 2008, Physiographically sensitive mapping of climatological temperature and precipitation across the conterminous United States: International Journal of Climatology, Vol. 28, p. 2031-2064.

Daly, C., Neilson, R.P., and Phillips, D.L., 1994, A statistical-topographic model for mapping climatological precipitation over mountainous terrain: Journal of Applied Meteorology, Vol. 33, No. 2, p. 140–158.

Daly, C., Taylor, G.H., and Gibson, W.P., 1997, The PRISM approach to mapping precipitation and temperature, *in* Proceedings of the 10th American Meteorological Society Conference on Applied Climatology, Reno, Nevada, October 20–23, p. 10–12.

Daly, C., Taylor, G.H., Gibson, W.P., Parzybok, T., Johnson, G.L., and Pasteris, P.A., 1998, Development of high-quality spatial climate datasets for the United States, *in* Arvanitis, L., ed., Proceedings of the First International Conference on Geospatial Information in Agriculture and Forestry, Lake Buena Vista, Florida, June 1–3, 1998: ERIM International, Inc., Ann Arbor, Michigan, p. I-512–I-519.

Davisson, M.L., and Rose, T.P., 2000, Maxey-Eakin methods for estimating groundwater recharge in the Fenner Watershed, southeastern California: U.S. Department of Energy, Lawrence Livermore National Laboratory, UCRL-ID-139027, 15 p.

DeMeo, G.A., Smith, J.L., Damar, N.A., and Darnell, J., 2008, Quantifying ground-water and surface-water discharge from evapotranspiration processes in 12 hydrographic areas of the Colorado Regional Ground-Water Flow System, Nevada, Utah, and Arizona: U.S. Geological Survey Scientific Investigations Report 2008-5116, 34 p.

Dettinger, M.D., 1989, Reconnaissance estimates of natural recharge to desert basins in Nevada, U.S.A., by using chloride-balance calculations: Journal of Hydrology, Vol. 106, p. 55–78.

Dettinger, M.D., Harrill, J.R., Schmidt, D.L., and Hess, J.W., 1995, Distribution of carbonate-rock aquifers and the potential for their development, southern Nevada and adjacent parts of California, Arizona, and Utah: U.S. Geological Survey Water-Resources Investigations Report 91-4146, 107 p.

Dettinger, M.D., and Schaefer, D.H., 1996, Hydrogeology of structurally extended terrain in the eastern Great Basin of Nevada, Utah, and adjacent states, from geologic and geophysical models: U.S. Geological Survey Hydrologic Atlas 694-D.

Deverel, S., Thomas, J., Decker, D., Earman, S., Mihevc, T., and Acheampong, S., 2005, Groundwater evaporation estimates using stable isotope and chloride data, Yelland Playa, Spring Valley, Nevada: Desert Research Institute, Division of Hydrologic Sciences, Publication No. 41219, 20 p.

Devitt, D.A., Sala, A., Smith, S.D., Cleverly, J., Shaulis, L.K., and Hammet, R., 1998, Bowen ratio estimates of evapotranspiration for *Tamarix Ramosissima* stands on the Virgin River in southern Nevada: Water Resources Research, Vol. 34, No. 9, p. 2407–2414.

Dixon, G.L., and Katzer, T., 2002, Geology and hydrology of the lower Virgin River Valley in Nevada, Arizona, and Utah: Virgin Valley Water District, Mesquite, Nevada, Report No. VVWD-01, 140 p.

Dixon, G.L., Rowley, P.D., Burns, A.G., Watrus, J.M., Donovan, D.J., and Ekren E.B., 2007, Geology of White Pine and Lincoln counties and adjacent areas, Nevada and Utah—The geologic framework of regional groundwater flow systems: Southern Nevada Water Authority, Las Vegas, Nevada, Doc. No. HAM-ED-0001, 157 p.

DOE, see U.S. Department of Energy.

Donovan, D.J., and Katzer, T., 2000, Hydrologic implications of greater ground-water recharge to Las Vegas Valley, Nevada: Journal of the American Water Resources Association, Vol. 36, No. 5, p. 1133–1148.

Dudley, W.W., Jr., and Larson, J.D., 1976, Effect of irrigation pumping on desert pupfish habitats in Ash Meadows, Nye County, Nevada: U.S. Geological Survey Professional Paper 927, 59 p.

Duebendorfer, E.M., and Black, R.A., 1992, The kinematic role of transverse structures in continental extension: An example from the Las Vegas Valley shear zone, Nevada: Geology, v. 20, p. 87–90.

Duell, L.F.W., Jr., 1990, Estimates of evapotranspiration in alkaline scrub and meadow communities of Owens Valley, California, using the Bowen-ratio, eddy-correlation, and Penman-combination methods: U.S. Geological Survey Water-Supply Paper 2370-E, 49 pp.

Eakin, T.E., 1962, Ground-water appraisal of Cave Valley in Lincoln and White Pine counties, Nevada: Nevada Department of Conservation and Natural Resources, Ground-Water Resources Reconnaissance Series Report 13, 27 p.

Eakin, T.E., 1963a, Ground-water appraisal of Dry Lake and Delamar valleys, Lincoln County, Nevada: Nevada Department of Conservation and Natural Resources, Ground-Water Resources Reconnaissance Series Report 16, 34 p.

Eakin, T.E., 1963b, Ground-water appraisal of Garden and Coal valleys, Lincoln and Nye counties, Nevada: Nevada Department of Conservation and Natural Resources, Ground-Water Resources Reconnaissance Series Report 18, 40 p.

Eakin, T.E., 1961, Ground-water appraisal of Long Valley, White Pine and Elko counties, Nevada: Nevada Department of Conservation and Natural Resources, Ground-Water Resources Reconnaissance Series Report 3, 82 p.

Eakin, T.E., 1963c, Ground-water appraisal of Pahranagat and Pahroc valleys, Lincoln and Nye counties, Nevada: Nevada Department of Conservation and Natural Resources, Ground-Water Resources Reconnaissance Series Report 21, 52 p.

Eakin, T.E., 1964, Ground-water appraisal of Coyote Spring and Kane Spring valleys and Muddy River Springs Area, Lincoln and Clark counties, Nevada: Nevada Department of Conservation and Natural Resources, Ground-Water Resources Reconnaissance Series Report 25, 55 p.

Eakin, T.E., 1966, A regional interbasin ground-water system in the White River area, southeastern Nevada: Water Resources Research, Vol. 2, No. 2, p. 251–271.

Eakin, T.E., Hughes, J.L., and Moore, D.O., 1967, Water-resources appraisal of Steptoe Valley, White Pine and Elko counties, Nevada: Nevada Department of Conservation and Natural Resources, Water Resources Reconnaissance Series Report 42, 62 p.

Eakin, T.E., Maxey, G.B., Robinson, T.W., Fredericks, J.C., and Loeltz, O.J., 1951, Contributions to the hydrology of eastern Nevada: State of Nevada, Office of the State Engineer, Water Resources Bulletin No. 12, 86 p.

Eakin, T.E., Price, D., and Harrill, J.R., 1976, Summary appraisals of the nation's ground-water resources - Great Basin Region: U.S. Geological Survey Professional Paper 813-G, 43 p.

Ekren, E.B., Orkild, P.P., Sargent, K.A., Dixon, G.L., 1977, Geologic map of Tertiary rocks, Lincoln County, Nevada: U.S. Geological Survey, Miscellaneous Investigations Series Map I-1041, scale 1:250,000.

Epstein, B.J., 2004, Development and uncertainty analysis of empirical recharge prediction models for Nevada's desert basins [M.S. thesis], University of Nevada, Reno, 215 p.

Ertec Western, Inc., 1981a, MX Siting Investigation—Water Resources Program—results of regional carbonate aquifer testing, Coyote Spring Valley, Nevada: U.S. Department of the Air Force, Ballistic Missile Office, Norton Air Force Base, California, Report E-TR-57, 65 p.

Ertec Western, Inc., 1981b, MX Siting Investigation—Water Resources Program—technical summary report, volume I: U.S. Department of the Air Force, Ballistic Missile Office, Norton Air Force Base, California, Report E-TR-52-I, 143 p.

Ertec Western, Inc., 1981c, MX Siting Investigation—Water Resources Program—technical summary report, volume II: U.S. Department of the Air Force, Ballistic Missile Office, Norton Air Force Base, California, Report E-TR-52-II, 286 p.

Ertec Western, Inc., 1981d, MX Siting Investigation—Water Resources Program—technical summary report, volume IIA: U.S. Department of the Air Force, Ballistic Missile Office, Norton Air Force Base, California, Report E-TR-52-II, 41 p.

Ertec Western, Inc., 1981e, MX Siting Investigation—Water Resources Program—technical summary report, volume IIB: U.S. Department of the Air Force, Ballistic Missile Office, Norton Air Force Base, California, Report E-TR-52-II, 138 p.

Faunt, C.C., 1997, Effect of faulting on ground-water movement in the Death Valley Region, Nevada and California: U.S. Geological Survey, Water-Resources Investigations Report Series, 95-4132, 47 p.

Faunt, C.C., Blainey, J.B., Hill, M.C., D'Agnese, F.A., and O'Brien, G.M., 2004, Chapter F—Transient numerical model, *in* Belcher, W.R., ed., 2004, Death Valley Regional Ground-water Flow System, Nevada and California—Hydrogeologic framework and transient ground-water flow model: U.S. Geological Survey Scientific Investigations Report 2004-5205.

Faybishenko, B., 2007, Climatic forecasting of net infiltration at Yucca Mountain using analogue meteorological data: Vadose Zone Journal, Vol. 6, p. 77–92.

Fenneman, N.M., 1931, Physiography of the western United States. First edition: New York, McGraw-Hill.

Flint, A.L., and Flint, L.E., 2007, Application of the Basin Characterization Model to estimate in-place recharge and runoff potential in the Basin and Range Carbonate-Rock Aquifer System, White Pine County, Nevada, and adjacent areas in Nevada and Utah: U.S. Geological Survey Scientific Investigations Report 2007-5099, 30 p.

Flint, A.L., Flint, L.E., Hevesi, J.A., and Blainey, J.M., 2004, Fundamental concepts of recharge in the Desert Southwest—A regional modeling perspective, *in* Hogan, J.F., Phillips, F.M., and Scanlon, B.R., eds., Ground-water recharge in a desert environment—The southwestern United States: American Geophysical Union, Water Science and Applications Series, Vol. 9, p. 159-184.

Flint, A.L., Flint, L.E., Kwicklis, E.M., Fabryka-Martin, J.T., and Bodvarsson, G.S., 2002, Estimating recharge at Yucca Mountain, Nevada, U.S.A.—Comparison of methods: Hydrogeology Journal, Vol. 10, p. 180–204.

Freeze R.A., and Cherry, J.A., 1979, Groundwater: Englewood Cliffs, New Jersey, Prentice-Hall.

Frick, E.A., 1985, Quantitative analysis of groundwater flow in valley-fill deposits in Steptoe Valley, Nevada [M.S. thesis]: University of Nevada, Reno, 208 p.

Gates, J.S., and Kruer, S.A., 1981, Hydrologic reconnaissance of the southern Great Salt Lake Desert and summary of the hydrology of west-central Utah: Utah Department of Natural Resources Technical Publication No. 71, 64 p.

Gatewood, J.S., Robinson, T.W., Colby, B.R., Hem, J.D., and Halpenny, L.C., 1950, Use of water by bottom-land vegetation in lower Safford Valley, Arizona: U.S. Geological Survey Water-Supply Paper 1103, 224 p.

Gillespie, J.M., 2008, A conceptual model of groundwater flow in Spring Valley, NV, and Snake Valley, NV-UT [M.S. thesis]: Brigham Young University, Utah, 91 p.

Glancy, P.A., 1968, Water-resources appraisal of Butte Valley, Elko and White Pine counties, Nevada: Nevada Department of Conservation and Natural Resources, Ground-Water Reconnaissance Series Report 49, 35 p.

Guth, P.L., 1981, Tertiary extension north of the Las Vegas Valley shear zone, Sheep and Desert ranges, Clark County, Nevada: Geological Society of America Bulletin, Vol. 92, no. 10, p. 763-771.

Guth, P.L., 1990, Superposed Mesozoic and Cenozoic deformation, Indian Springs Quadrangle, *in* Wernicke, B., ed., Basin and Range extensional tectonics near the latitude of Las Vegas, Geological Society of America Memoir 176, p. 237-249.

Halford, K.J., 2008, Personal communication of January 8 to Lari Knochenmus (U.S. Geological Survey) regarding Water Budgets—consistent application of a Maxey-Eakin approach to water-budgets and recharge estimates for the Ground-Water, Development EIS in Clark, Lincoln, and White Pine Counties: U.S. Geological Survey.

Hardman, G., 1936, Nevada precipitation and acreages of land by rainfall zones: University of Nevada, Reno, Agricultural Experiment Station, mimeographed report, 10 p.

Hardman, G., 1962, Precipitation Map of Nevada, *in* Lamke, R.D., and Moore, D.O., 1965, Interim inventory of surface water resources of Nevada: Nevada Department of Conservation and Natural Resources, Water Resources Bulletin No. 30, p. 5-6.

Hardman, G., 1965, Nevada Precipitation Map, adapted by George Hardman, July 1965, from map prepared by George Hardman, Victor Kral, and Victor Haffey, and others, 1936: University of Nevada, Reno, Agricultural Experiment Station.

Hardman, G., and Mason, H.G., eds., 1949, Irrigated lands of Nevada: University of Nevada, Reno, Agricultural Experiment Station, Bulletin No. 183, 57 p.

Harrill, J.R., 1971, Water-resources appraisal of the Pilot Creek Valley area, Elko and White Pine counties, Nevada: Nevada Department of Conservation and Natural Resources, Water Resources Reconnaissance Series Report 56, 52 p.

Harrill, J.R., Gates, J.S., and Thomas, J.M., 1988, Major ground-water flow systems in the Great Basin region of Nevada, Utah, and adjacent states: U.S. Geological Survey Hydrologic Investigations Atlas HA-694-C, 4 p., scale 1:1,000,000, two sheets.

Harrill, J.R., and Prudic, D.E., 1998, Aquifer systems in the Great Basin region of Nevada, Utah, and adjacent states—Summary report: U.S. Geological Survey Professional Paper 1409-A, 66 p.

Heath, R.C., 1984, Ground-water regions of the United States: U.S. Geological Survey Water Supply Paper 2242, 88 p.

Hershey, R.L, Hellweil, V.M., Gardner, D., Lyles, B.F., Earman, S., Thomas, J.M., and Lundmark, K.W., 2007, Ground-water chemistry interpretations supporting the Basin and Range Regional Carbonate-Rock Aquifer System (BARCAS) study, eastern Nevada and western Utah: Desert Research Institute, Publication No. 41230, 108 p.

Hess, J.W., and Mifflin, M.D., 1978, A feasibility study of water production from deep carbonate aquifers in Nevada: Desert Research Institute, Water Resources Center, Publication No. 41054, 135 p.

Hevesi, J.A., Flint, A.L., and Flint, L.E., 2002, Preliminary estimates of spatially distributed net infiltration and recharge for the Death Valley region, Nevada–California: U.S. Geological Survey Water-Resources Investigations Report 2002-4010, 41 p.

Hintze, L.F., 1978, Sevier attenuation faulting in the Fish Springs and House Ranges, western Utah: Brigham Young University Geology Studies, v. 25, pt. 1, p. 11-24.

Hintze, L.F., 1980a, Preliminary geologic map of the Fish Springs NW and Fish Springs SW quadrangles, Juab and Tooele counties, Utah: U.S. Geological Survey Miscellaneous Field Studies Map MF-1148, scale 1:24,000.

Hintze, L.F., 1980b, Preliminary geologic map of the Sand Pass NW quadrangle, Juab County, Utah: U.S. Geological Survey Miscellaneous Field Studies Map MF-1149, scale 1:24,000.

Hintze, L.F., and Davis, F.D., 2002a, Geologic map of the Wah Wah Mountains North 30' × 60' quadrangle and part of the Garrison 30' × 60' quadrangle, southwest Millard County and part of Beaver County, Utah: Utah Geological Survey Map 182, scale 1:100,000.

Hintze, L.F., and Davis, F.D., 2002b, Geologic map of the Tule Valley 30' × 60' quadrangle and parts of the Ely, Fish Springs, and Kern Mountains 30' × 60' quadrangles, northwest Millard County, Utah: Utah Geological Survey Map 186, scale 1:100,000.

Hood, J.W., and Rush, F.E., 1965, Water-resources appraisal of the Snake Valley area, Utah and Nevada: Nevada Department of Conservation and Natural Resources, Water-Resources Reconnaissance Series Report 34, 60 p.

Hood, J.W., and Waddell, K.M., 1968, Hydrologic reconnaissance of Skull Valley, Tooele County, Utah: State of Utah Department of Natural Resources Technical Publication No. 18, 54 p.

Hose, R.K., and Blake, M.C., Jr., 1976, Geology and mineral resources of White Pine County, Nevada, Part 1, Geology: Nevada Bureau of Mines and Geology Bulletin 85, p. 1-35.

Houghton, J.G., Sakamoto, C.M., and Gifford, R.O., 1975, Nevada's weather and climate: Nevada Bureau of Mines and Geology Special Publication 2, 84 p.

IT, see IT Corporation.

IT Corporation, 1996, Underground test area subproject, Phase I data analysis task—Volume IV. Hydrologic parameter data documentation package: IT Corporation, Las Vegas, Nevada, Report ITLV/10972-181, 78 p.

Jachens, R.C., and Moring, B.C., 1990, Maps of the thickness of Cenozoic deposits and the isostatic residual gravity over basement for Nevada: U.S. Geological Survey Open-File Report 90-404, 15 p.

Johnson, M., 2007, Hydrogeology of Pahranagat shear zone and surrounding area, *in* Coache, R., editor, Regional tour of the carbonate system guidebook: Reno, Nevada Water Resources Association, p. 11-12.

Kalnay, E., et al., 1996, The NCEP/NCAR Reanalysis 40-year Project: Bulletin of the American Meteorological Society, 77, pp. 437-471.

Kampf, S.K., Tyler, S.W., Ortiz, C.A., Muñoz, J.F., and Adkins, P.L., 2005, Evaporation and land surface energy budget at the Salar de Atacama, Northern Chile: Journal of Hydrology, Vol. 310, p. 236-252.

Katzer, T., and Donovan, D.J., 2003, Surface-water resources and basin water budget for Spring Valley, White Pine and Lincoln counties, Nevada: Las Vegas Valley Water District, Las Vegas, Nevada, 79 p.

Kepper, J.C., 1960, Stratigraphy and structure of the southern half of the Fish Springs Range, Juab County, Utah [M.S. thesis]: University of Washington, Seattle, 92 p.

Kirby, S., and Hurlow, H., 2005, Hydrogeologic setting of the Snake Valley hydrologic basin, Millard County, Utah, and White Pine and Lincoln counties, Nevada—Implications for possible effects of proposed water wells: Utah Geological Survey Report of Investigation 254, 39 p.

Kirk, S.T., and Campana, M.E., 1990, A deuterium-calibrated groundwater flow model of a regional carbonate-alluvial system: Journal of Hydrology, Vol. 119, p. 357–388.

Kirono, D.G.C., and Jones, R.N., 2007, A bivariate test for detecting inhomogeneities in pan evaporation time series: Australian Meteorological Magazine, Vol. 56, No. 2, pp. 93-103.

Kleinhampl, F.J., and Ziony, J.I., 1985, Geology of northern Nye County, Nevada: Nevada Bureau of Mines and Geology Bulletin 99A, 172 p.

Kumar, C.P., and Seethapathi, P.V., 2002, Assessment of natural ground water recharge in upper Ganga canal command area: Association of Hydrologists of India, Journal of Applied Hydrology, Vol. XV, No. 4, p. 13–20.

Laczniak, R.J., Cole, J.C., Sawyer, D.A., and Trudeau, D.A., 1996, Summary of hydrogeologic controls on ground-water flow at the Nevada Test Site, Nye County, Nevada: U.S. Geological Survey Water-Resources Investigations Report 96-4109, 67 p.

Laczniak, R.J., DeMeo, G.A., Reiner, S.R., Smith, J.L., and Nylund, W.E., 1999, Estimates of ground-water discharge as determined from measurements of evapotranspiration, Ash Meadows Area, Nye County, Nevada: U.S. Geological Survey Water-Resources Investigations Report 99-4079, 77 p.

Laczniak, R.J., Smith, J.L., Elliott, P.E., DeMeo, G.A., Chatigny, M.A., and Roemer, G.J., 2001, Ground-water discharge determined from estimates of evapotranspiration, Death Valley Regional Flow System, Nevada and California: U.S. Geological Survey Water-Resources Investigations Report 01-4195, 51 p.

Las Vegas Valley Water District, Woodward-Clyde Consultants, and Dames & Moore Consultants, 1994, Environmental report covering selected hydrographic basins in Clark, Lincoln, Nye, and White Pine counties, Nevada: Las Vegas Valley Water District, Cooperative Water Project Report No. 14, 235 p.

Las Vegas Valley Water District, 2001, Water resources and ground-water modeling in the White River and Meadow Valley flow systems, Clark, Lincoln, Nye, and White Pine counties, Nevada: Las Vegas Valley Water District, Las Vegas, Nevada, 285 p.

Leahy, P.P., and Lyttle, P.T., 1998, The re-emerging and critical role of geologic understanding in hydrology, *in* Brahana, J.V., Eckstein, Y., Ongley, L.K., Schneider, R., and Moore, J.E., eds., Gambling with groundwater—Physical, chemical, and biological aspects of aquifer-stream relations, Proceedings volume, joint conference of the International Association of Hydrologists and the American Institute of Hydrology, Las Vegas, Nevada, 1998: American Institute of Hydrology, p. 19-24.

Lee, C.H., 1912, An intensive study of the water resources of a part of Owens Valley, California: U.S. Geological Survey Water-Supply Paper 294, 173 p.

Longwell, C.R., 1960, Possible explanation of diverse structural patterns in southern Nevada: American Journal of Science, v. 258-A, p. 192-203.

Longwell, C.R., Pampeyan, E.H., Bowyer, B., and Roberts, R.J., 1965, Geology and mineral deposits of Clark County, Nevada: Nevada Bureau of Mines and Geology Bulletin 62, 218 p., scale 1:250,000.

Lundmark, K.W., 2007, Regional water budget accounting and uncertainty analysis using a deuterium-calibrated discrete state compartment model—White Pine County, Nevada, and adjacent areas in Nevada and Utah [M.S. thesis]: University of Nevada, Reno, 186 p.

Lundmark, K.W., Pohll, G.M., and Carroll, R.W.H., 2007, A steady-state water budget accounting model for the carbonate aquifer system in White Pine County, Nevada, and adjacent areas in Nevada and Utah: Desert Research Institute, Division of Hydrologic Studies, Publication No. 41235, 62 p.

LVVWD, see Las Vegas Valley Water District.

Mankinen, E.A., and McKee, E.H., 2009, Geophysical setting of western Utah and eastern Nevada between latitudes 37°45' and 40°, *in* Tripp, B.T., Krahulec, K., and Jordan, J.L., editors, Geology and geologic resources and issues of western Utah: Utah Geological Association Publication 38.

Maurer, D.K., and Berger, D.L., 1997, Subsurface flow and water yield from watersheds tributary to Eagle Valley hydrographic area, west-central Nevada: U.S. Geological Survey Water-Resources Investigations Report 97-4191, 61 p.

Maurer, D.K., and Halford, K.J., 2004, Updated estimates of the distribution of average annual precipitation in Carson Valley, 1971–2000, Douglas County, Nevada, and Alpine County, California: Journal of the Nevada Water Resources Association, Vol. 1, No. 1, p. 20–39.

Maxey, G.B., and Eakin, T.E., 1949, Groundwater in White River Valley, White Pine, Nye, and Lincoln counties, Nevada: State of Nevada, Office of the State Engineer, Water Resources Bulletin No. 8, 61 p.

McCurdy, G., and Albright, W., 2004, Estimates of potential evapotranspiration at selected sites in eastern Nevada from meteorological station data: Desert Research Institute Publication No. 41198, 118 p.

McDonald, M.G., and Harbaugh, A.W., 1988, A modular three- dimensional finite-difference ground-water flow model: U.S. Geological Survey Techniques of Water-Resources Investigations, book 6, chap. A1, 586 p.

Meinzer, O.E., 1917, Geology and water resources of Big Smoky, Clayton, and Alkali Spring valleys, Nevada: U.S. Geological Survey Water-Supply Paper 423, 180 p.

Meinzer, O.E., 1927, Plants as indicators of ground water: U.S. Geological Survey Water-Supply Paper 577, 114 p.

Meinzer, O.E., ed., 1942, Hydrology: New York, McGraw-Hill Book Company, Inc.

Mendenhall, W.C., 1909, Some desert watering places in southeastern California and southwestern Nevada: U.S. Geological Survey Water-Supply Paper 224, 107 p.

Menking, K.M., Anderson, R.Y., Brunsell, N.A., Allen, B.D., Ellwein, A.L., Loveland, T.A., and Hostetler, S.W., 2000, Evaporation from groundwater discharge playas, Estancia Basin, central New Mexico, *in* Yu, Z., and Barron, E.J., eds., Special Issue—Integrated study of regional climate and hydrology: Global and Planetary Change, Vol. 25, p. 133–147.

Mifflin, M.D., 1968, Delineation of ground-water flow systems in Nevada: Desert Research Institute, Water Resources Center, Technical Report Series H-W, Publication No. 4, 115 p.

Mifflin, M.D., and Wheat, M.M., 1979, Pluvial lakes and estimated pluvial climates of Nevada: Nevada Bureau of Mines and Geology Bulletin 94, 57 p.

Mizell, S.A., Russell, C.E., and Kluesner, T.L., 2007, Reconnaissance estimation of groundwater recharge to selected hydrographic basins of eastern Nevada and western Utah using the chloride mass-balance method: Desert Research Institute, Division of Hydrologic Sciences, Publication No. 41232, 35 p.

Moreo, M.T., Laczniak, R.J., and Stannard, D.I., 2007, Evapotranspiration rate measurements of vegetation typical of ground-water discharge areas in the Basin and Range Carbonate-Rock Aquifer System, White Pine County, Nevada, and adjacent areas in Nevada and Utah, September 2005–August 2006: U.S. Geological Survey Scientific Investigations Report 2007-5078, 48 p.

Morris, H.T., 1987, Preliminary geologic map of the Delta 2° quadrangle, Tooele, Juab, Millard, and Utah counties, Utah: U.S. Geological Survey Open-File Report 87-185, scale 1:250,000.

Mozingo, H.N., 1987, Shrubs of the Great Basin—A natural history: Las Vegas, Nevada, University of Nevada Press.

Mundorff, J.C., 1970, Major thermal springs of Utah: Utah Geological and Mineralogical Survey, Water Resources Bulletin 13, 70 p.

Nalder, I.A., and Wein, R.W., 1998, Spatial interpolation of climatic Normals—Test of a new method in the Canadian boreal forest: Agriculture and Forest Meteorology, Vol. 92, No. 4, p. 211–225.

National Academy of Sciences, 1996, Rock fractures and fluid flow contemporary understanding and applications: Committee on Fracture Characterization and Fluid Flow, Washington, D.C., National Academy Press.

National Land Cover Data, 1992, Data [Internet], available from http://landcover.usgs.gov/natllandcover.asp or http://www.mrlc.gov/mrlc2k_nlcd.asp or http://epa.gov/mrlc/ncld.html.

National Oceanic and Atmospheric Administration, 2009, Earth Science Research Laboratory Physical Science Division, timeseries extraction from U.S. Climate Division Precipitation Dataset, U.S. Department of Commerce [Internet], [accessed 28 May 2009] available from http://www.cdc.noaa.gov/cgi-bin/data/timeseries/timeseries1.pl.

NDWR, see Nevada Division of Water Resources.

Neuman, S.P., 1990, Universal scaling of hydraulic conductivities and dispersivities in geologic media: Water Resources Research, Vol. 26, No. 8, p. 1749–1758.

Nevada Division of Water Resources, 2007, Water Rights Database Special Hydrographic Abstracts [Internet], [accessed March 7, 2007], available from http://water.nv.gov/water%20Rights/permitdb/permitdb_index.cfm.

Nevada State Engineer (The office of the State Engineer of The State of Nevada), 2007a, Ruling (#5712) in the matter of applications 72218, 72219, 72220 and 72221 filed to appropriate the underground waters of the Kane Springs Valley hydrographic basin (206), Lincoln County, Nevada.

Nevada State Engineer (The office of the State Engineer of The State of Nevada), 2007b, Ruling (#5726) in the matter of applications 54003 through 54021, inclusive, filed to appropriate the underground waters of the Spring Valley hydrographic basin (184), White Pine County, Nevada.

Nichols, W.D., 1993, Estimating discharge of shallow groundwater by transpiration from greasewood in the northern Great Basin: Water Resources Research, Vol. 29, No. 8, p. 2771-2778.

Nichols, W.D., 1994, Groundwater discharge by phreatophyte shrubs in the Great Basin as related to depth to groundwater: Water Resources Research, Vol. 30, No. 12, p. 3265-3274.

Nichols, W.D, Laczniak, R.J., DeMeo, G.A., and Rapp, T.R., 1997, Estimated ground-water discharge by evapotranspiration, Ash Meadows area, Nye County, Nevada, 1994: U.S. Geological Survey Water-Resources Investigations Report 97-4025, 18 p.

Nichols, W.D., 2000, Regional ground-water evapotranspiration and ground-water budgets, Great Basin, Nevada: U.S. Geological Survey Professional Paper 1628, 101 p.

NLCD, see National Land Cover Data.

NOAA, see National Oceanic and Atmospheric Administration.

Olivera, M.E., 1975, Geology of the Fish Springs mining district, Fish Springs Range, Utah: Brigham Young University Geology Studies, v. 22, pt. 1, p. 69-104.

Oviatt, C.G., 1991, Quaternary geology of Fish Springs Flat, Juab County, Utah: Utah Geological Survey Special Study 77, 21 p., scale 1:50,000.

Page, W.R., Dixon, G.L., Rowley, P.D., and Brickey, D.W., 2005, Geologic map of parts of the Colorado, White River, and Death Valley groundwater flow systems—Nevada, Utah, and Arizona: Nevada Bureau of Mines and Geology Map 150, scale 1:250,000.

Phoenix, D.A., 1948, Geology and ground water in the Meadow Valley Wash drainage area, Nevada, above the vicinity of Caliente, Nevada: State of Nevada, Office of the State Engineer, Water Resources Bulletin 7, 117 p.

Plume, R.W., and Carlton, S.M., 1988, Hydrogeology of the Great Basin region of Nevada, Utah, and adjacent states: U.S. Geological Survey Hydrologic Atlas HA-694-A, scale 1:1,000,000, one sheet.

Pohlmann, K.F., Campagna, D.J., Chapman, J.B., and Earman, S., 1998, Investigation of the origin of springs in the Lake Mead National Recreation Area: Desert Research Institute, Water Resources Center, Publication No. 41161, 94 p.

SE ROA 50549

JA_15950

Prudic, D.E., Harrill, J.R., and Burbey, T.J., 1995, Conceptual evaluation of regional ground-water flow in the carbonate-rock province of the Great Basin, Nevada, Utah, and adjacent states—Regional aquifer-system analysis—Great Basin, Nevada–Utah: U.S. Geological Survey Professional Paper 1409-D, 117 p.

Qi, J., Chehbouni, A., Huete, A.R., and Kerr, Y.H., and Sorooshian, S., 1994, A modified soil adjusted vegetation index, *in* Remote Sensing of Environment, Vol. 48, p. 119-126.

Quiring, R.F., 1965, Annual precipitation amount as a function of elevation in Nevada south of 38 1/2 degrees latitude: U.S. Weather Bureau Research Station, Las Vegas, Nevada, 14 p.

Reiner, S.R., Laczniak, R.J., DeMeo, G.A., Smith, J.L., Elliott, P.E., Nylund, W.E., and Fridrich, C.J., 2002, Ground-water discharge determined from measurements of evapotranspiration, other available hydrologic components, and shallow water-level changes, Oasis Valley, Nye County, Nevada: U.S. Geological Survey Water-Resources Investigations Report 01-4239, 65 p.

Rich, L.R., 1951, Consumptive use of water by forest and range vegetation: Proceedings—American Society of Civil Engineers, Vol. 77, separate No. 90, 14 p.

Robinson, T.W., 1970, Evapotranspiration by woody phreatophytes in the Humboldt River Valley near Winnemucca, Nevada: U.S. Geological Survey Professional Paper 491-D, 46 p.

Rosenberry, D.O., Winter, T.C., Buso, D.C., and Likens, G.E., 2007, Comparison of 15 evaporation methods applied to a small mountain lake in the northeastern USA: Journal of Hydrology, Vol.340, p. 149-166.

Rowley, P.D., 1998, Cenozoic transverse zones and igneous belts in the Great Basin, western United States—Their tectonic and economic implications, *in* Faulds, J.E., and Stewart, J., eds., Accommodation zones and transfer zones—The regional segmentation of the Basin and Range Province: Geological Society of America Special Paper 323, p. 195–228.

Rowley, P.D., and Dixon, G.L., 2000, Cenozoic evolution of the Great Basin area, U.S.A.—New interpretations based on long-term field studies [abs.]: Geological Society of America Abstracts with Programs, Vol. 32, No.7, p. A461.

Rowley, P.D., and Dixon, G.L., 2001, The Cenozoic evolution of the Great Basin area, U.S.A.—New interpretations based on regional geologic mapping, *in* The geologic transition, high plateaus to Great Basin—A symposium and field guide (The Mackin Volume): Utah Geological Association Publication 30 and Pacific Section of the American Association of Petroleum Geologists Guidebook GB 78, p. 169–188.

Rowley, P.D., and Dixon, G.L., 2004, The role of geology in increasing Utah's ground-water resources from faulted terranes—Lessons from the Navajo Sandstone, Utah, and the Death Valley Flow System, Nevada–California, *in* Spangler, L.E., ed., Ground water in Utah—Resource, protection, and remediation: Utah Geological Association Publication 31, p. 27–41.

Rowley, P.D., and Dixon, G.L., 2006, Memorandum of June 29 to A.G. Burns, (Southern Nevada Water Authority) regarding USGS report by Elliott et al. (2006), Las Vegas, Nevada, 14 p.

Rush, F.E., 1964, Ground-water appraisal of the Meadow Valley area, Lincoln and Clark counties, Nevada: Nevada Department of Conservation and Natural Resources, Ground-Water Resources Reconnaissance Series Report 27, 65 p.

Rush, F.E, 1968a, Index of hydrographic areas: Nevada Division of Water Resources, Water Resources Information Series Report 6, 43 p.

Rush, F.E., 1968b, Water-resources appraisal of the Lower Moapa–Lake Mead area, Clark County, Nevada: Nevada Department of Conservation and Natural Resources, Water Resources Reconnaissance Series Report 50, 75 p.

Rush, F.E., and Eakin, T.E., 1963, Ground-water appraisal of Lake Valley in Lincoln and White Pine counties, Nevada: Nevada Department of Conservation and Natural Resources, Ground-Water Resources Reconnaissance Series Report 24, 43 p.

Rush, F.E., and Kazmi, S.A.T., 1965, Water resources appraisal of Spring Valley, White Pine and Lincoln counties, Nevada: Nevada Department of Conservation and Natural Resources, Water Resources Reconnaissance Series Report 33, 56 p.

Russell, C.E., and Minor, T., 2002, Reconnaissance estimates of recharge based on an elevation-dependent chloride mass-balance approach: U.S. Department of Energy, National Nuclear Security Administration, DOE/NV/11508-37 (Desert Research Institute, Publication No. 45164), 146 p.

Sack, D., 1990, Quaternary geologic map of Tule Valley, west-central Utah: Utah Geological and Mineral Survey Map 124, scale 1:100,000.

San Juan, C.A., Belcher, W.R., Laczniak, R.J., and Putnam, H.M., 2004, Hydrologic components for model development, *in* Belcher, W.R., ed., Death Valley Regional Ground-Water Flow System, Nevada and California—Hydrogeologic framework and transient ground-water flow model: U.S. Geological Survey Scientific Investigations Report 2004-5205, p. 99–136.

Scanlon, B.R., Keese, K.E., Flint, A.L., Flint, L.E., Gaye, C.B., Edmunds, W.M., and Simmers, I., 2006, Global synthesis of groundwater recharge in semiarid and arid regions: Hydrological Processes, Vol. 20, p. 3335–3370.

Scheirer, D.S., Page, W.R., and Miller, J.J., 2006, Geophysical studies based on gravity and seismic data of Tule Desert, Meadow Valley Wash, and California Wash basins, southern Nevada. U.S. Geological Survey Open-File Report 2006-1396, 44 p.

Scheirer, D.S., and Andreasen, A.D., 2008, Results of gravity fieldwork conducted in March 2008 in the Moapa Valley region of Clark County, Nevada: U.S. Geological Survey Open-File Report 2008-1300, 40 p.

Scott, B.R., Smales, T.J., Rush, F.E., and Van Denburgh, A.S., 1971, Water for Nevada—Report 3—Nevada's Water Resources: Nevada Department of Conservation and Natural Resources, 92 p.

Shah, N., Nachabe, M., and Ross, M., 2007, Extinction depth and evapotranspiration from ground water under selected land covers: Ground Water, Vol. 45, No. 3, p. 329-338.

Sibson, R.H., 1996, Structural permeability of fluid-driven fault-fracture meshes: Journal of Structural Geology, Vol. 18, No. 8, p. 1031-1042.

Simley, J.D., Carswell Jr., W.J., 2009, The National Map—Hydrography: U.S. Geological Survey Fact Sheet 2009-3054, 4 p.

Smales, T.J., and Harrill, J.R., 1971, Water for Nevada—Report 2—Estimated water use in Nevada: Nevada Department of Conservation and Natural Resources, Division of Water Resources, 32 p.

Smith, J.L., Laczniak, R.J., Moreo, M.T., and Welborn, T.L., 2007, Mapping evapotranspiration units in the Basin and Range Carbonate-Rock Aquifer System, White Pine County, Nevada, and adjacent areas in Nevada and Utah: U.S. Geological Survey Scientific Investigations Report 2007-5087, 21 p.

SNWA, see Southern Nevada Water Authority.

Southern Nevada Water Authority, 2004, Five Year Conservation Plan, 2004–2009—Submitted to the U.S. Bureau of Reclamation in fulfillment of the requirements for Section 210(b) of the Reclamation Reform Act of 1982: Southern Nevada Water Authority, Las Vegas, Nevada, 31 p.

Southern Nevada Water Authority, 2005, Analysis of potential water-related effects of Southern Nevada Water Authority's proposed groundwater development project in Three Lakes Valley South, Clark County, Nevada: Southern Nevada Water Authority, Las Vegas, Nevada, 118 p.

Southern Nevada Water Authority, 2006, Water resources assessment for Spring Valley—Presentation to the Office of the Nevada State Engineer: Southern Nevada Water Authority, Las Vegas, Nevada, 176 p.

Southern Nevada Water Authority, 2007, Part A—regional-scale evaluation of natural recharge, discharge, and interbasin flow for the White River Flow System, *in* Southern Nevada Water Authority, Water-Resources Assessment and Hydrogeologic Report for Cave, Dry Lake, and Delamar Valleys: Southern Nevada Water Authority, Las Vegas, Nevada, 352 p.

Southern Nevada Water Authority, 2008a, Baseline characterization report for Clark, Lincoln, and White Pine Counties Groundwater Development Project: Southern Nevada Water Authority, Las Vegas, Nevada, 1146 p.

Southern Nevada Water Authority, 2008b, Water resource plan 09: Southern Nevada Water Authority, Las Vegas, Nevada, 71 p.

Southern Nevada Water Authority, 2009a, Simulation of Groundwater Development Scenarios Using the Transient Numerical Model of Groundwater Flow for the Central Carbonate-Rock Province: Clark, Lincoln, and White Pine Counties Groundwater Development Project. Prepared in cooperation with the Bureau of Land Management. Las Vegas, Nevada.

Southern Nevada Water Authority, 2009b, Transient numerical model of groundwater flow for the central carbonate-rock province Clark, Lincoln, and White Pine Counties Groundwater Development Project: Southern Nevada Water Authority, Las Vegas, Nevada.

Spengler R.W., Maldonado, F., Weir, J.E., Jr., Hanna, W.F., and Dixon, G.L., 1979, Inventory of granitic masses in the State of Nevada: U.S. Geological Survey Open-File Report 79-235, 264 p. and 9 plates.

Stephens, J.C., 1977, Hydrologic reconnaissance of the Tule Valley drainage basin, Juab and Millard counties, Utah: Utah Department of Natural Resources Technical Publications No. 56, 43 p.

Stoeser, D.B., 1993, Tertiary calderas and regional extension of the east-central part of the Tintic-Deep Creek mineral belt, eastern Great Basin, Utah *in* Advances Related to United States and International Mineral Resources–Developing Frameworks and Exploration Technologies: U.S. Geological Survey Bulletin 2039, p. 5-23.

Stuart, W.T., 1955, Pumping test evaluates water problem at Eureka, Nevada: American Institute of Mining, Metallurgical, and Petroleum Engineers Transactions, Vol. 202, p. 148-156.

Thomas, J.M., Calhoun, S.C., and Apambire, W.B., 2001, A deuterium mass-balance interpretation of groundwater sources and flows in southeastern Nevada: Desert Research Institute, Publication No. 41169, 52 p.

Thomas, J.M., Mason, J.L., and Crabtree, J.D., 1986, Groundwater-levels in the Great Basin region of Nevada, Utah, and adjacent states: U.S. Geological Survey Hydrologic Investigation Atlas HA-694-B, scale 1:1,000,000, two sheets.

Thomas, J.M., and Mihevc, T., 2007, Stable isotope evaluation of water budgets for the White River and Meadow Valley Wash Regional Groundwater Flow Systems in east-central and southeastern Nevada: Letter Report to Southern Nevada Water Authority, Desert Research Institute, 189 p.

Thomas, J.M., Welch, A.H., and Dettinger, M.D., 1996, Geochemistry and isotope hydrology of representative aquifers in the Great Basin region of Nevada, Utah, and adjacent states: U.S. Geological Survey Professional Paper 1409-C, 108 p.

Tóth, J.A., 1963, A theoretical analysis of ground-water flow in small drainage basins: Journal of Geophysical Research, Vol. 68, No. 16, p. 4795–4812.

Tschanz, C.M., 1960, Geology of northern Lincoln County, Nevada, *in* Boettcher, J.W., and Sloan, W.W., Jr., Guidebook to the geology of east-central Nevada—11th Annual Field Conference Guidebook: Intermountain Association of Petroleum Geologists, p. 198–208.